Distribution Agreement

In presenting this thesis or dissertation as a partial fulfillment of the requirements for an advanced degree from Emory University, I hereby grant to Emory University and its agents the non-exclusive license to archive, make accessible, and display my thesis or dissertation in whole or in part in all forms of media, now or hereafter known, including display on the world wide web. I understand that I may select some access restrictions as part of the online submission of this thesis or dissertation. I retain all ownership rights to the copyright of the thesis or dissertation. I also retain the right to use in future works (such as articles or books) all or part of this thesis or dissertation.

Signature:

_____ _____

Brian Dobosh Date

Regulation of Leukocyte Inflammation by Small Particles
Including Extracellular Vesicles and Viruses

By

Brian Dobosh
Doctor of Philosophy

Graduate Division of Biological and Biomedical Sciences
Immunology and Molecular Pathogenesis

Rabindra Tirouvanziam, Ph.D Advisor	Gregory Melikian, Ph.D Committee Member
Eun-Hyung Lee, MD Committee Member	Joanna Goldberg, Ph.D Committee Member
Mehul Suthar, Ph.D Committee Member	

Accepted:

Kimberly Jacob Arriola, Ph.D, MPH

Dean of the James T. Laney School of Graduate Studies

Date

Regulation of Leukocyte Inflammation by Small Particles
Including Extracellular Vesicles and Viruses

By

Brian Dobosh
BS, Northeastern University, 2015

Advisor: Rabindra Tirouvanziam, Ph.D

An abstract of a dissertation submitted to the Faculty of the
James T. Laney School of Graduate Studies of Emory University in
partial fulfillment of the requirements for the degree of

Doctor of Philosophy
In Immunology and Molecular Pathogenesis

2022

Abstract

Regulation of Leukocyte Inflammation by Small Particles
Including Extracellular Vesicles and Viruses

By

Brian Dobosh

Innate immune cells, which include polymorphonuclear neutrophils (PMNs) and monocytes, are constantly patrolling tissues such as the lung, in search of damaged or dying cells. This dissertation describes two cases in which innate immune cells fail to resolve airway stress and thus promote disease.

In patients with cystic fibrosis (CF), the main cause of morbidity and mortality is lung disease, which is associated with an early, massive and chronic recruitment of PMNs into the airway lumen. Therein, PMNs release potent effector proteins such as neutrophil elastase, myeloperoxidase, interleukin (IL)-1β and IL-18, which can damage the airways. Such pathological PMNs, which we have dubbed "GRIM" (for granule releasing, immunomodulatory, and metabolically active) are observed not only in the airways of CF patients, but also in those of patients with chronic obstructive pulmonary disease (COPD), asthma, and severe coronavirus disease of 2019 (COVID-19). Although PMNs are professional phagocytes, they actively restrict killing of bacteria in CF airways, leading to chronic infections. To date, it is unclear what factors cause PMNs to become GRIM. Work presented here show that extracellular vesicles (EVs) released by GRIM airway PMNs cause naïve, newly immigrated airway PMNs to take on the same fate. More precisely, GRIM PMN-derived EVs carrying the long non-coding RNA MALAT1 cause expression the enzyme HDAC11 in naïve PMNs, which drives them to degranulate, reduce their bacterial killing capacity, and release a new wave of MALAT1+ EVs that perpetuate the pathological cycle. Inhibition or knockdown of HDAC11 or MALAT1 reverses the GRIM phenotype and promotes killing of bacteria.

COVID-19 patients are generally asymptomatic during initial severe acute respiratory syndrome coronavirus-2 (SARS-CoV-2) replication, but may suffer severe immunopathology after the virus has receded and blood monocytes have infiltrated the airways. Patients that lack an early PMN response tend to have a monocyte response that results in cytokine release syndrome and severe COVID-19. Using an in vitro model, we show that airway-infiltrating monocytes acquire SARS-CoV-2 from infected epithelium and upregulate expression and secretion of inflammatory mediators including CXCL8 and IL-1β, mirroring *in vivo* data. Next, we characterized viral burden, gene expression and inflammatory mediator secretion by lung epithelial cells and infiltrating monocytes in the absence or presence of the antiviral remdesivir and/or immunomodulatory drug baricitinib. As expected, remdesivir decreased viral burden in both the epithelium and monocytes, while baricitinib enhanced antiviral signaling and decreased specific inflammatory mediators in monocytes. Combined use of baricitinib and remdesivir enhanced the rate of virus clearance from SARS-CoV-2-positive monocytes.

Taken together, when monocytes and PMNs have a discordant immune response to stress, runaway inflammation and lung damage may occur. We have developed methods to interrogate and modulate *in vitro* how these cells behave in the context of various stressors including virus and extracellular vesicles and have initiated testing of novel treatment approaches including small molecule drugs and DNA- and RNA-based therapeutics to tackle these problems.

Regulation of Leukocyte Inflammation by Small Particles
Including Extracellular Vesicles and Viruses

By

Brian Dobosh
B.S., Northeastern University, 2015

Advisor: Rabindra Tirouvanziam, PhD

A dissertation submitted to the Faculty of the James T. Laney School of Graduate Studies of Emory University in partial fulfillment of the requirements for the degree of

Doctor of Philosophy
In Immunology and Molecular Pathogenesis

2022

Acknowledgments

It goes without saying that I could not have done the work contained here without the support and mentorship of many people, both personally and professionally. Firstly, my parents and brother have always supported and encouraged me to follow my interests both inside and outside of the sciences. I also want to acknowledge the support of my grandparents in giving me the freedom to be curious and fostered my love of reading and the pursuit of knowledge. From generation to generation, they have enabled the success of our family. In addition, many of my friends, with whom I have traveled and hiked around the world, provided much needed distractions from my work.

To the members of the Tirouvanziam lab, both past and present, I give my heartfelt thanks in providing a strong conceptual foundation for how to approach amazingly difficult questions. You have shown an incredible willingness to work together despite my prickly nature. Milton Brown guided and helped troubleshoot numerous experiments during the early parts of the Ph.D. and, without him, our COVID-19 projects would have crumbled in the early days of the pandemic. Milagros Aldeco has kept our lab running smoothly and has always offered unwavering support and advice. She also provided much needed support in cell culture and RNA extractions throughout the years. Camilla Margaroli trained me when I first joined the lab and has been an incredible sounding board for ideas and how to work with researchers of many different personalities. Vincent Giacalone is the anchor of our lab and could always be relied upon to be a good lab citizen. We have experienced and handled the fickleness of science and commiserated over our shared experiences. Diego Moncada-Giraldo conducted most of the bioinformatics analysis included within this work. I aspire to have an as equally lighthearted approach to life as him. I also want to thank my undergraduate trainee, Alex Rojas. Most of the work he has done is not included in this thesis as it is an independent project, but he has assisted with many of my other experiments. Alex has been patient with me as I learned how to be a mentor to the next generation of scientists and I cannot wait to see what he does going forward. To the other unnamed members of the lab, I thank you for your assistance with my many experiments and have greatly enjoyed our gatherings around a table full of food.

I am quite grateful for the many opportunities afforded to me to gain experience across a multitude of disciplines. In particular, I would like to thank my undergraduate mentor, Phyllis Strauss, and my supervisor from when I was a technician, Ely Porter. They imparted a terrific foundation in the underlying chemistry and physics of many biological assays. It is due to their work that I have a strong and diverse technical background, which has been paramount to tackle the many projects contained within and outside this thesis.

Lastly, I give my heartfelt thanks to my mentor, Rabindra Tirouvanziam. He has grown my love and curiosity for a wide variety of scientific disciplines and given me the freedom to pursue my interests in understanding and engineering cell biology. My success as a scientist is in large part due to his cheerful counseling and eager willingness to talk at length about any topic including philosophy, art culture, and of course biology.

Table of Contents

Chapter 1: INTRODUCTION TO EV BIOLOGY

EV NOMENCLATURE

In the late 1960s it was observed that lipid-rich particulates from platelets, termed *"platelet dust,"* could cause the coagulation of blood (Wolf, 1967; Mathieu et al., 2019). It was not until later that the secretions of platelets, and other cells, would be realized as extracellular vesicles (EVs) (Couch et al., 2021). EVs are complex particles surrounded by a lipid bilayer which contain a mixture of lipids, carbohydrates, proteins and nucleic acids including various RNAs such as messenger, micro and long non-coding RNAs (mRNAs, miRNAs and lncRNAs, respectively), as well as genomic and mitochondrial DNA. Since EVs contain some of the proteins, RNAs, and lipids of the producer cells the subsequent uptake of these signals by recipient cells is a method to influence proximal and distal tissue environments. The release of EVs appears to be a universal and evolutionally conserved cellular mechanism to maintain homeostasis and respond to stressors. Archaea, Prokarya and Eukarya, including plants and fungi, all release EVs containing proteins, RNAs, and lipids that may change in response to environmental cues (Gill et al., 2018).

Over the past six decades, there have been numerous terms attributed to subcategories of EVs, roughly based on size and location of origin within a cell, including exosomes, microvesicles/microparticles, apoptotic bodies/blebs, ectosomes (Gyorgy et al., 2011) and exomeres (Zhang et al., 2018). Particles that originate from multivesicular bodies and are released after fusion with the cell membrane are termed *exosomes* (typically <200 nm diameter), while those that bud directly from the membrane are typically referred to as *microvesicles* (100 nm-1 µm) **(Figure 1.1)**. Rarely, *ectosomes* may describe microvesicles

specifically originating from polymorphonuclear neutrophils (PMNs) or monocytes (Gasser and Schifferli, 2004; Gyorgy et al., 2011). More commonly, ectosomes refer to the shedding of a large particle, following cytoskeletal remodeling and increased cytosolic levels of Ca^{2+} ions. The equilibrium of lipids in the plasma membrane, including phosphatidylserine, cholesterol and phosphatidylethanolamine is disturbed by the increased Ca^{2+} concentration and these are shed from the membrane (Cocucci et al., 2009; Cocucci and Meldolesi, 2015). The term *microvesicle* can also collectively refer to ectosomes, oncosomes, and other microparticles shed directly from the membrane (van Niel et al., 2018). A cell undergoing apoptosis will form *blebs* (100 nm – 5 µm in diameter) off its membrane, resulting in the loss of ATP and the subsequent flipping of phosphatidylserine from the inner to the outer leaflet of the membrane, which is recognized by receptors, such as annexin V, lactadherin and TIM-4 on scavenger cells like macrophages and PMNs (Gyorgy et al., 2011). Lastly, *exomere* is a recently coined term for the smallest of EVs (~50-60 nm or less). Exomere formation has not been fully described, but preliminary evidence suggests they are sheared or shed directly from the plasma membrane, yet the fact that they lack tetraspanins indicates minimal active membrane reorganization (Zhang et al., 2018). A subset of exomeres, *supermeres*, was recently described as being able to contain, or at least be associated with, many glycolytic enzymes, signaling molecules, miRNAs and RNA-binding proteins (Zhang et al., 2021). Although the authors mark a differences in some miRNA and protein contents, the distinction between exomeres / “distinct nanoparticles” identified in an earlier paper (Zhang et al., 2018; Zhang et al., 2019a) and supermeres (Zhang et al., 2021) is still unclear based on other similar contents between. *Outer membrane vesicles* (OMV) are particles

secreted by bacteria that are typically gram positive and thus contains portions of the peptidoglycan cell wall (Jan, 2017).

Altogether, there are many terms referring to particles actively or passively secreted by a cell and their size definition is not absolute. Furthermore, the sizes of each particle subtype overlap, resulting in erroneous or misleading nomenclature. To avoid confusion, the catchall term *extracellular vesicle* (or *EV*) will be used throughout this work to denote a lipidated particle secreted from cells unless otherwise specified. The general use of *extracellular vesicle* is the recommendation of the International Society for Extracellular Vesicles (ISEV) unless a particular subset of particle can be determined experimentally, which is typically quite challenging (Thery et al., 2018).

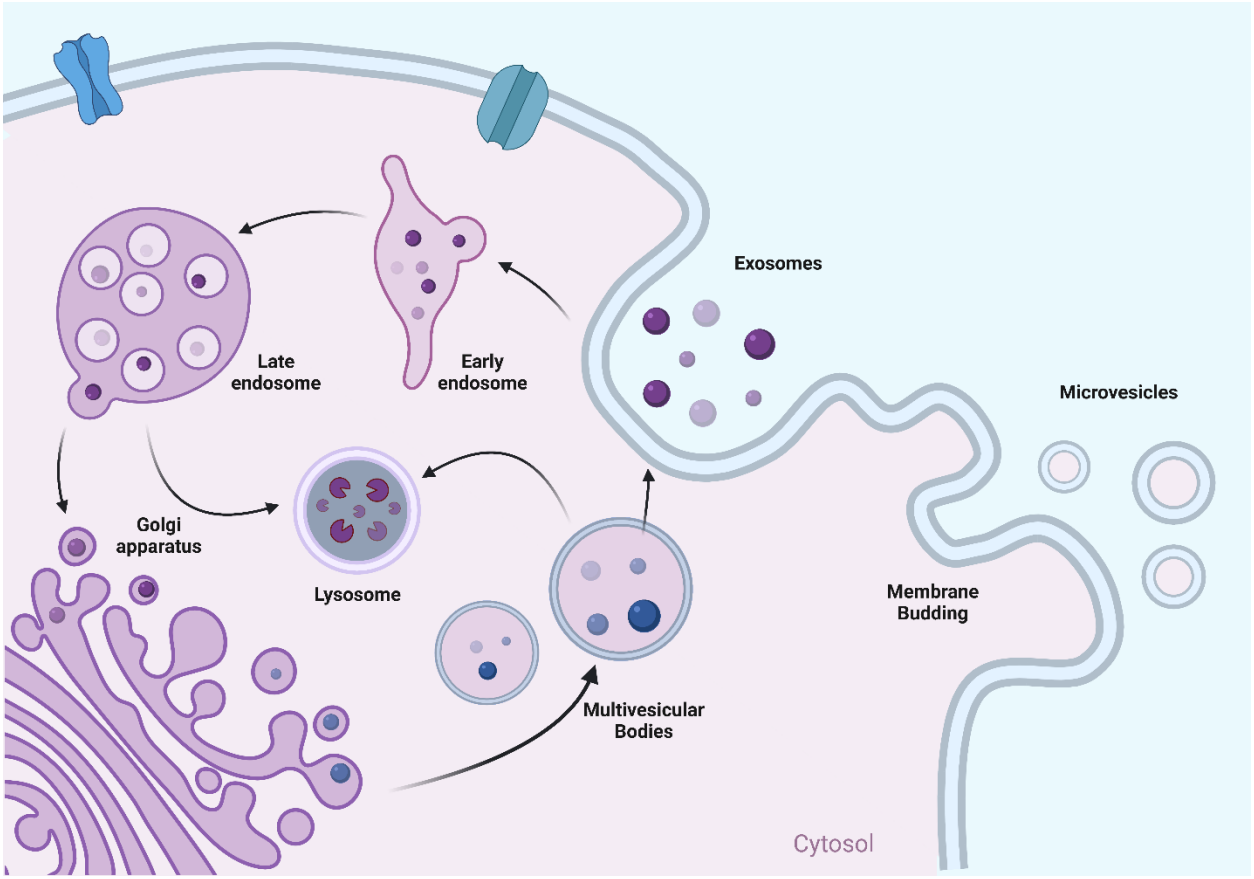

Figure 1.1. Vesicle trafficking throughout the cell and EV biogenesis. ***Extracellular particles such as exosomes and microvesicles may be taken up into a cell and trafficked via progressively more mature endosomes and contents may either be degraded or resorted by Golgi vesicles. Resorted cargo can be packaged within intraluminal vesicles and then multivesicular bodies. Fusion of the multivesicular body with the plasma membrane releases exosomes into the extracellular environment. Microvesicles are formed through direct budding from the plasma membrane.***

BIOLOGICAL EFFECTS OF EVS

The original function of EVs was thought to be that of a recycler whereby the contents and nutrients of a cell that were no longer needed and could not be stored nor degraded were expelled. Uptake by scavenger cells such as monocytes, macrophages, and PMNs would ensue, with EVs then being broken down into their base components and recycled for use in other cellular processes (Vidal, 2019). EVs not absorbed by scavenger cells would be expelled from the body in urine or other bodily secretions (Erdbrugger et al., 2021). The cellular use of EVs was analogous to the base functions of the proteasomal and lysosomal compartments.

However, just as the proteasome and lysosome are necessary not just for degradation of intracellular material but also for core cellular processes such as antigen presentation and autophagy, the role of EVs has also been expanded to include their broad potential for cell-to-cell communication. Indeed, EVs do not simply contain "obsolete membrane proteins" (Johnstone et al., 1991). As a result, the current in vivo functions of EVs can be observed to have four non-mutually exclusive facets: 1) Mediate cell-to-cell transfer of information; 2) Protect intra-EV cargo from degradation; 3) Reflect the current state of cells and tissues ("biomarkers"); and 4) Promote functional alterations to the extracellular milieu.

Cells may modulate their extracellular environment through the release of EVs, which contain bioactive components. As a consequence of their biogenesis, proteases, ligands and receptors, and other effector proteins associated with EVs may be active prior to their uptake and processing by the recipient cell. For example, EVs with surface-bound, catalytically active neutrophil elastase (NE) derived from patients with chronic obstructive pulmonary disease (COPD) promoted bronchiectasis upon transfer to mouse lungs (Genschmer et al., 2019). Furthermore, the receptors and ligands associated with the surface of EVs may be active independently of EV uptake, as shown by the induction of Ca^{2+} influx in T regulatory cells by surface-bound but not internalized EVs from U937 tumor cells (Muller et al., 2017).

EVs can also contain chemoattractants, cytokines, and inflammatory mediators to regulate the presence and activity of immune cells. For example, PMNs stimulated in the presence of endothelium released EVs that contained α2-macroglobulin, ceruloplasmid, and complement C3 whereas PMNs in suspension released EVs that were enriched for HSP70-1 (Dalli et al., 2013). The former EVs were also able to produce reactive oxygen species (ROS) and

leukotriene B4 (LTB4) and form their own chemotactic gradient (Dalli et al., 2013). Other studies have identified that most cytokines and inflammatory mediators such as CXCL8 (IL-8), IFNγ, IL-2, IL-10, and TNFα are not just present in soluble form, but also associated with EVs, potentially increasing the avidity of binding and enhancing their signaling potential to recipient cells (Fitzgerald et al., 2018; Kaur et al., 2021a). EVs can also be sampled from tissues or biofluids and used as a "snapshot" of the state of the cells and tissues at that time. For example, the presence of cancer may be reflected in the altered miRNA contents of a population of EVs in biofluids such as plasma (Shukuya et al., 2020; Ueta et al., 2021). Similarly, an increased concentration of PMNs present in the lung may show a concomitant increase in the amount of CD66b+ (PMN-specific) EVs in sputum or bronchoalveolar lavage fluid (BALF) (Genschmer et al., 2019; Margaroli et al., 2021; Margaroli et al., 2022).

EVs are one mechanism by which cell-to-cell communication occurs, adding a layer of complexity to the much-touted soluble mediator/hormone release and close-proximity juxtacrine signaling (Mulcahy et al., 2014). EVs may contain surface molecules such as free-associated light chains from B cells (Nazimek et al., 2020), the 'don't eat me signal' CD47 (Kaur et al., 2021a; Kaur et al., 2021b), integrins (Fedele et al., 2015; Akbar et al., 2022; Al Faruque et al., 2022), heat shock proteins, major histocompatibility complex (MHC) class I and II (Buschow et al., 2009; Kaur et al., 2021a; Marcoux et al., 2021), cell adhesion molecules (Segura et al., 2005), pattern recognition receptors like Toll-like receptors (TLRs) (Srinivasan et al., 2017), and other ligands and receptors which may influence recipient cells that receive particular subsets of EVs (Mulcahy et al., 2014; Swaim et al., 2020; Askenase, 2021, 2022). EV-associated receptors not only influence which cells receive particular subsets of EVs, but may also act as

decoys, as observed in the case of circulating EVs carrying the severe acute respiratory syndrome coronavirus-2 (SARS-CoV-2) ACE2 receptor on their surface, thereby decreasing the amount of virus able to infect target cells (El-Shennawy et al., 2022). This has led to the development of ACE2+ EVs and nanoparticles as potential therapeutics for SARS-CoV-2 infection (Cocozza et al., 2020).

EVs not only target particular cell populations, but also protect cargo from degradative enzymes such as RNAses and proteinases found in the systemic circulation (plasma) and other biofluids (Shelke et al., 2014; Cvjetkovic et al., 2016; O'Brien et al., 2020). In addition, EVs must also protect their contents from chemically harsh conditions such as those found in the stomach which is highly acidic and contains potent digestive enzymes (Izumi et al., 2012; Benmoussa et al., 2016), hypoxic environments as observed in many tissues and tumor microenvironments, or hyperoxic environments observed in the upper airways or during neonatal development (Patton et al., 2020; Askenase, 2021). EVs can be taken up by recipient cells via a variety of mechanisms including phagocytosis, micropinocytosis, endocytosis by both clathrin-dependent and -independent pathways, as well as associations with lipid rafts (Mulcahy et al., 2014; Mathieu et al., 2019). Prostate cancer-derived EVs labeled with a thiol-reactive fluorophore accumulated within the lysosomes of HeLa cells and primary lung fibroblasts before delivering cargo (Roberts-Dalton et al., 2017). Another study showed that EV-localized nanoluciferase can be observed within the endosome of HeLa cells for many days while slowly being degraded or released, although this is likely cell type-dependent (O'Brien et al., 2022). Thus, in addition to protection against degradation in the extracellular milieu, EVs

(and their cargo) can also survive the acidic and proteolytic lysosomal milieu where they tend to accumulate after entering recipient cells.

Damage-associated molecular patterns (DAMPs) released from injured or dying cells signal for the recruitment of scavenger cells (Todkar et al., 2021). Apoptotic blebs from these cells concentrate a variety of DAMPs into a single payload and their abnormal clearance results in the maturation of dendritic cells (DCs) and generation of systemic autoimmunity (Jiao et al., 2021; Bao et al., 2022). However, just as EVs protect their cargo from degradation in the extracellular environment, EVs may also prevent typically immunogenic cargo from being recognized as a DAMP. One study described that oxidized mitochondrial proteins, which are normally perceived as DAMPs, were occluded from conventional DAMP-sensing when packaged into EVs, preventing the release of pro-inflammatory mediators such as IL-6 (Todkar et al., 2021). Functional mitochondria, or fractions thereof, may be packaged into EVs and transferred to recipient cells (Amari and Germain, 2021). Conventionally, dysfunctional or damaged mitochondria are known to be degraded through “mitophagy” (i.e., autophagy of mitochondria). Thus, formation of mitochondria-encapsulated EVs by mitocytosis appears to functionally overlap with mitophagy (Jiao et al., 2021; Bao et al., 2022).

Prior studies have uncovered links between EV formation (typically within multivesicular bodies for exosomes) and EV fate after uptake. Many EVs that are taken up by recipient cells pass through the phagolysosome where they are degraded (Vidal, 2019). The degraded products may still contain some functional molecules or promote metabolic adaptations in recipient cells, but in all likelihood only a few escaped EVs are able to deliver functional cargo. Consistently, modulation of autophagy enhances functional EV delivery. Bone marrow (BM)

mesenchymal stromal cells (MSC)-released EVs able to inhibit autophagy of recipient cells promoted delivery of packaged miRNA-144-3p to cardiomyocytes (Wang et al., 2022). Similarly, the inclusion of autophagy inhibitors resulted in enhanced EV delivery and increased the efficiency of CRISPR/Cas9 gene editing in recipient cells (Zhang et al., 2022).

Due to the ubiquitous nature of EVs, understanding the unique aspects of each cell type, both in regard to the quality of EVs produced and how those EVs are handled once received, is challenging. Scavenger cells, which by nature consume a lot of extracellular material including large numbers of EVs, may be uniquely poised to degrade EVs and adapt to their environment by interpreting the message(s) encoded by the biomolecules within them (Akbar et al., 2022). One of the main functions of autophagy is to remove and recycle organelles damaged by ROS (Zhou et al., 2022). PMNs have a very short lifespan with a half-life of a few hours to just a few days, perhaps in part because of their rapid and massive generation of ROS, which is partially mitigated by highly efficient autophagy (Skendros et al., 2018; Dong et al., 2021). In inflammatory conditions, this may allow PMNs to release pathological EVs that cause them to recruit additional scavenger cells and components of the immune response (Dalli et al., 2013; Headland et al., 2014; Lorincz et al., 2015; Genschmer et al., 2019; Forrest et al., 2022).

The repertoire of EVs released by a cell is incredibly diverse, reflecting its current state and exposure to stressors. Furthermore, the tissue EV population is reflective of the multiple cell types present of varying origin, which are, potentially, both releasing and taking up EVs at the same time. This leads to a complex and dynamic EV environment which will change due to fluctuations in cell density an, poise, tissue health, circadian rhythms and environmental factors (Mulcahy et al., 2014; Yanez-Mo et al., 2015; Danielson et al., 2016; Mathieu et al., 2019). In

addition, EVs may also be present from external sources such as ingested food. EVs from human breast milk colostrum and milk from other animals have garnered a lot of interest since they are present in large numbers and able to survive ingestion (Jiang et al., 2021).

The contents of EVs include proteins, both cytosolic and membrane-bound, lipids, and RNAs, including micro RNAs (miRNA), long noncoding RNAs (lncRNA), messenger RNAs (mRNA) and transfer RNA (tRNA), and a variety of other small non-coding RNAs (Mulcahy et al., 2014; Janas et al., 2015). The membrane of EVs contains transmembrane proteins such as MHC and tetraspanins at the cell surface, although their density/concentration differ (Anand et al., 2019). Whether EVs contain ribosomal RNA (rRNA) (Lazaro-Ibanez et al., 2017; Mateescu et al., 2017; Sork et al., 2018) and mitochondrial (mtDNA) or genomic DNA (gDNA) is uncertain (Guescini et al., 2010; Shurtleff et al., 2018; Vagner et al., 2018; Yokoi et al., 2019). This likely stems from the types of cells from which the EVs were isolated (cancerous or not), the type of EVs analyzed (larger microvesicles and cancer-related EVs tended to carry larger nucleic acids such as rRNA and mtDNA/gDNA), and the method used to isolate the EVs (buoyant density centrifugation which may remove extra-EV bound material including gDNA from necrosed cells).

EV CARGO

The mechanisms by which a cell inputs its cargo into the EV package are under intense study. It is likely that the loading of cargo into EVs is not a passive process, nor due solely to passive diffusion of cellular cytosolic and membrane components since enrichment based on particular nucleotides (Zhang et al., 2010; Mittelbrunn et al., 2011; Nolte-'t Hoen et al., 2012; Villarroya-Beltri et al., 2014; Gao et al., 2018; Perez-Boza et al., 2018) and amino acids (Ghosh et al., 2014; Villarroya-Beltri et al., 2014; Janas et al., 2015; Rosa-Fernandes et al., 2017;

Whitham et al., 2018) motifs is observed. In addition to active packaging of cargo into and onto EVs, there can also be cross-complementation of EVs with extracellular protein or RNAs as shown by free miRNA-150, potentially in complex with argonaute-2 (Ago2), associating with EVs from B1a cells, which were then targeted directly to effector T cells (Bryniarski et al., 2015).

It has been well demonstrated that proteins can be transferred from one cell to another by EVs, as exemplified by TLR4-knockout cells receiving TLR4 from DCs (Zhang et al., 2019b). In addition to protein, the horizontal transfer of RNA from one cell to another is likely one of the most important functions of EVs *in vivo,* but details as to how much RNA is needed, and how many EVs need to be taken up by a cell to then be unpackaged and deliver an effective concentration of their cargo remains poorly defined. As mentioned above, EVs contain a variety of RNAs including, but not limited to snRNA, snoRNA, piRNA, scRNA, Y-RNA, miRNAs, as well as fragmented and intact tRNAs, rRNAs, lncRNAs, and mRNAs. These RNAs can have many downstream functional implications in recipient cells (Turchinovich et al., 2019). For example, during immune synapse formation, when antigen on MHC-bearing cells such as DCs is presented to T cells, the transfer of miRNAs via EVs (from DCs to T cells) enhanced antigen presentation, T-cell receptor signaling, and function (Bolukbasi et al., 2012; Szostak et al., 2014; Temoche-Diaz et al., 2019). Engineered DC-derived EVs have also been shown to transfer therapeutic cargo including cytokines (Mittelbrunn et al., 2011; Montecalvo et al., 2012).

One of the earliest studies to show the transfer of mRNA via EVs was in 2007 wherein human mast cells incubated with EVs from mouse mast cells were able to synthesize murine-encoded proteins (Valadi et al., 2007). Another early study used endothelial cells that expressed GFP mRNA, but GFP protein was not yet at detectable levels, yet the transfer of EVs resulted in

the production of GFP protein in a naïve endothelial cell population (Deregibus et al., 2007). This study did not inhibit ribosome machinery using a drug such as cycloheximide in the producer cell population, but other studies went on to show that RNA can be synthesized in one cell followed by packaging into EV, and translated in another cell (O'Brien et al., 2020).

EV Carrier Effects

As argued above, EVs are a universal and evolutionally conserved cellular mechanism to maintain homeostasis and respond to stressors (Gill et al., 2018). As EVs have been observed to be released from virtually all cell across all kingdoms of life, some have suggested an early evolutionary origin for the generation of small particles (Woith et al., 2019). As part of the 'RNA world' hypothesis and its many iterations (Joyce, 2002; Szostak, 2012; Muller et al., 2022), EVs may have been selected due to the ability to protect their ribonucleotide contents from degradation in harsh and noxious conditions such as low pH and hypoxia present in the "primordial soup" **(Figure 1.2).** Furthermore, fusion of distinct vesicles to form more complex protocells is on path towards the biogenesis of the first unicellular organism (Imai et al., 2022). In this vein, Askenase makes a compelling argument that EVs allow for "carrier effects" which enhance the ability of EVs to protect and deliver their cargo to recipient cells (Askenase, 2021).

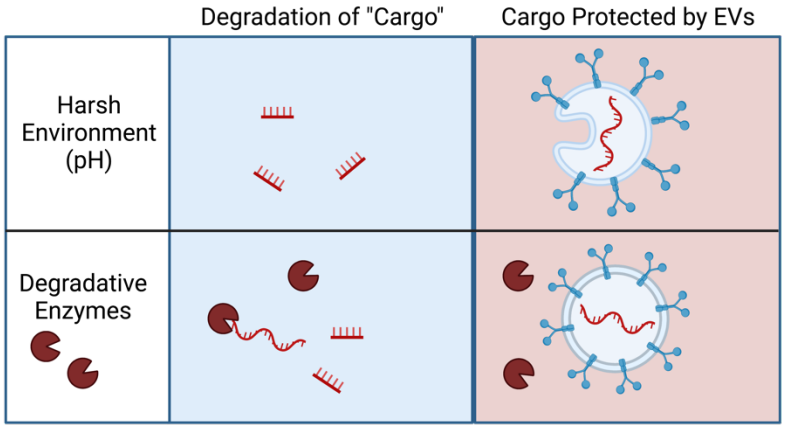

Figure 1.2. EVs protect cargo from degradation by harsh conditions such as pH or oxidative environments as well as from degradative enzymes such as RNAses and proteases. Top: RNA and protein released from cells or ingested food present in the stomach would get quickly degraded. However, RNAs and proteins encapsulated by EVs are stabilized and are less prone to degradation. The exact mechanisms of action are still not completely understood. Bottom: Circulating RNA and proteins in blood as well as other tissues may be degraded as a result of RNases and proteases. However, RNases and proteases may not cross the lipid bilayer membrane of EVs. Thus, molecules encapsulated by EVs are protected from enzymatic degradation.

One aspect of this is that the contents of an EV are at a greater effective concentration due to the potentially large number of RNA species contained within an individual EV of fairly low volume **(Figure 1.3)**. An EV with a 100 nm diameter has a volume of about 1e-18 L (or 1 attoliter). If only 1 RNA molecule is present, then it is at a concentration of approximately 1 µM. However, with millions of potential EV subsets there may be EVs which have 100 or 1,000 copies of a particular RNA resulting in an even greater concentration of cargo within the EVs (Askenase, 2021). Taking this a step further, based on Le Chatelier's principle and simple constant of dissociation (K_d) and Michaelis-Menten kinetics, estimates of association between RNA species, peptides or small molecule interactions within EVs should be quite strong as these theoretical molar concentrations allow for unusual RNA structures and activities to potentially be realized (Krishnan and Simmel, 2011; Wee et al., 2012; Chang et al., 2014; Briskin et al., 2020) and/or may increase the rate of a reaction.

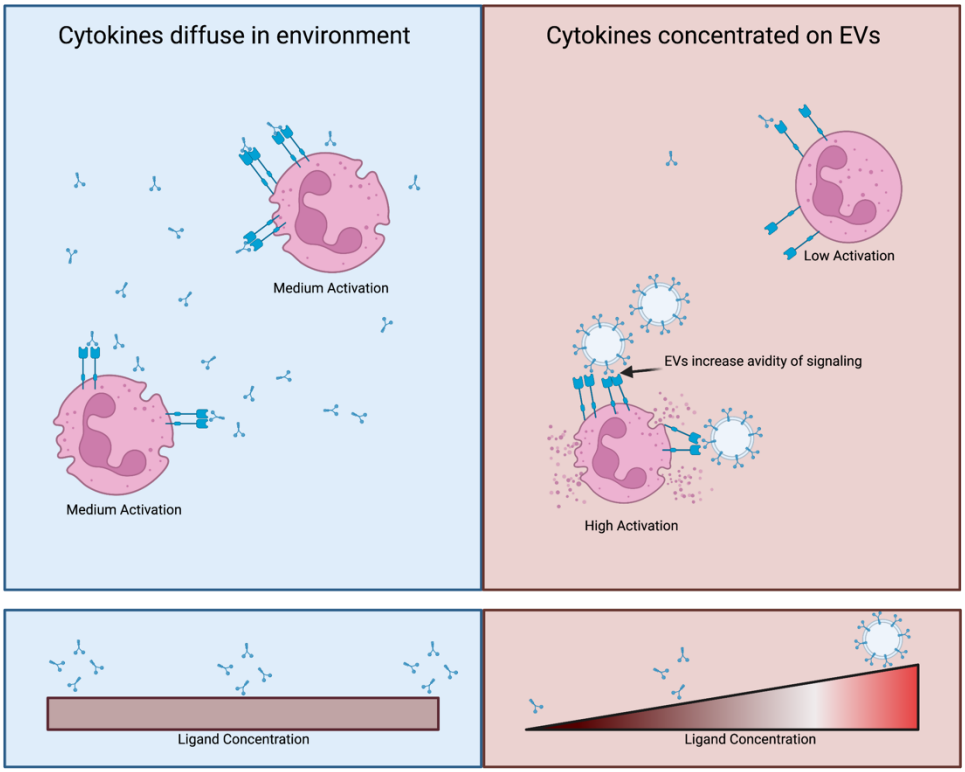

Figure 1.3. EVs Increase the effective concentration of ligands and EV cargo. Top: Soluble molecules, represented in light blue are homogenous in solution. Cells exposed to the soluble ligand are "activated" through receptor-ligand interactions. In this case, the magnitude of activation is deemed medium/intermediate. Ligands concentrated on the surface of an EV have a greater local concentration, thereby increasing the avidity of the receptor-ligand interaction, and thus have a higher degree of activation than the cells exposed to the same amount of soluble ligand. Since EVs increase the local concentration of a ligand, the non-local concentration of an EV-bound ligand will be lessened. Bottom: Assuming that ligands are no longer being produced or removed, soluble ligands are distributed evenly throughout the environment whereas EVs concentrate ligands resulting in a gradient.

There are differences in the RNA-binding properties and cleavage efficiencies of Ago2 complexed with miRNA/siRNA and a target mRNA among fly, mouse and human homologs (Wee et al., 2012). *Drosophila* Ago2 dissociates slowly from bound RNA, whereas murine and human homologs (which are 99% identical) dissociate rapidly and may not completely cleave their targets without assistance from other proteins. This observation led the authors to conclude that murine and human Ago2 are optimized for miRNA regulation and not RNA

interference, while Drosophila Ago2 uses the latter mechanism for antiviral immunity (Wee et al., 2012). However, owing to the hyper-concentration of contents within EVs, murine and human Ago2/RISC RNP complex may be more catalytically active on any RNA within the EV. EVs enclose their contents within a lipid bilayer, which protects the contents from degradation by RNAses and proteases (Skotland et al., 2020) **(Figure 1.2)**. Naturally, this also prevents the escape of intra-EV polar macromolecules by simple diffusion. Thus, there is a greater probability of effective reactions the longer EVs remain intact. This may lead to the presence of fragmented and smaller sized RNAs in EVs (Nolte-'t Hoen et al., 2012; Dellar et al., 2022).

Single RNA replicators have recently been demonstrated to be able to lead to the formation of a five-RNA replicator network when RNAs present at high concentrations are used (Mizuuchi et al., 2022), which has fueled the argument of a likely association between lipid-encapsulated RNA and the origin of cellular life in the pre-biotic soup (Czerniak and Saenz, 2022). As a practical consequence, when evaluating RNAs contained within EVs, one must not only uncover their primary sequence (including seed sequences of miRNAs), but also their arrangement in three-dimensional space in order to understand RNA binding and RNAzyme-like function (Eliscovich et al., 2017; Ganser et al., 2019).

EV Transfer Across Kingdoms

Cross-kingdom transfer of EVs is evidenced by the ability of EVs of ingested food products to affect immune development and gastrointestinal inflammation (Zhang et al., 2012; Benmoussa et al., 2017). EVs from plants can be detected in human breast milk, although it remains to be seen if such EVs carry specific effects on breastfed children (Lukasik et al., 2017). While it may appear that EV biogenesis pathways have been co-opted by viral particle synthesis pathways, it is also possible that viruses co-evolved with host mechanisms to generate EVs and

communicate between cells (Gould et al., 2003; Chahar et al., 2015; Gill and Forterre, 2015). Perhaps as a consequence of the same pathways being used for the synthesis of both EVs and viruses, the physical properties of many viruses and EVs including particle size, contents and mechanisms of release and uptake are broadly shared (Gould et al., 2003; Nolte-'t Hoen et al., 2016). The size range of EVs can be quite varied from 50 nm to perhaps 0.5-1 µm. However, many sources report a modal EV size between 90 and 150 nm in diameter, similar to that of many viruses including human immunodeficiency virus (HIV), influenza, SARS-CoV-2 and other coronaviruses, as well as Epstein-Barr virus (EBV) (Doyle and Wang, 2019; Parvez, 2020). Because of this similarity in size, many techniques developed to interrogate viral structure and function have been used for the study of EVs. These include nanoparticle tracking analysis (NTA), density-gradient centrifugation, and flow virometry/high resolution flow cytometry (Coumans et al., 2017). Nevertheless, viruses tend to be much better defined than EVs likely as a result of their historical importance for both the development of molecular biology techniques and public health.

Similar to an enveloped virus, the contents of an EV are surrounded by a lipid bilayer. Within this lipid membrane are also membrane proteins that could span the membrane, be anchored to the membrane, or simply associated with the membrane. Just as the receptor-binding domains influence which cells become infected by virus (Lakadamyali et al., 2004; Weston and Frieman, 2020; Nguyen et al., 2022), receptors and ligands on the surface of EVs may also determine which subsets of cells receive EVs thereby having targeted delivery of EV-cargo **(Figure 1.4).**

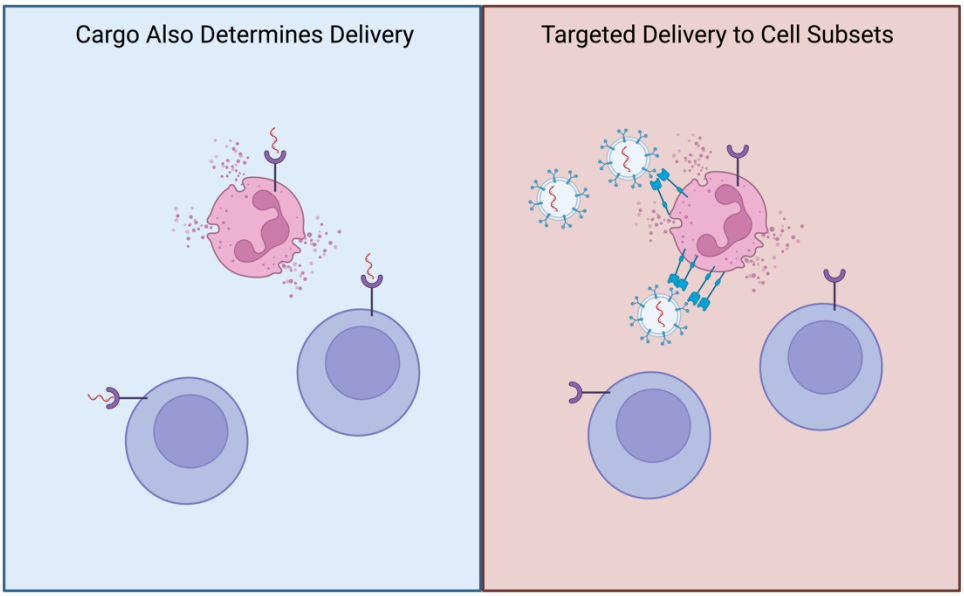

Figure 1.4. EVs have surface molecules which may bias which cells receive cargo. The molecule of interest in this case is depicted as RNA. Soluble RNA (left), not already degraded, is detected by pattern recognition receptors that in this case is present on both neutrophils (pink) and monocytes (blue). RNA encapsulated in an EV (right) is occluded from sensing by pattern recognition receptors. In addition, the ligands and receptors on the surface of the EV bias which cells receive the RNA. In this case, neutrophils have the proper receptor and thus receive more RNA cargo than the monocytes.

In addition to the canonical viral proteins, and viral genome, virions of several influenza viruses including A/WSN/33, A/PR/8/1934, and B/Brisbane/60/2008 grown in MDCK or chicken eggs contains host proteins such as ACTB, ANXA2, GAPDH, RPS2, ALDOA, EIF4A1. It was noted that many of the host proteins found associated with influenza virions were similar to that of EVs and that EVs and influenza virions were of a similar size, suggesting that influenza buds from a cell in a manner similar to EVs (Hutchinson et al., 2014). The notion that many viruses hijack cellular pathways essential to the biogenesis of EVs (both exosomes and microvesicles) to enhance formation and release of virions post-infection is termed the “Trojan Exosome Hypothesis.” (Gould et al., 2003). The genomes of viruses typically encode only those parts absolutely necessary for formation of infective virions that are not already furnished by the

host as well as accessory factors to evade or subvert the immune response. Thus, the relative simplicity of viral genomes may be partly enabled by the hijacking of cellular machinery for synthesis of virions.

The host protein Tsg101 is highly enriched in EVs and has been implicated in EV formation (Nabhan et al., 2012). It was found that HIV-1 Gag and Ebola virus matrix (EbVp40) interaction with Tsg101 is needed for viral budding (Garrus et al., 2001; Martin-Serrano et al., 2001). Since HIV and Ebola virus are evolutionarily distant, their shared interaction with the same host protein (here Tsg101) is likely a result of convergent evolution. In line with this reasoning, the myelin and lymphocyte (MAL) protein has been implicated in promoting vesicle trafficking to the plasma membrane via interactions with membrane rearrangement proteins such as synaptophysins, synaptogyrins, and occludins (Sanchez-Pulido et al., 2002). MAL is observed in highly ordered lipid domains and thus may also be involved in EV biogenesis, as well as viral budding (Gamage and Fraser, 2021; Rubio-Ramos et al., 2021). The conserved C-terminus of MAL promotes IAV HA to the apical surface (Puertollano et al., 2001). In addition, HIV-1 Nef changed the contents of EVs and released by infected T cells via interactions with MAL (Ventimiglia et al., 2015). The cooptation of MAL by HIV proteins in infected T cells may also impact T-cell receptor (TCR) signaling by reducing the recruitment of the TCR-associated kinase Lck and downstream *IL-2* transcription (Antón et al., 2008). The EBV protein BGLF2 intercalates between the envelope and nucleocapsid of the virion and was also observed to be packaged within exosomes, which repressed IFNα-induced phosphorylation of the signal transducer and activator of transcription (STAT) 3 and downstream innate immune signaling, thereby enhancing infectivity of EBV (Sato et al., 2022). Further, EBV and other herpesviruses

complete virion formation in proximity to the Golgi bodies and by interaction with exosome markers Rab11, Rab27a and CD63 (Nanbo et al., 2018).

Occurring in a space between viruses (typically assumed to be exogenous to the host) and EVs, are the endogenous retroviruses (ERVs), remnants of ancient infections that became stably integrated into the host genome. Amazingly, up to 8% of the human genome is made up of ERV-associated sequences with many duplication events and with the potential to still give rise to infectious units (Belshaw et al., 2004). Human endogenous retroviruses (HERVs) have been implicated in key physiological processes (e.g., placentation in mammals), as well as several diseases and immune reactions (Garcia-Montojo et al., 2018; Kuriyama et al., 2021; Rookhuizen et al., 2021; Temerozo et al., 2022), and have also been associated with EVs (Ferrari et al., 2019; Morozov and Morozov, 2021; Taylor et al., 2022).

Viruses show enormous diversity, yet their genomes end up encoding very similar functions including specialized polymerases, structural proteins, and mechanisms to evade the host immune response. Even amongst highly pleiomorphic viruses, such as influenza, there is a high degree of structural ubiquity, with most virions being around the same size (Kramberger et al., 2012) and containing the same number of structural proteins. Although it is difficult to physically separate purified exosomes from microparticles, it is clear that EVs do not have the same degree of structural uniformity as viruses (Tkach et al., 2018; Verweij et al., 2021).

Viruses serve as an extreme example of cargo sorting, with most virions including the same quantity of proteins. The efficient and specific cargo sorting of viruses is not limited to only proteins. Most virions typically only include a single genome (whether segmented or nonsegmented), suggesting a very specific sorting process for nucleic acids, as well. It was

reasoned that since the HIV genome (9.8 kb) can be packaged into a virion the size of an EV (~100 nm) about 500 copies of a miRNA should also be able to fit into a similarly sized particle (Zubarev et al., 2021). This is likely not even the maximum space that can be occupied within an approximately 100 nm diameter particle since the genome of SARS-CoV-2 is 30 kb. It is likely that as engineering of specific cargo into EVs improves, the observed cargo sorting efficiency of viruses, both for RNAs and proteins, will serve as a theoretical upper limit of what can be achieved artificially. However, the formation of HIV virions requires the packaging of only one genome whereas the packaging of miRNAs would actually be a 500-molar increase considering the number of transcripts to "drag" into a particle as it is formed. In addition, although viruses may be pleomorphic, their structure is much more ordered than that of EVs, which likely results in more orderly recruitment of cargo. It can therefore be inferred that the RNA contents of an EV result from active cargo sorting rather than only passive diffusion close to the membrane surface and/or spatial constraints. Consistently, the RNA and protein cargo of EVs show enrichment of nucleotide and amino acid motifs (Zhang et al., 2010; Mittelbrunn et al., 2011; Nolte-'t Hoen et al., 2012; Ghosh et al., 2014; Villarroya-Beltri et al., 2014; Janas et al., 2015; Rosa-Fernandes et al., 2017; Gao et al., 2018; Perez-Boza et al., 2018; Whitham et al., 2018).

RNA Sorting

Complexes of ribonucleoproteins (RNP) are formed through the interactions of RNA with RNA-binding domains (RBD)[1] of RNA-binding proteins (RBP) and are important for the cytosolic

[1] The acronym RBD sometimes refers to the receptor-binding domain on the surface proteins of viruses. The distinction will be made as needed. In particular, in the SARS-CoV-2 and monocyte chapter **(See Chapter 5)**, RBD refers to receptor binding domain of the SARS-CoV-2 Spike glycoprotein, which binds the ACE2 host cell surface receptor.

transfer and control of RNAs leaving the nucleus to the ribosome (Kohler and Hurt, 2007)[2]. RNP complexes are observed within EVs (Kossinova et al., 2017; Sork et al., 2018; Statello et al., 2018; Fabbiano et al., 2020). Whether this is due to sorting of RBP cargo to the EV bringing bound RNA with it, or RNA first being sorted to an EV and RBPs being bound to recruit or stabilize the RNP complex in a second phase is unclear. Likely, it is a mix of both scenarios.

There also appears to be a role for liquid-liquid phase condensates (LLPCs) in determining the cargo of EVs. For example, the RNP YBX1 (also referred to as YB-1) promotes loading of miRNA-223 into exosomes (Liu et al., 2021). The secondary structure of miRNA-223 RNA is key to recruiting YBX1 to EVs (Shurtleff et al., 2016; Shurtleff et al., 2017). YBX1 recognizes a variety of motifs depending upon its binding partners, as well as 5-methylcytosine modified nucleotides in some instances (Ray et al., 2009; Yanshina et al., 2018; Chen et al., 2019), and thus may control the sorting and stability of a wide variety of RNAs. For example, YBX1 in complex with IGF2BP-1, HNRNPU, SYNCRIP, and DHX9 stabilized *c-myc* mRNA (Weidensdorfer et al., 2009). Although it has not been formally shown that this specific RNA motif and complex is relevant for loading into EVs, each of these proteins and *c-myc* mRNA are highly abundant in EVs from a variety of cell types (Hong et al., 2009; Buschow et al., 2010; Skogberg et al., 2013; Hurwitz et al., 2016; Kowal et al., 2016; Choi et al., 2018; Spiniello et al., 2019). The transfer of YBX1 via EVs can have profound effects on recipient cells since it affects the regulation of key genes involved in DNA repair and antigen presentation at the DNA level,

[2] The *intracellular* complex of proteins and RNAs within a lipid vesicle transported from the nucleus to the cytosol is also called an *exosome* or *RNA exosome* (Kohler and Hurt, 2007). Confusingly, these are distinct entities from the exosomes that are found within multivesicular bodies that fuse to the plasma membrane upon release from cells (Cocucci and Meldolesi, 2015). RNA exosomes are not the subject of this review, nor mentioned elsewhere.

as well as RNA stability, packaging, and splicing (Prabhu et al., 2015; Suresh et al., 2018; Mordovkina et al., 2020). YBX1 is a known interactor of Ago2 (Hock et al., 2007; Liu et al., 2021), and thus may also affect processing and Ago2-dependent regulation and silencing of gene expression by miRNAs and siRNAs (Muller et al., 2019). Furthermore, there are many post-translational modifications (PTMs) that can regulate the activity and localization of YBX1 including ubiquitination, acetylation, methylation, and phosphorylation. These post-translation modifications are also relevant for the formation of LLPCs in general (Owen and Shewmaker, 2019). Notably, phosphorylation of YBX1 regulates its loading into EVs (Kossinova et al., 2017), although the relevance of this to LLPCs is unknown. The structure of RNAs outside of the primary sequence is also important in determining the characteristics of LLPCs (Alberti and Hyman, 2021; Tejedor et al., 2021). In line with these observations, the biophysics of EV formation must be studied further, in addition to and beyond the characterization of lipid membranes (Nicolson and Ferreira de Mattos, 2021).

Other RNA motifs and RBPs have also been observed to aid in the packaging of RNA cargo into EVs. For example, miRNA in B cells were found to have post-transcriptional addition of polyadenosines to the 3’ end of the transcripts whereas miRNAs in EVs had 3’ polyuridines (Koppers-Lalic et al., 2014). The heterogenous nuclear RBP A2B1 binds the EXOmotif 5’-GGAG-3’ in miRNAs and its subsequent SUMOylation promotes the packaging of bound miRNAs into EVs (Villarroya-Beltri et al., 2013). The motif 5’-CUGCC-3’ was found in the 3’UTR of mRNAs (Bolukbasi et al., 2012) and another group used untargeted RNA-seq to validate the heterogenous nuclear RBP A2B1 EXOmotif and YBX1 motifs in addition to sequences that had not been described before (Perez-Boza et al., 2018).

One approach to loading custom RNA into an EV is to include these RNA loading motifs in a minimally functional part of the RNA such as the 3'UTR of mRNAs or the non-seed region of miRNAs. In addition, generation of RBPs with RBDs that can bind novel sequences of RNA or are permissive to PTMs that promote EV loading may also allow for loading of custom RNA (Fukunaga and Yokobayashi, 2022). It has been speculated that exosomes are better than microvesicles at transferring miRNA contents to recipient cells due to the larger number of documented cases (Askenase, 2021). However, due to the massive variety of cells types used in EV studies as well as changing nomenclature or incorrect nomenclature of EV subsets (Thery et al., 2018), this claim is suspect and must likely be studied on a cell-by-cell basis (for producer and recipient cells) and for individual miRNAs.

Taken together, the contents of EVs are able to impact recipient cells as a result of EV-carrier effects. After ingestion, release by host cells, or injection, EVs containing concentrated biomolecules are able to survive the stomach and circulation (Nasiri Kenari et al., 2020), then mediate their uptake into particular populations of cells, survive the phagolysosome (O'Brien et al., 2018), potentially get repackaged within another population of EVs for retargeting to cells and tissues (Turchinovich et al., 2019), and then deliver their contents to an effector cell population (Valadi et al., 2007), which are often scavenger cells. As our understanding of the mechanisms regulating cargo sorting and offloading improves, we can harness these pathways to load custom cargo into EVs derived from cultured cells made to express a transgene or other product (Deregibus et al., 2007). Ironically, scientists have spent decades formulating lipid nanoparticles and viral vectors to great success, yet "Nature" already has a comparable and perhaps superior system of delivering material via EVs (Witwer and Wolfram, 2021).

EV ANALYSIS BY FLOW CYTOMETRY

Comparison with other methods

In order to investigate the role of EVs, it is first necessary to understand the current methods to analyze them and their contents. Common methods for EV analysis have been reviewed elsewhere (Hartjes et al., 2019), including western blot/ELISA, NTA, dynamic light scattering (DLS), asymmetrical flow field flow fractionation (aF4), and single particle interferometric reflectance imaging sensing (SP-IRIS) (Thery et al., 2018). This section will focus on flow cytometry, which can multiplex targeting of biomarkers and gate on subpopulations unlike the above methods, with the exception of SP-IRIS, which is a promising, but fledgling, technology and does not have the throughput of flow cytometry (Daaboul et al., 2016; Sevenler et al., 2018; Bachurski et al., 2019) **(Table 1.1)**. There are various terms for the flow cytometric analysis of single particles including nanoflow cytometry, high-sensitivity flow cytometry, high-resolution flow cytometry, and flow virometry (Lippe, 2018). With the exception of flow virometry, which is the flow cytometry of virions, these terms are fairly interchangeable in the literature. In this work, the term nanoflow cytometry will be used.

Single particle analysis of EVs by nanoflow cytometry is quite difficult due to the small size and subsequent small density of the target molecules. A prior study estimated that an ~8 µm monocyte bears ~110,000 molecules of CD14, a high abundance marker, on its surface (Nolan, 2015). Assuming that a monocyte is spherical and scaling the antigen density based on the surface area, an EV that is 100 nm in diameter is expected to have ~17 molecules of CD14 on its surface. For a lower abundance molecule such as CD16 with ~10,000 molecules on a monocyte and ~1.5 molecule on an EV, detection of the latter is understandably arduous. While there are approaches to modify the fluidics and settings of flow cytometers in order to amplify

signals from single EVs (Bari et al., 2021; Bordanaba-Florit et al., 2021; Gao et al., 2021; Silva et al., 2021; Verweij et al., 2021; Xu et al., 2021), these are pushing against the physical limits of this technology and are not necessarily applicable to every platform (Stoner et al., 2016; Nolan and Duggan, 2018; Brittain et al., 2019; Brittain et al., 2021; van der Pol et al., 2021). In practice, single EV analysis by nanoflow cytometry is a laborious technique for which the benefits must be weighed against the cost of reagents and time to conduct the experiment.

Method	Use	Pros	Cons	References
Nanoparticle Tracking Analysis (NTA)	Concentration, Size	Observe particle diffusion directly	Narrow range of effective sizes (~80-200 nm dimeter), fluorescence is not sensitive, sensitive to protein aggregate contamination	(Szatanek et al., 2017; Hou et al., 2018; Bachurski et al., 2019; Droste et al., 2021; Yahata et al., 2021)
Dynamic Light Scattering (DLS)	Concentration, Size	Fast, broader range of particle resolution compared to NTA	Assumes homogenous particle distribution	(Szatanek et al., 2017; Hou et al., 2018; Bachurski et al., 2019; Yahata et al., 2021)
Single Particle Interferometric Reflectance Imaging Sensing (SP-IRIS)	Surface protein content and other contents	multiplexed determination of surface protein markers	Laborious, low throughput	(Daaboul et al., 2016; Sevenler et al., 2018; Bachurski et al., 2019).
Asymmetrical Field Flow Fractionation (AF4)	Purification, Density determination	Gentle method for purifying EVs	Low throughput, loss of EVs, protocol development can be time-consuming	(Zhang et al., 2018; Zhang et al., 2019; Zhang et al., 2021)
Bead-based Flow Cytometry	Surface protein content and other contents	Aggregation of signal allows for detection of potentially rare targets	Population-based analysis, lose information about EV heterogeneity	(Morales-Kastresana and Jones, 2017)
Nanoflow Cytometry	Surface protein content and other contents, count, sizing	Single-EV analysis with multiplexed surface protein markers at once.	Laborious, sensitive to debris	(Nolan, 2015; Morales-Kastresana and Jones, 2017; Libregts et al., 2018; Nolan and Duggan, 2018; Droste et al., 2021)
Density-Gradient Ultracentrifugation	Purification	Highly pure population of EVs	Low throughput, loss of EVs	(Chhoy et al., 2021; Crescitelli et al., 2021)
Mass spectrometry-based proteomics	Protein content	Highly sensitive	Requires large amount of sample input, requires specialized analysis	(Rosa-Fernandes et al., 2017; Askeland et al., 2020)
Electron Microscopy	EV morphology, count, sizing	Highly sensitive, morphology of EV and view internal contents of EV	Laborious, low throughput	(Rikkert et al., 2019; Reclusa et al., 2020)

Table 1.1: Summary of some standard techniques to interrogate EVs with general pros and cons. This is not an exhaustive list of techniques, and the associated references are only introductions to the theory and/or application of the method for the study of EVs.

Population-based Analysis

One method to get around the low antigen density of EVs is to aggregate multiple EVs onto a larger particle (usually 4 µm or greater in diameter) either by using latex beads which bind lipids via hydrophobic interactions or by tethering an antibody to beads and performing immunoprecipitation followed by counterstaining with an antibody of interest (Nakai et al., 2016; Morales-Kastresana and Jones, 2017; Suarez et al., 2017; Wiklander et al., 2018) **(Table 1.2)**. In our own experimental work (Dobosh, unpublished), we calculated that one bead of ~9 µm diameter coated with a certain amount of streptavidin can bind ~3,000 PMN-derived (CD66b+) sputum EVs from patients with cystic fibrosis (CF). Taking the above calculation (Nolan, 2015) this amounts to ~17 molecules *3000 EVs = 51,000 molecules of CD66b available for binding. Applying some rough sphere packing calculations and estimating steric hindrance for fluorescent antibody binding between an EV and the bead (Campos-Silva et al., 2019), reduces this number by about 30% resulting in ~35,700 molecules to detect for highly abundant antigens. This will release sufficient signal on a flow cytometer and allows for population-based analysis of EVs in a fluid. It should be remembered though, that this number, and therefore the feasibility of detection, will depend on both the density of a given marker on a given subpopulation of EVs and the abundance of EVs that contain the marker in the biofluid of interest.

Problem	Reason for the Problem	Potential Solutions	Potential Disadvantages
Low Antigen Density	Low numbers of surface proteins and contained molecules in EVs due to their size	• Increase staining index of the antibody • Aggregate EVs on a bead	• Increasing the staining index may affect binding affinity of the antibody for the antigen • Bead pulldowns lose information about single EV parameters
Coincident Events (Swarming)	EVs are dramatically smaller than the width of the laser and thus multiple EVs may pass in front of the laser at the same time	• Have the flow rate as slow as possible • Titrate the sample until the event rate decreases linearly with the dilution factor and the median fluorescence intensity remains constant • Split sample equally into two tubes and stain with two antibodies of dyes of different fluorochromes then mix the samples back together and titrate until double positive events no longer occur	• Titrations dramatically increases the number of samples to be run and can be time consuming • The titrations must be analyzed before a suitable concentration is determined thus increasing the number of sessions on the flow cytometer • The two dyes or conjugated fluorochromes must have similar staining efficiencies and targets
Low Scatter	Mie Theory describes that FSC decreases faster than SSC as particle size becomes smaller than the wavelength of light being used. SSC still decreases thus using the violet laser (405 nm) rather than the blue laser (488 nm) is advantageous	• Lower the trigger threshold • Trigger off of the SSC or V-SSC channel or a fluorescence channel	• Lowering the trigger threshold increases the amount of noise being recorded as events • Not all flow cytometers are equipped with V-SSC capabilities • Fluorescent triggers remove most issues with instrument-intrinsic noise, but now require the antigen to be present for an EV to be analyzed

Table 1.2: Common Problems with nanoflow Cytometry and potential Solutions. Abbreviations: Side Scatter (SSC; assumed to be from the blue laser); Violet SSC (V-SSC); Forward Scatter (FSC; assumed to be from the blue laser). Most of the issues with nanoflow cytometry are due to the small size of the EV. As the typical experimenter cannot make hardware changes to the flow cytometer such as decreasing the width of the laser, installing more powerful lasers, or further decreasing the sheath flow rate the potential solutions presented here focus on how to prepare the sample as well as changes that can be made at the level of acquisition.

Bead-based pulldown (hereafter referred to as immunoprecipitation since latex beads are not as specific as antibody-based methods) is a powerful technique to isolate particular populations of EVs. For example, a bead coated in streptavidin is quite versatile since the antibody used for immunoprecipitation only has to be biotinylated, a process for which there are many kits and protocols available (Mao, 2010). Immunoprecipitation is also convenient to analyze subpopulations of EVs, such as those that are only PMN-derived (CD66b+), epithelial-derived (CD326+), or perhaps have effector molecules such as neutrophil elastase (NE), myeloperoxidase (MPO), or PD-L1 on their surface. Once a purified population of EVs is immunoprecipitated, RNA, proteins, or lipids can be extracted from them for transcriptomic, proteomic, or lipidomic analysis, respectively. It should be noted that once immunoprecipitated it is quite difficult to remove the EVs from the antibody for downstream functional experiments without destroying their integrity using denaturants such as urea or high salt buffers. Alternatively, a recombinant antibody or antigen may be used to outcompete antibody:EV binding, but this approach is not always successful. Examples of successful elution do exist, however. The protein Tim-4 bound to beads pulls down EVs expressing phosphatidylserine on the outer leaflet of the membrane. Since Tim-4 binding to phosphatidylserine is Ca^{2+}-dependent, adding a chelator such as EDTA can gently elute off EVs for downstream functional analysis without compromising their integrity (Nakai et al., 2016). We developed a similar method using Annexin V (Dobosh, unpublished), which exhibits reversible binding to phosphatidylserine based on the presence of Ca^{2+} ions in the medium. In addition to antibody staining, EVs can also be probed with cell-permeable, cleavage-sensitive dyes (Gray et al., 2015;

de Rond et al., 2018b), or stained for total RNA or specific RNA species using molecular beacons (Mateescu et al., 2017; Rhee and Jeong, 2017; Balducci et al., 2019).

While population-based analysis of EVs may answer many questions and begin to probe the diversity of EVs, it falls short when investigating variations in the density of a marker among individual EVs. Owing to the variety in EV morphology, contents and density it is likely that no two EVs are completely identical, resulting in potentially millions of different EV subsets (Gyorgy et al., 2011; Cocucci and Meldolesi, 2015; Tkach et al., 2018; Zhang et al., 2018; Zhang et al., 2019a; Askenase, 2021). Such a massive variety is also observed among EVs ingested from milk or plant-based products (Zhang et al., 2012; Benmoussa et al., 2017).

Coincident Events

In addition to the low antigen density on the surface of EVs, nanoflow cytometry is complicated by the fact that the typical laser beam width on a cytometer is approximately 5 µm in diameter, yet the size of the typical EV in our system is ~0.1 µm (Welsh et al., 2017). Thus, high scatter and fluorescence signals may result from EVs that are physically aggregated, are unbound but happen to be in the laser path coincidentally, or from a single large particle. This phenomenon is typically referred to as a *coincident event* or *swarming*[3]. In cell-based digital flow cytometry this conundrum is resolved by a *doublet* gate, i.e., typically by visualizing a given parameter's area against its height. This is made possible because cells passing in front of the laser are larger than or close to the width of the beam. Since this is not true for EVs, such doublet gates are not possible. Therefore, to ensure that only single EVs or physical aggregates

[3] Since swarming can also refer to the process of cellular transmigration, which will be discussed in other chapters, we will use *coincident event* in reference to multiple particles being detected as a single instance. However, although there is not a consensus, *swarming* appears to be the preferred term for this problem in the flow cytometry community.

of EVs, but not coinciding events, are being analyzed, samples should be serially diluted until the event rate decreases linearly with the dilution factor and the fluorescence of each marker remains constant (Libregts et al., 2018). An alternative method, inspired by flow virometry (Arakelyan et al., 2013; Arakelyan et al., 2015; Arakelyan et al., 2017) consists in splitting a population of EVs into tubes and staining each with two differently colored dyes or antibodies, followed by washing and remixing. The flow rate at which double positive events no longer appear allows for the analysis of single particles. However, one must ensure that both dyes/antibodies stain both particles with similar efficiency (de Rond et al., 2018b; Melling et al., 2022) **(Table 1.2)**.

Optics and Hardware

Mie theory describes the relationship between the wavelength of a laser hitting a particle of a particular size and the amount of scattered light at any angle (de Rond et al., 2018a; McVey et al., 2018). For particles smaller than the wavelength of light being used this relationship is important to get the most signal possible from a sample. Mie theory states that as the particle size gets smaller the amount of scattered light dramatically decreases, particularly in the forward scatter (FSC)/180˚ direction. In fact, using FSC at the sizes of an EV has very little relevance, while SSC decreases less dramatically. Thus, using the smallest wavelength possible is best for detecting EVs. This is typically achieved with SSC off of the 405 nm violet on most flow cytometers, noting that more advanced systems may include a better 350-355 nm or even better 320 nm ultraviolet laser. Switching from the conventional 488 nm blue laser to the 405 nm violet laser for SSC measurement makes an appreciable difference in the quality of EV-generated events detected (McVey et al., 2018). In addition, capturing the side-scattered violet light requires a special detector making optimal nanoflow analysis of EVs

less accessible (Nolan, 2015; Stoner et al.; de Rond et al.; McVey et al., 2018; Nolan and Duggan; Chiang and Chen, 2019). Additional hardware modifications to improve the amount of scattered light include increasing laser power and narrowing the diameter of the laser beam.

In flow cytometers, avalanche photodiodes or photomultiplier tubes are firing electrons as photons from the laser hit the detectors. This generates a constant stream of electrical information (called "events") that the hardware detects even when no particle is present in front of the laser. This electrical noise may in some part be due to debris present within the fluidics system, but may also derive from the natural physical state of the lasers and detectors. Yet, most of the time this noise is not visualized on the computer interface. At the software level, an event must have a particular magnitude for at least one parameter to be recorded as a real event and show up on the screen. This value, for which a particular event must be greater than, is called the trigger threshold. On a conventional flow cytometer, the trigger threshold is typically at least 20,000 on FSC-H. However, due to the weak FSC signal from small particles this is not an appropriate trigger for nanoflow cytometry. Thus, many groups will trigger off the violet SSC and/or a fluorescent channel (van der Vlist et al.; Pospichalova et al.; Arraud et al.; Groot Kormelink et al.; Mateescu et al., 2017; Morales-Kastresana and Jones, 2017). Using fluorescence-based triggers removes much of the noise related to scatter-based measurements and improves machine sensitivity since background debris and spontaneous detector firing generate little autofluorescence **(Table 1.2)**.

Since EVs have such weak scatter properties it would be ideal to have the brightest fluorochromes available. In addition to detecting all EVs this fluorochrome would have to be conjugated to an antibody or molecule that would specifically recognize all EVs. Unfortunately,

there is no pan-EV marker. For some time, CD63 and phosphatidylserine were considered as such, but this proved to be a false assumption (Yanez-Mo et al., 2015; Thery et al., 2018). To date, various markers and dyes are used by research groups in the field to detect EVs. In our group, specific interests in EVs from CF sputum, bronchoalveolar lavage fluid (BAL) (ex vivo), and conditioned media from human leukocyte trans-epithelial migration setups (in vitro) led us to select a mixture of Di-8-ANEPPS and calcein-based dyes (Stoner et al., 2016; Welsh et al.; de Rond et al., 2018b). Di-8-ANEPPS is a voltage-sensitive membrane dye that is nonfluorescent in solution and becomes fluorescent when bound to phospholipid membranes and proteins. Calcein-based dyes are membrane-permeable, but when cleaved by an esterase that *may* be present inside EVs become fluorescent and are retained inside the particle. These dyes tend to be bright, which is beneficial for fluorescence-based triggering of EV detection. In addition, for antibody-based detection of EV-associated markers, the brightest fluorochromes such as PE, APC and Brilliant Violet dyes (BD Biosciences) perform quite well. PE and APC should be used with caution however as they are large proteins potentially leading to steric hindrance of antibody (~10 nm in length on its longest axis) binding to EVs (~100 nm in diameter). Due to these size constraints, it has been postulated that only up to ~2-3 surface markers can be analyzed via antibody binding on single EVs. Lastly, many pre-conjugated antibodies come with a staining index of 1 or 2 (1-2 fluorochromes/antibody). While this is adequate for cells, and some EV markers, increasing the staining index (up to 5 or even 10 fluorochromes/antibody) will yield better signal. However, fluorochrome binding close to the Fab region of the antibody may compromise its binding capacity. Thus, increasing the staining index is a strategy that requires validation on an antibody-by-antibody (and lot-to-lot) basis.

Imaging flow cytometry may be an alternative method to the use of conventional flow cytometers for the study of EVs (Elborn, 2016; Margaroli and Tirouvanziam, 2016; Farrell et al., 2018). Once improvements to staining methods and flow cytometry hardware are made, advanced study of numerous subpopulations of EVs may be possible. Indeed, some have already begun to use spanning-tree progression analysis of density-normalized events (SPADE) to better understand the many populations of EVs present in biological fluids (Margaroli and Tirouvanziam, 2016; Chalmers et al.; Gramegna et al.; Dittrich et al.; Margaroli et al., 2019).

REFERENCES

1. Akbar, N., Braithwaite, A.T., Corr, E.M., Koelwyn, G.J., van Solingen, C., Cochain, C., Saliba, A.E., Corbin, A., Pezzolla, D., Moller Jorgensen, M.*, et al.* (2022). Rapid Neutrophil Mobilisation by VCAM-1+ Endothelial Extracellular Vesicles. Cardiovasc Res. 10.1093/cvr/cvac012.
2. Al Faruque, H., Choi, E.S., Kim, J.H., and Kim, E. (2022). Enhanced Effect of Autologous EVs Delivering Paclitaxel in Pancreatic Cancer. J Control Release *347*, 330-346. 10.1016/j.jconrel.2022.05.012.
3. Alberti, S., and Hyman, A.A. (2021). Biomolecular Condensates at the Nexus of Cellular Stress, Protein Aggregation Disease and Ageing. Nat Rev Mol Cell Biol *22*, 196-213. 10.1038/s41580-020-00326-6.
4. Amari, L., and Germain, M. (2021). Mitochondrial Extracellular Vesicles - Origins and Roles. Front Mol Neurosci *14*, 767219. 10.3389/fnmol.2021.767219. PMC8572053
5. Anand, S., Samuel, M., Kumar, S., and Mathivanan, S. (2019). Ticket to a Bubble Ride: Cargo Sorting into Exosomes and Extracellular Vesicles. Biochim Biophys Acta Proteins Proteom *1867*, 140203. 10.1016/j.bbapap.2019.02.005.
6. Antón , O., Batista , A., Millán , J., Andrés-Delgado , L., Puertollano , R., Correas , I., and Alonso , M.A. (2008). An Essential Role for the MAL Protein in Targeting Lck to the Plasma Membrane of Human T Lymphocytes. Journal of Experimental Medicine *205*, 3201-3213. 10.1084/jem.20080552.
7. Arakelyan, A., Fitzgerald, W., King, D.F., Rogers, P., Cheeseman, H.M., Grivel, J.C., Shattock, R.J., and Margolis, L. (2017). Flow Virometry Analysis of Envelope Glycoprotein Conformations on Individual HIV Virions. Sci Rep *7*, 948. 10.1038/s41598-017-00935-w. PMC5430429
8. Arakelyan, A., Fitzgerald, W., Margolis, L., and Grivel, J.C. (2013). Nanoparticle-Based Flow Virometry for the Analysis of Individual Virions. J Clin Invest *123*, 3716-3727. 10.1172/JCI67042. PMC3754246
9. Arakelyan, A., Ivanova, O., Vasilieva, E., Grivel, J.C., and Margolis, L. (2015). Antigenic Composition of Single Nano-Sized Extracellular Blood Vesicles. Nanomedicine *11*, 489-498. 10.1016/j.nano.2014.09.020. PMC5812487
10. Arraud, N., Gounou, C., Turpin, D., and Brisson, A.R. (2016). Fluorescence Triggering: A General Strategy for Enumerating and Phenotyping Extracellular Vesicles by Flow Cytometry. Cytometry A *89*, 184-195. 10.1002/cyto.a.22669.
11. Askenase, P.W. (2021). Exosomes Provide Unappreciated Carrier Effects That Assist Transfers of Their miRNAs to Targeted Cells; I. They Are 'the Elephant in the Room'. RNA Biol *18*, 2038-2053. 10.1080/15476286.2021.1885189. PMC8582996
12. Askenase, P.W. (2022). Exosome Carrier Effects; Resistance to Digestion in Phagolysosomes May Assist Transfers to Targeted Cells; II Transfers of miRNAs Are Better Analyzed Via Systems Approach as They Do Not Fit Conventional Reductionist Stoichiometric Concepts. Int J Mol Sci *23*. 10.3390/ijms23116192. PMC9181154
13. Bachurski, D., Schuldner, M., Nguyen, P.H., Malz, A., Reiners, K.S., Grenzi, P.C., Babatz, F., Schauss, A.C., Hansen, H.P., Hallek, M.*, et al.* (2019). Extracellular Vesicle Measurements with Nanoparticle Tracking Analysis - an Accuracy and Repeatability Comparison

between Nanosight NS300 and Zetaview. J Extracell Vesicles *8*, 1596016. 10.1080/20013078.2019.1596016. PMC6450530
14. Balducci, E., Leroyer, A.S., Lacroix, R., Robert, S., Todorova, D., Simoncini, S., Lyonnet, L., Chareyre, C., Zaegel-Faucher, O., Micallef, J.*, et al.* (2019). Extracellular Vesicles from T Cells Overexpress Mir-146b-5p in HIV-1 Infection and Repress Endothelial Activation. Sci Rep *9*, 10299. 10.1038/s41598-019-44743-w. PMC6635508
15. Bao, F., Zhou, L., Zhou, R., Huang, Q., Chen, J., Zeng, S., Wu, Y., Yang, L., Qian, S., Wang, M.*, et al.* (2022). Mitolysosome Exocytosis, a Mitophagy-Independent Mitochondrial Quality Control in Flunarizine-Induced Parkinsonism-Like Symptoms. Sci Adv *8*, eabk2376. 10.1126/sciadv.abk2376.
16. Bari, S.M.I., Hossain, F.B., and Nestorova, G.G. (2021). Advances in Biosensors Technology for Detection and Characterization of Extracellular Vesicles. Sensors (Basel) *21*. 10.3390/s21227645. PMC8621354
17. Belshaw, R., Pereira, V., Katzourakis, A., Talbot, G., Paces, J., Burt, A., and Tristem, M. (2004). Long-Term Reinfection of the Human Genome by Endogenous Retroviruses. Proc Natl Acad Sci U S A *101*, 4894-4899. 10.1073/pnas.0307800101. PMC387345
18. Benmoussa, A., Lee, C.H., Laffont, B., Savard, P., Laugier, J., Boilard, E., Gilbert, C., Fliss, I., and Provost, P. (2016). Commercial Dairy Cow Milk microRNAs Resist Digestion under Simulated Gastrointestinal Tract Conditions. J Nutr *146*, 2206-2215. 10.3945/jn.116.237651.
19. Benmoussa, A., Ly, S., Shan, S.T., Laugier, J., Boilard, E., Gilbert, C., and Provost, P. (2017). A Subset of Extracellular Vesicles Carries the Bulk of microRNAs in Commercial Dairy Cow's Milk. J Extracell Vesicles *6*, 1401897. 10.1080/20013078.2017.1401897. PMC5994974
20. Bolukbasi, M.F., Mizrak, A., Ozdener, G.B., Madlener, S., Strobel, T., Erkan, E.P., Fan, J.B., Breakefield, X.O., and Saydam, O. (2012). Mir-1289 and "Zipcode"-Like Sequence Enrich mRNAs in Microvesicles. Mol Ther Nucleic Acids *1*, e10. 10.1038/mtna.2011.2. PMC3381601
21. Bordanaba-Florit, G., Royo, F., Kruglik, S.G., and Falcon-Perez, J.M. (2021). Using Single-Vesicle Technologies to Unravel the Heterogeneity of Extracellular Vesicles. Nat Protoc *16*, 3163-3185. 10.1038/s41596-021-00551-z.
22. Briskin, D., Wang, P.Y., and Bartel, D.P. (2020). The Biochemical Basis for the Cooperative Action of microRNAs. Proc Natl Acad Sci U S A *117*, 17764-17774. 10.1073/pnas.1920404117. PMC7395462
23. Brittain, G.C.t., Chen, Y.Q., Martinez, E., Tang, V.A., Renner, T.M., Langlois, M.A., and Gulnik, S. (2019). A Novel Semiconductor-Based Flow Cytometer with Enhanced Light-Scatter Sensitivity for the Analysis of Biological Nanoparticles. Sci Rep *9*, 16039. 10.1038/s41598-019-52366-4. PMC6831566
24. Brittain, G.C.t., Langlois, M.A., and Gulnik, S. (2021). Reply To: Misinterpretation of Solid Sphere Equivalent Refractive Index Measurements and Smallest Detectable Diameters of Extracellular Vesicles by Flow Cytometry. Sci Rep *11*, 24170. 10.1038/s41598-021-03113-1. PMC8683426
25. Bryniarski, K., Ptak, W., Martin, E., Nazimek, K., Szczepanik, M., Sanak, M., and Askenase, P.W. (2015). Free Extracellular miRNA Functionally Targets Cells by Transfecting

Exosomes from Their Companion Cells. PLoS One *10*, e0122991. 10.1371/journal.pone.0122991. PMC4414541
26. Buschow, S.I., Nolte-'t Hoen, E.N., van Niel, G., Pols, M.S., ten Broeke, T., Lauwen, M., Ossendorp, F., Melief, C.J., Raposo, G., Wubbolts, R.*, et al.* (2009). MHC II in Dendritic Cells Is Targeted to Lysosomes or T Cell-Induced Exosomes Via Distinct Multivesicular Body Pathways. Traffic *10*, 1528-1542. 10.1111/j.1600-0854.2009.00963.x.
27. Buschow, S.I., van Balkom, B.W., Aalberts, M., Heck, A.J., Wauben, M., and Stoorvogel, W. (2010). MHC Class II-Associated Proteins in B-Cell Exosomes and Potential Functional Implications for Exosome Biogenesis. Immunol Cell Biol *88*, 851-856. 10.1038/icb.2010.64.
28. Campos-Silva, C., Suarez, H., Jara-Acevedo, R., Linares-Espinos, E., Martinez-Pineiro, L., Yanez-Mo, M., and Vales-Gomez, M. (2019). High Sensitivity Detection of Extracellular Vesicles Immune-Captured from Urine by Conventional Flow Cytometry. Sci Rep *9*, 2042. 10.1038/s41598-019-38516-8. PMC6376115
29. Chahar, H.S., Bao, X., and Casola, A. (2015). Exosomes and Their Role in the Life Cycle and Pathogenesis of RNA Viruses. Viruses *7*, 3204-3225. 10.3390/v7062770. PMC4488737
30. Chalmers, J.D., Moffitt, K.L., Suarez-Cuartin, G., Sibila, O., Finch, S., Furrie, E., Dicker, A., Wrobel, K., Elborn, J.S., Walker, B.*, et al.* (2017). Neutrophil Elastase Activity Is Associated with Exacerbations and Lung Function Decline in Bronchiectasis. Am J Respir Crit Care Med *195*, 1384-1393. 10.1164/rccm.201605-1027OC. PMC5443898
31. Chang, A.L., McKeague, M., Liang, J.C., and Smolke, C.D. (2014). Kinetic and Equilibrium Binding Characterization of Aptamers to Small Molecules Using a Label-Free, Sensitive, and Scalable Platform. Anal Chem *86*, 3273-3278. 10.1021/ac5001527. PMC3983011
32. Chen, X., Li, A., Sun, B.F., Yang, Y., Han, Y.N., Yuan, X., Chen, R.X., Wei, W.S., Liu, Y., Gao, C.C.*, et al.* (2019). 5-Methylcytosine Promotes Pathogenesis of Bladder Cancer through Stabilizing mRNAs. Nat Cell Biol *21*, 978-990. 10.1038/s41556-019-0361-y.
33. Chiang, C.Y., and Chen, C. (2019). Toward Characterizing Extracellular Vesicles at a Single-Particle Level. J Biomed Sci *26*, 9. 10.1186/s12929-019-0502-4. PMC6332877
34. Choi, D., Montermini, L., Kim, D.K., Meehan, B., Roth, F.P., and Rak, J. (2018). The Impact of Oncogenic Egfrviii on the Proteome of Extracellular Vesicles Released from Glioblastoma Cells. Mol Cell Proteomics *17*, 1948-1964. 10.1074/mcp.RA118.000644. PMC6166673
35. Cocozza, F., Nevo, N., Piovesana, E., Lahaye, X., Buchrieser, J., Schwartz, O., Manel, N., Tkach, M., Thery, C., and Martin-Jaular, L. (2020). Extracellular Vesicles Containing ACE2 Efficiently Prevent Infection by SARS-CoV-2 Spike Protein-Containing Virus. J Extracell Vesicles *10*, e12050. 10.1002/jev2.12050. PMC7769856
36. Cocucci, E., and Meldolesi, J. (2015). Ectosomes and Exosomes: Shedding the Confusion between Extracellular Vesicles. Trends Cell Biol *25*, 364-372. 10.1016/j.tcb.2015.01.004.
37. Cocucci, E., Racchetti, G., and Meldolesi, J. (2009). Shedding Microvesicles: Artefacts No More. Trends Cell Biol *19*, 43-51. 10.1016/j.tcb.2008.11.003.
38. Couch, Y., Buzas, E.I., Di Vizio, D., Gho, Y.S., Harrison, P., Hill, A.F., Lotvall, J., Raposo, G., Stahl, P.D., Thery, C.*, et al.* (2021). A Brief History of Nearly EV-Erything - the Rise and Rise of Extracellular Vesicles. J Extracell Vesicles *10*, e12144. 10.1002/jev2.12144. PMC8681215

39. Coumans, F.A.W., Brisson, A.R., Buzas, E.I., Dignat-George, F., Drees, E.E.E., El-Andaloussi, S., Emanueli, C., Gasecka, A., Hendrix, A., Hill, A.F*., et al.* (2017). Methodological Guidelines to Study Extracellular Vesicles. Circ Res *120*, 1632-1648. 10.1161/CIRCRESAHA.117.309417.
40. Cvjetkovic, A., Jang, S.C., Konecna, B., Hoog, J.L., Sihlbom, C., Lasser, C., and Lotvall, J. (2016). Detailed Analysis of Protein Topology of Extracellular Vesicles-Evidence of Unconventional Membrane Protein Orientation. Sci Rep *6*, 36338. 10.1038/srep36338. PMC5099568
41. Czerniak, T., and Saenz, J.P. (2022). Lipid Membranes Modulate the Activity of RNA through Sequence-Dependent Interactions. Proc Natl Acad Sci U S A *119*, e2119235119. 10.1073/pnas.2119235119. PMC8794826
42. Daaboul, G.G., Gagni, P., Benussi, L., Bettotti, P., Ciani, M., Cretich, M., Freedman, D.S., Ghidoni, R., Ozkumur, A.Y., Piotto, C*., et al.* (2016). Digital Detection of Exosomes by Interferometric Imaging. Sci Rep *6*, 37246. 10.1038/srep37246. PMC5112555
43. Dalli, J., Montero-Melendez, T., Norling, L.V., Yin, X., Hinds, C., Haskard, D., Mayr, M., and Perretti, M. (2013). Heterogeneity in Neutrophil Microparticles Reveals Distinct Proteome and Functional Properties. Mol Cell Proteomics *12*, 2205-2219. 10.1074/mcp.M113.028589. PMC3734580
44. Danielson, K.M., Estanislau, J., Tigges, J., Toxavidis, V., Camacho, V., Felton, E.J., Khoory, J., Kreimer, S., Ivanov, A.R., Mantel, P.Y*., et al.* (2016). Diurnal Variations of Circulating Extracellular Vesicles Measured by Nano Flow Cytometry. PLoS One *11*, e0144678. 10.1371/journal.pone.0144678. PMC4706300
45. de Rond, L., Coumans, F.A.W., Nieuwland, R., van Leeuwen, T.G., and van der Pol, E. (2018a). Deriving Extracellular Vesicle Size from Scatter Intensities Measured by Flow Cytometry. Curr Protoc Cytom *86*, e43. 10.1002/cpcy.43.
46. de Rond, L., van der Pol, E., Hau, C.M., Varga, Z., Sturk, A., van Leeuwen, T.G., Nieuwland, R., and Coumans, F.A.W. (2018b). Comparison of Generic Fluorescent Markers for Detection of Extracellular Vesicles by Flow Cytometry. Clin Chem *64*, 680-689. 10.1373/clinchem.2017.278978.
47. Dellar, E.R., Hill, C., Melling, G.E., Carter, D.R.F., and Baena-Lopez, L.A. (2022). Unpacking Extracellular Vesicles: RNA Cargo Loading and Function. Journal of Extracellular Biology *1*, e40. 10.1002/jex2.40.
48. Deregibus, M.C., Cantaluppi, V., Calogero, R., Lo Iacono, M., Tetta, C., Biancone, L., Bruno, S., Bussolati, B., and Camussi, G. (2007). Endothelial Progenitor Cell Derived Microvesicles Activate an Angiogenic Program in Endothelial Cells by a Horizontal Transfer of mRNA. Blood *110*, 2440-2448. 10.1182/blood-2007-03-078709.
49. Dittrich, A.S., Kuhbandner, I., Gehrig, S., Rickert-Zacharias, V., Twigg, M., Wege, S., Taggart, C.C., Herth, F., Schultz, C., and Mall, M.A. (2018). Elastase Activity on Sputum Neutrophils Correlates with Severity of Lung Disease in Cystic Fibrosis. Eur Respir J *51*. 10.1183/13993003.01910-2017.
50. Dong, Y., Jin, C., Ding, Z., Zhu, Y., He, Q., Zhang, X., Ai, R., Yin, Y., and He, Y. (2021). TLR4 Regulates ROS and Autophagy to Control Neutrophil Extracellular Traps Formation against Streptococcus Pneumoniae in Acute Otitis Media. Pediatr Res *89*, 785-794. 10.1038/s41390-020-0964-9.

51. Doyle, L.M., and Wang, M.Z. (2019). Overview of Extracellular Vesicles, Their Origin, Composition, Purpose, and Methods for Exosome Isolation and Analysis. Cells *8*. 10.3390/cells8070727. PMC6678302
52. El-Shennawy, L., Hoffmann, A.D., Dashzeveg, N.K., McAndrews, K.M., Mehl, P.J., Cornish, D., Yu, Z., Tokars, V.L., Nicolaescu, V., Tomatsidou, A.*, et al.* (2022). Circulating ACE2-Expressing Extracellular Vesicles Block Broad Strains of SARS-CoV-2. Nat Commun *13*, 405. 10.1038/s41467-021-27893-2. PMC8776790
53. Elborn, J.S. (2016). Cystic Fibrosis. Lancet *388*, 2519-2531. 10.1016/S0140-6736(16)00576-6. 27140670
54. Eliscovich, C., Shenoy, S.M., and Singer, R.H. (2017). Imaging mRNA and Protein Interactions within Neurons. Proc Natl Acad Sci U S A *114*, E1875-E1884. 10.1073/pnas.1621440114. PMC5347572
55. Erdbrugger, U., Blijdorp, C.J., Bijnsdorp, I.V., Borras, F.E., Burger, D., Bussolati, B., Byrd, J.B., Clayton, A., Dear, J.W., Falcon-Perez, J.M.*, et al.* (2021). Urinary Extracellular Vesicles: A Position Paper by the Urine Task Force of the International Society for Extracellular Vesicles. J Extracell Vesicles *10*, e12093. 10.1002/jev2.12093. PMC8138533
56. Fabbiano, F., Corsi, J., Gurrieri, E., Trevisan, C., Notarangelo, M., and D'Agostino, V.G. (2020). RNA Packaging into Extracellular Vesicles: An Orchestra of RNA-Binding Proteins? J Extracell Vesicles *10*, e12043. 10.1002/jev2.12043. PMC7769857
57. Farrell, P., Ferec, C., Macek, M., Frischer, T., Renner, S., Riss, K., Barton, D., Repetto, T., Tzetis, M., Giteau, K.*, et al.* (2018). Estimating the Age of P.(Phe508del) with Family Studies of Geographically Distinct European Populations and the Early Spread of Cystic Fibrosis. Eur J Hum Genet *26*, 1832-1839. 10.1038/s41431-018-0234-z. PMC6244163
58. Fedele, C., Singh, A., Zerlanko, B.J., Iozzo, R.V., and Languino, L.R. (2015). The Alphavbeta6 Integrin Is Transferred Intercellularly Via Exosomes. J Biol Chem *290*, 4545-4551. 10.1074/jbc.C114.617662. PMC4335196
59. Ferrari, L., Cafora, M., Rota, F., Hoxha, M., Iodice, S., Tarantini, L., Dolci, M., Delbue, S., Pistocchi, A., and Bollati, V. (2019). Extracellular Vesicles Released by Colorectal Cancer Cell Lines Modulate Innate Immune Response in Zebrafish Model: The Possible Role of Human Endogenous Retroviruses. Int J Mol Sci *20*. 10.3390/ijms20153669. PMC6695895
60. Fitzgerald, W., Freeman, M.L., Lederman, M.M., Vasilieva, E., Romero, R., and Margolis, L. (2018). A System of Cytokines Encapsulated in Extracellular Vesicles. Sci Rep *8*, 8973. 10.1038/s41598-018-27190-x. PMC5997670
61. Forrest, O.A., Dobosh, B., Ingersoll, S.A., Rao, S., Rojas, A., Laval, J., Alvarez, J.A., Brown, M.R., Tangpricha, V., and Tirouvanziam, R. (2022). Neutrophil-Derived Extracellular Vesicles Promote Feed-Forward Inflammasome Signaling in Cystic Fibrosis Airways. J Leukoc Biol. 10.1002/JLB.3AB0321-149R.
62. Fukunaga, K., and Yokobayashi, Y. (2022). Directed Evolution of Orthogonal RNA-Rbp Pairs through Library-Vs-Library in Vitro Selection. Nucleic Acids Res *50*, 601-616. 10.1093/nar/gkab527. PMC8789040
63. Gamage, T., and Fraser, M. (2021). The Role of Extracellular Vesicles in the Developing Brain: Current Perspective and Promising Source of Biomarkers and Therapy for Perinatal Brain Injury. Front Neurosci *15*, 744840. 10.3389/fnins.2021.744840. PMC8498217

64. Ganser, L.R., Kelly, M.L., Herschlag, D., and Al-Hashimi, H.M. (2019). The Roles of Structural Dynamics in the Cellular Functions of RNAs. Nat Rev Mol Cell Biol *20*, 474-489. 10.1038/s41580-019-0136-0. PMC7656661
65. Gao, T., Shu, J., and Cui, J. (2018). A Systematic Approach to RNA-Associated Motif Discovery. BMC Genomics *19*, 146. 10.1186/s12864-018-4528-x. PMC5813387
66. Gao, X., Teng, X., Dai, Y., and Li, J. (2021). Rolling Circle Amplification-Assisted Flow Cytometry Approach for Simultaneous Profiling of Exosomal Surface Proteins. ACS Sens *6*, 3611-3620. 10.1021/acssensors.1c01163.
67. Garcia-Montojo, M., Doucet-O'Hare, T., Henderson, L., and Nath, A. (2018). Human Endogenous Retrovirus-K (Hml-2): A Comprehensive Review. Crit Rev Microbiol *44*, 715-738. 10.1080/1040841X.2018.1501345. PMC6342650
68. Garrus, J.E., von Schwedler, U.K., Pornillos, O.W., Morham, S.G., Zavitz, K.H., Wang, H.E., Wettstein, D.A., Stray, K.M., Cote, M., Rich, R.L*., et al.* (2001). Tsg101 and the Vacuolar Protein Sorting Pathway Are Essential for HIV-1 Budding. Cell *107*, 55-65. 10.1016/s0092-8674(01)00506-2.
69. Gasser, O., and Schifferli, J.A. (2004). Activated Polymorphonuclear Neutrophils Disseminate Anti-Inflammatory Microparticles by Ectocytosis. Blood *104*, 2543-2548. 10.1182/blood-2004-01-0361.
70. Genschmer, K.R., Russell, D.W., Lal, C., Szul, T., Bratcher, P.E., Noerager, B.D., Abdul Roda, M., Xu, X., Rezonzew, G., Viera, L*., et al.* (2019). Activated PMN Exosomes: Pathogenic Entities Causing Matrix Destruction and Disease in the Lung. Cell *176*, 113-126 e115. 10.1016/j.cell.2018.12.002. PMC6368091
71. Ghosh, A., Davey, M., Chute, I.C., Griffiths, S.G., Lewis, S., Chacko, S., Barnett, D., Crapoulet, N., Fournier, S., Joy, A*., et al.* (2014). Rapid Isolation of Extracellular Vesicles from Cell Culture and Biological Fluids Using a Synthetic Peptide with Specific Affinity for Heat Shock Proteins. PLoS One *9*, e110443. 10.1371/journal.pone.0110443. PMC4201556
72. Gill, S., Catchpole, R., and Forterre, P. (2018). Extracellular Membrane Vesicles in the Three Domains of Life and Beyond. FEMS microbiology reviews *43*, 273-303.
73. Gill, S., and Forterre, P. (2015). Origin of Life: Luca and Extracellular Membrane Vesicles (Emvs). International Journal of Astrobiology *15*, 7-15. 10.1017/s1473550415000282.
74. Gould, S.J., Booth, A.M., and Hildreth, J.E. (2003). The Trojan Exosome Hypothesis. Proc Natl Acad Sci U S A *100*, 10592-10597. 10.1073/pnas.1831413100. PMC196848
75. Gramegna, A., Amati, F., Terranova, L., Sotgiu, G., Tarsia, P., Miglietta, D., Calderazzo, M.A., Aliberti, S., and Blasi, F. (2017). Neutrophil Elastase in Bronchiectasis. Respir Res *18*, 211. 10.1186/s12931-017-0691-x. PMC5735855
76. Gray, W.D., Mitchell, A.J., and Searles, C.D. (2015). An Accurate, Precise Method for General Labeling of Extracellular Vesicles. MethodsX *2*, 360-367. 10.1016/j.mex.2015.08.002. PMC4589801
77. Groot Kormelink, T., Arkesteijn, G.J., Nauwelaers, F.A., van den Engh, G., Nolte-'t Hoen, E.N., and Wauben, M.H. (2016). Prerequisites for the Analysis and Sorting of Extracellular Vesicle Subpopulations by High-Resolution Flow Cytometry. Cytometry A *89*, 135-147. 10.1002/cyto.a.22644.

78. Guescini, M., Genedani, S., Stocchi, V., and Agnati, L.F. (2010). Astrocytes and Glioblastoma Cells Release Exosomes Carrying Mtdna. J Neural Transm (Vienna) *117*, 1-4. 10.1007/s00702-009-0288-8.
79. Gyorgy, B., Szabo, T.G., Pasztoi, M., Pal, Z., Misjak, P., Aradi, B., Laszlo, V., Pallinger, E., Pap, E., Kittel, A*., et al.* (2011). Membrane Vesicles, Current State-of-the-Art: Emerging Role of Extracellular Vesicles. Cell Mol Life Sci *68*, 2667-2688. 10.1007/s00018-011-0689-3. PMC3142546
80. Hartjes, T.A., Mytnyk, S., Jenster, G.W., van Steijn, V., and van Royen, M.E. (2019). Extracellular Vesicle Quantification and Characterization: Common Methods and Emerging Approaches. Bioengineering (Basel) *6*. 10.3390/bioengineering6010007. PMC6466085
81. Headland, S.E., Jones, H.R., D'Sa, A.S., Perretti, M., and Norling, L.V. (2014). Cutting-Edge Analysis of Extracellular Microparticles Using Imagestream(X) Imaging Flow Cytometry. Sci Rep *4*, 5237. 10.1038/srep05237. PMC4050385
82. Hock, J., Weinmann, L., Ender, C., Rudel, S., Kremmer, E., Raabe, M., Urlaub, H., and Meister, G. (2007). Proteomic and Functional Analysis of Argonaute-Containing mRNA-Protein Complexes in Human Cells. EMBO Rep *8*, 1052-1060. 10.1038/sj.embor.7401088. PMC2247381
83. Hong, B.S., Cho, J.H., Kim, H., Choi, E.J., Rho, S., Kim, J., Kim, J.H., Choi, D.S., Kim, Y.K., Hwang, D*., et al.* (2009). Colorectal Cancer Cell-Derived Microvesicles Are Enriched in Cell Cycle-Related mRNAs That Promote Proliferation of Endothelial Cells. BMC Genomics *10*, 556. 10.1186/1471-2164-10-556. PMC2788585
84. Hurwitz, S.N., Rider, M.A., Bundy, J.L., Liu, X., Singh, R.K., and Meckes, D.G., Jr. (2016). Proteomic Profiling of NCI-60 Extracellular Vesicles Uncovers Common Protein Cargo and Cancer Type-Specific Biomarkers. Oncotarget *7*, 86999-87015. 10.18632/oncotarget.13569. PMC5341331
85. Hutchinson, E.C., Charles, P.D., Hester, S.S., Thomas, B., Trudgian, D., Martinez-Alonso, M., and Fodor, E. (2014). Conserved and Host-Specific Features of Influenza Virion Architecture. Nat Commun *5*, 4816. 10.1038/ncomms5816. PMC4167602
86. Imai, M., Sakuma, Y., Kurisu, M., and Walde, P. (2022). From Vesicles toward Protocells and Minimal Cells. Soft Matter. 10.1039/d1sm01695d.
87. Izumi, H., Kosaka, N., Shimizu, T., Sekine, K., Ochiya, T., and Takase, M. (2012). Bovine Milk Contains microRNA and Messenger RNA That Are Stable under Degradative Conditions. J Dairy Sci *95*, 4831-4841. 10.3168/jds.2012-5489.
88. Jan, A.T. (2017). Outer Membrane Vesicles (OMVs) of Gram-Negative Bacteria: A Perspective Update. Front Microbiol *8*, 1053. 10.3389/fmicb.2017.01053. PMC5465292
89. Janas, T., Janas, M.M., Sapon, K., and Janas, T. (2015). Mechanisms of RNA Loading into Exosomes. FEBS Lett *589*, 1391-1398. 10.1016/j.febslet.2015.04.036.
90. Jiang, X., You, L., Zhang, Z., Cui, X., Zhong, H., Sun, X., Ji, C., and Chi, X. (2021). Biological Properties of Milk-Derived Extracellular Vesicles and Their Physiological Functions in Infant. Front Cell Dev Biol *9*, 693534. 10.3389/fcell.2021.693534. PMC8267587
91. Jiao, H., Jiang, D., Hu, X., Du, W., Ji, L., Yang, Y., Li, X., Sho, T., Wang, X., Li, Y*., et al.* (2021). Mitocytosis, a Migrasome-Mediated Mitochondrial Quality-Control Process. Cell *184*, 2896-2910 e2813. 10.1016/j.cell.2021.04.027.

92. Johnstone, R.M., Mathew, A., Mason, A.B., and Teng, K. (1991). Exosome Formation During Maturation of Mammalian and Avian Reticulocytes: Evidence That Exosome Release Is a Major Route for Externalization of Obsolete Membrane Proteins. J Cell Physiol *147*, 27-36. 10.1002/jcp.1041470105.
93. Joyce, G.F. (2002). The Antiquity of RNA-Based Evolution. Nature *418*, 214-221. 10.1038/418214a.
94. Kaur, S., Elkahloun, A.G., Petersen, J.D., Arakelyan, A., Livak, F., Singh, S.P., Margolis, L., Zimmerberg, J., and Roberts, D.D. (2021a). CD63(+) and MHC Class I(+) Subsets of Extracellular Vesicles Produced by Wild-Type and Cd47-Deficient Jurkat T Cells Have Divergent Functional Effects on Endothelial Cell Gene Expression. Biomedicines *9*. 10.3390/biomedicines9111705. PMC8615535
95. Kaur, S., Saldana, A.C., Elkahloun, A.G., Petersen, J.D., Arakelyan, A., Singh, S.P., Jenkins, L.M., Kuo, B., Reginauld, B., Jordan, D.G.*, et al.* (2021b). Cd47 Interactions with Exportin-1 Limit the Targeting of M(7)G-Modified RNAs to Extracellular Vesicles. J Cell Commun Signal. 10.1007/s12079-021-00646-y.
96. Kohler, A., and Hurt, E. (2007). Exporting RNA from the Nucleus to the Cytoplasm. Nat Rev Mol Cell Biol *8*, 761-773. 10.1038/nrm2255.
97. Koppers-Lalic, D., Hackenberg, M., Bijnsdorp, I.V., van Eijndhoven, M.A.J., Sadek, P., Sie, D., Zini, N., Middeldorp, J.M., Ylstra, B., de Menezes, R.X.*, et al.* (2014). Nontemplated Nucleotide Additions Distinguish the Small RNA Composition in Cells from Exosomes. Cell Rep *8*, 1649-1658. 10.1016/j.celrep.2014.08.027.
98. Kossinova, O.A., Gopanenko, A.V., Tamkovich, S.N., Krasheninina, O.A., Tupikin, A.E., Kiseleva, E., Yanshina, D.D., Malygin, A.A., Ven'yaminova, A.G., Kabilov, M.R.*, et al.* (2017). Cytosolic YB-1 and NSUN2 Are the Only Proteins Recognizing Specific Motifs Present in mRNAs Enriched in Exosomes. Biochim Biophys Acta Proteins Proteom *1865*, 664-673. 10.1016/j.bbapap.2017.03.010.
99. Kowal, J., Arras, G., Colombo, M., Jouve, M., Morath, J.P., Primdal-Bengtson, B., Dingli, F., Loew, D., Tkach, M., and Thery, C. (2016). Proteomic Comparison Defines Novel Markers to Characterize Heterogeneous Populations of Extracellular Vesicle Subtypes. Proc Natl Acad Sci U S A *113*, E968-977. 10.1073/pnas.1521230113. PMC4776515
100. Kramberger, P., Ciringer, M., Strancar, A., and Peterka, M. (2012). Evaluation of Nanoparticle Tracking Analysis for Total Virus Particle Determination. Virol J *9*, 265. 10.1186/1743-422X-9-265. PMC3503628
101. Krishnan, Y., and Simmel, F.C. (2011). Nucleic Acid Based Molecular Devices. Angew Chem Int Ed Engl *50*, 3124-3156. 10.1002/anie.200907223.
102. Kuriyama, Y., Shimizu, A., Kanai, S., Oikawa, D., Motegi, S.I., Tokunaga, F., and Ishikawa, O. (2021). Coordination of Retrotransposons and Type I Interferon with Distinct Interferon Pathways in Dermatomyositis, Systemic Lupus Erythematosus and Autoimmune Blistering Disease. Sci Rep *11*, 23146. 10.1038/s41598-021-02522-6. PMC8632942
103. Lakadamyali, M., Rust, M.J., and Zhuang, X. (2004). Endocytosis of Influenza Viruses. Microbes Infect *6*, 929-936. 10.1016/j.micinf.2004.05.002. PMC2715838
104. Lazaro-Ibanez, E., Lunavat, T.R., Jang, S.C., Escobedo-Lucea, C., Oliver-De La Cruz, J., Siljander, P., Lotvall, J., and Yliperttula, M. (2017). Distinct Prostate Cancer-Related

mRNA Cargo in Extracellular Vesicle Subsets from Prostate Cell Lines. BMC Cancer *17*, 92. 10.1186/s12885-017-3087-x. PMC5286827
105. Libregts, S., Arkesteijn, G.J.A., Nemeth, A., Nolte-'t Hoen, E.N.M., and Wauben, M.H.M. (2018). Flow Cytometric Analysis of Extracellular Vesicle Subsets in Plasma: Impact of Swarm by Particles of Non-Interest. J Thromb Haemost *16*, 1423-1436. 10.1111/jth.14154.
106. Lippe, R. (2018). Flow Virometry: A Powerful Tool to Functionally Characterize Viruses. J Virol *92*. 10.1128/JVI.01765-17. PMC5774884
107. Liu, X.M., Ma, L., and Schekman, R. (2021). Selective Sorting of microRNAs into Exosomes by Phase-Separated YBX1 Condensates. Elife *10*. 10.7554/eLife.71982. PMC8612733
108. Lorincz, A.M., Schutte, M., Timar, C.I., Veres, D.S., Kittel, A., McLeish, K.R., Merchant, M.L., and Ligeti, E. (2015). Functionally and Morphologically Distinct Populations of Extracellular Vesicles Produced by Human Neutrophilic Granulocytes. J Leukoc Biol *98*, 583-589. 10.1189/jlb.3VMA1014-514R.
109. Lukasik, A., Brzozowska, I., Zielenkiewicz, U., and Zielenkiewicz, P. (2017). Detection of Plant miRNAs Abundance in Human Breast Milk. Int J Mol Sci *19*. 10.3390/ijms19010037. PMC5795987
110. Mao, S.Y. (2010). Biotinylation of Antibodies. Methods Mol Biol *588*, 49-52. 10.1007/978-1-59745-324-0_7.
111. Marcoux, G., Laroche, A., Hasse, S., Bellio, M., Mbarik, M., Tamagne, M., Allaeys, I., Zufferey, A., Levesque, T., Rebetz, J.*, et al.* (2021). Platelet EVs Contain an Active Proteasome Involved in Protein Processing for Antigen Presentation Via MHC-I Molecules. Blood *138*, 2607-2620. 10.1182/blood.2020009957.
112. Margaroli, C., Garratt, L.W., Horati, H., Dittrich, A.S., Rosenow, T., Montgomery, S.T., Frey, D.L., Brown, M.R., Schultz, C., Guglani, L.*, et al.* (2019). Elastase Exocytosis by Airway Neutrophils Is Associated with Early Lung Damage in Children with Cystic Fibrosis. Am J Respir Crit Care Med *199*, 873-881. 10.1164/rccm.201803-0442OC. PMC6444666
113. Margaroli, C., Madison, M.C., Viera, L., Russell, D.W., Gaggar, A., Genschmer, K.R., and Blalock, J.E. (2022). An in Vivo Model for Extracellular Vesicle-Induced Emphysema. JCI Insight *7*. 10.1172/jci.insight.153560. PMC8876451
114. Margaroli, C., Moncada-Giraldo, D., Gulick, D.A., Dobosh, B., Giacalone, V.D., Forrest, O.A., Sun, F., Gu, C., Gaggar, A., Kissick, H.*, et al.* (2021). Transcriptional Firing Represses Bactericidal Activity in Cystic Fibrosis Airway Neutrophils. Cell Rep Med *2*, 100239. 10.1016/j.xcrm.2021.100239. PMC8080108
115. Margaroli, C., and Tirouvanziam, R. (2016). Neutrophil Plasticity Enables the Development of Pathological Microenvironments: Implications for Cystic Fibrosis Airway Disease. Mol Cell Pediatr *3*, 38. 10.1186/s40348-016-0066-2. PMC5136534
116. Martin-Serrano, J., Zang, T., and Bieniasz, P.D. (2001). HIV-1 and Ebola Virus Encode Small Peptide Motifs That Recruit Tsg101 to Sites of Particle Assembly to Facilitate Egress. Nature medicine *7*, 1313.
117. Mateescu, B., Kowal, E.J., van Balkom, B.W., Bartel, S., Bhattacharyya, S.N., Buzas, E.I., Buck, A.H., de Candia, P., Chow, F.W., Das, S.*, et al.* (2017). Obstacles and Opportunities in the Functional Analysis of Extracellular Vesicle RNA - an ISEV Position Paper. J Extracell Vesicles *6*, 1286095. 10.1080/20013078.2017.1286095. PMC5345583

118. Mathieu, M., Martin-Jaular, L., Lavieu, G., and Thery, C. (2019). Specificities of Secretion and Uptake of Exosomes and Other Extracellular Vesicles for Cell-to-Cell Communication. Nat Cell Biol *21*, 9-17. 10.1038/s41556-018-0250-9.
119. McVey, M.J., Spring, C.M., and Kuebler, W.M. (2018). Improved Resolution in Extracellular Vesicle Populations Using 405 Instead of 488 nm Side Scatter. J Extracell Vesicles *7*, 1454776. 10.1080/20013078.2018.1454776. PMC5912191
120. Melling, G.E., Conlon, R., Pantazi, P., Dellar, E.R., Samuel, P., Baena-Lopez, L.A., Simpson, J.C., and Carter, D.R.F. (2022). Confocal Microscopy Analysis Reveals That Only a Small Proportion of Extracellular Vesicles Are Successfully Labelled with Commonly Utilised Staining Methods. Sci Rep *12*, 262. 10.1038/s41598-021-04225-4. PMC8741769
121. Mittelbrunn, M., Gutierrez-Vazquez, C., Villarroya-Beltri, C., Gonzalez, S., Sanchez-Cabo, F., Gonzalez, M.A., Bernad, A., and Sanchez-Madrid, F. (2011). Unidirectional Transfer of microRNA-Loaded Exosomes from T Cells to Antigen-Presenting Cells. Nat Commun *2*, 282. 10.1038/ncomms1285. PMC3104548
122. Mizuuchi, R., Furubayashi, T., and Ichihashi, N. (2022). Evolutionary Transition from a Single RNA Replicator to a Multiple Replicator Network. Nat Commun *13*, 1460. 10.1038/s41467-022-29113-x. PMC8933500
123. Montecalvo, A., Larregina, A.T., Shufesky, W.J., Stolz, D.B., Sullivan, M.L., Karlsson, J.M., Baty, C.J., Gibson, G.A., Erdos, G., Wang, Z.*, et al.* (2012). Mechanism of Transfer of Functional microRNAs between Mouse Dendritic Cells Via Exosomes. Blood *119*, 756-766. 10.1182/blood-2011-02-338004. PMC3265200
124. Morales-Kastresana, A., and Jones, J.C. (2017). Flow Cytometric Analysis of Extracellular Vesicles. Methods Mol Biol *1545*, 215-225. 10.1007/978-1-4939-6728-5_16. PMC7888554
125. Mordovkina, D., Lyabin, D.N., Smolin, E.A., Sogorina, E.M., Ovchinnikov, L.P., and Eliseeva, I. (2020). Y-Box Binding Proteins in Mrnp Assembly, Translation, and Stability Control. Biomolecules *10*. 10.3390/biom10040591. PMC7226217
126. Morozov, V.A., and Morozov, A.V. (2021). A Comprehensive Analysis of Human Endogenous Retroviruses Herv-K (Hml.2) from Teratocarcinoma Cell Lines and Detection of Viral Cargo in Microvesicles. Int J Mol Sci *22*. 10.3390/ijms222212398. PMC8619701
127. Mulcahy, L.A., Pink, R.C., and Carter, D.R. (2014). Routes and Mechanisms of Extracellular Vesicle Uptake. J Extracell Vesicles *3*, 24641. 10.3402/jev.v3.24641. PMC4122821
128. Muller, F., Escobar, L., Xu, F., Wegrzyn, E., Nainyte, M., Amatov, T., Chan, C.Y., Pichler, A., and Carell, T. (2022). A Prebiotically Plausible Scenario of an RNA-Peptide World. Nature *605*, 279-284. 10.1038/s41586-022-04676-3. PMC9095488
129. Muller, L., Simms, P., Hong, C.S., Nishimura, M.I., Jackson, E.K., Watkins, S.C., and Whiteside, T.L. (2017). Human Tumor-Derived Exosomes (Tex) Regulate Treg Functions Via Cell Surface Signaling Rather Than Uptake Mechanisms. Oncoimmunology *6*, e1261243. 10.1080/2162402X.2016.1261243. PMC5593709
130. Muller, M., Fazi, F., and Ciaudo, C. (2019). Argonaute Proteins: From Structure to Function in Development and Pathological Cell Fate Determination. Front Cell Dev Biol *7*, 360. 10.3389/fcell.2019.00360. PMC6987405
131. Nabhan, J.F., Hu, R., Oh, R.S., Cohen, S.N., and Lu, Q. (2012). Formation and Release of Arrestin Domain-Containing Protein 1-Mediated Microvesicles (Armms) at Plasma

Membrane by Recruitment of Tsg101 Protein. Proc Natl Acad Sci U S A *109*, 4146-4151. 10.1073/pnas.1200448109. PMC3306724
132. Nakai, W., Yoshida, T., Diez, D., Miyatake, Y., Nishibu, T., Imawaka, N., Naruse, K., Sadamura, Y., and Hanayama, R. (2016). A Novel Affinity-Based Method for the Isolation of Highly Purified Extracellular Vesicles. Sci Rep *6*, 33935. 10.1038/srep33935. PMC5034288
133. Nanbo, A., Noda, T., and Ohba, Y. (2018). Epstein-Barr Virus Acquires Its Final Envelope on Intracellular Compartments with Golgi Markers. Front Microbiol *9*, 454. 10.3389/fmicb.2018.00454. PMC5864893
134. Nasiri Kenari, A., Cheng, L., and Hill, A.F. (2020). Methods for Loading Therapeutics into Extracellular Vesicles and Generating Extracellular Vesicles Mimetic-Nanovesicles. Methods *177*, 103-113. 10.1016/j.ymeth.2020.01.001.
135. Nazimek, K., Bryniarski, K., Ptak, W., Groot Kormelink, T., and Askenase, P.W. (2020). Orally Administered Exosomes Suppress Mouse Delayed-Type Hypersensitivity by Delivering miRNA-150 to Antigen-Primed Macrophage Apc Targeted by Exosome-Surface Anti-Peptide Antibody Light Chains. Int J Mol Sci *21*. 10.3390/ijms21155540. PMC7432818
136. Nguyen, L., McCord, K.A., Bui, D.T., Bouwman, K.M., Kitova, E.N., Elaish, M., Kumawat, D., Daskhan, G.C., Tomris, I., Han, L.*, et al.* (2022). Sialic Acid-Containing Glycolipids Mediate Binding and Viral Entry of SARS-CoV-2. Nat Chem Biol *18*, 81-90. 10.1038/s41589-021-00924-1.
137. Nicolson, G.L., and Ferreira de Mattos, G. (2021). A Brief Introduction to Some Aspects of the Fluid-Mosaic Model of Cell Membrane Structure and Its Importance in Membrane Lipid Replacement. Membranes (Basel) *11*. 10.3390/membranes11120947. PMC8708848
138. Nolan, J.P. (2015). Flow Cytometry of Extracellular Vesicles: Potential, Pitfalls, and Prospects. Curr Protoc Cytom *73*, 13 14 11-13 14 16. 10.1002/0471142956.cy1314s73.
139. Nolan, J.P., and Duggan, E. (2018). Analysis of Individual Extracellular Vesicles by Flow Cytometry. Methods Mol Biol *1678*, 79-92. 10.1007/978-1-4939-7346-0_5.
140. Nolte-'t Hoen, E., Cremer, T., Gallo, R.C., and Margolis, L.B. (2016). Extracellular Vesicles and Viruses: Are They Close Relatives? Proc Natl Acad Sci U S A *113*, 9155-9161. 10.1073/pnas.1605146113. PMC4995926
141. Nolte-'t Hoen, E.N., Buermans, H.P., Waasdorp, M., Stoorvogel, W., Wauben, M.H., and t Hoen, P.A. (2012). Deep Sequencing of RNA from Immune Cell-Derived Vesicles Uncovers the Selective Incorporation of Small Non-Coding RNA Biotypes with Potential Regulatory Functions. Nucleic Acids Res *40*, 9272-9285. 10.1093/nar/gks658. PMC3467056
142. O'Brien, J., Hayder, H., Zayed, Y., and Peng, C. (2018). Overview of Microrna Biogenesis, Mechanisms of Actions, and Circulation. Front Endocrinol (Lausanne) *9*, 402. 10.3389/fendo.2018.00402. PMC6085463
143. O'Brien, K., Breyne, K., Ughetto, S., Laurent, L.C., and Breakefield, X.O. (2020). RNA Delivery by Extracellular Vesicles in Mammalian Cells and Its Applications. Nat Rev Mol Cell Biol *21*, 585-606. 10.1038/s41580-020-0251-y. PMC7249041

144. O'Brien, K., Ughetto, S., Mahjoum, S., Nair, A.V., and Breakefield, X.O. (2022). Uptake, Functionality, and Re-Release of Extracellular Vesicle-Encapsulated Cargo. Cell Rep *39*, 110651. 10.1016/j.celrep.2022.110651.
145. Owen, I., and Shewmaker, F. (2019). The Role of Post-Translational Modifications in the Phase Transitions of Intrinsically Disordered Proteins. Int J Mol Sci *20*. 10.3390/ijms20215501. PMC6861982
146. Parvez, M.K. (2020). Geometric Architecture of Viruses. World J Virol *9*, 5-18. 10.5501/wjv.v9.i2.5. PMC7459239
147. Patton, M.C., Zubair, H., Khan, M.A., Singh, S., and Singh, A.P. (2020). Hypoxia Alters the Release and Size Distribution of Extracellular Vesicles in Pancreatic Cancer Cells to Support Their Adaptive Survival. J Cell Biochem *121*, 828-839. 10.1002/jcb.29328. PMC6878126
148. Perez-Boza, J., Lion, M., and Struman, I. (2018). Exploring the RNA Landscape of Endothelial Exosomes. RNA *24*, 423-435. 10.1261/rna.064352.117. PMC5824360
149. Pospichalova, V., Svoboda, J., Dave, Z., Kotrbova, A., Kaiser, K., Klemova, D., Ilkovics, L., Hampl, A., Crha, I., Jandakova, E.*, et al.* (2015). Simplified Protocol for Flow Cytometry Analysis of Fluorescently Labeled Exosomes and Microvesicles Using Dedicated Flow Cytometer. J Extracell Vesicles *4*, 25530. 10.3402/jev.v4.25530. PMC4382613
150. Prabhu, L., Hartley, A.V., Martin, M., Warsame, F., Sun, E., and Lu, T. (2015). Role of Post-Translational Modification of the Y Box Binding Protein 1 in Human Cancers. Genes Dis *2*, 240-246. 10.1016/j.gendis.2015.05.001. PMC6150071
151. Puertollano, R., Martinez-Menarguez, J.A., Batista, A., Ballesta, J., and Alonso, M.A. (2001). An Intact Dilysine-Like Motif in the Carboxyl Terminus of MAL Is Required for Normal Apical Transport of the Influenza Virus Hemagglutinin Cargo Protein in Epithelial Madin-Darby Canine Kidney Cells. Mol Biol Cell *12*, 1869-1883. 10.1091/mbc.12.6.1869. PMC37348
152. Ray, D., Kazan, H., Chan, E.T., Pena Castillo, L., Chaudhry, S., Talukder, S., Blencowe, B.J., Morris, Q., and Hughes, T.R. (2009). Rapid and Systematic Analysis of the RNA Recognition Specificities of RNA-Binding Proteins. Nat Biotechnol *27*, 667-670. 10.1038/nbt.1550.
153. Rhee, W.J., and Jeong, S. (2017). Extracellular Vesicle miRNA Detection Using Molecular Beacons. Methods Mol Biol *1660*, 287-294. 10.1007/978-1-4939-7253-1_23.
154. Roberts-Dalton, H.D., Cocks, A., Falcon-Perez, J.M., Sayers, E.J., Webber, J.P., Watson, P., Clayton, A., and Jones, A.T. (2017). Fluorescence Labelling of Extracellular Vesicles Using a Novel Thiol-Based Strategy for Quantitative Analysis of Cellular Delivery and Intracellular Traffic. Nanoscale *9*, 13693-13706. 10.1039/c7nr04128d.
155. Rookhuizen, D.C., Bonte, P.-E., Ye, M., Hoyler, T., Gentili, M., Burgdorf, N., Durand, S., Aprahamian, F., Kroemer, G., Manel, N.*, et al.* (2021). Induction of Transposable Element Expression Is Central to Innate Sensing. bioRxiv, 2021.2009.2010.457789. 10.1101/2021.09.10.457789.
156. Rosa-Fernandes, L., Rocha, V.B., Carregari, V.C., Urbani, A., and Palmisano, G. (2017). A Perspective on Extracellular Vesicles Proteomics. Front Chem *5*, 102. 10.3389/fchem.2017.00102. PMC5702361

157. Rubio-Ramos, A., Labat-de-Hoz, L., Correas, I., and Alonso, M.A. (2021). The MAL Protein, an Integral Component of Specialized Membranes, in Normal Cells and Cancer. Cells *10*. 10.3390/cells10051065. PMC8145151
158. Sanchez-Pulido, L., Martin-Belmonte, F., Valencia, A., and Alonso, M.A. (2002). Marvel: A Conserved Domain Involved in Membrane Apposition Events. Trends Biochem Sci *27*, 599-601. 10.1016/s0968-0004(02)02229-6.
159. Sato, Y., Yaguchi, M., Okuno, Y., Ishimaru, H., Sagou, K., Ozaki, S., Suzuki, T., Inagaki, T., Umeda, M., Watanabe, T*., et al.* (2022). Epstein-Barr Virus Tegument Protein Bglf2 in Exosomes Released from Virus-Producing Cells Facilitates De Novo Infection. Cell Commun Signal *20*, 95. 10.1186/s12964-022-00902-7. PMC9210680
160. Segura, E., Nicco, C., Lombard, B., Veron, P., Raposo, G., Batteux, F., Amigorena, S., and Thery, C. (2005). ICAM-1 on Exosomes from Mature Dendritic Cells Is Critical for Efficient Naive T-Cell Priming. Blood *106*, 216-223. 10.1182/blood-2005-01-0220.
161. Sevenler, D., Daaboul, G.G., Ekiz Kanik, F., Unlu, N.L., and Unlu, M.S. (2018). Digital Microarrays: Single-Molecule Readout with Interferometric Detection of Plasmonic Nanorod Labels. ACS Nano *12*, 5880-5887. 10.1021/acsnano.8b02036.
162. Shelke, G.V., Lasser, C., Gho, Y.S., and Lotvall, J. (2014). Importance of Exosome Depletion Protocols to Eliminate Functional and RNA-Containing Extracellular Vesicles from Fetal Bovine Serum. J Extracell Vesicles *3*, 24783. 10.3402/jev.v3.24783. PMC4185091
163. Shukuya, T., Ghai, V., Amann, J.M., Okimoto, T., Shilo, K., Kim, T.K., Wang, K., and Carbone, D.P. (2020). Circulating Micrornas and Extracellular Vesicle-Containing Micrornas as Response Biomarkers of Anti-Programmed Cell Death Protein 1 or Programmed Death-Ligand 1 Therapy in Nsclc. J Thorac Oncol *15*, 1773-1781. 10.1016/j.jtho.2020.05.022. PMC7641981
164. Shurtleff, M.J., Temoche-Diaz, M.M., Karfilis, K.V., Ri, S., and Schekman, R. (2016). Y-Box Protein 1 Is Required to Sort microRNAs into Exosomes in Cells and in a Cell-Free Reaction. Elife *5*, e19276. 10.7554/eLife.19276. PMC5047747
165. Shurtleff, M.J., Temoche-Diaz, M.M., and Schekman, R. (2018). Extracellular Vesicles and Cancer: Caveat Lector. Annual Review of Cancer Biology, Vol 2 *2*, 395-411. 10.1146/annurev-cancerbio-030617-050519.
166. Shurtleff, M.J., Yao, J., Qin, Y., Nottingham, R.M., Temoche-Diaz, M.M., Schekman, R., and Lambowitz, A.M. (2017). Broad Role for YBX1 in Defining the Small Noncoding RNA Composition of Exosomes. Proc Natl Acad Sci U S A *114*, E8987-E8995. 10.1073/pnas.1712108114. PMC5663387
167. Silva, A.M., Lazaro-Ibanez, E., Gunnarsson, A., Dhande, A., Daaboul, G., Peacock, B., Osteikoetxea, X., Salmond, N., Friis, K.P., Shatnyeva, O*., et al.* (2021). Quantification of Protein Cargo Loading into Engineered Extracellular Vesicles at Single-Vesicle and Single-Molecule Resolution. J Extracell Vesicles *10*, e12130. 10.1002/jev2.12130. PMC8329990
168. Skendros, P., Mitroulis, I., and Ritis, K. (2018). Autophagy in Neutrophils: From Granulopoiesis to Neutrophil Extracellular Traps. Front Cell Dev Biol *6*, 109. 10.3389/fcell.2018.00109. PMC6131573
169. Skogberg, G., Gudmundsdottir, J., van der Post, S., Sandstrom, K., Bruhn, S., Benson, M., Mincheva-Nilsson, L., Baranov, V., Telemo, E., and Ekwall, O. (2013). Characterization of

Human Thymic Exosomes. PLoS One *8*, e67554. 10.1371/journal.pone.0067554. PMC3699640
170. Skotland, T., Sagini, K., Sandvig, K., and Llorente, A. (2020). An Emerging Focus on Lipids in Extracellular Vesicles. Adv Drug Deliv Rev *159*, 308-321. 10.1016/j.addr.2020.03.002.
171. Sork, H., Corso, G., Krjutskov, K., Johansson, H.J., Nordin, J.Z., Wiklander, O.P.B., Lee, Y.X.F., Westholm, J.O., Lehtio, J., Wood, M.J.A*., et al.* (2018). Heterogeneity and Interplay of the Extracellular Vesicle Small RNA Transcriptome and Proteome. Sci Rep *8*, 10813. 10.1038/s41598-018-28485-9. PMC6050237
172. Spiniello, M., Steinbrink, M.I., Cesnik, A.J., Miller, R.M., Scalf, M., Shortreed, M.R., and Smith, L.M. (2019). Comprehensive in Vivo Identification of the c-Myc mRNA Protein Interactome Using Hypr-Ms. RNA *25*, 1337-1352. 10.1261/rna.072157.119. PMC6800478
173. Srinivasan, S., Su, M., Ravishankar, S., Moore, J., Head, P., Dixon, J.B., and Vannberg, F. (2017). TLR-Exosomes Exhibit Distinct Kinetics and Effector Function. Sci Rep *7*, 41623. 10.1038/srep41623. PMC5349571
174. Statello, L., Maugeri, M., Garre, E., Nawaz, M., Wahlgren, J., Papadimitriou, A., Lundqvist, C., Lindfors, L., Collen, A., Sunnerhagen, P*., et al.* (2018). Identification of RNA-Binding Proteins in Exosomes Capable of Interacting with Different Types of RNA: Rbp-Facilitated Transport of RNAs into Exosomes. PLoS One *13*, e0195969. 10.1371/journal.pone.0195969. PMC5918169
175. Stoner, S.A., Duggan, E., Condello, D., Guerrero, A., Turk, J.R., Narayanan, P.K., and Nolan, J.P. (2016). High Sensitivity Flow Cytometry of Membrane Vesicles. Cytometry A *89*, 196-206. 10.1002/cyto.a.22787.
176. Suarez, H., Gamez-Valero, A., Reyes, R., Lopez-Martin, S., Rodriguez, M.J., Carrascosa, J.L., Cabanas, C., Borras, F.E., and Yanez-Mo, M. (2017). A Bead-Assisted Flow Cytometry Method for the Semi-Quantitative Analysis of Extracellular Vesicles. Sci Rep *7*, 11271. 10.1038/s41598-017-11249-2. PMC5595788
177. Suresh, P.S., Tsutsumi, R., and Venkatesh, T. (2018). YBX1 at the Crossroads of Non-Coding Transcriptome, Exosomal, and Cytoplasmic Granular Signaling. Eur J Cell Biol *97*, 163-167. 10.1016/j.ejcb.2018.02.003.
178. Swaim, C.D., Canadeo, L.A., Monte, K.J., Khanna, S., Lenschow, D.J., and Huibregtse, J.M. (2020). Modulation of Extracellular Isg15 Signaling by Pathogens and Viral Effector Proteins. Cell Rep *31*, 107772. 10.1016/j.celrep.2020.107772. PMC7297157
179. Szostak, J.W. (2012). The Eightfold Path to Non-Enzymatic RNA Replication. Journal of Systems Chemistry *3*, 2. 10.1186/1759-2208-3-2.
180. Szostak, N., Royo, F., Rybarczyk, A., Szachniuk, M., Blazewicz, J., del Sol, A., and Falcon-Perez, J.M. (2014). Sorting Signal Targeting mRNA into Hepatic Extracellular Vesicles. RNA Biol *11*, 836-844. 10.4161/rna.29305. PMC4179958
181. Taylor, S., Isobe, S., Cao, A., Contrepois, K., Benayoun, B.A., Jiang, L., Wang, L., Melemenidis, S., Ozen, M.O., Otsuki, S*., et al.* (2022). Endogenous Retroviral Elements Generate Pathologic Neutrophils in Pulmonary Arterial Hypertension. Am J Respir Crit Care Med. 10.1164/rccm.202102-0446OC.

182. Tejedor, A.R., Garaizar, A., Ramirez, J., and Espinosa, J.R. (2021). 'RNA Modulation of Transport Properties and Stability in Phase-Separated Condensates. Biophys J *120*, 5169-5186. 10.1016/j.bpj.2021.11.003. PMC8715277
183. Temerozo, J.R., Fintelman-Rodrigues, N., Dos Santos, M.C., Hottz, E.D., Sacramento, C.Q., de Paula Dias da Silva, A., Mandacaru, S.C., Dos Santos Moraes, E.C., Trugilho, M.R.O., Gesto, J.S.M.*, et al.* (2022). Human Endogenous Retrovirus K in the Respiratory Tract Is Associated with COVID-19 Physiopathology. Microbiome *10*, 65. 10.1186/s40168-022-01260-9. PMC9024070
184. Temoche-Diaz, M.M., Shurtleff, M.J., Nottingham, R.M., Yao, J., Fadadu, R.P., Lambowitz, A.M., and Schekman, R. (2019). Distinct Mechanisms of microRNA Sorting into Cancer Cell-Derived Extracellular Vesicle Subtypes. Elife *8*, 612069. 10.7554/eLife.47544. PMC6728143
185. Thery, C., Witwer, K.W., Aikawa, E., Alcaraz, M.J., Anderson, J.D., Andriantsitohaina, R., Antoniou, A., Arab, T., Archer, F., Atkin-Smith, G.K.*, et al.* (2018). Minimal Information for Studies of Extracellular Vesicles 2018 (MISEV2018): A Position Statement of the International Society for Extracellular Vesicles and Update of the MISEV2014 Guidelines. J Extracell Vesicles *7*, 1535750. 10.1080/20013078.2018.1535750. PMC6322352
186. Tkach, M., Kowal, J., and Thery, C. (2018). Why the Need and How to Approach the Functional Diversity of Extracellular Vesicles. Philos Trans R Soc Lond B Biol Sci *373*. 10.1098/rstb.2016.0479. PMC5717434
187. Todkar, K., Chikhi, L., Desjardins, V., El-Mortada, F., Pepin, G., and Germain, M. (2021). Selective Packaging of Mitochondrial Proteins into Extracellular Vesicles Prevents the Release of Mitochondrial Damps. Nat Commun *12*, 1971. 10.1038/s41467-021-21984-w. PMC8009912
188. Turchinovich, A., Drapkina, O., and Tonevitsky, A. (2019). Transcriptome of Extracellular Vesicles: State-of-the-Art. Front Immunol *10*, 202. 10.3389/fimmu.2019.00202. PMC6404625
189. Ueta, E., Tsutsumi, K., Kato, H., Matsushita, H., Shiraha, H., Fujii, M., Matsumoto, K., Horiguchi, S., and Okada, H. (2021). Extracellular Vesicle-Shuttled miRNAs as a Diagnostic and Prognostic Biomarker and Their Potential Roles in Gallbladder Cancer Patients. Sci Rep *11*, 12298. 10.1038/s41598-021-91804-0. PMC8192895
190. Vagner, T., Spinelli, C., Minciacchi, V.R., Balaj, L., Zandian, M., Conley, A., Zijlstra, A., Freeman, M.R., Demichelis, F., De, S.*, et al.* (2018). Large Extracellular Vesicles Carry Most of the Tumour DNA Circulating in Prostate Cancer Patient Plasma. J Extracell Vesicles *7*, 1505403. 10.1080/20013078.2018.1505403. PMC6084494
191. Valadi, H., Ekstrom, K., Bossios, A., Sjostrand, M., Lee, J.J., and Lotvall, J.O. (2007). Exosome-Mediated Transfer of mRNAs and microRNAs Is a Novel Mechanism of Genetic Exchange between Cells. Nat Cell Biol *9*, 654-659. 10.1038/ncb1596.
192. van der Pol, E., van Leeuwen, T.G., and Yan, X. (2021). Misinterpretation of Solid Sphere Equivalent Refractive Index Measurements and Smallest Detectable Diameters of Extracellular Vesicles by Flow Cytometry. Sci Rep *11*, 24151. 10.1038/s41598-021-03015-2. PMC8683472
193. van der Vlist, E.J., Nolte-'t Hoen, E.N., Stoorvogel, W., Arkesteijn, G.J., and Wauben, M.H. (2012). Fluorescent Labeling of Nano-Sized Vesicles Released by Cells and Subsequent

Quantitative and Qualitative Analysis by High-Resolution Flow Cytometry. Nat Protoc *7*, 1311-1326. 10.1038/nprot.2012.065.
194. van Niel, G., D'Angelo, G., and Raposo, G. (2018). Shedding Light on the Cell Biology of Extracellular Vesicles. Nat Rev Mol Cell Biol *19*, 213-228. 10.1038/nrm.2017.125.
195. Ventimiglia, L.N., Fernandez-Martin, L., Martinez-Alonso, E., Anton, O.M., Guerra, M., Martinez-Menarguez, J.A., Andres, G., and Alonso, M.A. (2015). Cutting Edge: Regulation of Exosome Secretion by the Integral MAL Protein in T Cells. J Immunol *195*, 810-814. 10.4049/jimmunol.1500891.
196. Verweij, F.J., Balaj, L., Boulanger, C.M., Carter, D.R.F., Compeer, E.B., D'Angelo, G., El Andaloussi, S., Goetz, J.G., Gross, J.C., Hyenne, V.*, et al.* (2021). The Power of Imaging to Understand Extracellular Vesicle Biology in Vivo. Nat Methods *18*, 1013-1026. 10.1038/s41592-021-01206-3. PMC8796660
197. Vidal, M. (2019). Exosomes: Revisiting Their Role as "Garbage Bags". Traffic *20*, 815-828. 10.1111/tra.12687.
198. Villarroya-Beltri, C., Baixauli, F., Gutiérrez-Vázquez, C., Sánchez-Madrid, F., and Mittelbrunn, M. (2014). Sorting It Out: Regulation of Exosome Loading. Paper presented at: Seminars in cancer biology (Elsevier).
199. Villarroya-Beltri, C., Gutierrez-Vazquez, C., Sanchez-Cabo, F., Perez-Hernandez, D., Vazquez, J., Martin-Cofreces, N., Martinez-Herrera, D.J., Pascual-Montano, A., Mittelbrunn, M., and Sanchez-Madrid, F. (2013). Sumoylated hnRNPA2B1 Controls the Sorting of miRNAs into Exosomes through Binding to Specific Motifs. Nat Commun *4*, 2980. 10.1038/ncomms3980. PMC3905700
200. Wang, W., Peng, X., Zhao, L., Zhao, H., and Gu, Q. (2022). Extracellular Vesicles from Bone Marrow Mesenchymal Stem Cells Inhibit Apoptosis and Autophagy of Ischemia-Hypoxia Cardiomyocyte Line in Vitro by Carrying Mir-144-3p to Inhibit ROCK1. Curr Stem Cell Res Ther. 10.2174/1574888X17666220503192941.
201. Wee, L.M., Flores-Jasso, C.F., Salomon, W.E., and Zamore, P.D. (2012). Argonaute Divides Its RNA Guide into Domains with Distinct Functions and RNA-Binding Properties. Cell *151*, 1055-1067. 10.1016/j.cell.2012.10.036. PMC3595543
202. Weidensdorfer, D., Stohr, N., Baude, A., Lederer, M., Kohn, M., Schierhorn, A., Buchmeier, S., Wahle, E., and Huttelmaier, S. (2009). Control of C-Myc mRNA Stability by IGF2BP1-associated Cytoplasmic RNPs. RNA *15*, 104-115. 10.1261/rna.1175909. PMC2612774
203. Welsh, J.A., Holloway, J.A., Wilkinson, J.S., and Englyst, N.A. (2017). Extracellular Vesicle Flow Cytometry Analysis and Standardization. Front Cell Dev Biol *5*, 78. 10.3389/fcell.2017.00078. PMC5582084
204. Weston, S., and Frieman, M.B. (2020). COVID-19: Knowns, Unknowns, and Questions. mSphere *5*, e00203-00220. 10.1128/mSphere.00203-20. PMC7082143
205. Whitham, M., Parker, B.L., Friedrichsen, M., Hingst, J.R., Hjorth, M., Hughes, W.E., Egan, C.L., Cron, L., Watt, K.I., Kuchel, R.P.*, et al.* (2018). Extracellular Vesicles Provide a Means for Tissue Crosstalk During Exercise. Cell Metab *27*, 237-251 e234. 10.1016/j.cmet.2017.12.001.
206. Wiklander, O.P.B., Bostancioglu, R.B., Welsh, J.A., Zickler, A.M., Murke, F., Corso, G., Felldin, U., Hagey, D.W., Evertsson, B., Liang, X.M.*, et al.* (2018). Systematic Methodological Evaluation of a Multiplex Bead-Based Flow Cytometry Assay for

Detection of Extracellular Vesicle Surface Signatures. Front Immunol *9*, 1326. 10.3389/fimmu.2018.01326. PMC6008374
207. Witwer, K.W., and Wolfram, J. (2021). Extracellular Vesicles Versus Synthetic Nanoparticles for Drug Delivery. Nature Reviews Materials *6*, 103-106. 10.1038/s41578-020-00277-6.
208. Woith, E., Fuhrmann, G., and Melzig, M.F. (2019). Extracellular Vesicles-Connecting Kingdoms. Int J Mol Sci *20*. 10.3390/ijms20225695. PMC6888613
209. Wolf, P. (1967). The Nature and Significance of Platelet Products in Human Plasma. Br J Haematol *13*, 269-288. 10.1111/j.1365-2141.1967.tb08741.x.
210. Xu, H., Zheng, L., Zhou, Y., and Ye, B.C. (2021). An Artificial Enzyme Cascade Amplification Strategy for Highly Sensitive and Specific Detection of Breast Cancer-Derived Exosomes. Analyst *146*, 5542-5549. 10.1039/d1an01071a.
211. Yanez-Mo, M., Siljander, P.R., Andreu, Z., Zavec, A.B., Borras, F.E., Buzas, E.I., Buzas, K., Casal, E., Cappello, F., Carvalho, J.*, et al.* (2015). Biological Properties of Extracellular Vesicles and Their Physiological Functions. J Extracell Vesicles *4*, 27066. 10.3402/jev.v4.27066. PMC4433489
212. Yanshina, D.D., Kossinova, O.A., Gopanenko, A.V., Krasheninina, O.A., Malygin, A.A., Venyaminova, A.G., and Karpova, G.G. (2018). Structural Features of the Interaction of the 3'-Untranslated Region of mRNA Containing Exosomal RNA-Specific Motifs with YB-1, a Potential Mediator of mRNA Sorting. Biochimie *144*, 134-143. 10.1016/j.biochi.2017.11.007.
213. Yokoi, A., Villar-Prados, A., Oliphint, P.A., Zhang, J., Song, X., De Hoff, P., Morey, R., Liu, J., Roszik, J., Clise-Dwyer, K.*, et al.* (2019). Mechanisms of Nuclear Content Loading to Exosomes. Sci Adv *5*, eaax8849. 10.1126/sciadv.aax8849. PMC6867874
214. Zhang, H., Freitas, D., Kim, H.S., Fabijanic, K., Li, Z., Chen, H., Mark, M.T., Molina, H., Martin, A.B., Bojmar, L.*, et al.* (2018). Identification of Distinct Nanoparticles and Subsets of Extracellular Vesicles by Asymmetric Flow Field-Flow Fractionation. Nat Cell Biol *20*, 332-343. 10.1038/s41556-018-0040-4. PMC5931706
215. Zhang, L., Hou, D., Chen, X., Li, D., Zhu, L., Zhang, Y., Li, J., Bian, Z., Liang, X., Cai, X.*, et al.* (2012). Exogenous Plant Mir168a Specifically Targets Mammalian LDLRAP1: Evidence of Cross-Kingdom Regulation by microRNA. Cell Res *22*, 107-126. 10.1038/cr.2011.158. PMC3351925
216. Zhang, Q., Higginbotham, J.N., Jeppesen, D.K., Yang, Y.P., Li, W., McKinley, E.T., Graves-Deal, R., Ping, J., Britain, C.M., Dorsett, K.A.*, et al.* (2019a). Transfer of Functional Cargo in Exomeres. Cell Rep *27*, 940-954 e946. 10.1016/j.celrep.2019.01.009. PMC6559347
217. Zhang, Q., Jeppesen, D.K., Higginbotham, J.N., Graves-Deal, R., Trinh, V.Q., Ramirez, M.A., Sohn, Y., Neininger, A.C., Taneja, N., McKinley, E.T.*, et al.* (2021). Supermeres Are Functional Extracellular Nanoparticles Replete with Disease Biomarkers and Therapeutic Targets. Nat Cell Biol *23*, 1240-1254. 10.1038/s41556-021-00805-8. PMC8656144
218. Zhang, Y., Huang, M., Jiang, L., Li, T., Wang, J., Zhao, L., and Zhou, J. (2022). Autophagy Inhibitors Enhance Biomolecular Delivery Efficiency of Extracellular Vesicles. Biochem Biophys Res Commun *603*, 130-137. 10.1016/j.bbrc.2022.03.006.
219. Zhang, Y., Liu, D., Chen, X., Li, J., Li, L., Bian, Z., Sun, F., Lu, J., Yin, Y., Cai, X.*, et al.* (2010). Secreted Monocytic miR-150 Enhances Targeted Endothelial Cell Migration. Mol Cell *39*, 133-144. 10.1016/j.molcel.2010.06.010. PMID: 20603081

220. Zhang, Y., Meng, J., Zhang, L., Ramkrishnan, S., and Roy, S. (2019b). Extracellular Vesicles with Exosome-Like Features Transfer Tlrs between Dendritic Cells. Immunohorizons *3*, 186-193. 10.4049/immunohorizons.1900016. PMC8011940
221. Zhou, J., Li, X.Y., Liu, Y.J., Feng, J., Wu, Y., Shen, H.M., and Lu, G.D. (2022). Full-Coverage Regulations of Autophagy by ROS: From Induction to Maturation. Autophagy *18*, 1240-1255. 10.1080/15548627.2021.1984656.
222. Zubarev, I., Vladimirtsev, D., Vorontsova, M., Blatov, I., Shevchenko, K., Zvereva, S., Lunev, E.A., Faizuloev, E., and Barlev, N. (2021). Viral Membrane Fusion Proteins and RNA Sorting Mechanisms for the Molecular Delivery by Exosomes. Cells *10*. 10.3390/cells10113043. PMC8622164

Chapter 2: INTRODUCTION TO NEUTROPHIL BIOLOGY

NEUTROPHIL DEVELOPMENT IN THE BONE MARROW

Polymorphonuclear neutrophils (PMNs) are the most abundant leukocyte in the bone marrow (BM) and circulation. PMNs are short-lived cells with an estimated half-life of just a few hours to at most a few days (Pillay et al., 2010). Thus, to constantly replenish the circulating population of PMNs, granulopoiesis is a rapid and energy-intensive process with an estimated 1e9 PMNs/kg/day (roughly 1e11 PMNs/day) being produced in the BM of humans (Dancey et al., 1976; Price et al., 1996). It takes a remarkable amount of cellular division occurring in the BM for granulopoiesis to proceed from hematopoietic stem cells (HSCs) to the multipotent progenitors (MPPs) to promyelocytes all the way through to mature PMNs. This process is under strict regulation to prevent the emergence of cancerous cells or cells that may be damaging to the host. Mature PMNs released from the BM circulate in the bloodstream looking for damage-associated molecular patterns (DAMPs) and pathogen-associated molecular patterns (PAMPs) that may be present in either a sterile or infected tissue microenvironments. PMNs, and the other innate immune cells such as eosinophils, basophils, monocytes, macrophages, and myeloid-derived dendritic cells, are constantly patrolling and interacting with cells and their remnants to maintain homeostasis.

The HSCs are slowly dividing cells capable of self-renewal and differentiation into MPPs (Orkin and Zon, 2008). MPPs differentiate into lineage-restricted, e.g., common myeloid (CMP) or common lymphoid (CLP), progenitors. In humans, PMNs originate primarily from CMPs. Granulocyte-monocyte progenitors (GMPs) are the typical intermediate population between CMPs and committed neutrophil progenitors in the human BM at steady-state. GMPs are a key

branch point between neutrophil and monocyte/macrophage production, under control of several transcription factors including PU.1, Gfi-1, and Irf8. However, alternative paths exist under stress conditions that may bypass the CMP stage and proceed via the recently discovered PMN-restricted precursor (NeuP) (Kwok et al., 2020; Hidalgo and Casanova-Acebes, 2021; McKenna et al., 2021). In addition, mature segmented PMNs may be subcategorized based upon their transcriptional states as recently shown using scRNA-seq data of circulating PMNs (Wigerblad et al., 2022).

PMN differentiation occurs in six stages, beginning with myeloblasts [Stage 1], which differentiate into promyelocytes [Stage 2] and then myelocytes [Stage 3]. These first 3 stages are pre-mitotic, i.e., these precursors are endowed with the ability to expand. The next three stages are post-mitotic, i.e., the cells differentiate without expanding, yielding metamyelocytes [Stage 4], then band cells [Stage 5], and finally segmented neutrophils [Stage 6], which can leave the BM (Borregaard, 2010). Under certain inflammatory conditions, band cells as well as lower density segmented PMNs are observed in circulation (Sun et al., 2022). Low density PMNs are also observed in certain healthy individuals at rest (Hardisty et al., 2021). Mature PMNs are considered terminally differentiated, and replication-incompetent as they appear arrested in the G0 phase and yet, contain various cyclin-dependent kinases and express the proliferating cell nuclear antigen (Rossi et al., 2006; Leitch et al., 2010; Witko-Sarsat et al., 2010). Despite this apparent arrested state, mature PMNs have been demonstrated in recent years to exhibit significant plasticity upon recruitment to peripheral tissues, leading to starkly different downstream fates and effector functions including phagocytosis, NETosis (neutrophil

extracellular trap formation), and hyperexocytosis, which may be affected to differing extents by precursor poise and tissue cues (Margaroli and Tirouvanziam, 2016; Rosales, 2018).

PMNs compartmentalize their effector proteins into different granule and secretory vesicle fractions. The primary (azurophilic) granules contain the most potent effector molecules such as NE and other proteases and cathepsins, MPO, and α-defensins and are coated in the tetraspanin CD63 (Borregaard and Cowland, 1997). They are formed during the promyelocyte stage and are the last subset of granules to be released upon activation of a mature PMN. The secondary (specific) granules contain lactoferrin, lysozyme, collagenases and other proteins that aid in initiating an immune response against invading pathogens, as well as CD66b on the membrane. The tertiary (gelatinase) granules are readily mobilized upon PMN activation, and as their name suggests contain gelatinase as well as lysozyme and matrix metalloprotease 9 (MMP9). The secretory vesicles, which are formed by inward pinching of the plasma membrane at the segmented PMN stage contain CR1, CD16 and pattern recognition receptors that can be rapidly mobilized to the cell membrane in the early phase of PMN priming prior to activation.

There is no clear signal peptide sequence that target specific proteins to each type of PMN granule. This has led to the notion that the cargo of granules reflects the gene expression pattern during the differentiation stage in which they were formed (Bardoel et al., 2014). Since the loading is nonspecific, the classification of granules is not completely discrete. For example, gelatinase, which gives its name to the tertiary granules is also found in small amounts in secondary granules. In addition, particular amino acid motifs are enriched in granular compared to cytosolic proteins, as well as between granule subsets (Benson et al., 2003; Nakatsu and Ohno, 2003; Borregaard, 2010; Kallquist et al., 2010; Sheshachalam et al., 2014) and certain

post-translational modifications such as paucimannose N-glycans and N-acetyllactosamine (Venkatakrishnan et al., 2020; Reiding et al., 2021) may contribute to granule protein sorting.

There is a variety of transcription factors relevant for maturation of developing PMNs and expression of granule proteins, however the transcription factor family of CCAAT enhancer binding proteins (C/EBP) is clearly central to this process (Ramji and Foka, 2002). The C/EBP family has six members and many including the α and β members can have multiple isoforms generated through alternative splicing, differential promoter use, translation initiation and/or proteolysis (Ramji and Foka, 2002). G-CSF is the main cytokine promoting proliferation and maturation of PMNs in the BM. Stimulation of the G-CSF receptor induces STAT3 phosphorylation in BM progenitor cells, which results in C/EBPα and β expression (Akagi et al., 2008; Iida et al., 2008). The other C/EBP members are thought to be more inhibitory due to lacking the transactivation domain, which is present at the N-terminus (Cloutier et al., 2009).

During homeostatic ("steady-state") conditions, the differentiation of PMNs is controlled mainly by the transcription factors C/EBPα, as well as Gfi-1 and Lef1, which quickly decrease upon reaching the promyelocyte stage, whereas C/EBPα is expressed in GMPs and myeloblasts and then decreases (Radomska et al., 1998; Yeamans et al., 2007). C/EBPβ is the main transcription factor needed to reach the final stage of mature, segmented PMNs and is used during "emergency granulopoiesis" as observed during active infections (Bjerregaard et al., 2003; Cain et al., 2011). Other stimuli in addition to G-CSF, such as GM-CSF, IL-3, and IL-6, can induce the expression of C/EBPβ in myeloblasts and promyelocytes, thereby mobilizing PMN progenitors and increasing their rate of differentiation (Hirai et al., 2006). Understanding the interplay of these stimuli as well as what controls the direction and rate of differentiation of

the various progenitor stages in both steady state and emergency conditions remains an area of active study.

There is strict control of a variety of transcription factors during granulopoiesis. To this point, C/EBPα and β may antagonize the activity of one another regulating the rate and poise of developing PMNs (Hirai et al., 2006; Lourenco and Coffer, 2017). Indeed, there are no known cases of "neutrophil cancer". Despite this, approximately 9-20% of patients with acute myeloid leukemia exhibit a mutation in the Cebpa gene and many oncogenes have been shown to attenuate C/EBPα function or expression (Nerlov, 2004; Lourenco and Coffer, 2017). In line with these observations, C/EBP regulates steady state granulopoiesis and may serve as an early checkpoint for the induction of PMN differentiation and maturation (Zhang et al., 1997). C/EBPβ$^{-/-}$ mice do not show increased circulating PMN counts upon injection of G-CSF or challenge with *Candida albicans* compared to wild-type mice (Hirai et al., 2006). In addition, over half of mature C/EBPβ$^{-/-}$ PMNs are apoptotic 18 hours after injection with FBS (a negative control which may still be inflammatory due to a response to bovine protein), LPS, and GM-CSF, suggesting that C/EBPβ may also have a functional role in preventing the apoptosis of PMNs (Akagi et al., 2008).

C/EBPβ was observed to be already bound to the IL-8 promoter of primary human PMNs and was phosphorylated after just 15 minutes of LPS stimulation (Cloutier et al., 2009). In addition, C/EBPβ can bind the promoter region of many other inflammatory genes including IL-1α and β, IFNγ, NE, MPO, tumor necrosis factor (TNF) α, nitric oxide synthase (NOS), lactoferrin and many others (Ramji and Foka, 2002). PMNs that have matured in the BM as a result of

C/EBPβ during a phase of emergency granulopoiesis may be predisposed towards expressing these inflammatory molecules once PMNs enter the stressed tissue microenvironment.

The loss of C/EBPα, and expression of other members (mainly C/EBPβ) has been suggested to be a switch for differentiation towards mature PMNs (Nauseef and Borregaard, 2014). However, it has also been observed that C/EBPα can remain level throughout the differentiation process only being lost upon emigration from the BM, although C/EBP family members such as C/EBPδ and ζ are also increased (Bjerregaard et al., 2003). C/EBPγ was observed to quickly decrease after the myeloblast and promyelocyte stages and is considered the only C/EBP member not expressed in post-mitotic PMNs (Bjerregaard et al., 2003).

Typically, only mature PMNs are released from the BM in circulation. During development, the retention marker CXCR4 (which binds to its cognate ligand stromal cell derived factor 1 on the bone marrow stroma) is present on PMN precursors, gradually decreasing as the cells advance through maturation. Meanwhile, the chemokine receptor CXCR2 gradually increases from the myeloblast stage to the mature PMN stage, likely under induction by G-CSF and downstream STAT3 signaling (Nguyen-Jackson et al., 2010). During infection or some other stress, the circulating pool of PMNs is consumed, thus PMN progenitors in the BM are rapidly mobilized to replenish them and meet the increased demand for PMNs at the site of inflammation (Manz and Boettcher, 2014). A constant state of heightened granulopoiesis may result in the release of incompletely differentiated granulocytes into circulation such as band cells and low-density PMNs (Carmona-Rivera and Kaplan, 2013; Ostendorf et al., 2019). Both band cells and low-density PMNs, which are observed at increased

numbers in patients with chronic stress, show an increased propensity for activation than mature PMNs (Carmona-Rivera and Kaplan, 2013; Blanco-Camarillo et al., 2021).

CLEARANCE OF PMNS

To main a steady-state level of circulating PMNs, production and release of mature PMNs must match the rate of PMN clearance by macrophages in the BM, spleen, and liver (Rankin, 2010; Bratton and Henson, 2011; Gordy et al., 2011). It has been observed that efferocytosis of apoptotic PMNs by macrophages results in positive feedback signaling for inflammation resolution via induction the liver X receptor (LXR) family of cholesterol-sensing transcription factors suppressing the production of proinflammatory cytokines such as IL-1β, IL-8, G-CSF, and TNFα by macrophages (Fadok et al., 1998; A. Gonzalez et al., 2009; Korns et al., 2011). The production of the anti-inflammatory cytokine IL-10 does not appear as consistent and may depend on other factors such as age or microbiome (Fadok et al., 1998; A. Gonzalez et al., 2009; Meriwether et al., 2022). In addition, different subsets of macrophages will either increase or decrease production of G-CSF depending upon context. For example, BM stromal macrophages increase G-CSF production upon clearing senescent PMNs (Furze and Rankin, 2008) whereas tissue macrophages decrease G-CSF production as stresses are resolved (Stark et al., 2005; Gordy et al., 2011).

Notably, many of the cytokines that are inhibited as a result of macrophage efferocytosis of PMNs are the same ones involved in cytokine release syndrome or “cytokine storm” observed in cases of sepsis and severe COVID-19, pathologies which also feature massive tissue influx and death of PMNs (Coperchini et al., 2020; Chan et al., 2021). Since the early recruitment of PMNs is impaired in COVID-19 via inhibition of pro-PMN signaling in the

infected epithelium by SARS-CoV-2 (Dobosh et al., 2022) **(See Chapter 5)**, alveolar macrophages, recruited macrophages and/or inflammatory monocytes may initiate the cytokine storm as a consequence of decreased efferocytosis of dying and dead PMNs (Merad and Martin, 2020; Subbarao and Mahanty, 2020). Recruited PMNs may then hyperexocytose their granules and inflammatory cytokines to deal with rampant inflammation resulting in acute respiratory distress syndrome (ARDS), which is a major complication of severe COVID-19 (Chan et al., 2021). Other pathogens have also developed methods to impair the efficacy of PMN efferocytosis by macrophages. For example, phagocytosis of *S. aureus* by PMNs prevented their efferocytosis by cocultured macrophages, allowing the bacterium to persist (Greenlee-Wacker et al., 2014). On the flipside, the association of *P. aeruginosa* with apoptotic PMNs and epithelial cells allows for their co-clearance, making efferocytosis another method of pathogen removal (Capasso et al., 2016; Jager et al., 2021).

Cigarette smoke, in a model of COPD (an acquired disease which mirrors CF in terms of pulmonary presentation) also results in decreased efficiency of PMN efferocytosis, suggesting that the disease process may be driven in part by impaired airway macrophage function (Ito et al., 2020). Interestingly, NE released by activated PMNs can cleave the phosphatidylserine receptor, CD36, thereby decreasing the detection and efferocytosis of apoptotic cells (Vandivier et al., 2002). In addition, oxidized lipoproteins accumulating in the oxidizing conditions of the CF airways (Benabdeslam et al., 1999; Garrel et al., 2007) decrease the activity of c-Mer tyrosine kinase (MerTK), also resulting in decreased efferocytosis (Cai et al., 2017). Taken together, impairment of PMN clearance by tissue-resident macrophages can result in discordant immune responses and failure to clear invading pathogens. In the context of inflammatory airway

diseases, particularly CF, the failure of tissue-resident macrophages to clear apoptotic PMNs and debris is a major contributor to chronic inflammation (Turton et al., 2021).

It is important to consider that the body is constantly challenged by incoming microorganisms. Such a continual presence of an even minimal burden of microorganisms in mucosal areas such as the gut or the airways provides impetus for the BM to sustain a constant rate of PMN production and circulation. This is supported by the observation that aseptic mice have lower levels of circulating PMNs than mice caged under normal conditions. Upon occurrence of a larger microbial load (acute infection in the lung, chronic dysbiosis in the gut), the release of typical inflammatory factors such as the IL-1 family of cytokines, TNFα, G-CSF, and GM-CSF can upregulate the production of PMNs from the BM into circulation.

PMN ACTIVATION

PMN activation in tissue is preceded by their *diapedesis* through the endothelial barrier, and their subsequent *swarming* into tissue entry and migration, which may culminate in their trans-epithelial migration ("*transmigration*") in mucosal environments. Diapedesis of PMNs through the activated endothelium close to the site of stress/injury depends on β2 integrins, while swarming depends on PMN-to-PMN signaling via the lipid chemoattractant leukotriene B4 (LTB4) (Lammermann et al., 2013; Kriebel et al., 2018; Majumdar et al., 2021). PMNs may also enter the tissue distally from the site of injury and follow the LTB4 chemoattractant gradient generated by PMNs proximal to the injury site to surround the site of injury or infection and have additional PMNs present. Interestingly, EVs from PMNs contain both LTB4 and leukotriene A4 hydrolase (LTA4H), the enzyme that synthesizes LTB4, and can therefore promote PMN chemotaxis (Dalli et al., 2013; Majumdar et al., 2021). Thus, it is possible that a

chemotactic gradient can be created not only by soluble mediators, but also EVs, a swarming mechanism that is evolutionary conserved in the social amoeba *Dictyostelium discoideum* via cAMP gradient generation (Kriebel et al., 2018). Taken together, PMNs are able to release EVs that allows them to both form their own chemotactic gradient as well as attract additional PMNs and immune cells to the site of injury. Autologous generation of chemotactic gradients allows cells to steer themselves through complex paths such as mazes, allowing them to navigate to distal and difficult to find sites of injury and stress (Insall et al., 2022). As another example, PMNs activated with the bacterial formyl peptide formyl methionine leucine phenylalanine (fMLF) release EVs that can prime and activate naïve PMNs, showing a transfer of information across waves of recruited PMNs (Amjadi et al., 2021), occurring in spite of their limited lifespan. PMNs may be thus able to sustain, or quell, inflammation via EVs, as well as control the recruitment of additional immune cells.

In yet another example, human whole blood incubated with the supernatant of *S. aureus* resulted in PMN activation, as evidenced by increased CD66b, CD11a, CD11b, and CD11c, which likely reflect secondary granule release (Schmidt et al., 2012). The increase of CD66b was closely associated with the amount of PMN aggregation observed and PMN aggregation itself was reduced upon replacement of the activating stimulus (plasma and *S. aureus* secreted products) with cell culture media. This suggests that PMN aggregation is directly correlated with immune stimulation, which may play a role in PMNs forming cast-like aggregates around bacteria in the CF airways, particularly *P. aeruginosa* (Kragh et al., 2014; Rada, 2017; Jennings et al., 2021). Both injury and infection can result in swarms of PMNs. However, recruited PMNs are cleared away upon healing of the wound or pathogen

destruction, perhaps as a result of short PMN half-life and tight regulation of tissue entry (Bratton and Henson, 2011). PMN clearance allows for a return to homeostatic conditions.

The primary granules of PMNs, which are mobilized last upon activation, may fuse with one of three compartments: a) the phagosome to enable intracellular killing [Fate 1]; b) the nucleus to initiate complexation of cationic granule effectors with anionic DNA for NETosis [Fate 2]; or c) the plasma membrane resulting in exocytosis [Fate 3] (Mollinedo et al., 2006; Margaroli and Tirouvanziam, 2016). These different fates of the primary granules and resulting pattern of PMN activation may or may not be mutually exclusive (Margaroli and Tirouvanziam, 2016). During NETosis [Fate 2], the chromatin is decondensed, followed by rapid cell death and extracellular release of DNA and citrullinated histones complexed with NE, MPO and other primary granule cationic proteins. Such NETs may serve as bacteriostatic meshes (Brinkmann and Zychlinsky, 2012; Thiam et al., 2020). Fusion of the primary granules with the PMN plasma membrane [Fate 3] results in an increase of CD63 at the PMN surface and the release of contained cargo (NE, MPO) into the extracellular environment. This latter fate of PMNs is not associated with rapidly ensuing cell death as phagocytosis and NETosis, and has now been observed in many diseases, although it has been best characterized by our group in the context of CF airway disease.

PMNS IN CF LUNG DISEASE

Progressive lung disease is the leading cause of mortality in CF, a chronic condition characterized by impaired mucociliary clearance, mucus plugging, bacterial and fungal colonization of the lungs, and chronic recruitment of PMNs to the airways (Elborn, 2016; Margaroli and Tirouvanziam, 2016; Farrell et al., 2018). Despite the large numbers of PMNs

present in CF airways, opportunistic microbes like *P. aeruginosa* and *S. aureus* persist therein. The number of PMNs in expectorated CF sputum correlates strongly with the severity of airway disease. Additionally, the concentration and activity of the PMN primary granule effectors NE and MPO strongly correlate with disease severity in infants, preschool and school-age children, as well as adolescents and adults, emphasizing the pathogenic role for PMN exocytosis throughout the course of CF airway disease (Brown et al., 1996; Margaroli and Tirouvanziam, 2016; Chalmers et al., 2017; Gramegna et al., 2017; Dittrich et al., 2018; Margaroli et al., 2019).

Our group showed previously that a large fraction of PMNs in CF airways is alive and non-apoptotic, and actively fuses primary granules to the membrane (Tirouvanziam et al., 2008). In addition, these PMNs downregulate the activity of T-cells and airway macrophages through the secretion of arginase-1 (Ingersoll et al., 2015). These cells are metabolically active, as evidenced by high rates of glucose uptake and glycolysis and anabolic signaling downstream of the mechanistic target of rapamycin (mTOR) and cAMP-response element binding protein (CREB), yet actively repress their bacterial killing activity (Makam et al., 2009; Laval et al., 2013; Margaroli et al., 2021). These activated, tissue-differentiated, PMNs have been named based on core phenotypic traits which include excessive granule release, immunoregulatory activities toward T-cells and macrophages and metabolic licensing (GRIM) (Forrest et al., 2018; Mitchell, 2018). Beyond CF, PMNs with similar features to GRIM cells have also been observed in COPD, severe asthma, COVID-19, and arguably some cancers (Bergin et al., 2013; Stockley et al., 2013; Fine et al., 2020; Bost et al., 2021; Grant et al., 2021; Wang et al., 2021; Quail et al., 2022).

The best-studied consequence of PMN hyperexocytosis in diseased environments such as the CF airways is the release of NE in the extracellular milieu, which results in activation or

inhibition of an array of epithelial/PMN/macrophage/T-cell proteins (Margaroli and Tirouvanziam, 2016). In healthy individuals, the amount and subsequent activity of NE is kept in check by a range of antiproteases secreted in high amounts at baseline, and by the compartmentalization of NE within PMN primary granules and phagosomes. However, in inflammatory airway diseases, such as CF and COPD, the concentration of NE is so high that the antiprotease shield is inefficient at limiting its activity, resulting in bronchiectasis (Chalmers et al., 2017; Gramegna et al., 2017; Dittrich et al., 2018; Genschmer et al., 2019).

In addition, the PMN tertiary granule protease MMP9 may be activated by NE directly or via NE-mediated degradation of the MMP9 inhibitor, TIMP-1, which also leads to collagen degradation, tissue damage, and bronchiectasis in patients with CF (Jackson et al., 2010; Garratt et al., 2015). An isoform of IL-8 secreted by PMNs was shown to enhance its potency after cleavage by NE and other PMN-derived proteases (Padrines et al., 1994), although this may be mitigated by further cleavage (Leavell et al., 1997). NE can also mediate proteolytic activation of the epithelial sodium channel (ENaC), exacerbating the ionic imbalance of airway milieu in CF and COPD (Caldwell et al., 2005; Harris et al., 2007). NE is also able to cleave antibodies and CD2, CD4, CD8 and CD25 surface receptors on T cells, thereby disarming the adaptive immune system (Korkmaz et al.; Gramegna et al., 2017). This may play a role in the localization of T-cells in the submucosa rather than the PMN-rich lumen within the CF lung (Ingersoll et al., 2015). Finally, NE may also epigenetically control transcription of key genes in various airway cells.

ASSOCIATION OF NE AND OTHER EFFECTOR MOLECULES WITH EVS

The resistance of NE to antiprotease inhibition in CF and COPD airways results not only from its high concentrations (Delacourt et al., 2002) but also from its binding to cellular and EV membranes, masking its regulatory region. Indeed, NE associated with PMNs and PMN-derived EVs had a greater specific activity and were less prone to inhibition by antiproteases such as α1-antitrypsin than its free form (Owen et al., 1995; Genschmer et al., 2019). The packaging of effector molecules on PMN-derived EVs seems to be relevant in a number of inflammatory contexts, beyond NE and CF/COPD. For example, it was observed that PMNs with high plasmin generation capacity and urokinase could promote coagulation and fibrinolysis and enhance host survival in a murine model of sepsis. While the injection of soluble urokinase did not show benefits (Cointe et al., 2022), EVs from pneumolysin-exposed PMNs efficiently promoted activation of platelets and mediated host protection (Letsiou et al., 2021).

The exocytosis of PMN primary granules appear to overlap with EV formation, particularly exosomes, via secretory autophagy (Sheshachalam et al., 2014; Anand et al., 2019). CD63 is essential for EV biogenesis and enriched in lysosomal compartments of many cells (Hurwitz et al., 2016a; Hurwitz et al., 2016b; Hurwitz et al., 2018). Interestingly, knockout of CD63 results in signaling via the mTOR pathway in HEK293 cells (Hurwitz et al., 2018). However, whether the removal of CD63 from PMNs via mobilization to the plasma membrane (following primary granule exocytosis) or release of CD63+ EVs is able to induce mTOR signaling in PMNs, as we described previously in CF (Tirouvanziam et al., 2008), is currently unknown. In addition, CD63 appears to promote the sorting of cargo into both PMN primary granules, which bear many similarities to lysosomal vesicles, and EV cargo via routing from the trans-Golgi network into multivesicular bodies/late endosome (Rous et al., 2002; Pols and Klumperman, 2009).

Moreover, CD63 and NE are binding partners and their co-expression results in the concentration of NE in the lysosome of COS and HL-60 cells (Kallquist et al., 2008). Conversely, CD63 depletion results in decreased maturation of NE and secretion of granule contents (Kallquist et al., 2008), consistent with the observation that CD63 is necessary for multivesicular body/late endosome maturation during exosome generation (Mathieu et al., 2021).

As shown for NE, secreted proteins may be soluble, present as part of plaques or aggregates, crosslinked with other proteins (e.g., mucins), electrostatically bound to extracellular DNA (NETs) or functionalized on the surface of particles such as EVs, which affects their activity (Fitzgerald et al., 2018). A prominent example is that of cytokines and other signaling molecules that are typically thought of as free, unbound molecules functioning in an autocrine and/or paracrine fashion. Binding of such mediators to EVs may increase effective molarity and deliver concentrated payloads to recipient cells. In addition, such mediators could be delivered more rapidly to a particular location as bound or tethered to a scaffold, such as an EV decorated with targeting molecules, than if released in a soluble form **(Figure 1.2)**. For example, EV-bound rather than soluble PD-L1 was more effective at inhibiting CD8 T cells in a mouse model of lymphoma (Chen et al., 2018) and correlated with decreased patient survival while soluble PD-L1 did not (Fan et al., 2019). Taken together, association of proteins with EVs may alter their physical properties, causing differences in activity profile as demonstrated for NE (Genschmer et al., 2019). Furthermore, the packaging of such proteins, along with other membrane-bound receptors and ligands able to interact with specific cell membranes with high affinity, may enable preferential targeting of EVs toward certain recipient cells over others.

IN VITRO MODELING OF PMN EV SIGNALING

A limitation of most human PMN studies to date is that they rely on the stimulation of blood PMNs with various ligands, which fail to recapitulate transcriptional, metabolic and functional changes these cells undergo upon recruitment to tissue microenvironments in vivo. To tackle this problem in the context of human airway inflammation as it occurs in patients with CF, COPD and other debilitating lung diseases, we developed an organotypic model that relies on primary human blood neutrophils recruited through a differentiated human airway epithelium into patient airway fluid. When using CF patient sputum supernatant as the apical fluid, this model recapitulates the main hallmarks of GRIM PMNs described above including, but not limited to, primary granule exocytosis, T-cell blockade, metabolic licensing, and active inhibition of their bactericidal capacity (Forrest et al., 2018; Dobosh et al., 2021).

GRIM PMNs undergo a transcriptional program that results in a high rate of release of EVs (Margaroli et al., 2021). GRIM PMN EVs are in part characterized by a high content of active caspase-1 promoting inflammasome signaling in neighboring PMNs and epithelial cells via paracrine signaling (Forrest et al., 2022) **(See Chapter 3)**. Additional work presented in **Chapter 4** generated with our transmigration model suggest that EVs (isolated by 300 kDa molecular weight cutoff tangential flow filtration) are the necessary and sufficient component in CF patient sputum supernatant for induction of the GRIM phenotype in recruited PMNs, following rapid expression of the histone deacetylase HDAC11. HDAC11+ $CD63^{hi}$ GRIM PMNs release EVs that contain the lncRNA MALAT1. In turn, MALAT1+ PMN EVs cause naïve PMNs to become GRIM, thus delineating a feed-forward, EV-driven, PMN-to-PMN cycle of inflammation. In fact, such a PMN-centric axis of communication may an essential driving force in tissue homeostasis and inflammation **(Table 2.1)**, including but not limited to CF airway disease.

Type of EV	Conditions	Main Contents	Main Functional Effects	References
EVs	fMLF	flavocytochrome b558, NE, MPO	Induced LFA-1, CD35, CD66, flavocytochrome b558, p47 phosphorylation induced in recipient naive PMNs	(Amjadi et al., 2021)
EVs	LPS	Annexin V, CD15, PAI1	Lyse thrombus, high plasmin generation capacity, activate platelets	(Letsiou et al., 2021; Cointe et al., 2022)
EVs	fMLF +/- HUVEC pre-incubation	NE, CD66b, A2MG, CO3, MPO, S100-A8, HSP70, G3P, LTB4	Generate ROS, LTB4, regulates inflammatory profile of endothelial cells	(Dalli et al., 2013)
EVs	None	CD66b, CD62P, CD11b	Induce M1-like phenotype in monocytes	(Danesh et al., 2018)
EVs	CF sputum	CASP1, CD63, TSG101, CD66b	Induce inflammasome signaling in airway epithelial cells	(Forrest et al., 2022)
EVs	fMLF	NE, MPO, proteinase-3, MMP-9, CR-1, F-actin, HLA-1, CD16, CD66b, phosphatidyl serine	Binds THP-1 and HUVEC cells	(Gasser et al., 2003)
EVs	fMLF, LPS, PMA, TNFα + anti-PR3	miRNA-223, miRNA-142-3p, miRNA-451	Induce endothelial apoptosis, IL-6, IL-8, CXCL10, CXCL11, impair angiogenesis	(Glemain et al., 2022)
EVs	opsonized Zymosan A particles	lactoferrin, proteomics	anti-bacterial	(Lorincz et al., 2015)
EVs	fMLF	CD63, MMP9, MPO, LTB4, 5-LO, LTA4H, Hsc70, FLAP	Induce PMN migration	(Majumdar et al., 2021)
EVs	fMLF, IL-8, C5a, opsonized zymosan A	Phosphatidyl serine	Inhibited IFN-γ and TNFα, induced TGF-β in IL-2/IL-12 stimulated NK cells	(Pliyev et al., 2014)
EVs	fMLF	MPO, phosphatidyl serine,	Inhibit gut epithelial wound healing	(Slater et al., 2017)
EVs	PMA, opsonized S. aureus	CR3, LFA-1, CD16, gp91, p22, CD63, CD81, CD82, CD9, ALIX, TSG101, Annexin V, proteomics	Antibacterial	(Timar et al., 2013)
EVs	LPS	ITGB1, ITGB2, CD9, CD63, TSG101, LTA4H, TLR4,	Promote smooth airway remodeling	(Vargas et al., 2016)
EVs	LPS, fMLF, airway isolation from COPD patients	NE, CD66b, LFA-1	Promotes bronchiectasis	(Genschmer et al., 2019)
ENDS	LPS	CD66b, MPO, CD16, CD11a, CD11b, S110A8, S100A9, MRP8/14 complex, proteomics, phosphatidyl serine	Release S100A8/S100A9 in plasma	(Marki et al., 2021)
Migrasome	migration and mitochondria stress	LFA-1, CXCL12, mitochondria	Transfer of mitochondria to other cells	(Jiao et al., 2021)

Table 2.1: Main studies that have analyzed the contents and functional outcomes of human PMN-derived EVs and related particles. If proteomics is included in the third column (Main Contents) then the protein content was either entirely or mostly derived by mass spectrometry-based proteomics. For details of the method and amount/type of stimulation refer to the methods section of the indicated reference. Some of these papers use terms such as exosomes, microvesicles, or ectosomes to refer to the EV particle. In accordance with MISEV2018 guidelines we have used EV in this table.

To start with, it is well established that a major fraction of PMN-derived EVs presents the granulocyte-specific marker CD66b on their surface (Dalli et al., 2013; Headland et al., 2014; Lorincz et al., 2015; Genschmer et al., 2019; Letsiou et al., 2021; Forrest et al., 2022). CD66b (also referred to as CEACAM8/CGM6/W272 in older literature) (Zhao et al., 2002) can bind to the more broadly expressed CD66a and CD66c (referred to as CEACAM6/NCA in older literature) (Zhou et al., 1993; Kuroki et al., 2001). CD66c is expressed only on granulocytes, epithelial cells and endothelial cells (Blumenthal et al., 2007) and also shows homotypic adhesion properties and heterotypic binding to CD66b (Kuroki et al., 2001; Shikotra et al., 2017), thus potentially allowing CD66c+ and CD66b+ EVs to mediate communications within a "private network" of PMNs, epithelial cells and endothelial cells. CD66b and CD66c on the EV surface may bind to CD66c on the surface of recipient PMNs, thereby increasing the likelihood of processing of PMN-derived EVs by PMNs. In a related example, it was recently shown that fMLF-primed PMNs release EVs that can, in turn, activate naïve PMNs without concomitant fMLF exposure (Amjadi et al., 2021). Thus, our data suggest that GRIM PMN EVs are able to activate and drive GRIM fate acquisition in newly recruited PMNs via similar mechanisms.

As PMNs roll along activated endothelium, they release elongated neutrophil-derived structures (ENDS) which contain DAMPs and can activate nearby cells (Marki et al., 2021). Activated PMNs release EVs with surface-exposed phosphatidylserine and intra-EV proteins associated with granules including CD16, CD66b, NE, MMP9, proteinase 3, and bioactive MPO. In addition, these EVs were found to bind to complement proteins, endothelial cells, and monocytes (Gasser et al., 2003). Furthermore, activated PMN EVs contain various miRNAs including miRNA-223, miRNA-142-3p, and miRNA-451, which, upon delivery to endothelial cells,

affected their migration, proliferation and expression of the inflammatory cytokines IL-6, CXCL8 (IL-8), CXCL10, and CXCL11 (Glemain et al., 2022). It is important to note that CF sputum contains a heterogenous population of EVs derived not only from PMNs, but also from airway epithelial cells, macrophages, monocytes, T-cells and even microorganisms. EVs (termed OMVs) from *S. aureus* present in CF sputum can inhibit blood PMN killing of this particular bacteria in vitro (Fantone et al., 2021). EVs may also use surface integrins and lipids such as phosphatidylserine (Solomon et al., 2015) for preferential uptake by scavenger cells, such as PMNs, allowing them to modulate the activity of these cells (Askenase, 2022).

THERAPEUTIC POTENTIAL OF EV-BASED APPROACHES

Patients with CF receive ever-improving care, in part through the use of various drugs including antibiotics, inhaled mucolytic therapies, and CFTR modulators (tackling the basic molecular defect underlying the disease), resulting in an improved quality of life with greater longevity (Solomon et al., 2015; Hudock and Clancy, 2017; Strug et al., 2018). Despite the effectiveness of CFTR-directed therapies in improving lung function, their use is limited to patients with particular CFTR mutations, and patients continue to experience a steady decline, albeit delayed, in health (Ramsey et al., 2011; Jones and Barry, 2015). For example, adult CF patients with the G551D mutation eligible for treatment with the CFTR modulator ivacaftor saw an increase in lung function in the first three years post-treatment inception, but then displayed lung function decline at the same rate as the control, untreated group (Volkova et al., 2020). The ivacaftor-treatment group showed an initial reduction and then a rebound in *P. aeruginosa* burden in the lung. In addition, although sputum IL-8 and NE were substantially decreased by the treatment, they still remained at pathologically high levels (Hisert et al., 2017). Although we

are awaiting cohort data from the novel generation of CFTR modulator therapy (triple combination), data to date suggest that even the most advanced CF treatment plans are not sufficient to completely curb inflammatory airway disease. Thus, additional therapies must be developed, particularly with regards to PMN activation, since this aspect is central to the progression of the disease (Giacalone et al., 2020) yet remains unaddressed. Beyond our work described in **Chapters 3 and 4**, it is unknown what subtypes and molecular components of EVs drive PMN pathological features in CF. The mechanisms by which these disease-inducing EVs are made remain to be elucidated. Understanding these processes will allow targeting of therapeutics toward the EV compartment, which in turn could enable development of more efficacious drugs for CF and other intractable inflammatory airway diseases such as COPD, asthma, and COVID-19.

Concomitantly with therapeutic development, it has become increasingly important to identify patients which may be at a greater risk of rapid decline in lung function, infections, increased frequency of pulmonary exacerbations, or even onset of other complications such as CF-related diabetes. Unfortunately, current CF biomarkers do not fully predict the course of disease. Thus, it is necessary to develop a cadre of novel biomarkers to form a more complete picture of CF disease throughout the lifespan of people with CF. EVs are released by all cells and thus are always present in biofluids such as plasma, urine, bronchoalveolar lavage fluid (BALF), as well as induced or spontaneously expectorated sputum, and retain long-term stability in standard freezers. Thus, EVs are well situated to track and predict the course of disease in CF. The protein and RNA contents of EVs are typically used as biomarkers for the diagnosis of various cancers. While some groups have begun to analyze EVs in the context of CF, a

longitudinal study on the presence and stability of EV-associated molecules from multiple patient cohorts has yet to be implemented. Understanding the burden of EVs in CF will allow for the discovery and characterization of novel biomarkers. This will ultimately enable: 1) finer tracking of early CF disease when many of the current biomarkers are not yet present or do not demonstrate large enough variation to allow for patient-to-patient comparison or treatment evaluation; and 2) better subcategorization of late-stage CF disease when many current biomarkers are highly saturated. Based on the work presented herein, we propose that EVs, carrying the biomolecules of the cells from which they were derived, constitute rich and stable sources of biomarkers for CF.

REFERENCES

1. A. Gonzalez, N., Bensinger, S.J., Hong, C., Beceiro, S., Bradley, M.N., Zelcer, N., Deniz, J., Ramirez, C., Diaz, M., Gallardo, G.*, et al.* (2009). Apoptotic Cells Promote Their Own Clearance and Immune Tolerance through Activation of the Nuclear Receptor LXR. Immunity *31*, 245-258. 10.1016/j.immuni.2009.06.018. PMC2791787
2. Akagi, T., Saitoh, T., O'Kelly, J., Akira, S., Gombart, A.F., and Koeffler, H.P. (2008). Impaired Response to GM-CSF and G-CSF, and Enhanced Apoptosis in C/Ebpbeta-Deficient Hematopoietic Cells. Blood *111*, 2999-3004. 10.1182/blood-2007-04-087213. PMC2265449
3. Amjadi, M.F., Avner, B.S., Greenlee-Wacker, M.C., Horswill, A.R., and Nauseef, W.M. (2021). Neutrophil-Derived Extracellular Vesicles Modulate the Phenotype of Naive Human Neutrophils. J Leukoc Biol *110*, 917-925. 10.1002/JLB.3AB0520-339RR. PMC8423865
4. Anand, S., Samuel, M., Kumar, S., and Mathivanan, S. (2019). Ticket to a Bubble Ride: Cargo Sorting into Exosomes and Extracellular Vesicles. Biochim Biophys Acta Proteins Proteom *1867*, 140203. 10.1016/j.bbapap.2019.02.005.
5. Askenase, P.W. (2022). Exosome Carrier Effects; Resistance to Digestion in Phagolysosomes May Assist Transfers to Targeted Cells; II Transfers of miRNAs Are Better Analyzed Via Systems Approach as They Do Not Fit Conventional Reductionist Stoichiometric Concepts. Int J Mol Sci *23*. 10.3390/ijms23116192. PMC9181154
6. Bardoel, B.W., Kenny, E.F., Sollberger, G., and Zychlinsky, A. (2014). The Balancing Act of Neutrophils. Cell Host Microbe *15*, 526-536. 10.1016/j.chom.2014.04.011.
7. Benabdeslam, H., Abidi, H., Garcia, I., Bellon, G., Gilly, R., and Revol, A. (1999). Lipid Peroxidation and Antioxidant Defenses in Cystic Fibrosis Patients. Clin Chem Lab Med *37*, 511-516. 10.1515/CCLM.1999.082.
8. Benson, K.F., Li, F.Q., Person, R.E., Albani, D., Duan, Z., Wechsler, J., Meade-White, K., Williams, K., Acland, G.M., Niemeyer, G.*, et al.* (2003). Mutations Associated with Neutropenia in Dogs and Humans Disrupt Intracellular Transport of Neutrophil Elastase. Nat Genet *35*, 90-96. 10.1038/ng1224.
9. Bergin, D.A., Hurley, K., Mehta, A., Cox, S., Ryan, D., O'Neill, S.J., Reeves, E.P., and McElvaney, N.G. (2013). Airway Inflammatory Markers in Individuals with Cystic Fibrosis and Non-Cystic Fibrosis Bronchiectasis. J Inflamm Res *6*, 1-11. 10.2147/JIR.S40081. PMC3576001
10. Bjerregaard, M.D., Jurlander, J., Klausen, P., Borregaard, N., and Cowland, J.B. (2003). The in Vivo Profile of Transcription Factors During Neutrophil Differentiation in Human Bone Marrow. Blood *101*, 4322-4332. 10.1182/blood-2002-03-0835.
11. Blanco-Camarillo, C., Aleman, O.R., and Rosales, C. (2021). Low-Density Neutrophils in Healthy Individuals Display a Mature Primed Phenotype. Front Immunol *12*, 672520. 10.3389/fimmu.2021.672520. PMC8285102
12. Blumenthal, R.D., Leon, E., Hansen, H.J., and Goldenberg, D.M. (2007). Expression Patterns of CEACAM5 and CEACAM6 in Primary and Metastatic Cancers. BMC Cancer *7*, 2. 10.1186/1471-2407-7-2. PMC1769503
13. Borregaard, N. (2010). Neutrophils, from Marrow to Microbes. Immunity *33*, 657-670. 10.1016/j.immuni.2010.11.011.

14. Borregaard, N., and Cowland, J.B. (1997). Granules of the Human Neutrophilic Polymorphonuclear Leukocyte. Blood *89*, 3503-3521. https://doi.org/10.1182/blood.V89.10.3503.
15. Bost, P., De Sanctis, F., Cane, S., Ugel, S., Donadello, K., Castellucci, M., Eyal, D., Fiore, A., Anselmi, C., Barouni, R.M.*, et al.* (2021). Deciphering the State of Immune Silence in Fatal COVID-19 Patients. Nat Commun *12*, 1428. 10.1038/s41467-021-21702-6. PMC7935849
16. Bratton, D.L., and Henson, P.M. (2011). Neutrophil Clearance: When the Party Is over, Clean-up Begins. Trends Immunol *32*, 350-357. 10.1016/j.it.2011.04.009. PMC3151332
17. Brinkmann, V., and Zychlinsky, A. (2012). Neutrophil Extracellular Traps: Is Immunity the Second Function of Chromatin? J Cell Biol *198*, 773-783. 10.1083/jcb.201203170. PMC3432757
18. Brown, R.K., Wyatt, H., Price, J.F., and Kelly, F.J. (1996). Pulmonary Dysfunction in Cystic Fibrosis Is Associated with Oxidative Stress. European Respiratory Journal *9*, 334-339. Doi 10.1183/09031936.96.09020334.
19. Cai, B., Thorp, E.B., Doran, A.C., Sansbury, B.E., Daemen, M.J., Dorweiler, B., Spite, M., Fredman, G., and Tabas, I. (2017). Mertk Receptor Cleavage Promotes Plaque Necrosis and Defective Resolution in Atherosclerosis. J Clin Invest *127*, 564-568. 10.1172/JCI90520. PMC5272169
20. Cain, D.W., Snowden, P.B., Sempowski, G.D., and Kelsoe, G. (2011). Inflammation Triggers Emergency Granulopoiesis through a Density-Dependent Feedback Mechanism. PLoS One *6*, e19957. 10.1371/journal.pone.0019957. PMC3104996
21. Caldwell, R.A., Boucher, R.C., and Stutts, M.J. (2005). Neutrophil Elastase Activates near-Silent Epithelial Na+ Channels and Increases Airway Epithelial Na+ Transport. Am J Physiol Lung Cell Mol Physiol *288*, L813-819. 10.1152/ajplung.00435.2004.
22. Capasso, D., Pepe, M.V., Rossello, J., Lepanto, P., Arias, P., Salzman, V., and Kierbel, A. (2016). Elimination of Pseudomonas Aeruginosa through Efferocytosis Upon Binding to Apoptotic Cells. PLoS Pathog *12*, e1006068. 10.1371/journal.ppat.1006068. PMC5158079
23. Carmona-Rivera, C., and Kaplan, M.J. (2013). Low-Density Granulocytes: A Distinct Class of Neutrophils in Systemic Autoimmunity. Semin Immunopathol *35*, 455-463. 10.1007/s00281-013-0375-7. PMC4007274
24. Chalmers, J.D., Moffitt, K.L., Suarez-Cuartin, G., Sibila, O., Finch, S., Furrie, E., Dicker, A., Wrobel, K., Elborn, J.S., Walker, B.*, et al.* (2017). Neutrophil Elastase Activity Is Associated with Exacerbations and Lung Function Decline in Bronchiectasis. Am J Respir Crit Care Med *195*, 1384-1393. 10.1164/rccm.201605-1027OC. PMC5443898
25. Chan, L., Karimi, N., Morovati, S., Alizadeh, K., Kakish, J.E., Vanderkamp, S., Fazel, F., Napoleoni, C., Alizadeh, K., Mehrani, Y.*, et al.* (2021). The Roles of Neutrophils in Cytokine Storms. Viruses *13*. 10.3390/v13112318. PMC8624379
26. Chen, G., Huang, A.C., Zhang, W., Zhang, G., Wu, M., Xu, W., Yu, Z., Yang, J., Wang, B., Sun, H.*, et al.* (2018). Exosomal PD-L1 Contributes to Immunosuppression and Is Associated with Anti-PD-1 Response. Nature *560*, 382-386. 10.1038/s41586-018-0392-8. PMC6095740

27. Cloutier, A., Guindi, C., Larivee, P., Dubois, C.M., Amrani, A., and McDonald, P.P. (2009). Inflammatory Cytokine Production by Human Neutrophils Involves C/Ebp Transcription Factors. J Immunol *182*, 563-571. 10.4049/jimmunol.182.1.563.
28. Cointe, S., Vallier, L., Esnault, P., Dacos, M., Bonifay, A., Macagno, N., Harti Souab, K., Chareyre, C., Judicone, C., Frankel, D.*, et al.* (2022). Granulocyte Microvesicles with a High Plasmin Generation Capacity Promote Clot Lysis and Improve Outcome in Septic Shock. Blood *139*, 2377-2391. 10.1182/blood.2021013328.
29. Coperchini, F., Chiovato, L., Croce, L., Magri, F., and Rotondi, M. (2020). The Cytokine Storm in COVID-19: An Overview of the Involvement of the Chemokine/Chemokine-Receptor System. Cytokine Growth Factor Rev *53*, 25-32. 10.1016/j.cytogfr.2020.05.003. PMC7211650
30. Dalli, J., Montero-Melendez, T., Norling, L.V., Yin, X., Hinds, C., Haskard, D., Mayr, M., and Perretti, M. (2013). Heterogeneity in Neutrophil Microparticles Reveals Distinct Proteome and Functional Properties. Mol Cell Proteomics *12*, 2205-2219. 10.1074/mcp.M113.028589. PMC3734580
31. Dancey, J.T., Deubelbeiss, K.A., Harker, L.A., and Finch, C.A. (1976). Neutrophil Kinetics in Man. J Clin Invest *58*, 705-715. 10.1172/JCI108517. PMC333229
32. Delacourt, C., Herigault, S., Delclaux, C., Poncin, A., Levame, M., Harf, A., Saudubray, F., and Lafuma, C. (2002). Protection against Acute Lung Injury by Intravenous or Intratracheal Pretreatment with Epi-Hne-4, a New Potent Neutrophil Elastase Inhibitor. Am J Respir Cell Mol Biol *26*, 290-297. 10.1165/ajrcmb.26.3.4611.
33. Dittrich, A.S., Kuhbandner, I., Gehrig, S., Rickert-Zacharias, V., Twigg, M., Wege, S., Taggart, C.C., Herth, F., Schultz, C., and Mall, M.A. (2018). Elastase Activity on Sputum Neutrophils Correlates with Severity of Lung Disease in Cystic Fibrosis. Eur Respir J *51*. 10.1183/13993003.01910-2017.
34. Dobosh, B., Giacalone, V.D., Margaroli, C., and Tirouvanziam, R. (2021). Mass Production of Human Airway-Like Neutrophils Via Transmigration in an Organotypic Model of Human Airways. STAR Protoc *2*, 100892. 10.1016/j.xpro.2021.100892. PMC8551927
35. Dobosh, B., Zandi, K., Giraldo, D.M., Goh, S.L., Musall, K., Aldeco, M., LeCher, J., Giacalone, V.D., Yang, J., Eddins, D.J.*, et al.* (2022). Baricitinib Attenuates the Proinflammatory Phase of COVID-19 Driven by Lung-Infiltrating Monocytes. Cell Rep *39*, 110945. 10.1016/j.celrep.2022.110945.
36. Elborn, J.S. (2016). Cystic Fibrosis. Lancet *388*, 2519-2531. 10.1016/S0140-6736(16)00576-6. 27140670
37. Fadok, V.A., Bratton, D.L., Konowal, A., Freed, P.W., Westcott, J.Y., and Henson, P.M. (1998). Macrophages That Have Ingested Apoptotic Cells in Vitro Inhibit Proinflammatory Cytokine Production through Autocrine/Paracrine Mechanisms Involving TGF-beta, PGE2, and PAF. J Clin Invest *101*, 890-898. 10.1172/JCI1112. PMC508637
38. Fan, Y., Che, X., Qu, J., Hou, K., Wen, T., Li, Z., Li, C., Wang, S., Xu, L., Liu, Y.*, et al.* (2019). Exosomal PD-L1 Retains Immunosuppressive Activity and Is Associated with Gastric Cancer Prognosis. Ann Surg Oncol *26*, 3745-3755. 10.1245/s10434-019-07431-7.
39. Fantone, K., Tucker, S.L., Miller, A., Yadav, R., Bernardy, E.E., Fricker, R., Stecenko, A.A., Goldberg, J.B., and Rada, B. (2021). Cystic Fibrosis Sputum Impairs the Ability of

Neutrophils to Kill Staphylococcus Aureus. Pathogens *10*. 10.3390/pathogens10060703. PMC8229215
40. Farrell, P., Ferec, C., Macek, M., Frischer, T., Renner, S., Riss, K., Barton, D., Repetto, T., Tzetis, M., Giteau, K.*, et al.* (2018). Estimating the Age of P.(Phe508del) with Family Studies of Geographically Distinct European Populations and the Early Spread of Cystic Fibrosis. Eur J Hum Genet *26*, 1832-1839. 10.1038/s41431-018-0234-z. PMC6244163
41. Fine, N., Tasevski, N., McCulloch, C.A., Tenenbaum, H.C., and Glogauer, M. (2020). The Neutrophil: Constant Defender and First Responder. Front Immunol *11*, 571085. 10.3389/fimmu.2020.571085. PMC7541934
42. Fitzgerald, W., Freeman, M.L., Lederman, M.M., Vasilieva, E., Romero, R., and Margolis, L. (2018). A System of Cytokines Encapsulated in Extracellular Vesicles. Sci Rep *8*, 8973. 10.1038/s41598-018-27190-x. PMC5997670
43. Forrest, O.A., Dobosh, B., Ingersoll, S.A., Rao, S., Rojas, A., Laval, J., Alvarez, J.A., Brown, M.R., Tangpricha, V., and Tirouvanziam, R. (2022). Neutrophil-Derived Extracellular Vesicles Promote Feed-Forward Inflammasome Signaling in Cystic Fibrosis Airways. J Leukoc Biol. 10.1002/JLB.3AB0321-149R.
44. Forrest, O.A., Ingersoll, S.A., Preininger, M.K., Laval, J., Limoli, D.H., Brown, M.R., Lee, F.E., Bedi, B., Sadikot, R.T., Goldberg, J.B.*, et al.* (2018). Frontline Science: Pathological Conditioning of Human Neutrophils Recruited to the Airway Milieu in Cystic Fibrosis. J Leukoc Biol *104*, 665-675. 10.1002/JLB.5HI1117-454RR. PMC6956843
45. Furze, R.C., and Rankin, S.M. (2008). The Role of the Bone Marrow in Neutrophil Clearance under Homeostatic Conditions in the Mouse. FASEB J *22*, 3111-3119. 10.1096/fj.08-109876. PMC2593561
46. Garratt, L.W., Sutanto, E.N., Ling, K.M., Looi, K., Iosifidis, T., Martinovich, K.M., Shaw, N.C., Kicic-Starcevich, E., Knight, D.A., Ranganathan, S.*, et al.* (2015). Matrix Metalloproteinase Activation by Free Neutrophil Elastase Contributes to Bronchiectasis Progression in Early Cystic Fibrosis. Eur Respir J *46*, 384-394. 10.1183/09031936.00212114.
47. Garrel, C., Ceballos-Picot, I., Germain, G., and Al-Gubory, K.H. (2007). Oxidative Stress-Inducible Antioxidant Adaptive Response During Prostaglandin F2alpha-Induced Luteal Cell Death in Vivo. Free Radic Res *41*, 251-259. 10.1080/10715760601067493.
48. Gasser, O., Hess, C., Miot, S., Deon, C., Sanchez, J.C., and Schifferli, J.A. (2003). Characterisation and Properties of Ectosomes Released by Human Polymorphonuclear Neutrophils. Exp Cell Res *285*, 243-257. 10.1016/s0014-4827(03)00055-7.
49. Genschmer, K.R., Russell, D.W., Lal, C., Szul, T., Bratcher, P.E., Noerager, B.D., Abdul Roda, M., Xu, X., Rezonzew, G., Viera, L.*, et al.* (2019). Activated PMN Exosomes: Pathogenic Entities Causing Matrix Destruction and Disease in the Lung. Cell *176*, 113-126 e115. 10.1016/j.cell.2018.12.002. PMC6368091
50. Giacalone, V.D., Dobosh, B.S., Gaggar, A., Tirouvanziam, R., and Margaroli, C. (2020). Immunomodulation in Cystic Fibrosis: Why and How? Int J Mol Sci *21*. 10.3390/ijms21093331. PMC7247557
51. Glemain, A., Neel, M., Neel, A., Andre-Gregoire, G., Gavard, J., Martinet, B., Le Bloas, R., Riquin, K., Hamidou, M., Fakhouri, F.*, et al.* (2022). Neutrophil-Derived Extracellular

Vesicles Induce Endothelial Inflammation and Damage through the Transfer of miRNAs. J Autoimmun *129*, 102826. 10.1016/j.jaut.2022.102826.
52. Gordy, C., Pua, H., Sempowski, G.D., and He, Y.W. (2011). Regulation of Steady-State Neutrophil Homeostasis by Macrophages. Blood *117*, 618-629. 10.1182/blood-2010-01-265959. PMC3031484
53. Gramegna, A., Amati, F., Terranova, L., Sotgiu, G., Tarsia, P., Miglietta, D., Calderazzo, M.A., Aliberti, S., and Blasi, F. (2017). Neutrophil Elastase in Bronchiectasis. Respir Res *18*, 211. 10.1186/s12931-017-0691-x. PMC5735855
54. Grant, R.A., Morales-Nebreda, L., Markov, N.S., Swaminathan, S., Querrey, M., Guzman, E.R., Abbott, D.A., Donnelly, H.K., Donayre, A., Goldberg, I.A*., et al.* (2021). Circuits between Infected Macrophages and T Cells in SARS-CoV-2 Pneumonia. Nature *590*, 635-641. 10.1038/s41586-020-03148-w. PMC7987233
55. Greenlee-Wacker, M.C., Rigby, K.M., Kobayashi, S.D., Porter, A.R., DeLeo, F.R., and Nauseef, W.M. (2014). Phagocytosis of Staphylococcus Aureus by Human Neutrophils Prevents Macrophage Efferocytosis and Induces Programmed Necrosis. J Immunol *192*, 4709-4717. 10.4049/jimmunol.1302692. PMC4011196
56. Hardisty, G.R., Llanwarne, F., Minns, D., Gillan, J.L., Davidson, D.J., Gwyer Findlay, E., and Gray, R.D. (2021). High Purity Isolation of Low Density Neutrophils Casts Doubt on Their Exceptionality in Health and Disease. Front Immunol *12*, 625922. 10.3389/fimmu.2021.625922. PMC8217868
57. Harris, M., Firsov, D., Vuagniaux, G., Stutts, M.J., and Rossier, B.C. (2007). A Novel Neutrophil Elastase Inhibitor Prevents Elastase Activation and Surface Cleavage of the Epithelial Sodium Channel Expressed in Xenopus Laevis Oocytes. J Biol Chem *282*, 58-64. 10.1074/jbc.M605125200.
58. Headland, S.E., Jones, H.R., D'Sa, A.S., Perretti, M., and Norling, L.V. (2014). Cutting-Edge Analysis of Extracellular Microparticles Using Imagestream(X) Imaging Flow Cytometry. Sci Rep *4*, 5237. 10.1038/srep05237. PMC4050385
59. Hidalgo, A., and Casanova-Acebes, M. (2021). Dimensions of Neutrophil Life and Fate. Semin Immunol *57*, 101506. 10.1016/j.smim.2021.101506.
60. Hirai, H., Zhang, P., Dayaram, T., Hetherington, C.J., Mizuno, S., Imanishi, J., Akashi, K., and Tenen, D.G. (2006). C/Ebpbeta Is Required for 'Emergency' Granulopoiesis. Nat Immunol *7*, 732-739. 10.1038/ni1354.
61. Hisert, K.B., Heltshe, S.L., Pope, C., Jorth, P., Wu, X., Edwards, R.M., Radey, M., Accurso, F.J., Wolter, D.J., Cooke, G*., et al.* (2017). Restoring Cystic Fibrosis Transmembrane Conductance Regulator Function Reduces Airway Bacteria and Inflammation in People with Cystic Fibrosis and Chronic Lung Infections. Am J Respir Crit Care Med *195*, 1617-1628. 10.1164/rccm.201609-1954OC. PMC5476912
62. Hudock, K.M., and Clancy, J.P. (2017). An Update on New and Emerging Therapies for Cystic Fibrosis. Expert opinion on emerging drugs *22*, 331-346. 10.1080/14728214.2017.1418324.
63. Hurwitz, S.N., Cheerathodi, M.R., Nkosi, D., York, S.B., and Meckes, D.G., Jr. (2018). Tetraspanin CD63 Bridges Autophagic and Endosomal Processes to Regulate Exosomal Secretion and Intracellular Signaling of Epstein-Barr Virus Lmp1. J Virol *92*. 10.1128/JVI.01969-17. PMC5809724

64. Hurwitz, S.N., Conlon, M.M., Rider, M.A., Brownstein, N.C., and Meckes, D.G., Jr. (2016a). Nanoparticle Analysis Sheds Budding Insights into Genetic Drivers of Extracellular Vesicle Biogenesis. J Extracell Vesicles *5*, 31295. 10.3402/jev.v5.31295. PMC4947197
65. Hurwitz, S.N., Rider, M.A., Bundy, J.L., Liu, X., Singh, R.K., and Meckes, D.G., Jr. (2016b). Proteomic Profiling of NCI-60 Extracellular Vesicles Uncovers Common Protein Cargo and Cancer Type-Specific Biomarkers. Oncotarget *7*, 86999-87015. 10.18632/oncotarget.13569. PMC5341331
66. Iida, S., Watanabe-Fukunaga, R., Nagata, S., and Fukunaga, R. (2008). Essential Role of C/Ebpalpha in G-CSF-Induced Transcriptional Activation and Chromatin Modification of Myeloid-Specific Genes. Genes Cells *13*, 313-327. 10.1111/j.1365-2443.2008.01173.x.
67. Ingersoll, S.A., Laval, J., Forrest, O.A., Preininger, M., Brown, M.R., Arafat, D., Gibson, G., Tangpricha, V., and Tirouvanziam, R. (2015). Mature Cystic Fibrosis Airway Neutrophils Suppress T Cell Function: Evidence for a Role of Arginase 1 but Not Programmed Death-Ligand 1. J Immunol *194*, 5520-5528. 10.4049/jimmunol.1500312. PMC4433848
68. Insall, R.H., Paschke, P., and Tweedy, L. (2022). Steering Yourself by the Bootstraps: How Cells Create Their Own Gradients for Chemotaxis. Trends Cell Biol *32*, 585-596. 10.1016/j.tcb.2022.02.007.
69. Ito, H., Yamashita, Y., Tanaka, T., Takaki, M., Le, M.N., Yoshida, L.M., and Morimoto, K. (2020). Cigarette Smoke Induces Endoplasmic Reticulum Stress and Suppresses Efferocytosis through the Activation of Rhoa. Sci Rep *10*, 12620. 10.1038/s41598-020-69610-x. PMC7387437
70. Jackson, P.L., Xu, X., Wilson, L., Weathington, N.M., Clancy, J.P., Blalock, J.E., and Gaggar, A. (2010). Human Neutrophil Elastase-Mediated Cleavage Sites of MMP-9 and TIMP-1: Implications to Cystic Fibrosis Proteolytic Dysfunction. Mol Med *16*, 159-166. 10.2119/molmed.2009.00109. PMC2811559
71. Jager, A.V., Arias, P., Tribulatti, M.V., Brocco, M.A., Pepe, M.V., and Kierbel, A. (2021). The Inflammatory Response Induced by Pseudomonas Aeruginosa in Macrophages Enhances Apoptotic Cell Removal. Sci Rep *11*, 2393. 10.1038/s41598-021-81557-1. PMC7841155
72. Jennings, L.K., Dreifus, J.E., Reichhardt, C., Storek, K.M., Secor, P.R., Wozniak, D.J., Hisert, K.B., and Parsek, M.R. (2021). Pseudomonas Aeruginosa Aggregates in Cystic Fibrosis Sputum Produce Exopolysaccharides That Likely Impede Current Therapies. Cell Rep *34*, 108782. 10.1016/j.celrep.2021.108782. PMC7958924
73. Jones, A.M., and Barry, P.J. (2015). Lumacaftor/Ivacaftor for Patients Homozygous for Phe508del-CFTR: Should We Curb Our Enthusiasm? Thorax *70*, 615-616. 10.1136/thoraxjnl-2015-207369.
74. Kallquist, L., Hansson, M., Persson, A.M., Janssen, H., Calafat, J., Tapper, H., and Olsson, I. (2008). The Tetraspanin CD63 Is Involved in Granule Targeting of Neutrophil Elastase. Blood *112*, 3444-3454. 10.1182/blood-2007-10-116285.
75. Kallquist, L., Rosen, H., Nordenfelt, P., Calafat, J., Janssen, H., Persson, A.M., Hansson, M., and Olsson, I. (2010). Neutrophil Elastase and Proteinase 3 Trafficking Routes in Myelomonocytic Cells. Exp Cell Res *316*, 3182-3196. 10.1016/j.yexcr.2010.08.016.
76. Korkmaz, B., Horwitz, M.S., Jenne, D.E., and Gauthier, F. (2010). Neutrophil Elastase, Proteinase 3, and Cathepsin G as Therapeutic Targets in Human Diseases. Pharmacol Rev *62*, 726-759. 10.1124/pr.110.002733. PMC2993259

77. Korns, D., Frasch, S.C., Fernandez-Boyanapalli, R., Henson, P.M., and Bratton, D.L. (2011). Modulation of Macrophage Efferocytosis in Inflammation. Front Immunol *2*, 57. 10.3389/fimmu.2011.00057. PMC3342042
78. Kragh, K.N., Alhede, M., Jensen, P.O., Moser, C., Scheike, T., Jacobsen, C.S., Seier Poulsen, S., Eickhardt-Sorensen, S.R., Trostrup, H., Christoffersen, L*., et al.* (2014). Polymorphonuclear Leukocytes Restrict Growth of Pseudomonas Aeruginosa in the Lungs of Cystic Fibrosis Patients. Infect Immun *82*, 4477-4486. 10.1128/IAI.01969-14. PMC4249348
79. Kriebel, P.W., Majumdar, R., Jenkins, L.M., Senoo, H., Wang, W., Ammu, S., Chen, S., Narayan, K., Iijima, M., and Parent, C.A. (2018). Extracellular Vesicles Direct Migration by Synthesizing and Releasing Chemotactic Signals. J Cell Biol *217*, 2891-2910. 10.1083/jcb.201710170. PMC6080930
80. Kuroki, M., Abe, H., Imakiirei, T., Liao, S., Uchida, H., Yamauchi, Y., Oikawa, S., and Kuroki, M. (2001). Identification and Comparison of Residues Critical for Cell-Adhesion Activities of Two Neutrophil Cd66 Antigens, CEACAM6 and Ceacam8. J Leukoc Biol *70*, 543-550.
81. Kwok, I., Becht, E., Xia, Y., Ng, M., Teh, Y.C., Tan, L., Evrard, M., Li, J.L.Y., Tran, H.T.N., Tan, Y*., et al.* (2020). Combinatorial Single-Cell Analyses of Granulocyte-Monocyte Progenitor Heterogeneity Reveals an Early Uni-Potent Neutrophil Progenitor. Immunity *53*, 303-318 e305. 10.1016/j.immuni.2020.06.005.
82. Lammermann, T., Afonso, P.V., Angermann, B.R., Wang, J.M., Kastenmuller, W., Parent, C.A., and Germain, R.N. (2013). Neutrophil Swarms Require LTB4 and Integrins at Sites of Cell Death in Vivo. Nature *498*, 371-375. 10.1038/nature12175. PMC3879961
83. Laval, J., Touhami, J., Herzenberg, L.A., Conrad, C., Taylor, N., Battini, J.L., Sitbon, M., and Tirouvanziam, R. (2013). Metabolic Adaptation of Neutrophils in Cystic Fibrosis Airways Involves Distinct Shifts in Nutrient Transporter Expression. J Immunol *190*, 6043-6050. 10.4049/jimmunol.1201755.
84. Leavell, K.J., Peterson, M.W., and Gross, T.J. (1997). Human Neutrophil Elastase Abolishes Interleukin-8 Chemotactic Activity. J Leukoc Biol *61*, 361-366. 10.1002/jlb.61.3.361.
85. Leitch, A.E., Riley, N.A., Sheldrake, T.A., Festa, M., Fox, S., Duffin, R., Haslett, C., and Rossi, A.G. (2010). The Cyclin-Dependent Kinase Inhibitor R-Roscovitine Down-Regulates Mcl-1 to Override Pro-Inflammatory Signalling and Drive Neutrophil Apoptosis. Eur J Immunol *40*, 1127-1138. 10.1002/eji.200939664.
86. Letsiou, E., Teixeira Alves, L.G., Felten, M., Mitchell, T.J., Muller-Redetzky, H.C., Dudek, S.M., and Witzenrath, M. (2021). Neutrophil-Derived Extracellular Vesicles Activate Platelets after Pneumolysin Exposure. Cells *10*. 10.3390/cells10123581. PMC8700313
87. Lorincz, A.M., Schutte, M., Timar, C.I., Veres, D.S., Kittel, A., McLeish, K.R., Merchant, M.L., and Ligeti, E. (2015). Functionally and Morphologically Distinct Populations of Extracellular Vesicles Produced by Human Neutrophilic Granulocytes. J Leukoc Biol *98*, 583-589. 10.1189/jlb.3VMA1014-514R.
88. Lourenco, A.R., and Coffer, P.J. (2017). A Tumor Suppressor Role for C/Ebpalpha in Solid Tumors: More Than Fat and Blood. Oncogene *36*, 5221-5230. 10.1038/onc.2017.151.
89. Majumdar, R., Tavakoli Tameh, A., Arya, S.B., and Parent, C.A. (2021). Exosomes Mediate LTB4 Release During Neutrophil Chemotaxis. PLoS Biol *19*, e3001271. 10.1371/journal.pbio.3001271. PMC8262914

90. Makam, M., Diaz, D., Laval, J., Gernez, Y., Conrad, C.K., Dunn, C.E., Davies, Z.A., Moss, R.B., Herzenberg, L.A., Herzenberg, L.A.*, et al.* (2009). Activation of Critical, Host-Induced, Metabolic and Stress Pathways Marks Neutrophil Entry into Cystic Fibrosis Lungs. Proc Natl Acad Sci U S A *106*, 5779-5783. 10.1073/pnas.0813410106. PMC2667067
91. Manz, M.G., and Boettcher, S. (2014). Emergency Granulopoiesis. Nat Rev Immunol *14*, 302-314. 10.1038/nri3660.
92. Margaroli, C., Garratt, L.W., Horati, H., Dittrich, A.S., Rosenow, T., Montgomery, S.T., Frey, D.L., Brown, M.R., Schultz, C., Guglani, L.*, et al.* (2019). Elastase Exocytosis by Airway Neutrophils Is Associated with Early Lung Damage in Children with Cystic Fibrosis. Am J Respir Crit Care Med *199*, 873-881. 10.1164/rccm.201803-0442OC. PMC6444666
93. Margaroli, C., Moncada-Giraldo, D., Gulick, D.A., Dobosh, B., Giacalone, V.D., Forrest, O.A., Sun, F., Gu, C., Gaggar, A., Kissick, H.*, et al.* (2021). Transcriptional Firing Represses Bactericidal Activity in Cystic Fibrosis Airway Neutrophils. Cell Rep Med *2*, 100239. 10.1016/j.xcrm.2021.100239. PMC8080108
94. Margaroli, C., and Tirouvanziam, R. (2016). Neutrophil Plasticity Enables the Development of Pathological Microenvironments: Implications for Cystic Fibrosis Airway Disease. Mol Cell Pediatr *3*, 38. 10.1186/s40348-016-0066-2. PMC5136534
95. Marki, A., Buscher, K., Lorenzini, C., Meyer, M., Saigusa, R., Fan, Z., Yeh, Y.T., Hartmann, N., Dan, J.M., Kiosses, W.B.*, et al.* (2021). Elongated Neutrophil-Derived Structures Are Blood-Borne Microparticles Formed by Rolling Neutrophils During Sepsis. J Exp Med *218*. 10.1084/jem.20200551. PMC7721910
96. Mathieu, M., Nevo, N., Jouve, M., Valenzuela, J.I., Maurin, M., Verweij, F.J., Palmulli, R., Lankar, D., Dingli, F., Loew, D.*, et al.* (2021). Specificities of Exosome Versus Small Ectosome Secretion Revealed by Live Intracellular Tracking of CD63 and CD9. Nat Commun *12*, 4389. 10.1038/s41467-021-24384-2. PMC8289845
97. McKenna, E., Mhaonaigh, A.U., Wubben, R., Dwivedi, A., Hurley, T., Kelly, L.A., Stevenson, N.J., Little, M.A., and Molloy, E.J. (2021). Neutrophils: Need for Standardized Nomenclature. Front Immunol *12*, 602963. 10.3389/fimmu.2021.602963. PMC8081893
98. Merad, M., and Martin, J.C. (2020). Pathological Inflammation in Patients with COVID-19: A Key Role for Monocytes and Macrophages. Nat Rev Immunol *20*, 355-362. 10.1038/s41577-020-0331-4. PMC7201395
99. Meriwether, D., Jones, A.E., Ashby, J.W., Solorzano-Vargas, R.S., Dorreh, N., Noori, S., Grijalva, V., Ball, A.B., Semis, M., Divakaruni, A.S.*, et al.* (2022). Macrophage COX2 Mediates Efferocytosis, Resolution Reprogramming, and Intestinal Epithelial Repair. Cell Mol Gastroenterol Hepatol *13*, 1095-1120. 10.1016/j.jcmgh.2022.01.002. PMC8873959
100. Mitchell, T.C. (2018). A Grim Fate for Human Neutrophils in Airway Disease. J Leukoc Biol *104*, 657-659. 10.1002/JLB.5CE0418-162R. PMC7309533
101. Mollinedo, F., Calafat, J., Janssen, H., Martin-Martin, B., Canchado, J., Nabokina, S.M., and Gajate, C. (2006). Combinatorial Snare Complexes Modulate the Secretion of Cytoplasmic Granules in Human Neutrophils. J Immunol *177*, 2831-2841. 10.4049/jimmunol.177.5.2831.
102. Nakatsu, F., and Ohno, H. (2003). Adaptor Protein Complexes as the Key Regulators of Protein Sorting in the Post-Golgi Network. Cell Struct Funct *28*, 419-429. 10.1247/csf.28.419.

103. Nauseef, W.M., and Borregaard, N. (2014). Neutrophils at Work. Nat Immunol *15*, 602-611. 10.1038/ni.2921.
104. Nerlov, C. (2004). C/Ebpalpha Mutations in Acute Myeloid Leukaemias. Nat Rev Cancer *4*, 394-400. 10.1038/nrc1363.
105. Nguyen-Jackson, H., Panopoulos, A.D., Zhang, H., Li, H.S., and Watowich, S.S. (2010). Stat3 Controls the Neutrophil Migratory Response to CXCR2 Ligands by Direct Activation of G-CSF-Induced CXCR2 Expression and Via Modulation of CXCR2 Signal Transduction. Blood *115*, 3354-3363. 10.1182/blood-2009-08-240317. PMC2858484
106. Orkin, S.H., and Zon, L.I. (2008). Hematopoiesis: An Evolving Paradigm for Stem Cell Biology. Cell *132*, 631-644. 10.1016/j.cell.2008.01.025. PMC2628169
107. Ostendorf, L., Mothes, R., van Koppen, S., Lindquist, R.L., Bellmann-Strobl, J., Asseyer, S., Ruprecht, K., Alexander, T., Niesner, R.A., Hauser, A.E*., et al.* (2019). Low-Density Granulocytes Are a Novel Immunopathological Feature in Both Multiple Sclerosis and Neuromyelitis Optica Spectrum Disorder. Front Immunol *10*, 2725. 10.3389/fimmu.2019.02725. PMC6896820
108. Owen, C.A., Campbell, M.A., Sannes, P.L., Boukedes, S.S., and Campbell, E.J. (1995). Cell Surface-Bound Elastase and Cathepsin G on Human Neutrophils: A Novel, Non-Oxidative Mechanism by Which Neutrophils Focus and Preserve Catalytic Activity of Serine Proteinases. J Cell Biol *131*, 775-789. 10.1083/jcb.131.3.775. PMC2120617
109. Padrines, M., Wolf, M., Walz, A., and Baggiolini, M. (1994). Interleukin-8 Processing by Neutrophil Elastase, Cathepsin G and Proteinase-3. FEBS Lett *352*, 231-235. 10.1016/0014-5793(94)00952-x.
110. Pillay, J., den Braber, I., Vrisekoop, N., Kwast, L.M., de Boer, R.J., Borghans, J.A., Tesselaar, K., and Koenderman, L. (2010). In Vivo Labeling with 2h2o Reveals a Human Neutrophil Lifespan of 5.4 Days. Blood *116*, 625-627. 10.1182/blood-2010-01-259028.
111. Pols, M.S., and Klumperman, J. (2009). Trafficking and Function of the Tetraspanin CD63. Exp Cell Res *315*, 1584-1592. 10.1016/j.yexcr.2008.09.020.
112. Price, T.H., Chatta, G.S., and Dale, D.C. (1996). Effect of Recombinant Granulocyte Colony-Stimulating Factor on Neutrophil Kinetics in Normal Young and Elderly Humans. Blood *88*, 335-340.
113. Quail, D.F., Amulic, B., Aziz, M., Barnes, B.J., Eruslanov, E., Fridlender, Z.G., Goodridge, H.S., Granot, Z., Hidalgo, A., Huttenlocher, A*., et al.* (2022). Neutrophil Phenotypes and Functions in Cancer: A Consensus Statement. J Exp Med *219*. 10.1084/jem.20220011. PMC9086501
114. Rada, B. (2017). Interactions between Neutrophils and Pseudomonas Aeruginosa in Cystic Fibrosis. Pathogens *6*. 10.3390/pathogens6010010. PMC5371898
115. Radomska, H.S., Huettner, C.S., Zhang, P., Cheng, T., Scadden, D.T., and Tenen, D.G. (1998). CCAAT/Enhancer Binding Protein Alpha Is a Regulatory Switch Sufficient for Induction of Granulocytic Development from Bipotential Myeloid Progenitors. Mol Cell Biol *18*, 4301-4314. 10.1128/MCB.18.7.4301. PMC109014
116. Ramji, D.P., and Foka, P. (2002). CCAAT/Enhancer-Binding Proteins: Structure, Function and Regulation. Biochem J *365*, 561-575. 10.1042/BJ20020508. PMC1222736
117. Ramsey, B.W., Davies, J., McElvaney, N.G., Tullis, E., Bell, S.C., Drevinek, P., Griese, M., McKone, E.F., Wainwright, C.E., Konstan, M.W*., et al.* (2011). A CFTR Potentiator in

Patients with Cystic Fibrosis and the G551d Mutation. N Engl J Med *365*, 1663-1672. 10.1056/NEJMoa1105185. PMC3230303
118. Rankin, S.M. (2010). The Bone Marrow: A Site of Neutrophil Clearance. J Leukoc Biol *88*, 241-251. 10.1189/jlb.0210112.
119. Reiding, K.R., Lin, Y.H., van Alphen, F.P.J., Meijer, A.B., and Heck, A.J.R. (2021). Neutrophil Azurophilic Granule Glycoproteins Are Distinctively Decorated by Atypical Pauci- and Phosphomannose Glycans. Commun Biol *4*, 1012. 10.1038/s42003-021-02555-7. PMC8390755
120. Rosales, C. (2018). Neutrophil: A Cell with Many Roles in Inflammation or Several Cell Types? Front Physiol *9*, 113. 10.3389/fphys.2018.00113. PMC5826082
121. Rossi, A.G., Sawatzky, D.A., Walker, A., Ward, C., Sheldrake, T.A., Riley, N.A., Caldicott, A., Martinez-Losa, M., Walker, T.R., Duffin, R.*, et al.* (2006). Cyclin-Dependent Kinase Inhibitors Enhance the Resolution of Inflammation by Promoting Inflammatory Cell Apoptosis. Nat Med *12*, 1056-1064. 10.1038/nm1468.
122. Rous, B.A., Reaves, B.J., Ihrke, G., Briggs, J.A., Gray, S.R., Stephens, D.J., Banting, G., and Luzio, J.P. (2002). Role of Adaptor Complex AP-3 in Targeting Wild-Type and Mutated CD63 to Lysosomes. Mol Biol Cell *13*, 1071-1082. 10.1091/mbc.01-08-0409. PMC99620
123. Schmidt, T., Zundorf, J., Gruger, T., Brandenburg, K., Reiners, A.L., Zinserling, J., and Schnitzler, N. (2012). Cd66b Overexpression and Homotypic Aggregation of Human Peripheral Blood Neutrophils after Activation by a Gram-Positive Stimulus. J Leukoc Biol *91*, 791-802. 10.1189/jlb.0911483.
124. Sheshachalam, A., Srivastava, N., Mitchell, T., Lacy, P., and Eitzen, G. (2014). Granule Protein Processing and Regulated Secretion in Neutrophils. Front Immunol *5*, 448. 10.3389/fimmu.2014.00448. PMC4168738
125. Shikotra, A., Choy, D.F., Siddiqui, S., Arthur, G., Nagarkar, D.R., Jia, G., Wright, A.K., Ohri, C.M., Doran, E., Butler, C.A.*, et al.* (2017). A CEACAM6-High Airway Neutrophil Phenotype and CEACAM6-High Epithelial Cells Are Features of Severe Asthma. J Immunol *198*, 3307-3317. 10.4049/jimmunol.1600606.
126. Solomon, G.M., Marshall, S.G., Ramsey, B.W., and Rowe, S.M. (2015). Breakthrough Therapies: Cystic Fibrosis (Cf) Potentiators and Correctors. Pediatric pulmonology *50 Suppl 40*, S3-S13. 10.1002/ppul.23240. PMC4620567
127. Stark, M.A., Huo, Y., Burcin, T.L., Morris, M.A., Olson, T.S., and Ley, K. (2005). Phagocytosis of Apoptotic Neutrophils Regulates Granulopoiesis Via IL-23 and IL-17. Immunity *22*, 285-294. 10.1016/j.immuni.2005.01.011.
128. Stockley, J.A., Walton, G.M., Lord, J.M., and Sapey, E. (2013). Aberrant Neutrophil Functions in Stable Chronic Obstructive Pulmonary Disease: The Neutrophil as an Immunotherapeutic Target. Int Immunopharmacol *17*, 1211-1217. 10.1016/j.intimp.2013.05.035.
129. Strug, L.J., Stephenson, A.L., Panjwani, N., and Harris, A. (2018). Recent Advances in Developing Therapeutics for Cystic Fibrosis. Hum Mol Genet *27*, R173-R186. 10.1093/hmg/ddy188. PMC6061831
130. Subbarao, K., and Mahanty, S. (2020). Respiratory Virus Infections: Understanding COVID-19. Immunity *52*, 905-909. 10.1016/j.immuni.2020.05.004. PMC7237932

131. Sun, R., Huang, J., Yang, Y., Liu, L., Shao, Y., Li, L., and Sun, B. (2022). Dysfunction of Low-Density Neutrophils in Peripheral Circulation in Patients with Sepsis. Sci Rep *12*, 685. 10.1038/s41598-021-04682-x. PMC8758723
132. Thiam, H.R., Wong, S.L., Qiu, R., Kittisopikul, M., Vahabikashi, A., Goldman, A.E., Goldman, R.D., Wagner, D.D., and Waterman, C.M. (2020). Netosis Proceeds by Cytoskeleton and Endomembrane Disassembly and Pad4-Mediated Chromatin Decondensation and Nuclear Envelope Rupture. Proc Natl Acad Sci U S A *117*, 7326-7337. 10.1073/pnas.1909546117. PMC7132277
133. Tirouvanziam, R., Gernez, Y., Conrad, C.K., Moss, R.B., Schrijver, I., Dunn, C.E., Davies, Z.A., Herzenberg, L.A., and Herzenberg, L.A. (2008). Profound Functional and Signaling Changes in Viable Inflammatory Neutrophils Homing to Cystic Fibrosis Airways. Proc Natl Acad Sci U S A *105*, 4335-4339. 10.1073/pnas.0712386105. PMC2393742
134. Turton, K.B., Ingram, R.J., and Valvano, M.A. (2021). Macrophage Dysfunction in Cystic Fibrosis: Nature or Nurture? J Leukoc Biol *109*, 573-582. 10.1002/JLB.4RU0620-245R.
135. Vandivier, R.W., Fadok, V.A., Hoffmann, P.R., Bratton, D.L., Penvari, C., Brown, K.K., Brain, J.D., Accurso, F.J., and Henson, P.M. (2002). Elastase-Mediated Phosphatidylserine Receptor Cleavage Impairs Apoptotic Cell Clearance in Cystic Fibrosis and Bronchiectasis. J Clin Invest *109*, 661-670. 10.1172/JCI13572. PMC150889
136. Venkatakrishnan, V., Dieckmann, R., Loke, I., Tjondro, H.C., Chatterjee, S., Bylund, J., Thaysen-Andersen, M., Karlsson, N.G., and Karlsson-Bengtsson, A. (2020). Glycan Analysis of Human Neutrophil Granules Implicates a Maturation-Dependent Glycosylation Machinery. J Biol Chem *295*, 12648-12660. 10.1074/jbc.RA120.014011. PMC7476722
137. Volkova, N., Moy, K., Evans, J., Campbell, D., Tian, S., Simard, C., Higgins, M., Konstan, M.W., Sawicki, G.S., Elbert, A.*, et al.* (2020). Disease Progression in Patients with Cystic Fibrosis Treated with Ivacaftor: Data from National US and UK Registries. J Cyst Fibros *19*, 68-79. 10.1016/j.jcf.2019.05.015.
138. Wang, J., Wang, X., Guo, Y., Ye, L., Li, D., Hu, A., Cai, S., Yuan, B., Jin, S., Zhou, Y.*, et al.* (2021). Therapeutic Targeting of Spib/Spi1-Facilitated Interplay of Cancer Cells and Neutrophils Inhibits Aerobic Glycolysis and Cancer Progression. Clin Transl Med *11*, e588. 10.1002/ctm2.588. PMC8567044
139. Wigerblad, G., Cao, Q., Brooks, S., Naz, F., Gadkari, M., Jiang, K., Gupta, S., O'Neil, L., Dell'Orso, S., Kaplan, M.J.*, et al.* (2022). Single-Cell Analysis Reveals the Range of Transcriptional States of Circulating Human Neutrophils. J Immunol. 10.4049/jimmunol.2200154.
140. Witko-Sarsat, V., Mocek, J., Bouayad, D., Tamassia, N., Ribeil, J.A., Candalh, C., Davezac, N., Reuter, N., Mouthon, L., Hermine, O.*, et al.* (2010). Proliferating Cell Nuclear Antigen Acts as a Cytoplasmic Platform Controlling Human Neutrophil Survival. J Exp Med *207*, 2631-2645. 10.1084/jem.20092241. PMC2989777
141. Yeamans, C., Wang, D., Paz-Priel, I., Torbett, B.E., Tenen, D.G., and Friedman, A.D. (2007). C/Ebpalpha Binds and Activates the PU.1 Distal Enhancer to Induce Monocyte Lineage Commitment. Blood *110*, 3136-3142. 10.1182/blood-2007-03-080291. PMC2200910
142. Zhang, D.E., Zhang, P., Wang, N.D., Hetherington, C.J., Darlington, G.J., and Tenen, D.G. (1997). Absence of Granulocyte Colony-Stimulating Factor Signaling and Neutrophil

Development in CCAAT Enhancer Binding Protein Alpha-Deficient Mice. Proc Natl Acad Sci U S A *94*, 569-574. 10.1073/pnas.94.2.569. PMC19554

143. Zhao, L., Xu, S., Peterson, C., Kuroki, M., Kuroki, M., and Venge, P. (2002). Purification and Characterization of a 95-Kda Protein--Carcinoembryonic Antigen-Related Cell Adhesion Molecule 8--from Normal Human Granulocytes. J Immunol Methods *270*, 27-35. 10.1016/s0022-1759(02)00215-6.
144. Zhou, H., Stanners, C.P., and Fuks, A. (1993). Specificity of Anti-Carcinoembryonic Antigen Monoclonal Antibodies and Their Effects on Cea-Mediated Adhesion. Cancer Res *53*, 3817-3822.

This chapter has been published in the Journal of Leukocyte Biology (Forrest et al., 2022)

Chapter 3: NEUTROPHIL-DERIVED EXTRACELLULAR VESICLES PROMOTE FEED-FORWARD INFLAMMASOME SIGNALING IN CYSTIC FIBROSIS AIRWAYS

ABSTRACT

Cystic fibrosis (CF) airways feature high extracellular levels of the interleukin-1 (IL-1) family of pro-inflammatory mediators. These mediators are cleavage products of caspase-1, the final protease in the inflammasome cascade. Due to the proven chronic presence of reprogrammed neutrophils in the CF airway lumen, understanding inflammasome signaling in these cells is of great importance to understand how disease is perpetuated in this milieu. Here, we hypothesized that CF airway neutrophils contribute to chronic inflammation, in part, via the packaging of inflammasome-inducing signals in extracellular vesicles (EVs). We confirmed that CF airway fluid is enriched in IL-1α, IL-1β and IL-18, and that CF airway neutrophils upregulate the activating receptor IL-1R1. Meanwhile, down-modulatory signals such as IL-1R2 and IL-1RA are unchanged. Active caspase-1 itself is present in CF airway fluid EVs, with neutrophil derived-EVs being most enriched. Using a transmigration model of CF airway inflammation, we show that CF airway fluid EVs are necessary and sufficient to induce primary granule exocytosis by naïve neutrophils (hallmark of reprogramming), and concomitantly activate caspase-1 and IL-1β production by these cells and the addition of triple combination highly effective modulator therapy does not abrogate these effects. Finally, EVs from activated neutrophils can deliver active caspase-1 to naïve primary tracheal epithelial cells and induce their release of IL-1α. These findings support the existence of a feed-forward inflammatory process by which

reprogrammed CF airway neutrophils bypass normal two-step control of inflammasome activation in neighboring cells (naïve neutrophils and epithelial cells) via the transfer of bioactive EVs.

INTRODUCTION

Mediators of the interleukin-1 (IL-1) family, including IL-1α, IL1β and IL-18, are key to the induction of sterile and infection-induced inflammatory responses (dos Santos et al., 2012; Lukens et al., 2012). IL-1α / β signal by binding to the activating IL-1 receptor, IL-1R1 (Besnard et al., 2012; Lukens et al., 2012; Mahmutovic Persson et al., 2018), while IL-18 binds to IL-18R. Both IL-1R1 and IL-18R are expressed broadly and can lead to production of IL-1α, IL1β and IL-18 by target cells, emphasizing the potential for feed-forward IL-1 signaling. To mitigate this risk, IL-1 signaling is countered at the target cell level by IL-1α / β binding to the decoy receptor, IL-R2 and competitive binding of IL-1 receptor antagonist (IL-1RA) to IL-1R1 (Sims and Smith, 2010; Nold et al., 2013). In addition, IL-1 mediator production is under two-step control: signal #1 induces transcription and translation of pro-forms of IL-1 mediators, and signal #2 regulates their cleavage into bioactive forms (Iula et al., 2018; Gritsenko et al., 2020).

Cleavage of the IL-1 mediator pro-forms follows the assembly of multimolecular intracellular scaffolds named “inflammasomes”. Inflammasome assembly is initiated by binding of stress stimuli (signal #1) to NOD-like receptors (NLRs). This in turn recruits the adaptor molecule apoptosis-associated speck-like protein (ASC), which contains a caspase activation and recruitment domain (CARD) able to proteolytically activate the effector protease caspase-1. In the last step of the cascade, active caspase-1 activation cleaves pro-forms of IL-1 IL-1α, IL1β and IL-18 (Sutterwala et al., 2007). Pro-forms of IL-1α / β may also be activated in neutrophils in a caspase 1-independent manner through serine proteases such as neutrophil elastase (NE), although there is conflicting evidence on this (Alfaidi et al., 2015; Clancy et al., 2018). NE is stored within primary granules (Karmakar et al., 2015; Johnson et al., 2017) and can be released

upon neutrophil exocytosis, leading to its presence in the extracellular fluid and its recapture at the surface of cells and on extracellular vesicles (EVs) (Genschmer et al., 2019). Key components of the inflammasome (ASC, caspase-1) normally induced by signal #2 can also be released by activated cells for uptake by bystander cells to perpetuate inflammasome activation (Baroja-Mazo et al., 2014; Venegas et al., 2017).

Inflammasome activation is not only critical to myeloid cell-mediated immunity, but it is also a central innate response in epithelial cells (Schroder and Tschopp, 2010; Thinwa et al., 2014; Venegas et al., 2017). In macrophages, inflammasome activation is followed by pyroptotic cell death, which leads to the mass release of IL-1β and perpetuation of inflammation (Brennan and Cookson, 2000). In neutrophils and epithelial cells, however, IL-1 secretion can occur without concomitant cell death (Chen et al., 2014; Gaidt and Hornung, 2017). Notably, one of the final effectors of pyroptosis is gasdermin D, which upon cleavage of its pro-form will oligomerize and generate pores in the plasma membrane. However, in neutrophils gasdermin D can associate with the primary granules and facilitate release of IL-1β without cell death (Karmakar et al., 2020). Although incompletely understood, another mechanism of release for these mediators is through packaging within EVs, which are then released extracellularly by viable cells and endocytosed by target cells (MacKenzie et al., 2001; Exline et al., 2014).

In cystic fibrosis (CF), progressive lung disease is caused by a pathological triad of airway obstruction, bacterial infection, and sustained recruitment of neutrophils. This results in neutrophils being the dominant leukocyte subset in CF airways starting in infancy (Cohen and Prince, 2012; Margaroli and Tirouvanziam, 2016), with characteristic reprogramming marked by

rapid transcription, primary granule exocytosis, immunomodulatory activity toward T-cells, metabolic licensing, and loss of bacterial killing (Margaroli et al., 2021). Inflammasome activation is thought to contribute to the chronic recruitment of neutrophils to CF airways, via both IL-1α from the stressed epithelium and IL-1β from activated leukocytes (Sutterwala et al., 2007; Fritzsching et al., 2015; Rimessi et al., 2015). In leukocytes, activation of caspase-1 (signal #2) may be initiated, in part, by the gram-negative bacterium *P. aeruginosa,* which infects a majority of CF patients (Reiniger et al., 2007; Cohen and Prince, 2013). However, it remains unclear how much inflammasome activation within activated CF airway neutrophils themselves contributes to perpetuating IL-1 signaling and chronic inflammation in patients.

In this study, we focused on the role of inflammasome activation in neutrophils as a potential driving force in CF airway pathogenesis. We show that the inflammasome pathway is activated in CF airway neutrophils, while inhibitory signals are unchanged. Moreover, we show that CF airway fluid EVs, and predominantly the neutrophil-derived EVs therein, carry active caspase-1 and directly induce inflammasome signaling in naïve neutrophils and epithelial cells, resulting in a feed-forward inflammatory process.

MATERIALS AND METHODS

Human subjects and samples. Samples were accrued per Emory University IRB-approved protocols. Informed consent was obtained before sample collection from a total of 76 adults with CF **(Supplementary Table 1)** and 10 HC adults. CF was diagnosed using a quantitative iontophoresis test and/or documentation of two identifiable CFTR mutations. Neutrophils were purified from whole blood from healthy control (HC) and CF donors as previously described(Tirouvanziam et al., 2008)and used for transmigration experiments (below) or flow cytometry **(Supplementary Methods)**. Sputum was collected from HC subjects by induction, and from CF patients by expectoration and processed as previously described (Tirouvanziam et al., 2008) to yield live neutrophils and airway supernatant (ASN). Airway neutrophils were analyzed by flow and image cytometry **(Supplementary Methods)**. ASN was stored at -80˚C until use for EV purification (below), transmigration experiments (below), or ELISA **(Supplementary Methods)**.

Primary airway epithelial cell culture. Primary healthy control tracheal epithelial cells (NhTE) were grown on semi-permeable Transwell supports (Corning, Herndon, VA, USA) in conditionally reprogrammed cell (CRC) culture medium by the Emory Experimental Models Core, as previously described (Liu et al., 2012). In brief, NhTE cells were first plated on human type IV placental collagen-coated 12 mm plates in CRC culture medium and fed every other day basolaterally for differentiation at ALI. Experiments were performed between 2 and 4 weeks of ALI culture and epithelial cells analyzed by confocal microscopy **(Supplementary Methods)**.

***In vitro* transmigration model of CF airway inflammation.** The model was set up as described (Forrest et al., 2018; Dobosh et al., 2021). In brief, the H441 human club-like cell line was seeded on Alvetex scaffolds (Reprocell, Glasgow, UK) and grown at air-liquid interface (ALI) over two weeks. Subsequently, 0.5-1 x 10^6 purified blood neutrophils (either from healthy controls or from patients diagnosed with cystic fibrosis not currently on highly effective modulator therapy) per scaffold were transmigrated at 37˚C under 5% CO_2 for 2 or 18 hours toward apical CFASN, or fractions thereof (e.g., flow-through of 300 kDa MWCO column devoid of EVs, and reconstituted flow-through plus retentate adding back EVs). For experiments utilizing CF neutrophils highly effective modulator therapy (HEMT; 5 µM VX445, 18 µM VX661, 1 µM VX770) was added to the apical CFASN. Transmigrated neutrophils were used for media conditioning (below), flow cytometry and western blot analyses **(Supplementary Methods)**.

As a control for the act of transmigration being necessary to activate the neutrophils, blood neutrophils were incubated in either DMEM + 10% FBS or the CFASN for 2 or 18 hours. The same downstream assays were then conducted.

***In vitro* inflammasome activation.** Transmigrated neutrophils were stimulated with LPS (10 ng/mL, Gibco Life Technologies Inc, Waltham MA, USA) in RPMI at 37˚C and 5% CO_2 for 4 hours followed by nigericin (10 µM, Sigma Aldrich, St. Louis MO, USA) treatment for 2 additional hours.

Generation of EVs from conditioned media. Blood neutrophils activated by LPS (10 ng/mL for 4 hours) and nigericin (10 µM for an additional 2 hours) or neutrophils transmigrated

towards CFASN for 8 hours were incubated in RPMI at a density of 1e6 cells/mL for 12 hours and then EVs were purified as described below.

Purification of EVs. EVs were isolated from ASN or conditioned media by taking the supernatant from sequential centrifugations at 800, 3,000, and 20,000 x *g,* applying to a 300 kDa MWCO (Vivaspin 500, Sartorius, Germany) followed by a 3,000 x *g* spin. Characterization of EVs was by nanoparticle tracking analysis (NTA), flow cytometry and transmission electron microscopy **(Supplementary Methods)**.

Data Analysis. Statistical analyses were preformed using Prism 9.0.0 (GraphPad, La Jolla, CA, USA). Comparisons between two groups was performed with a Mann-Whitney U-test (unpaired) with a threshold of * for $p<0.05$, ** for $p<0.01$, and *** for $p<0.001$, and between two or more groups with a Kruskal-Wallis test and Dunn's multiple comparisons, * $p<0.0332$, ** $p<0.0021$, ***$p<0.0002$. For analysis of the difference in discontinuous distribution of FLICA puncta **(Figure 3.2B)** the Kolmogorov-Smirnov test was used.

Supplementary Methods

Characterization of EVs by nanoparticle tracking analysis, flow cytometry, and electron microscopy. Concentration and size of EVs was determined using the Nanosight NS3000 (Malvern Panalytical, Westborough, MA, USA). For flow cytometry, 30 µL of magnetic beads coated with streptavidin (SVM-80-5 Spherotech, Lake Forest, IL, USA) and washed with PBS + 2.5 mM EDTA then incubated with 10 µL of biotinylated antibody (0.5 mg/mL, Biolegend for 2 hours rotating at 4 ˚C brought to a final volume of 200 µL with PBS + EDTA. Biotinylated antibodies were CD63: 353018, CD66b: 305120, CD326: 324216. CD63 is expressed on many EVs. CD66b is to immunoprecipitate neutrophil-derived EVs, and CD326 is to

immunoprecipitate epithelial-derived EVs.(Takao et al., 2018; Genschmer et al., 2019)Beads were washed 3 times with PBS + EDTA and then approximately $2x10^9$ EVs were applied to the beads and rotated overnight at 4˚C. Bead:EV conjugates were washed 3 times with PBS + EDTA then stained with FLICA and run on a Cytoflex S flow cytometer (Beckman Coulter, Pasadena, CA, USA).

For electron microscopy, EVs were applied to a discharged formvar-carbon coated grid. Excess liquid was wicked away and 1% uranyl acetate stain was added, then wicked away. The samples were air-dried at room temperature. Grids were visualized on a Hitachi 7700 TEM at 80 kV.

ELISA of CFASN and culture supernatants. IL1α, IL-1β, IL-1RA (Cat# DY200, DY201 and DY280, respectively, from R&D Systems, Minneapolis, MN, USA), and IL-18 (ELH-IL18-1, RayBiotech, Peachtree Corners, GA, USA) were measured in CFASN and culture supernatants per manufacturer guidelines.

Flow cytometry analysis of neutrophils. Blood and airway cells from CF and HC subjects, and from the in vitro transmigration model, were stained with fluorescently labeled antibodies: CD63 (H5C6), CD66b (G10F5), EpCAM (9C4), and ICAM (HA58) (Biolegend, San Diego CA, USA), IL-1R1 (FAB269P), IL-1R2 (FAB663A), and IL-1B (IC201) (R&D Systems, Minneapolis, MN, USA). Cells were also stained with the Zombie Aqua or NIR probe (Biolegend) to determine viability. The caspase-1 probe (FAM-YVAD-FMK, Immunochemistry Technologies, Bloomington, MN, USA) was used to assess active caspase-1 activity. Data were acquired on a LSRII cytometer (BD

biosciences) or Cytoflex S and compensation and analysis were performed using FlowJo software 10.6.1 (Becton Dickinson and Company, Franklin Lakes, NJ, USA). The voltages across all acquisitions were calibrated using Spherotech Rainbow Calibration Particles (RCP-30-5) to ensure that all samples were acquired under the same conditions and the cytometer was performing as expected.

Image cytometry analysis of neutrophils. Cells were fixed in Lyse/Fix Phosflow (BD Biosciences), were washed with PBS-EDTA, permeabilized with Perm Buffer I (BD Biosciences) and stained for active caspase-1 (FAM-FLICA-YVAD-FMK), and Hoechst 3334 (nuclear stain). Cells were acquired on the Amnis Imagestream X Mark II (EMD Millipore), with 40x magnification and low flow rate/high sensitivity on the INSPIRE software. Brightfield was set on channels 01 and 09, while scattering was set in channel 06. Data were analyzed using the IDEAS software v6.2 (EMD Millipore).

Lactate Dehydrogenase Assay. To normalize the assay conditions, after each conditioning, which can take varying amounts of time, cells were washed once in PBS, then resuspended in RPMI for 1 hour. Cells were removed and an aliquot of the conditioned media was taken and frozen at -20 ˚C for up to 3 days and then extracellular LDH was measured using the CyQUANT LDH cytotoxicity assay following the manufacturer's instructions. All measurements were normalized to the equivalent number of purified blood neutrophils lysed with 1% TritonX-100.

Western Blot analysis of neutrophils and EVs. 10^6 neutrophils were pelleted and then resuspended in RIPA + HALT protease inhibitor cocktail (Thermo Fisher Scientific, Waltham MA, USA). EVs (~$2x10^9$) were concentrated on the 300 kDa MWCO column and then lysed in RIPA + protease inhibitor cocktail. Primary antibodies diluted in TBST+BSA were TSG101 (1:1000, 4A10, Abcam, Cambridge, UK), calnexin (1:1000, ab10286, Abcam) anti-CD63 (1:15000 System Biosciences EXOAB-CD63A-1), anti-GAPDH (1:400, sc-47724, Santa Cruz), anti-caspase-1 (1:400, NBP1-45433, Novus), and anti-gasdermin D (1:500, #96458, Cell Signaling Technologies). Secondary antibodies were goat anti-rabbit IRdye 800 CW and goat anti-mouse IRdye 680RD (both 1:15000, LICOR, Lincoln NE, USA). Images were taken on a LICOR ODYSSEY per manufacturer guidelines. Images were analyzed in ImageJ 1.52.

Confocal microscopy analysis of epithelial cells. NhTE cells were stimulated for 24 hours with either isolated EVs or LPS + nigericin and stained with FLICA for 1 hour at 37 ˚C, after which the Transwells were washed twice with PBS, and fixed with 4% paraformaldehyde. Fixed Transwells were washed, permeabilized with 0.5% Tween-20 in PBS, followed by two washes with PBS + tween supplemented with 2% goat serum. After the last wash, Transwells were incubated overnight at 4 ˚C with anti-ZO-1 antibody (ZMD.437, Thermo Fisher Scientific, Waltham MA, USA) diluted 1:250 in PBS + 2% goat serum. Transwells were then washed three times with PBS + 2 % goat serum, then incubated for 1 hour at room temperature with a secondary goat anti-rabbit antibody (A27039, Thermo Fisher Scientific, Waltham MA, USA), and 0.5 μg/mL DAPI (Biolegend, San Diego CA, USA) as a nuclear counterstain. Transwells were then washed dried and mounted and stored for confocal imaging. Z-stack images were acquired

using an inverted FV1000 confocal microscope (Olympus Tokyo, Japan), and analyzed using the Fiji image analysis software (National Institutes of Health, Bethesda MD, USA).

Generation of caspase-1 knockout H441 epithelial cells. Two plasmids, pBD245 and pBD246 were cloned, which each express a gRNA **(Supplementary Table 2)** that targets a different portion of the human caspase-1 loci with purported minimal off-target effects. gRNA sequences were designed by Synthego. pSpCas9(BB)-2A-Puro (PX459) V2.0 was acquired from Addgene (Plasmid #62988, Feng Zhang). The plasmid was digested with Bbs1 (New England Biolabs), and purified with a PCR clean up kit. Complementary oligos, with overhangs complementary to the sticky ends of the Bbs1 plasmid digestion **(Supplementary Table 2)**, were annealed together by heating to 95 ˚C and slowly cooled to room temperature. Oligos were diluted 1:100 and ligated to the digested plasmid in the presence of T4 PNK, T4 DNA Ligase and Bbs1 in T4 DNA Ligase Buffer at 37 ˚C. Samples were heat inactivated at 80 ˚C, and then fresh Bbs1 was added to cleave any rejoined plasmid. Ligation reactions were cloned into STBL3 cells plasmids and verified for the correct insertion by Sanger sequencing (Genewiz).

H441 cells were cultured in 50/50 DMEM/F12 media supplemented with antibiotics and 10% FBS. To generate a polyclonal caspase-1 knockout line, the cells were grown to ~80% confluency in a T-25 flask then transfected with both plasmids (pBD245 and pBD246) in one reaction using Lipofectamine 3000 (Invitrogen) in media without serum for 6 hours. The transfection media was replaced with the typical growth media containing serum. After 24 hours, puromycin was added at a concentration of 5 μg/mL and replaced every day for a total

of 6 days. A non-transfected flask was used as a negative control for complete cell death. A standard protocol can be found here (Ran et al., 2013).

RESULTS AND DISCUSSION

Inflammasome pathway mediators IL-1β, IL-1α and IL-18, and activating receptor IL-1R1 are upregulated in CF airways. We first sought to validate previous work linking soluble mediators of the inflammasome pathway to CF airways (Osika et al.) in a large cohort of patients. We found that IL-1α, IL-1β, and IL-18, were elevated in the sputum of patients with CF compared to that of healthy control (HC) subjects **(Figure 3.1A-C)**. However, commensurate changes in IL-1RA levels were not observed **(Figure 3.1D)**. Next, we assessed if inflammasome activation in CF airways also involved altered receptor expression on neutrophils by flow cytometry **(Supplementary Figure 3.1A,B)**. We found increased surface expression of activating IL-1R1 receptor on CF airway compared to blood neutrophils in both inpatient (exacerbation) and outpatient (stable) settings **(Figure 3.1E, Supplementary Figure 3.1C)**, while surface expression of decoy IL-1R2 receptor remained unchanged **(Figure 3.1F, Supplementary Figure 3.1D)**. Together, our data establish a strong baseline inflammasome signaling in CF airways with high levels of IL-1α, IL-1β, IL-18 and IL-1R1, and no evidence for compensatory increases in IL-1RA and IL-1R2.

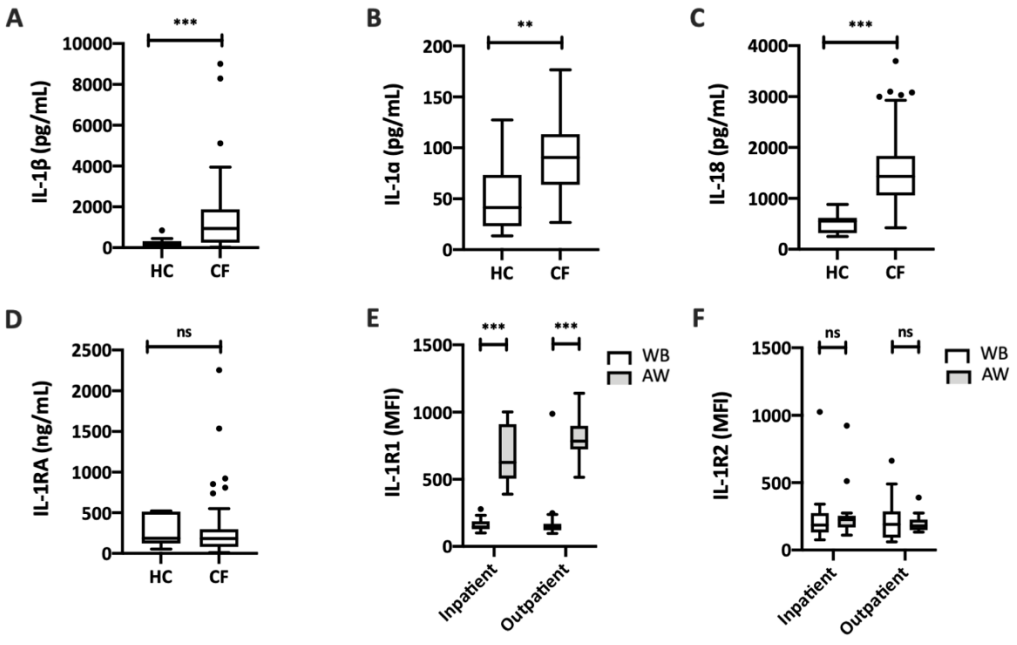

Figure 3.1. Upregulated IL-1 pathway effectors in CF airway fluid and neutrophils. (A) *IL-1β (HC: n= 9, CF: n=60),* ***(B)*** *IL-1α (HC: n=10, CF: n=43),* ***(C)*** *IL-18 (HC: n=9, CF: n=64), and* ***(D)*** *IL-1RA (HC: n=9 CF: n= 55) measured in sputum supernatant by ELISA.* ***(E)*** *Surface expression of the activating IL-1R1 receptor, and* ***(F)*** *surface expression of the decoy IL-1R2 receptor, measured by flow cytometry on whole blood (WB, white) and airway (gray) neutrophils from CF patients at inpatient (WB: n=17, AW: n=16) and outpatient (WB: n=15, AW: n=14) visits. Inpatient visits were conducted 1-4 days after an acute pulmonary exacerbation and outpatient visits were conducted in stable condition at least 3 months from an exacerbation. All statistics were calculated using the Mann-Whitney U-test. * p<0.05, ** p<0.01, ***p<0.001.*

Neutrophils recruited to CF airways *in vivo* and *in vitro* contain active caspase-1. Next, we assessed neutrophils recruited to CF airways for the intracellular presence of active caspase-1, a key step in inflammasome activation, using the caspase 1-specific probe, FAM-FLICA-YVAD-FMK (FLICA). We observed increased intracellular caspase-1 activity in live CF airway neutrophils compared to blood neutrophils in both inpatient and outpatient settings **(Figure 3.2A, Supplementary Figure 3.2A)**. By image cytometry, we confirmed a large number of intracellular nucleation of caspase-1 in typical specks within CF airway neutrophils, while blood neutrophils predominantly had none, or very few puncta **(Figure 3.2B, Supplementary Figure 3.2B, C.)**. To expand beyond these *in vivo* findings, we used an *in vitro* transmigration (TM)

model that we developed to recapitulate the recruitment and reprogramming of neutrophils in CF airways (Forrest et al., 2018). Unstimulated whole blood (WB) neutrophils from HCs did not show strong staining with the FLICA probe in contrast to WB neutrophils activated by signal #1 LPS (10 ng/μL, 4 hours) followed by signal #2 nigericin (10 μM, additional 2 hours). We observed that neutrophils recruited to CF sputum airway supernatant (CFASN), but not the control chemoattractant leukotriene B4 (LTB4), had increased intracellular caspase-1 activity 2 hours post-TM, which was further increased 18 hours post-TM compared to WB neutrophils **(Figure 3.3A)**. Furthermore, we confirmed live CF airway-like neutrophils showed increased production of IL-1β compared to WB and LTB4 TM neutrophils by intracellular cytokine staining **(Figure 3.3B).** Increased cleavage of caspase-1 in the 18-hour CFASN TM neutrophils compared to the LTB4 TM and WB neutrophils was confirmed by western blot (**Supplementary Figure 3.3A).** We also noted that the caspase-1 bands in CFASN TM neutrophils ran at a slightly lower molecular weight (~7 kDa), which to our knowledge has not been previously described. Finally, addition of a NOD-, LRR- and pyrin domain-containing protein 3 (NLRP3) inflammasome-specific inhibitor prevented activation of caspase-1 in neutrophils upon a 2-hour TM, but not at the longer timepoint **(Supplementary Figure 3.3B)**. Thus, inflammasome signaling is activated and inhibitable in live neutrophils recently immigrated into CF airways, resulting in IL-1β production.

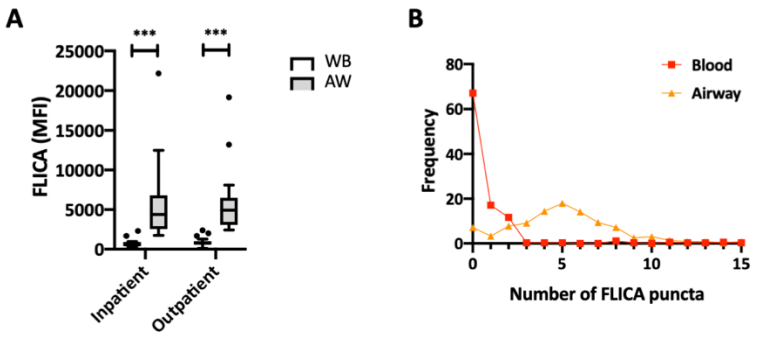

Figure 3.2. Active caspase-1 and IL-1β in CF airway neutrophils in vivo and in vitro. (A) *Intracellular staining with the FAM-FLICA-YVAD-FMK probe specific for active caspase-1 measured by flow cytometry on whole blood (WB, white) and airway (gray) neutrophils from CF patients at inpatient (WB: n=17, AW: n=20) and outpatient (WB: n=15, AW: n=14) visits. Statistics were calculated with Mann-Whitney U-test. * p<0.05, ** p<0.01, ***p<0.001* ***(B)*** *Blood and airway neutrophils from CF patients were analyzed by image cytometry with brightfield (BF), active caspase-1 (FAM-FLICA-YVAD-FMK), and DNA (Hoechst 33342) channels shown. Airway, but not blood neutrophils (paired n=5), show punctate FLICA staining reflecting multiple caspase 1-positive aggregates. The difference in the distribution was calculated using the Kolmogorov-Smirnov test; p= 0.0001.*

After a 2-hour TM, ~75% of the neutrophils were alive as measured by flow cytometry staining of Zombie Aqua, an amine-reactive dye that is impermeant to live cells. After the 18-hour TM the neutrophils were about 50% alive. The damage-associated molecular patterns (DAMPs) as a result of cell death occurring in some cells may play a role in further activation of inflammasome signaling in live neutrophils. To determine whether caspase-1 activation is inevitable in neutrophils after an extended amount of time, WB neutrophils were incubated in either DMEM + 10% FBS or the CFASN without TM. The blood neutrophils showed similar viability as the concomitant TM time points **(Figure 3.3C, Supplementary Figure 3.3C)**. Furthermore, WB neutrophils incubated in CFASN for 18 hours showed a very small increase in FLICA staining, but not to the same extent as the CFASN 18-hour TM neutrophils **(Figure 3.3A, Supplementary Figure 3.3D)**. WB neutrophils incubated in DMEM + 10% FBS or CFASN showed increased lactate dehydrogenase (LDH) secretion compared to the LTB4- and CFASN-transmigrated neutrophils **(Supplementary Figure 3.3E)**. With the exception of unstimulated

WB neutrophils (likely an artifact of low cell number and cells activated by the mechanical processing of blood), dead neutrophils did not show increased FLICA signal compared to their live counterparts **(Supplementary Figure 3.3F)**. We also observed that expression gasdermin-D, and the amount of gasdermin-D that was cleaved remained unchanged in WB, WB LPS + nig stimulated, CFASN TM neutrophils (**Supplementary Figure 3.3G).** Taken together, the process of transmigration in addition to inflammatory cues in the extracellular milieu are necessary to activate inflammasome signaling in live and naïve neutrophils.

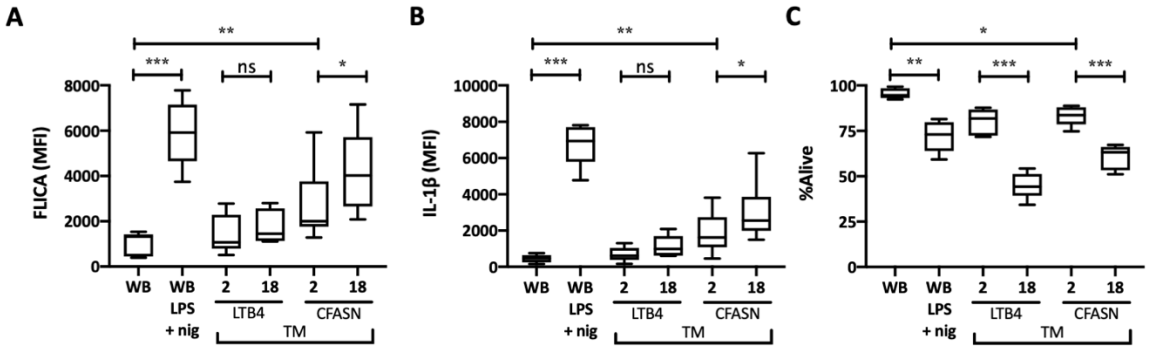

Figure 3.3: Airway-like neutrophils are alive and contain active caspase-1 and IL-1β*. Neutrophils from healthy control (HC) donors transmigrated across NCI-H441 club epithelial cells grown at air-liquid interface towards either leukotriene B4 (LTB4), a control chemoattractant, or CF airway supernatant (CFASN) in a model of CF airway inflammation. Following transmigration (TM) for 2 or 18 hours,* ***(A)*** *intracellular staining with the FAM-FLICA-YVAD-FMK probe, and* ***(B)*** *intracellular IL-1β in live HC neutrophils.* ***(C)*** *Viability of the neutrophils was determined by staining with Fixable Zombie Aqua using flow cytometry. Whole Blood (WB) and WB neutrophils stimulated with LPS (10 ng/μL for 4 hours) and nigericin (10 μM, additional 2 hours) serve as controls. Data from n=6 independent experiments. Statistics were calculated with a Kruskal-Wallis test then selected multiple comparisons between groups using Dunn's test. * p<0.0332, ** p<0.0021, ***p<0.0002.*

Highly effective modulator therapy (HEMT) does not alter caspase-1 or IL-1β in airway-like CF neutrophils. WB neutrophils from donors diagnosed with CF and not currently receiving highly effective combination therapy (HEMT defined as Ivacaftor or Trikafta/Kaftrio) were transmigrated towards either CFASN or CFASN containing triple-HEMT (5 μM VX445, 18 μM VX661, 1 μM VX770) for 2 or 18 hours. The pooled CFASN was not autologously matched with the blood donor, although this may be an area of further research to assess personalized

therapeutics in addition to the use of donor-matched epithelial cells. Similar to the neutrophils derived from HCs, following transmigration staining with the FLICA probe increased with time of transmigration, although was unchanged with the addition of HEMT **(Figure 3.4A)**. Intracellular staining of bioactive IL-1β in live CF neutrophils also showed no change with the addition of HEMT, although the CFASN + HEMT condition at 18-hour TM showed a decrease in the range suggesting that there could be effects of HEMT on inflammasome activation over increased periods of time **(Figure 3.4B)**. Viability of the neutrophils also remained unchanged with the addition of HEMT measured by both flow cytometry **(Figure 3.4C)** and LDH assay **(Supplementary Figure 3.4A).** HEMT may not have a noticeable effect on neutrophil-inflammasome drive inflammation in short term assays although its effect over generations of recruited immune cells remains to be determined. Furthermore, the expression and activity of CFTR, and thus the direct effects of HEMT, on neutrophils must be further investigated (Pohl et al., 2014).

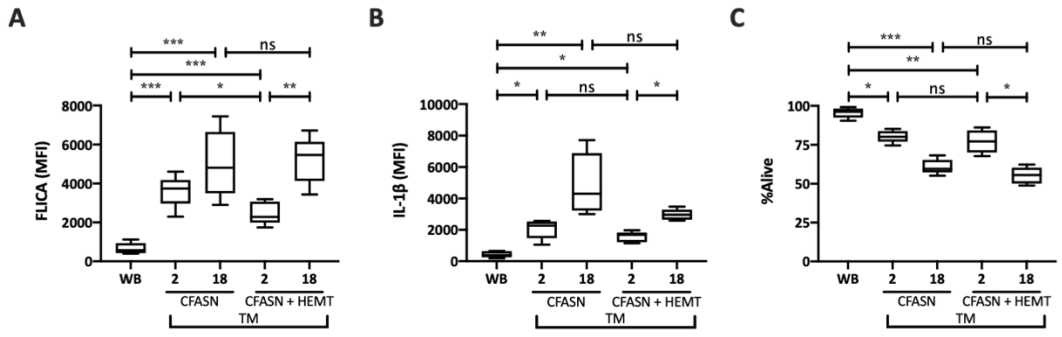

Figure 3.4. Highly effective modulator therapy (HEMT) does not alter caspase-1 or IL-1ϐ in airway-like CF neutrophils. *Neutrophils from donors with CF were transmigrated (TM) towards either CFASN or CFASN containing triple-combination HEMT (5 µM VX445, 18 µM VX661, 1 µM VX770) for 2 or 18 hours. DMSO was used as a vehicle control. The CFASN is a pool of CFASN and there was no autologous matching between the blood neutrophils and the source of the CFASN or the epithelial cells. Following transmigration, **(A)** intracellular staining with the FAM-FLICA-YVAD-FMK probe, and **(B)** intracellular IL-1ϐ in live CF neutrophils. **(C)** Total viability of the neutrophils was determined by staining with amine-reactive Zombie Aqua using flow cytometry. Data from n=5 independent experiments. Statistics were calculated with a Kruskal-Wallis test then selected multiple comparisons between groups using Dunn's test. * p<0.0332, ** p<0.0021, ***p<0.0002.*

EVs from CF sputum activate inflammasome signaling in naïve neutrophils. Building on the observation that CF airway fluid activates inflammasome signaling in recruited neutrophils *in vitro*, we next sought to determine which fluid component resulted in that activity. After differential centrifugations of 800, 3,000, and 20,000 x *g*, the resulting supernatant was applied to a 300 kDa molecular weight cut-off (MWCO) column. Neutrophils were then transmigrated either towards the supernatant of the 20,000 x *g* spin (Pre-300 kDa), the column flow-through (Low MWCO), or the control (reconstituted) fraction with column flow-through and retentate added back to one another (Low + Hi MWCO). Only the conditions including the high molecular weight fraction resulted in the primary granule exocytosis characteristic of CF airway neutrophils **(Figure 3.5A)**, and concomitant increase in intracellular active caspase-1 **(Figure 3.5B)**. According to the minimal information for studies of EVs 2018 (MISEV2018), this is considered an acceptable "intermediate recovery, intermediate specificity" EV enrichment method (Thery et al., 2018). The 300 kDa retentate was then analyzed by a variety of methods to confirm the presence of EVs in accordance with the MISEV2018 guidelines. Western blot analysis of the retentate (Hi MWCO) fraction confirmed the likely presence of EVs as evidenced by inclusion of prototypical EV markers TSG101, a component of the ESRCT machinery involved in EV biogenesis, and the tetraspanin CD63. Meanwhile, the endoplasmic reticulum marker calnexin was not detectable in this fraction, confirming that this fraction is not constituted of apoptotic blebs or cellular debris **(Figure 3.5C, Supplementary Figure A-C).** The presence of EVs was also confirmed by transmission electron microscopy (TEM) negatively stained with 1% uranyl acetate **(Figure 3.5D, Supplementary Figure 5D)** and the global size matched the expected profile by nanoparticle tracking analysis (NTA, **Figure 5E)**. The EVs were also shown to

contain the transmembrane proteins CD66b (neutrophils) or CD326 (epithelial cells) by immunoprecipitation, which colocalized with caspase-1 measured by FLICA **(Figure 3.5F)**. The immunoprecipitated EVs from the retentate, using either CD63 (general EV marker), or the cell-specific markers CD66b and CD326 confirmed that all EV subsets from CF sputum were positive for active caspase-1, although neutrophil-derived EVs (CD66b+) had the highest level **(Figure 3.5F)**. By both TEM and NTA it is clear that the population of EVs is heterogenous in its composition. Indeed, we do not distinguish between different classes of EVs, such as exosomes, exomeres, and microvesicles to name a few (Thery et al., 2018). Likely, the variety of particles we observe originate from the many cells present in the airways such as neutrophils, epithelial cells, macrophages and monocytes, and T-cells, but also invading pathogens such as bacteria and perhaps even fungi. Further diversity is introduced through the multiple pathways of EV biogenesis. Taken together, EVs are present in CF sputum, and notably those derived from airway neutrophils, carry active caspase-1 and induce feed-forward inflammasome activity in neutrophils freshly recruited from blood.

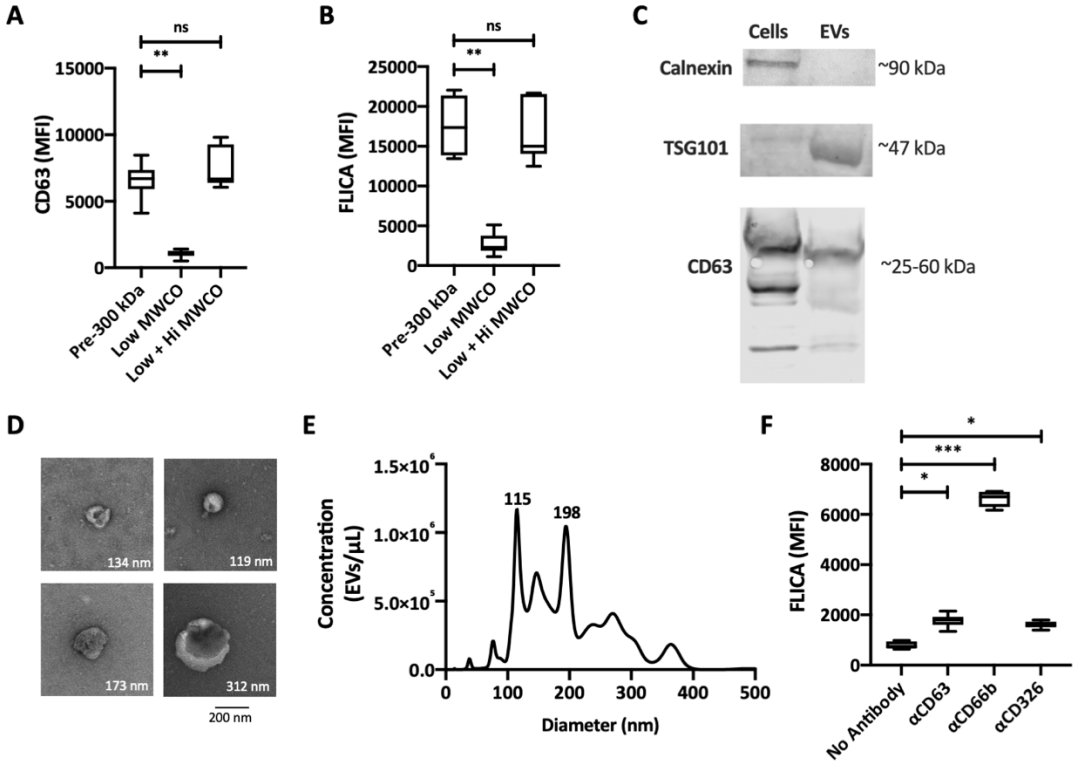

Figure 3.5. CF airway fluid EVs promote caspase-1 signaling in lung-recruited neutrophils. (A) *Surface CD63 expression (reflecting primary granule exocytosis), and* ***(B)*** *intracellular staining with the FAM-FLICA-YVAD-FMK probe in HC neutrophils transmigrated for 18 hours to either of three apical milieus: (i) CF airway supernatant (CFASN) devoid of cells and debris but rich in EVs (Pre-300 kDa); (ii) its 300 kDa flow-through devoid of EVs (Low MWCO); or (iii) the reconstituted fraction with 300 kDa flow-through (EV-free) and retentate (EV-rich) added back together (Low + Hi MWCO). n = 8 independent experiments* ***(C)*** *Western blot of CF airway neutrophils (cells) and 300 kDa retentate fraction thereof (EVs) probing for the presence of the endoplasmic reticulum marker calnexin (common in cell debris like apoptotic blebs but typically excluded from EVs) and canonical EV markers TSG101 and CD63.* ***(D)*** *Transmission electron micrographs of EVs negatively stained with 1% uranyl acetate. A scale bar corresponding to 200 nm is included.* ***(E)*** *Nanoparticle tracking analysis to determine the size and concentration of EVs in the retentate (high MWCO, EV-rich) fraction of CF airway fluid. Data from n=5 replicates.* ***(F)*** *Staining with the FAM-FLICA-YVAD-FMK probe specific for active caspase-1 measured by flow cytometry on the total retentate (high MWCO, EV-rich) fraction of CF airway fluid (No antibody) and immunopurified subsets therefrom using magnetic beads coated with streptavidin with biotinylated antibodies reflecting pan-EV (anti-CD63), neutrophil-derived EV (anti-CD66b) and epithelial-derived EV (anti-CD326) subsets. Data from n=6 independent experiments. All Statistics were calculated with a Kruskal-Wallis test then selected multiple comparisons between groups using Dunn's test. * p<0.0332, ** p<0.0021, ***p<0.0002.*

Neutrophil-derived EVs induce inflammasome activation in naïve epithelial cells. Next, we sought to determine if neutrophil-derived EVs could also induce inflammasome signaling in naïve epithelial cells. Neutrophils were transmigrated to CF airway fluid or as a control, WB neutrophils were treated with LPS (10 ng/mL, serving as signal 1) plus nigericin (10 µM, serving as signal 2). After stimulation (either LPS + nigericin or CFASN TM), neutrophils were washed and allowed to condition fresh media with their own EVs for 12 hours **(Figure 3.6A)**. EVs from

conditioned media were isolated by differential centrifugation and column purification (300 kDa MWCO), and added to primary normal (healthy) tracheal epithelial (NhTE) cells. The NhTE cells were stained for ZO-1 to confirm the presence of tight junctions and also to confirm that the cells were grown in a monolayer **(Figure 3.6B)**. Upon EV application, the NhTE cells showed clear upregulation of active caspase-1 **(Figure 3.6B)**, To measure association of the neutrophil-derived EVs with the NhTE cells, the EVs were labeled with the membrane dye PKH26 and applied to the NhTE cells. By flow cytometry, the NhTE cells show clear PKH26 signal compared to the untreated control **(Figure 3.6C).** The extracellular inflammatory mediators IL-1α, IL-1β, IL-18 and intercellular adhesion molecule-1 (ICAM-1) levels were also similar increased compared to the unstimulated NhTE cells (Figure 3.**6D-G).** The levels were similar, albeit slightly reduced compared to direct stimulation of the NhTE with LPS + nigericin as opposed to stimulation with EVs from stimulated neutrophils **(Supplementary Figure 3.6A-D)**.

In order to determine the extent to which endogenously expressed caspase-1 vs caspase-1 from neutrophil-derived EVs resulted in FLICA signal, we generated a polyclonal caspase-1 knockout NCI-H441 club epithelial cell line, which exhibited ~92.9% caspase-1 protein reduction **(Supplementary 7A)**. Control stimulation of the casp1$^{-/-}$ cells with LPS + nigericin further confirmed that the knockout removes FLICA staining in these cells **(Supplementary Figure 3.7B).** The application of EVs from neutrophils stimulated with LPS + nigericin or transmigrated towards CFASN only resulted in a minor, and statistically insignificant, increase of FLICA compared to the unstimulated knockout cells. As with the NhTE cells, WT caspase-1 H441 cells showed increased FLICA signal in the appropriate conditions. Labeling of the EVs with PKH26 showed similar association of EVs across all conditions suggesting that endogenous

caspase-1 does not affect EV uptake **(Supplementary Figure 3.7C).** Furthermore, the casp1$^{-/-}$ cells were unable to secrete bioactive IL-1α, IL-1β, and IL-18 **(Supplementary Figure 3.7D-F).** Taken together, these findings demonstrate that EVs derived from neutrophils recruited to and conditioned by the CF airway milieu are able to activate inflammasome signaling in naïve epithelial cells, similarly to treatment with prototypical signals 1 + 2 (LPS plus nigericin).

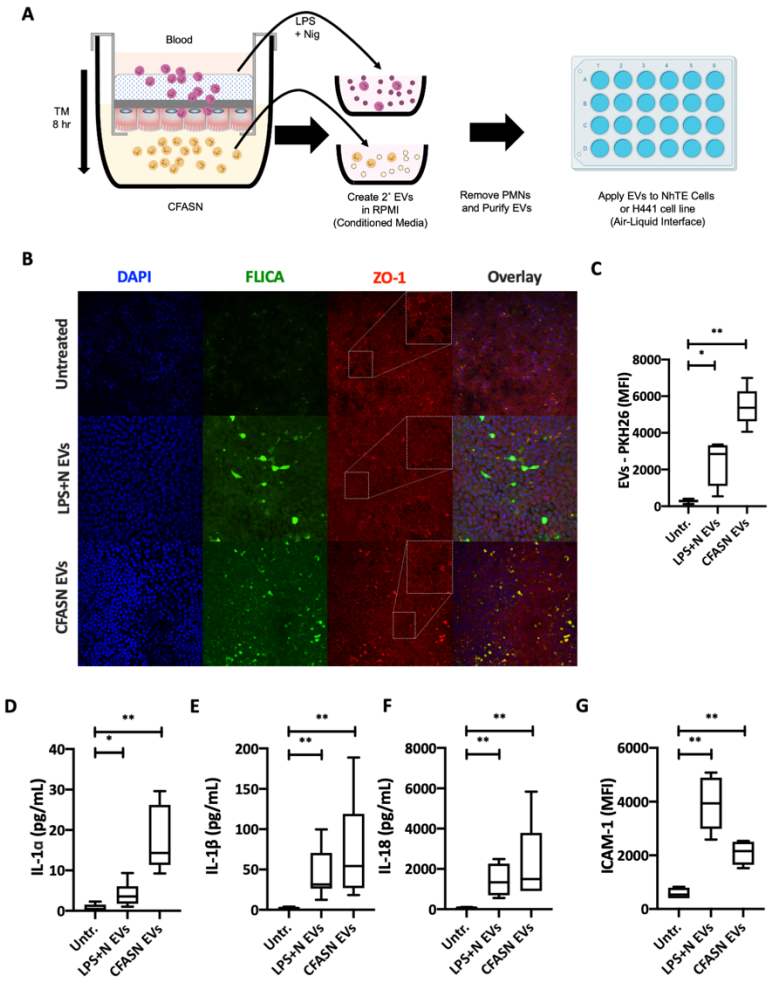

Figure 3.6. CF airway fluid EVs promote caspase-1 signaling in primary lung epithelial cells. (A) *Schematic of experimental setup: blood neutrophils were stimulated with LPS (4 hours, 10 ng/mL) plus nigericin (2 additional hours, 10 μM) or transmigrated into CFASN for 8 hours. These activated neutrophils were then allowed to condition fresh media (without serum) for 12 hours, after which EVs from the conditioned media were isolated.* ***(B)*** *Normal human tracheal epithelial cells (NhTE) grown on semi-permeable Transwell supports at air-liquid interface (ALI) were exposed to EVs from the conditioned media generated from either blood neutrophils stimulated with LPS and nigericin (LPS + N EVs) or from neutrophils that transmigrated towards CFASN (CFASN EVs) and stained for tight junctional complexes (ZO-1) and nucleus (DAPI).* ***(C)*** *The EVs were stained with the membrane dye PKH26 and added to ALI NhTE cultures. Association of EVs with the NhTE cells was assessed by flow*

cytometry analysis of PKH26. ***(D)*** *IL-1α,* ***(E)*** *IL-1β, and* ***(F)*** *IL-18 measured in the conditioned media of NhTE cells stimulated by EVs from neutrophils by ELISA.* ***(G)*** *Surface expression of ICAM-1 on NhTE cells stimulated by EVs from neutrophils measured by flow cytometry. Data from n=8 independent experiments. Statistics were calculated with a Kruskal-Wallis test then multiple comparisons using Dunn's test. * p<0.0332, ** p<0.0021, ***p<0.0002.*

EVs contribute to sustained inflammasome signaling between recruited neutrophils and epithelial cells in CF airways. Neutrophilic inflammation is a hallmark of CF airway disease. In prior in vivo studies from our group, neutrophils were found to enter into the small airway lumen in infants with CF within the first months of life, and notably before chronic infection with proinflammatory pathogens known to induce strong inflammasome activation like *P. aeruginosa*, *S. aureus*, *H. influenzae*, or *A. fumigatus* (Margaroli et al., 2019). Work in epithelial cell and mouse models suggested that local accumulation of apical material (mucus "flakes", or other) may induce hypoxic stress and IL-1a production, providing the impetus for neutrophilic influx (Fritzsching et al., 2015). How this early influx may lead to chronic disease remains unclear. Findings presented here suggest that neutrophils recruited to and conditioned by the CF airway milieu may provide sufficient driving force for sustained inflammasome activation not only in resident, long-lived epithelial cells, but also in freshly recruited neutrophils **(Figure 3.5, 6)**. The critical role of EVs in this process may explain how acute local inflammation in discrete areas of the bronchiolar tree may become chronic and facilitate seeding of adjacent areas by EV transport and uptake. Further studies are needed to determine whether small molecule inflammasome inhibitors (Becker et al.) or recombinant IL-1RA (anakinra)(Iannitti et al.) may counter feed-forward inflammasome signaling when spread via EVs. In chronic obstructive pulmonary disease (COPD) and acute respiratory distress syndrome (ARDS), NE present on the

surface of EVs is less prone to inhibition by $\alpha 1$-antitrypsin and can drive disease (Genschmer et al., 2019).

In fact, EVs can be generated from all of the cells present in the CF lung including, but not limited to the neutrophils and epithelial cells, such as macrophages, monocytes, T-cells, as well as bacteria and fungus (Woith et al., 2019). This communication between the cells in the airways must be heavily investigated and targeted for therapeutic development. There have been recent studies that EVs from neutrophils can cause activation of other neutrophils (Amjadi et al., 2021), and that EVs from *S. aureus* can downregulate the ability of neutrophils to kill bacterial pathogens (Fantone et al., 2021). EVs from CFTR mutated epithelial cells were able to activate neutrophils (Useckaite et al., 2020) and our study now adds communication in the other direction from neutrophils to epithelial cells. It remains unclear what the initial incidence, and whether it is EV-related, is that causes feed-forward neutrophilic inflammation in the CF airways. Due to their high abundance in sputum, inflammasome- and NE-laden, neutrophil-derived EVs are emerging as critical mediators of pathological signaling in CF, COPD and ARDS. In-depth studies attempting to specifically target the entire EV population and specifically these neutrophil-derived EVs for therapeutic benefit are now warranted.

AUTHORSHIP

O.A.F., B.D. and R.T. conceived the study; O.A.F., B.D., S.A.I., S.R., J.L., M.R.B., J.A.A., V.T., AR collected data; O.A.F., B.D., S.A.I., S.R., R.T. analyzed data; A.G., R.W., G.G. contributed methods; O.A.F., B.D. and R.T. drafted the manuscript.

ACKNOWLEDGMENTS

This study was supported by a Cystic Fibrosis Foundation award to R.T. (TIROUV17G0), CF@LANTA RDP Fellowship funded under MCCART15A0 to C.M., and NIH/NHLBI to R.T. (R01HL126603). We thank Dr. Matthew Cooper for providing the NLRP3 inflammasome inhibitor MCC950. We thank the Emory University Pediatrics Department and Winship Cancer Institute Flow Cytometry and Integrated Cellular Imaging Cores and the Apkarian Integrated Electron Microscopy Core for their cooperation. Cystic fibrosis sputum samples for in vitro studies were provided by the CF Biospecimen Repository at the Children's Healthcare of Atlanta and Emory University CF Discovery Core and NhTE cell cultures at ALI were provided by the Emory University CF Experimental Models Core.

CONFLICT OF INTEREST DISCLOSURE

The authors declare no conflict of interest.

FIGURES

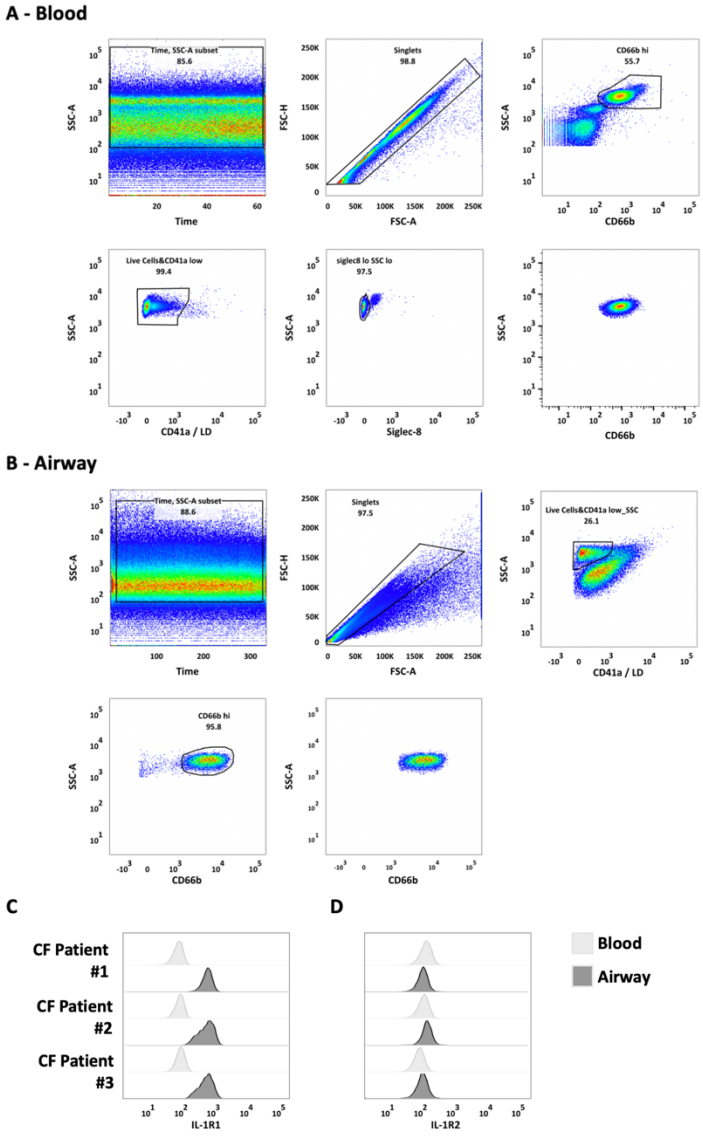

Supplementary Figure 3.1. Flow cytometry analysis of blood and airway neutrophils. (A) Sequential gating strategy for blood neutrophils, and (B) sequential gating strategy for airway neutrophils. (C) Histograms for IL-1R1 and IL1-R2 expression on blood (white) and airway (gray) neutrophils from 3 representative patients with CF.

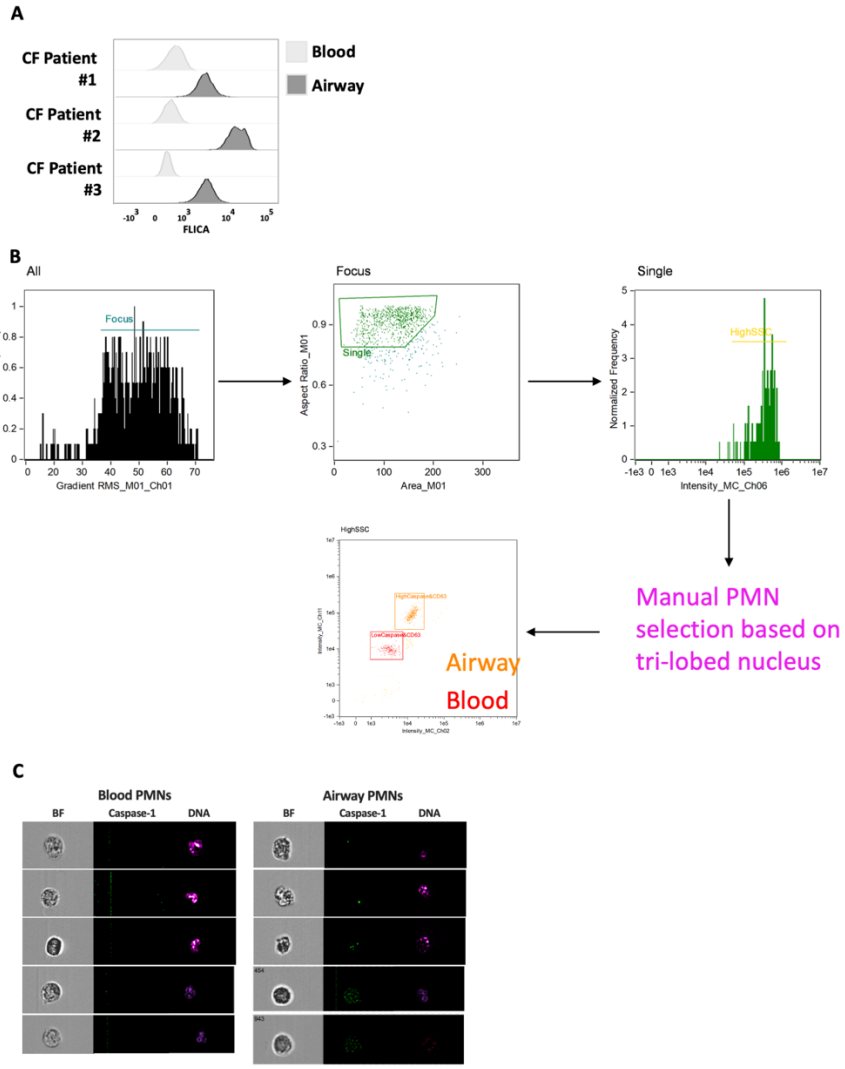

Supplementary Figure 3.2. (A) Representative histograms of the FAM-FLICA-YVAD-FMK probe specific for active caspase-1 on blood (white) and airway (gray) neutrophils. Aggregate data shown in Figure 3.2A. (B) Image flow cytometry (Imagestream) sequential gating strategy to identify neutrophils in blood and airway samples from patients with CF. (C). Representative pictures of caspase-1 (FAM-FLICA-YVAD-FMK) and DNA (Hoechst 33342) from Image flow cytometry. Aggregate quantification of caspase-1 specks in Figure 3.2B.

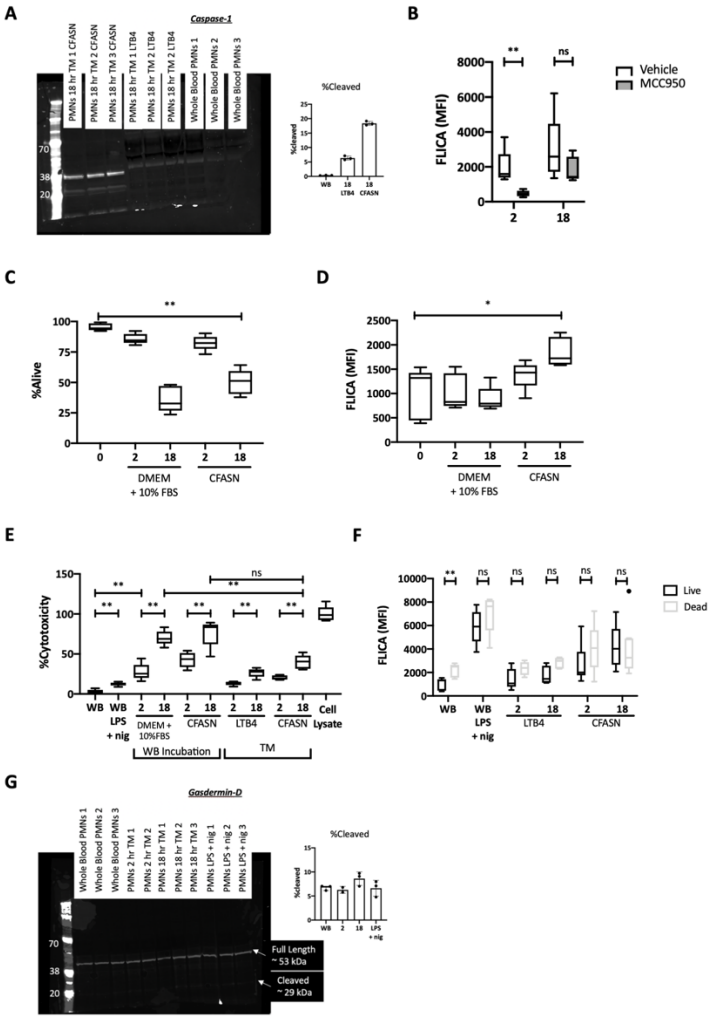

*Supplementary Figure 3.3. (A) Raw western blot for caspase-1 and quantification of the amount of cleaved caspase-1. (B) The specific NLRP3 inhibitor MCC950 (gray) was added at 10 μM to apical CFASN during transmigration. Vehicle (white) was 0.1% v/v water. Data from n=6 independent experiments. Statistics were calculated using the Mann-Whitney U-test. * p<0.05, ** p<0.01, ***p<0.001. (C) Whole blood (WB) neutrophils from healthy control patients were incubated for the prescribed amount of time in either DMEM + 10% FBS or CFASN and viability was measured by retention of the amine reactive Zombie Aqua dye by flow cytometry. (D) Active caspase-1 in blood neutrophils incubated as above was measured with the FLICA probe using flow cytometry. (E) Quantification of lactate dehydrogenase (LDH) activity in the extracellular environment from each condition. To normalize the amount of time that LDH was allowed to be secreted, the cells were conducted to either an incubation in or transmigration towards the marked apical fluid (either DMEM + 10% FBS or CFASN or LTB4 or CFASN) for 2 or 18 hours. Cells were then washed, and allowed to condition fresh media for 1 hour. An aliquot was taken and stored at -20 ˚C for up to 3 days. LDH activity was measured using the CyQUANT kit. The cell lysate is the same number of whole blood cells lysed in 1% TritonX100. Data from n = 6 independent experiments. Statistics were calculated with a Kruskal-Wallis test then selected multiple comparisons between groups using Dunn's test. * p<0.0332, ** p<0.0021, ***p<0.0002. (F) After live or dead flow cytometry gating of the Zombie Aqua dye the median fluorescence intensity (MFI) of the FLICA probe was assessed in both the live and dead cells. Data from n=6 independent experiments. Statistics were calculated using the Mann-Whitney U-test. * p<0.05, ** p<0.01, ***p<0.001. (G) Raw western blot for gasdermin-D and quantification of the amount of cleaved gasdermin-D.*

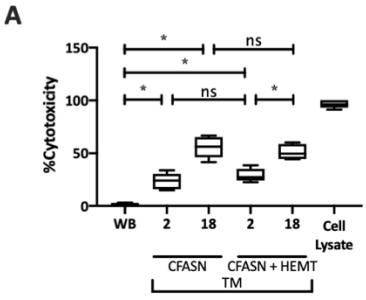

*Supplementary Figure 3.4. Whole blood neutrophils transmigrated towards CFASN or CFASN + HEMT (5 µM VX445, 18 µM VX661, 1 µM VX770) for 2 or 18 hours. DMSO was used as a vehicle control. The cells were then washed and allowed to condition fresh media for 1 hour. An aliquot was taken and stored at -20 ˚C for up to 3 days. LDH activity was measured using the CyQUANT kit. The cell lysate is the same number of whole blood cells lysed in 1% TritonX100. Data from n = 6 independent experiments. Statistics were calculated with a Kruskal-Wallis test then selected multiple comparisons between groups using Dunn's test. * p<0.0332, ** p<0.0021, ***p<0.0002.*

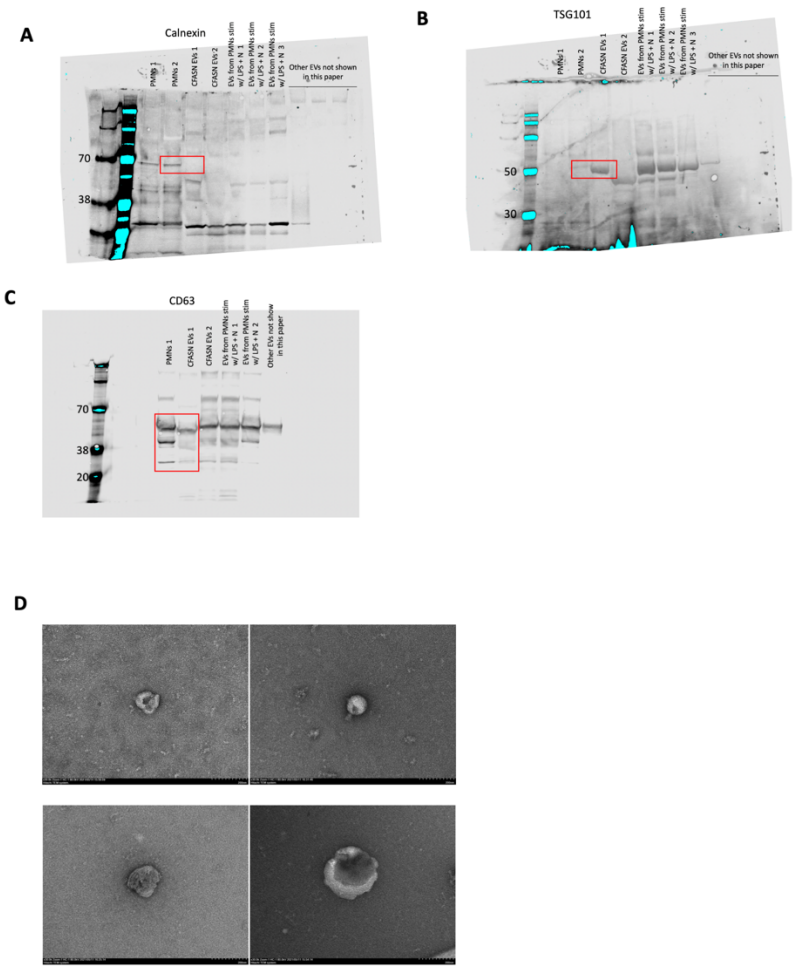

Supplementary Figure 3.5. Raw unprocessed western blots and electron micrographs. This figure relates to Figure 3.5C and 3.5D.

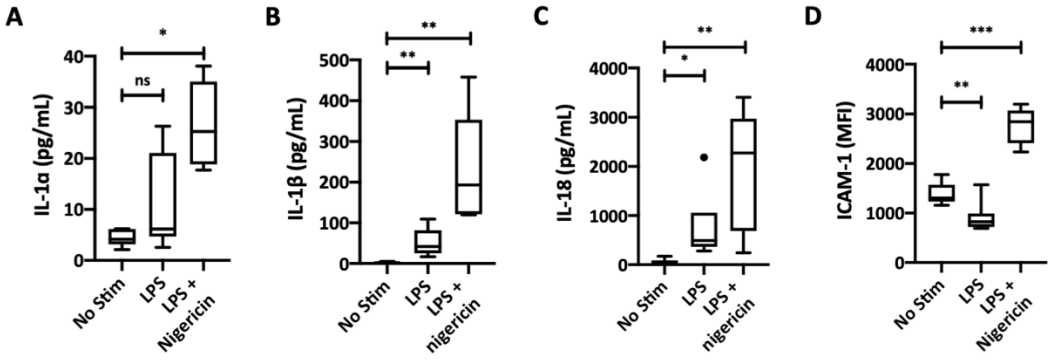

Supplementary Figure 3.6. Control experiment showing direct inflammasome activation in NhTE cultures by LPS and nigericin. (A-C) IL-1α, IL-1β, and IL-18 measured in the extracellular medium by ELISA, and (D) surface expression of ICAM-1 measured by flow cytometry on NhTE cells maintained in ALI culture and stimulated with LPS (10 ng/mL, signal 1) alone or in combination

*with nigericin (10 μM, signal 2). Data from n=8 independent experiments. Statistics were calculated with a Kruskal-Wallis test then multiple comparisons using Dunn's test. * p<0.0332, ** p<0.0021, ***p<0.0002.*

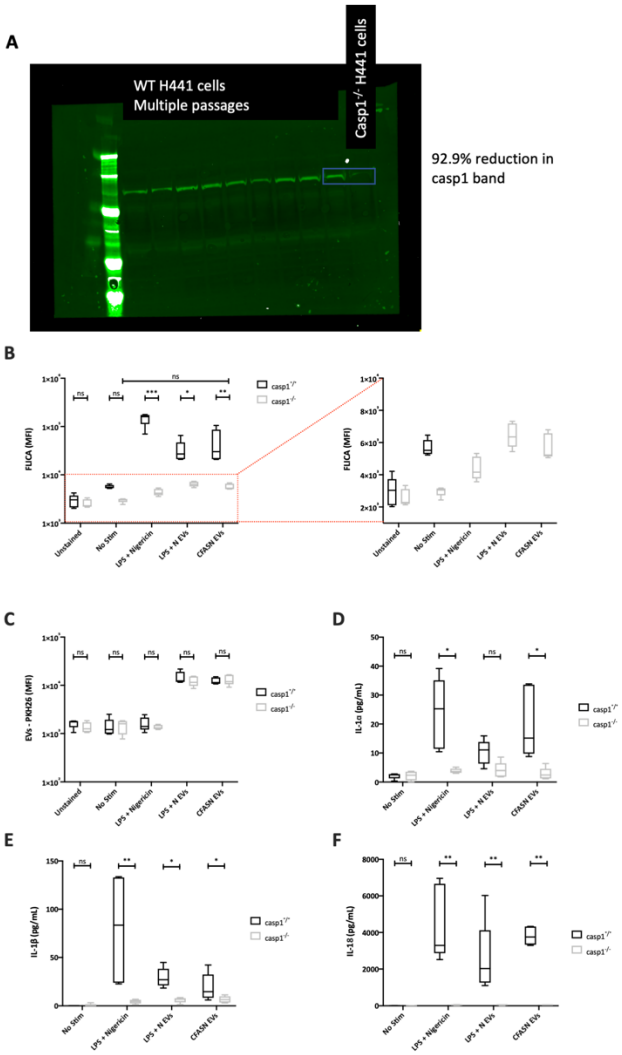

*Supplementary Figure 3.7. Generation and validation of caspase-1 knockout cells (A) Raw western blot showing ~92.9% reduction of caspase-1 in a polyclonal knockout of caspase-1 in H441 cells. H441 cells grown at ALI were either mock-stimulated with media or with LPS (10 ng/mL, signal 1) then with nigericin (10 μM, signal 2) or with EVs labeled with PKH26 from neutrophils stimulated with LPS + nigericin or EVs labeled with PKH26 from neutrophils transmigrated towards CFASN. (B) Quantification of active caspase-1 or (C) association of EVs with the cells. (D-F) IL-1α, IL-1β, and IL-18 was measured in the extracellular medium by ELISA. Data from n=6 independent experiments. Statistics were calculated with a Kruskal-Wallis test then multiple comparisons using Dunn's test. * p<0.0332, ** p<0.0021, ***p<0.0002.*

REFERENCES

1. Alfaidi, M., Wilson, H., Daigneault, M., Burnett, A., Ridger, V., Chamberlain, J., and Francis, S. (2015). Neutrophil Elastase Promotes Interleukin-1beta Secretion from Human Coronary Endothelium. J Biol Chem *290*, 24067-24078. 10.1074/jbc.M115.659029. PMC4591798
2. Amjadi, M.F., Avner, B.S., Greenlee-Wacker, M.C., Horswill, A.R., and Nauseef, W.M. (2021). Neutrophil-Derived Extracellular Vesicles Modulate the Phenotype of Naive Human Neutrophils. J Leukoc Biol *110*, 917-925. 10.1002/JLB.3AB0520-339RR. PMC8423865
3. Baroja-Mazo, A., Martin-Sanchez, F., Gomez, A.I., Martinez, C.M., Amores-Iniesta, J., Compan, V., Barbera-Cremades, M., Yague, J., Ruiz-Ortiz, E., Anton, J.*, et al.* (2014). The NLRP3 Inflammasome Is Released as a Particulate Danger Signal That Amplifies the Inflammatory Response. Nat Immunol *15*, 738-748. 10.1038/ni.2919.
4. Becker, K.A., Li, X., Seitz, A., Steinmann, J., Koch, A., Schuchman, E., Kamler, M., Edwards, M.J., Caldwell, C.C., and Gulbins, E. (2017). Neutrophils Kill Reactive Oxygen Species-Resistant Pseudomonas Aeruginosa by Sphingosine. Cell Physiol Biochem *43*, 1603-1616. 10.1159/000482024.
5. Besnard, A.G., Togbe, D., Couillin, I., Tan, Z., Zheng, S.G., Erard, F., Le Bert, M., Quesniaux, V., and Ryffel, B. (2012). Inflammasome-IL-1-Th17 Response in Allergic Lung Inflammation. J Mol Cell Biol *4*, 3-10. 10.1093/jmcb/mjr042.
6. Brennan, M.A., and Cookson, B.T. (2000). Salmonella Induces Macrophage Death by Caspase-1-Dependent Necrosis. Mol Microbiol *38*, 31-40. 10.1046/j.1365-2958.2000.02103.x.
7. Chen, K.W., Gross, C.J., Sotomayor, F.V., Stacey, K.J., Tschopp, J., Sweet, M.J., and Schroder, K. (2014). The Neutrophil Nlrc4 Inflammasome Selectively Promotes Il-1beta Maturation without Pyroptosis During Acute Salmonella Challenge. Cell Rep *8*, 570-582. 10.1016/j.celrep.2014.06.028.
8. Clancy, D.M., Sullivan, G.P., Moran, H.B.T., Henry, C.M., Reeves, E.P., McElvaney, N.G., Lavelle, E.C., and Martin, S.J. (2018). Extracellular Neutrophil Proteases Are Efficient Regulators of IL-1, Il-33, and Il-36 Cytokine Activity but Poor Effectors of Microbial Killing. Cell Rep *22*, 2937-2950. 10.1016/j.celrep.2018.02.062.
9. Cohen, T.S., and Prince, A. (2012). Cystic Fibrosis: A Mucosal Immunodeficiency Syndrome. Nat Med *18*, 509-519. 10.1038/nm.2715. PMC3577071
10. Cohen, T.S., and Prince, A.S. (2013). Activation of Inflammasome Signaling Mediates Pathology of Acute P. Aeruginosa Pneumonia. J Clin Invest *123*, 1630-1637. 10.1172/JCI66142. PMC3613922
11. Dobosh, B., Giacalone, V.D., Margaroli, C., and Tirouvanziam, R. (2021). Mass Production of Human Airway-Like Neutrophils Via Transmigration in an Organotypic Model of Human Airways. STAR Protoc *2*, 100892. 10.1016/j.xpro.2021.100892. PMC8551927
12. dos Santos, G., Kutuzov, M.A., and Ridge, K.M. (2012). The Inflammasome in Lung Diseases. Am J Physiol Lung Cell Mol Physiol *303*, L627-633. 10.1152/ajplung.00225.2012. PMC4747913
13. Exline, M.C., Justiniano, S., Hollyfield, J.L., Berhe, F., Besecker, B.Y., Das, S., Wewers, M.D., and Sarkar, A. (2014). Microvesicular Caspase-1 Mediates Lymphocyte Apoptosis in Sepsis. PLoS One *9*, e90968. 10.1371/journal.pone.0090968. PMC3958341

14. Fantone, K., Tucker, S.L., Miller, A., Yadav, R., Bernardy, E.E., Fricker, R., Stecenko, A.A., Goldberg, J.B., and Rada, B. (2021). Cystic Fibrosis Sputum Impairs the Ability of Neutrophils to Kill Staphylococcus Aureus. Pathogens *10*. 10.3390/pathogens10060703. PMC8229215
15. Forrest, O.A., Dobosh, B., Ingersoll, S.A., Rao, S., Rojas, A., Laval, J., Alvarez, J.A., Brown, M.R., Tangpricha, V., and Tirouvanziam, R. (2022). Neutrophil-Derived Extracellular Vesicles Promote Feed-Forward Inflammasome Signaling in Cystic Fibrosis Airways. J Leukoc Biol. 10.1002/JLB.3AB0321-149R.
16. Forrest, O.A., Ingersoll, S.A., Preininger, M.K., Laval, J., Limoli, D.H., Brown, M.R., Lee, F.E., Bedi, B., Sadikot, R.T., Goldberg, J.B.*, et al.* (2018). Frontline Science: Pathological Conditioning of Human Neutrophils Recruited to the Airway Milieu in Cystic Fibrosis. J Leukoc Biol *104*, 665-675. 10.1002/JLB.5HI1117-454RR. PMC6956843
17. Fritzsching, B., Zhou-Suckow, Z., Trojanek, J.B., Schubert, S.C., Schatterny, J., Hirtz, S., Agrawal, R., Muley, T., Kahn, N., Sticht, C.*, et al.* (2015). Hypoxic Epithelial Necrosis Triggers Neutrophilic Inflammation Via IL-1 Receptor Signaling in Cystic Fibrosis Lung Disease. Am J Respir Crit Care Med *191*, 902-913. 10.1164/rccm.201409-1610OC. PMC4435455
18. Gaidt, M.M., and Hornung, V. (2017). Alternative Inflammasome Activation Enables Il-1beta Release from Living Cells. Curr Opin Immunol *44*, 7-13. 10.1016/j.coi.2016.10.007. PMC5894802
19. Genschmer, K.R., Russell, D.W., Lal, C., Szul, T., Bratcher, P.E., Noerager, B.D., Abdul Roda, M., Xu, X., Rezonzew, G., Viera, L.*, et al.* (2019). Activated PMN Exosomes: Pathogenic Entities Causing Matrix Destruction and Disease in the Lung. Cell *176*, 113-126 e115. 10.1016/j.cell.2018.12.002. PMC6368091
20. Gritsenko, A., Green, J.P., Brough, D., and Lopez-Castejon, G. (2020). Mechanisms of NLRP3 Priming in Inflammaging and Age Related Diseases. Cytokine Growth Factor Rev *55*, 15-25. 10.1016/j.cytogfr.2020.08.003. PMC7571497
21. Iannitti, R.G., Napolioni, V., Oikonomou, V., De Luca, A., Galosi, C., Pariano, M., Massi-Benedetti, C., Borghi, M., Puccetti, M., Lucidi, V.*, et al.* (2016). IL-1 Receptor Antagonist Ameliorates Inflammasome-Dependent Inflammation in Murine and Human Cystic Fibrosis. Nat Commun *7*, 10791. 10.1038/ncomms10791. PMC4793079
22. Iula, L., Keitelman, I.A., Sabbione, F., Fuentes, F., Guzman, M., Galletti, J.G., Gerber, P.P., Ostrowski, M., Geffner, J.R., Jancic, C.C.*, et al.* (2018). Autophagy Mediates Interleukin-1beta Secretion in Human Neutrophils. Front Immunol *9*, 269. 10.3389/fimmu.2018.00269. PMC5825906
23. Johnson, J.L., Ramadass, M., Haimovich, A., McGeough, M.D., Zhang, J., Hoffman, H.M., and Catz, S.D. (2017). Increased Neutrophil Secretion Induced by NLRP3 Mutation Links the Inflammasome to Azurophilic Granule Exocytosis. Front Cell Infect Microbiol *7*, 507. 10.3389/fcimb.2017.00507. PMC5732154
24. Karmakar, M., Katsnelson, M., Malak, H.A., Greene, N.G., Howell, S.J., Hise, A.G., Camilli, A., Kadioglu, A., Dubyak, G.R., and Pearlman, E. (2015). Neutrophil Il-1beta Processing Induced by Pneumolysin Is Mediated by the NLRP3/Asc Inflammasome and Caspase-1 Activation and Is Dependent on K+ Efflux. J Immunol *194*, 1763-1775. 10.4049/jimmunol.1401624. PMC4369676

25. Karmakar, M., Minns, M., Greenberg, E.N., Diaz-Aponte, J., Pestonjamasp, K., Johnson, J.L., Rathkey, J.K., Abbott, D.W., Wang, K., Shao, F.*, et al.* (2020). N-Gsdmd Trafficking to Neutrophil Organelles Facilitates Il-1beta Release Independently of Plasma Membrane Pores and Pyroptosis. Nat Commun *11*, 2212. 10.1038/s41467-020-16043-9. PMC7200749
26. Liu, X., Ory, V., Chapman, S., Yuan, H., Albanese, C., Kallakury, B., Timofeeva, O.A., Nealon, C., Dakic, A., Simic, V.*, et al.* (2012). Rock Inhibitor and Feeder Cells Induce the Conditional Reprogramming of Epithelial Cells. Am J Pathol *180*, 599-607. 10.1016/j.ajpath.2011.10.036. PMC3349876
27. Lukens, J.R., Gross, J.M., and Kanneganti, T.D. (2012). IL-1 Family Cytokines Trigger Sterile Inflammatory Disease. Front Immunol *3*, 315. 10.3389/fimmu.2012.00315. PMC3466588
28. MacKenzie, A., Wilson, H.L., Kiss-Toth, E., Dower, S.K., North, R.A., and Surprenant, A. (2001). Rapid Secretion of Interleukin-1beta by Microvesicle Shedding. Immunity *15*, 825-835. 10.1016/s1074-7613(01)00229-1.
29. Mahmutovic Persson, I., Menzel, M., Ramu, S., Cerps, S., Akbarshahi, H., and Uller, L. (2018). Il-1beta Mediates Lung Neutrophilia and Il-33 Expression in a Mouse Model of Viral-Induced Asthma Exacerbation. Respir Res *19*, 16. 10.1186/s12931-018-0725-z. PMC5781288
30. Margaroli, C., Garratt, L.W., Horati, H., Dittrich, A.S., Rosenow, T., Montgomery, S.T., Frey, D.L., Brown, M.R., Schultz, C., Guglani, L.*, et al.* (2019). Elastase Exocytosis by Airway Neutrophils Is Associated with Early Lung Damage in Children with Cystic Fibrosis. Am J Respir Crit Care Med *199*, 873-881. 10.1164/rccm.201803-0442OC. PMC6444666
31. Margaroli, C., Moncada-Giraldo, D., Gulick, D.A., Dobosh, B., Giacalone, V.D., Forrest, O.A., Sun, F., Gu, C., Gaggar, A., Kissick, H.*, et al.* (2021). Transcriptional Firing Represses Bactericidal Activity in Cystic Fibrosis Airway Neutrophils. Cell Rep Med *2*, 100239. 10.1016/j.xcrm.2021.100239. PMC8080108
32. Margaroli, C., and Tirouvanziam, R. (2016). Neutrophil Plasticity Enables the Development of Pathological Microenvironments: Implications for Cystic Fibrosis Airway Disease. Mol Cell Pediatr *3*, 38. 10.1186/s40348-016-0066-2. PMC5136534
33. Nold, M.F., Mangan, N.E., Rudloff, I., Cho, S.X., Shariatian, N., Samarasinghe, T.D., Skuza, E.M., Pedersen, J., Veldman, A., Berger, P.J.*, et al.* (2013). Interleukin-1 Receptor Antagonist Prevents Murine Bronchopulmonary Dysplasia Induced by Perinatal Inflammation and Hyperoxia. Proc Natl Acad Sci U S A *110*, 14384-14389. 10.1073/pnas.1306859110. PMC3761642
34. Osika, E., Cavaillon, J.M., Chadelat, K., Boule, M., Fitting, C., Tournier, G., and Clement, A. (1999). Distinct Sputum Cytokine Profiles in Cystic Fibrosis and Other Chronic Inflammatory Airway Disease. Eur Respir J *14*, 339-346. 10.1034/j.1399-3003.1999.14b17.x.
35. Pohl, K., Hayes, E., Keenan, J., Henry, M., Meleady, P., Molloy, K., Jundi, B., Bergin, D.A., McCarthy, C., McElvaney, O.J.*, et al.* (2014). A Neutrophil Intrinsic Impairment Affecting Rab27a and Degranulation in Cystic Fibrosis Is Corrected by CFTR Potentiator Therapy. Blood *124*, 999-1009. 10.1182/blood-2014-02-555268. PMC4133506

36. Ran, F.A., Hsu, P.D., Wright, J., Agarwala, V., Scott, D.A., and Zhang, F. (2013). Genome Engineering Using the CRISPR-Cas9 System. Nat Protoc *8*, 2281-2308. 10.1038/nprot.2013.143. PMC3969860
37. Reiniger, N., Lee, M.M., Coleman, F.T., Ray, C., Golan, D.E., and Pier, G.B. (2007). Resistance to Pseudomonas Aeruginosa Chronic Lung Infection Requires Cystic Fibrosis Transmembrane Conductance Regulator-Modulated Interleukin-1 (IL-1) Release and Signaling through the IL-1 Receptor. Infect Immun *75*, 1598-1608. 10.1128/IAI.01980-06. PMC1865697
38. Rimessi, A., Bezzerri, V., Patergnani, S., Marchi, S., Cabrini, G., and Pinton, P. (2015). Mitochondrial Ca2+-Dependent NLRP3 Activation Exacerbates the Pseudomonas Aeruginosa-Driven Inflammatory Response in Cystic Fibrosis. Nat Commun *6*, 6201. 10.1038/ncomms7201.
39. Schroder, K., and Tschopp, J. (2010). The Inflammasomes. Cell *140*, 821-832. 10.1016/j.cell.2010.01.040.
40. Sims, J.E., and Smith, D.E. (2010). The IL-1 Family: Regulators of Immunity. Nat Rev Immunol *10*, 89-102. 10.1038/nri2691.
41. Sutterwala, F.S., Mijares, L.A., Li, L., Ogura, Y., Kazmierczak, B.I., and Flavell, R.A. (2007). Immune Recognition of Pseudomonas Aeruginosa Mediated by the Ipaf/Nlrc4 Inflammasome. J Exp Med *204*, 3235-3245. 10.1084/jem.20071239. PMC2150987
42. Takao, M., Nagai, Y., Ito, M., and Ohba, T. (2018). Flow Cytometric Quantitation of Epcam-Positive Extracellular Vesicles by Immunomagnetic Separation and Phospholipid Staining Method. Genes Cells *23*, 963-973. 10.1111/gtc.12645.
43. Thery, C., Witwer, K.W., Aikawa, E., Alcaraz, M.J., Anderson, J.D., Andriantsitohaina, R., Antoniou, A., Arab, T., Archer, F., Atkin-Smith, G.K*., et al.* (2018). Minimal Information for Studies of Extracellular Vesicles 2018 (MISEV2018): A Position Statement of the International Society for Extracellular Vesicles and Update of the MISEV2014 Guidelines. J Extracell Vesicles *7*, 1535750. 10.1080/20013078.2018.1535750. PMC6322352
44. Thinwa, J., Segovia, J.A., Bose, S., and Dube, P.H. (2014). Integrin-Mediated First Signal for Inflammasome Activation in Intestinal Epithelial Cells. J Immunol *193*, 1373-1382. 10.4049/jimmunol.1400145. PMC4174679
45. Tirouvanziam, R., Gernez, Y., Conrad, C.K., Moss, R.B., Schrijver, I., Dunn, C.E., Davies, Z.A., Herzenberg, L.A., and Herzenberg, L.A. (2008). Profound Functional and Signaling Changes in Viable Inflammatory Neutrophils Homing to Cystic Fibrosis Airways. Proc Natl Acad Sci U S A *105*, 4335-4339. 10.1073/pnas.0712386105. PMC2393742
46. Useckaite, Z., Ward, M.P., Trappe, A., Reilly, R., Lennon, J., Davage, H., Matallanas, D., Cassidy, H., Dillon, E.T., Brennan, K*., et al.* (2020). Increased Extracellular Vesicles Mediate Inflammatory Signalling in Cystic Fibrosis. Thorax *75*, 449-458. 10.1136/thoraxjnl-2019-214027. PMC7279202
47. Venegas, C., Kumar, S., Franklin, B.S., Dierkes, T., Brinkschulte, R., Tejera, D., Vieira-Saecker, A., Schwartz, S., Santarelli, F., Kummer, M.P*., et al.* (2017). Microglia-Derived Asc Specks Cross-Seed Amyloid-Beta in Alzheimer's Disease. Nature *552*, 355-361. 10.1038/nature25158.
48. Woith, E., Fuhrmann, G., and Melzig, M.F. (2019). Extracellular Vesicles-Connecting Kingdoms. Int J Mol Sci *20*. 10.3390/ijms20225695. PMC6888613

Chapter 4: EXTRACELLULAR VESICLE lncRNA MALAT1 DRIVES HDAC11 DEPENDENT CHRONIC INFLAMMATION IN AIRWAY NEUTROPHILS

ABSTRACT

Polymorphonuclear neutrophils (PMNs) are the most abundant leukocyte in the bone marrow and circulation and are central to the pathogenesis of many airway diseases including cystic fibrosis (CF), chronic obstructive pulmonary disease (COPD), asthma, and COVID-19. In CF, airway PMNs adopt a fate associated with granule release, immunomodulatory activity, and metabolic licensing (GRIM) and fail to completely clear invading pathogens. The number of airway GRIM PMNs as well as their secreted products are the strongest correlates for disease severity, however, it is unknown what pathological factors cause naïve PMNs to differentiate into GRIM PMNs. In this study we fractionated CF sputum to determine what components of the lung milieu condition PMNs to become inflammatory. We found that CD66b+ PMN-derived EVs contain the lncRNA MALAT1, which induced the expression of the histone deacetylase HDAC11 in PMNs. Either component was necessary and sufficient to differentiate naïve PMNs into GRIM PMNs. HDAC11 + GRIM PMNs secreted MALAT1+ EVs that were able to cause other PMNs to become GRIM in a cycle of feed-forward inflammation. Knockdown or inhibition of both MALAT1 and HDAC11 prevented the induction of the GRIM phenotype. Thus, MALAT1 and HDAC11 are therapeutic targets for the treatment of diseases featuring inflammatory airway PMNs. MALAT1 may also serve as a biomarker of lung disease as the amount of MALAT1 relative to the concentration of EVs strongly correlated with lung function (%FEV1).

INTRODUCTION

Polymorphonuclear neutrophils (PMNs) are the most abundant leukocyte in the bone marrow and circulation with an estimated half-life of just a few hours to at most a few days (Pillay et al., 2010). The traditional view that these cells are only capable of phagocytosis or releasing DNA and histones in the form of neutrophil extracellular traps (NETosis) has been challenged in recent years as the remarkable heterogeneity of PMNs in the bone marrow, circulation, and tissue has been realized (Margaroli and Tirouvanziam, 2016; Rosales, 2018; Sumagin, 2021). It has become clear that during the process of swarming into a tissue PMNs are able to initiate a transcriptional program to adapt to their environment (Bost et al., 2021; Grieshaber-Bouyer et al., 2021; Margaroli et al., 2021). In addition, PMNs, and their secreted products, have been implicated in the severity of many diseases including cystic fibrosis (CF), chronic obstructive pulmonary disease (COPD), asthma, and respiratory infections caused by influenza virus and severe acute respiratory syndrome coronavirus (SARS-CoV-2), the causative agent of coronavirus disease 2019 (COVID-19) (Margaroli and Tirouvanziam, 2016; Genschmer et al., 2019; Grunwell et al., 2019; Bost et al., 2021; Reusch et al., 2021). Contrary to their pivotal importance in these diseases, PMNs remain poorly studied likely as a consequence of their propensity for spontaneous activation and incapacity for viable cryopreservation (Blanter et al., 2021). In light of these advancements, activated PMNs are excellent targets for the development of host-directed therapeutics for the treatment of many inflammatory diseases (Grieshaber-Bouyer and Nigrovic, 2019; Fine et al., 2020).

Progressive lung disease is the leading cause of mortality in cystic fibrosis (CF), a chronic condition characterized by impaired mucociliary clearance and mucus plugging of the small airways, bacterial and fungal colonization of the lungs, and chronic recruitment of inflammatory

PMNs into the airways (Elborn, 2016; Margaroli and Tirouvanziam, 2016; Farrell et al., 2018). Airway PMNs actively hyperexocytose their primary granules and release damaging, inflammatory mediators such as neutrophil elastase (NE), a potent serine protease with many targets. In fact, PMN-related measurements, including the number of PMNs and concentration of NE and MPO in the airways are the strongest negative correlates with CF-disease severity and lung function (Brown et al., 1996; Chandler et al., 2018; Dittrich et al., 2018). Despite the large numbers of activated, inflammatory PMNs present in the airways of patients diagnosed with CF, common bacterial pathogens such as *P. aeruginosa* and *S. aureus* persist. These airway PMNs are non-apoptotic and alive, and actively fuse their primary granules to the membrane, while also featuring high rates of glucose uptake and glycolysis as well as anabolic mTOR and CREB signaling (Tirouvanziam et al., 2008; Makam et al., 2009; Laval et al., 2013; Margaroli et al., 2021). In addition, CF airway PMNs downregulate the activity of T-cells and airway macrophages through the production of arginase-1 (Ingersoll et al., 2015). Furthermore, CF airway PMNs are metabolically active This fate of PMNs has been described based on the above profound changes as granule-releasing, immunomodulatory, and metabolically active (GRIM) PMNs (Mitchell, 2018; Laucirica et al., 2022) and have decreased bactericidal capabilities.

GRIM PMNs undergo a transcriptional program that results in a high rate of release of extracellular vesicles (EVs) (Margaroli et al., 2021), which therein can transfer active caspase-1 to other cells bypassing the need for a stress stimulus (Forrest et al., 2022) (See Chapter 3). Notably, the heterogenous population of EVs in CF sputum, which are likely derived from airway epithelial cells and PMNs, as well as T-cells, monocytes, macrophages and bacteria were able to induce exocytosis in transmigrating PMNs (Forrest et al., 2022). It was recently shown

that fMLF primed-PMNs release EVs that activate naïve PMNs in turn (Amjadi et al., 2021). However, it is unclear if this mechanism occurs in the airways and in activated GRIM PMNs. To this end, we hypothesized that GRIM PMNs create chronic inflammation by secreting pathological EVs that differentiate future waves of naïve PMNs into GRIM PMNs resulting in a cycle of feed-forward inflammation.

RESULTS

PMN-derived EVs are abundant in CF sputum

EVs were purified from expectorated sputum from patients diagnosed with CF using a combination of differential centrifugation and tangential flow filtration with a 300 kDa molecular weight cutoff (MWCO) column **(Figure 4.1A)**. This method is easily applicable to patient samples and scalable for cell culture-generated material. EDTA was first added to the sputum to a final concentration of 2.5 mM in order to prevent spontaneous activation of the PMNs and other immune cells present, then dissociated and aspirated using an 18G 1.5" needle (Tirouvanziam et al., 2008; Forrest et al., 2018; Margaroli et al., 2019).The sample was then centrifuged at 800 xg to pellet the cells and the supernatant was then centrifuged at 3,000 xg to remove bacteria and apoptotic cells. Supernatants were then frozen at -80 ˚C so that all EV samples could be analyzed with minimal batch effects. Banked sputum was stable for at least up to a year (Genschmer et al., 2019). After thawing the samples were centrifuged at 20,000 xg to remove larger debris which generated CF airway supernatant (CFASN), a mixture of EVs, soluble proteins, nucleic acids, and metabolites. The supernatant was separated on a 300 kDa MWCO column into a retentate (high MW) fraction and a filtrate (low MW) fraction. The high MW fraction is expected to contain EVs (Forrest et al., 2022). According to the minimal information for studies of EVs 2018 (MISEV2018) this is considered an acceptable "intermediate recovery, intermediate specificity" EV enrichment method (Thery et al., 2018).

The high MW fraction contains particles that resemble EVs as measured by two orthogonal methods. Transmission electron microscopy (TEM) (**Figures 4.1B, Supplementary Figure 4.1A)** and nanoparticle tracking analysis (NTA) show particles of the expected size range

and concentration (Figures 4.1C). We previously observed that sputum from adult patients with CF contained EVs at a concentration of about 5e10 EVs/mL by nanoparticle tracking analysis and that the particle size ranged from about 100-200 nm in diameter (Forrest et al., 2022). The CFASN samples had a median concentration of 3.30e11 EVs/mL, while the healthy control (HC) airway supernatant had a median of 3.47e9 EVs/mL and a modal diameter of 156 nm (Figures 4.1D). The EV fraction of CFASN contains the tetraspanin CD63 and TSG101, a component of the ESCRT machinery involved in EV biogenesis, and does not contain calnexin, which is specific to the endoplasmic reticulum **(Supplementary Figure 4.1B).** Since EVs are ubiquitously released by all cells, including bacteria, we wanted to determine the percentage of the total EV population that was PMN-derived. It is well established that many PMN-derived EVs present surface-accessible CD66b, a granulocyte-specific marker (Dalli et al., 2013; Headland et al., 2014; Lorincz et al., 2015; Genschmer et al., 2019; Letsiou et al., 2021; Forrest et al., 2022). To accomplish this, EVs were stained with anti-CD66b-AF488 and analyzed by fluorescent NTA. About 62% of the EVs in CFASN were CD66b+ **(Figures 4.1D).** Taken together, the high molecular weight fraction of CFASN contains pure EVs and not cell debris, with over half of the EVs originating from PMNs or complexed with PMN-derived EVs. CD66b+ NE+ PMN EVs have been shown to cause emphysema and transfer a COPD-like phenotype to mice (Genschmer et al., 2019). Thus, we wanted to investigate if NE on PMN-derived EVs correlated with lung function, as measured by the forced exhaled volume in one second compared to the full, forced vital capacity (%FEV1). We conjugated anti-CD66b-biotin to 8 µm magnetic beads coated with streptavidin and incubated the complex with the total population of EVs to immunoprecipitate just the PMN-derived EVs. Then, the EV-bead complexes were counterstained with an antibody

against NE and quantified by flow cytometry. The total amount of NE on the CD66b+ EVs correlated negatively with %FEV1 **(Figures 4.1E)**. Since PMNs stimulated with fMLF release EVs that can activate naïve PMNs (Amjadi et al., 2021), we wanted to investigate the effect that CFASN EVs, with the majority being PMN-derived, had on naïve airway PMNs.

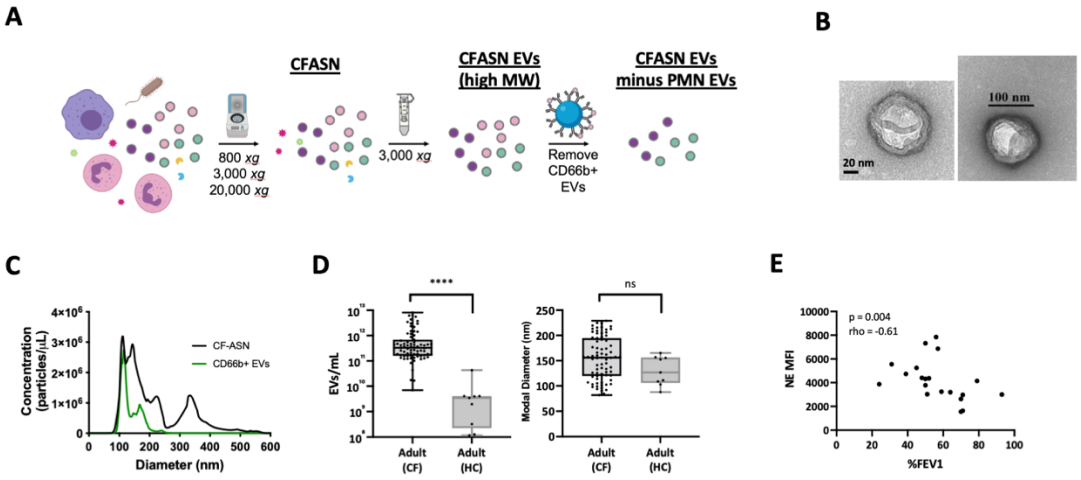

Figure 4.1: ***Neutrophil-derived EVs are abundant in CF airway fluid and track with disease severity. A)*** *Schematic for purification of EVs from CFASN and immunoprecipitation and depletion of cell-type specific EVs. CF sputum was differentially centrifuged at 800 xg to remove cells, 3,000 xg to remove bacteria and very large debris, 20,000 xg to remove other debris and apoptotic blebs. The supernatant was loaded onto a 300 kDa MWCO to remove small proteins, metabolites and other low molecular weight contaminants (filtrate). The high MW fraction (EV-containing) was normalized to 1e10 EVs/mL. Cell-type specific EVs can be depleted by immunoprecipitation with 8 um streptavidin beads* conjugated to anti-CD66b-biotin ***B)*** *TEM of EVs purified from CF sputum show spherical particles with a lipid bilayer.* ***C)*** *Nanoparticle tracking analysis (NTA) size and concentration determination of purified EVs in CFASN. EVs were stained with an anti-CD66b-AF488 antibody, and unbound antibody was removed by another 300 kDa MWCO centrifugation.* ***D,E)*** *Concentration and size of EVs in adult CF sputum (n=75) and healthy controls (HC; n=8). Statistics were calculated using the Mann-Whitney U-test. * p<0.05, ** p<0.01, ***p<0.001.* **F)** EVs were immunoprecipitated with 8 um streptavidin beads conjugated to anti-CD66b-biotin then counterstained with anti-NE-FITC and washed. Surface NE median fluorescence intensity was analyzed by flow cytometry and compared with %FEV1. n= 27; Statistics were calculated with a Spearman's correlation.

GRIM PMN-derived EVs are sufficient to transmit the GRIM phenotype to naïve PMNs

The induction of the GRIM phenotype in vivo is not observed in circulating PMNs and requires transmigration into a tissue (Tirouvanziam et al., 2008; Margaroli et al., 2021). To this end, we have previously developed and validated an organotypic transmigration model that allows for the conditioning of primary blood leukocytes into an airway-like phenotype (Forrest et al., 2018; Dobosh et al., 2021; Dobosh et al., 2022; Forrest et al., 2022). Human lung

epithelium (HLE) monolayers are grown at air-liquid interface (ALI) for two weeks, followed by transmigration of primary human blood PMNs into the apical fluid, which is either CFASN or fractions of CFASN or chemical stimuli and chemoattractants. The amount of time allotted for the transmigration step may vary. Many previous papers have used up to 18 hours (h) or more in order to ensure fully stimulated, airway-like PMNs (Forrest et al., 2018; Grunwell et al., 2019). However, therapeutic interventions are more likely to succeed if applied to a naïve PMN, or early migrant, rather than a PMN that is terminally GRIM. Indeed, a time-course of PMN transmigration revealed that PMNs over 1 h, 2 h, 4 h, 6 h, and 10 h had dynamic transcriptional changes (Margaroli et al., 2021). The transmigration for 4 h showed high CD63, correlating with primary granule exocytosis, and transcriptional activity and was an earlier timepoint. Therefore, we elected to use 4 h transmigrations for each of these experiments to understand what factors result in the early commitment to the GRIM fate particularly in regard to primary granule release, which positively correlates with surface CD63 as measured by flow cytometry (Supplementary Figure 4.1), and a bacteria killing assay generally with *P. aeruginosa* (PA01) at a multiplicity of infection (MOI) of 1 for one hour.

Leukotriene B4 (LTB4; 100 nM) was used as a control to stimulate transmigration without any pathological material present akin to PMNs patrolling tissues during homeostatic and noninflammatory conditions. Another group made the observation that PMN EVs contain LTB4 as well as the enzyme LTA4H and could induce migration of PMNs (Majumdar et al., 2021). We did not quantify LTB4 or LTA4H in CFASN EVs, but noted inefficient transmigration efficiencies when the apical fluid contained only CFASN EVs (data not shown), however this study and the above study used different PMN chemotaxis models which may account for the

difference in PMN behavior. To compensate, LTB4 (100 nM) was added to all EV conditions to induce PMN transmigration. PMNs transmigrated towards CFASN presented with low CD63 **(Figure 4.2A)** and was killed about 60% of P. aeruginosa **(Figure 4.2B).** In contrast, PMNs transmigrated towards CFASN or the total EVs derived from CFASN had increased CD63 and cleared about 40% and 20% of P. aeruginosa, respectively. As a control, PMNs transmigrating towards the filtrate (no EVs) did not show primary granule exocytosis and were able to kill P. aeruginosa equally as efficient as LTB4 transmigrated PMNs. Interestingly, GRIM PMNs transmigrated towards the high MW fraction (EVs) cleared less bacteria than the transmigration towards total CFASN, a more complex fluid. This suggests that the low MW fraction contains factors that condition PMN to kill bacteria efficiently or are bactericidal and associate with transmigrating PMNs. GRIM PMNs have also been shown to have low surface CD16, likely as a result of NE-mediated cleavage of the epitope, and high CD66b correlating with secondary granule release.

Using bead immunoprecipitation, CD66b+ EVs (PMN-derived) were depleted from the total CFASN EV population. The remaining EVs were no longer able to induce primary granule release in transmigrating PMNs **(Figures 4.2A),** although a moderate decrease in CD16 **(Supplementary Figure 4.3A)** and CD66b **(Supplementary Figure 4.3B)** was observed. In line with the data linking bacteria killing ability with measurement of surface CD63, PMNs transmigrated towards CD66b-depleted EVs were able to efficiently clear bacteria whereas CD326- and CD115-depleted EVs showed a slight reduction in bacterial clearance **(Figures 4.2B),** which confirms the pathological role of PMN-derived EVs in causing naïve PMNs to become GRIM.

The loss of the pathological GRIMming factor as a result of depleting CD66b+ EVs suggests that GRIM PMNs are able to impart the GRIM phenotype upon naïve, newly arrived PMNs. To confirm this, after PMNs were transmigrated towards LTB4 alone or CFASN EVs the PMNs were purified and allowed to condition plain RPMI media for 12 hours. After which the PMNs were removed and the EVs were purified as before **(Supplementary Figure 4.4A).** GRIM PMNs released ~3 times the number of EVs over the 12 hour incubation than LTB4-transmigrated PMNs although there was no difference in the size **(Supplementary Figures 4.4B,C)**. The total amount of EVs released is difficult to determine since some EVs may have been taken up by the PMNs and the rate of EV synthesis may not be constant throughout the incubation. Based on the hypothesis that EVs released by GRIM PMNs can cause naïve PMNs to differentiate into GRIM PMNs we used the EVs that comprised the conditioned media as the apical fluid in a new transmigration. EVs purified from the conditioned media are referred to as "secondary EVs" and can be generated from either LTB4 or CFASN EV transmigrated PMNs. Naïve blood PMNs were applied to the basal side of the model and were transmigrated towards either LTB4 secondary EVs (EVs generated by LTB4 transmigrated PMNs) or towards CFASN secondary EVs (EVs generated by GRIM, CFASN EV transmigrated, PMNs) **(Supplementary Figure 4.4A).** PMNs that transmigrated towards GRIM PMN-generated EVs showed heightened surface CD63 compared to PMNs that transmigrated towards LTB4 secondary EVs **(Figures 4.2C).** Furthermore, PMNs that transmigrated towards CFASN secondary EVs also had lower bacterial killing ability compared to the PMNs that transmigrated towards LTB4 secondary EVs **(Figures 4.2D).** These data demonstrate the transfer of a pathological phenotype between different waves of recruited PMNs.

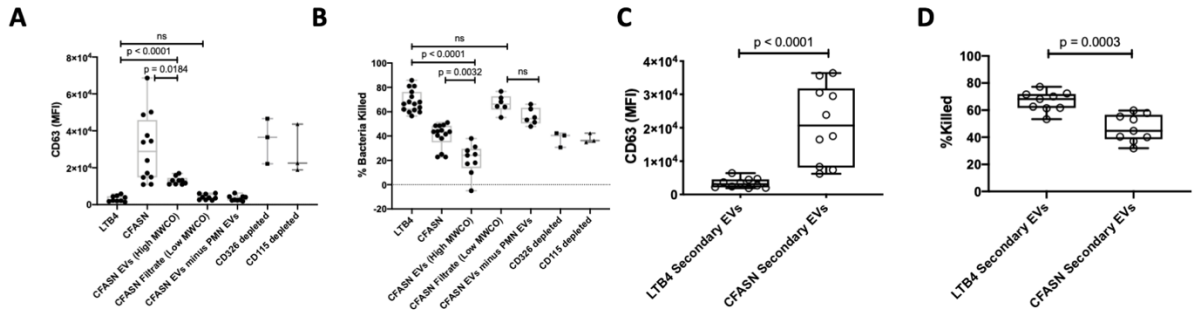

Figure 4.2: ***PMN-derived EVs cause multiple waves of recruited PMNs to become inflammatory.*** *1e6 primary human blood PMNs were transmigrated for 4 hours towards LTB4 (100 nM), CFASN, CFASN EVs, the filtrate from the EV purification, the remaining CFASN EVs from which CD66b+(PMN), or CD326+ (epithelial), CD115+(monocyte/macrophage) EVs were immunoprecipitated and depleted with 8 um streptavidin beads conjugated to biotinylated antibodies.* ***A)*** *PMN surface CD63 as a measure of primary granule exocytosis following transmigration* ***B)*** *PMNs transmigrated towards various conditions were incubated with PA01 at an MOI of 1 and then the amount of bacteria remaining after 1 hour incubation was calculated.* ***C)*** *PMNs transmigrated towards LTB4 or CFASN EVs were allowed to release their own EVs for 12 hours and then EVs were purified and normalized to 1e10 EVs/mL. Naïve PMNs were then transmigrated towards the generated secondary EVs and phenotyped by for primary granule release* ***(C)*** *and bacteria-killing capacity* ***(D).*** *Statistics were calculated using the Mann-Whitney U-test. * p<0.05, ** p<0.01, ***p<0.001.*

HDAC11 and MALAT1 expression regulates induction of the GRIM phenotype

We revisited the RNA-seq data of PMNs transmigrating towards CFASN for 1-10 hours to determine the differential expression of transcription factors or transcriptional regulators (Margaroli et al., 2021). We observed that the histone deacetylase and deacylase HDAC11 was continually upregulated over the entire dataset **(Figures 4.3A).** Interestingly, HDAC11 is also known to suppress the expression of the anti-inflammatory cytokine, IL-10 (Villagra et al., 2009; Cheng et al., 2014), which is notably absent or at low concentrations in the CF airways (Osika et al., 1999; Colombo et al., 2005; Giacalone et al., 2022). From the RNA-seq data we confirmed that cofilin was an appropriate loading control for relative mRNA quantification in PMNs **(Supplementary Figure 4.5).** We performed qRT-PCR and western blot to confirm the expression of HDAC11 in PMNs that become GRIM as a consequence of CFASN EVs. HDAC11 mRNA and protein were present in all transmigrating cells, but ~2-4 fold higher in CFASN- and CFASN EV-transmigrated PMNs than LTB4 PMNs **(Figures 4.3B,C, Supplementary Figure 4.6A).** In addition to its activities as a deacetylase HDAC11 is also a lysine defatty-acylase. In fact, the

defatty-acylase activity, which focuses on long-chain fatty acyl chains is also 10,000 times more active than the deacetylase activity (Kutil et al., 2018; Moreno-Yruela et al., 2018; Cao et al., 2019), further, a small-molecule inhibitor of the deacylase activity, SIS17, was developed recently (Son et al., 2019). Inclusion of SIS17 in the apical fluid (25 μM) of LTB4-transmigrating PMNs showed no differences in the amount of degranulation or bacterial killing ability compared to the LTB4 + vehicle controls. In contrast however, CFASN EVs + SIS17 transmigrated PMNs were $CD63^{med}$, which was significantly lower than PMNs transmigrated towards only CFASN EVs **(Figures 4.3D)**. To confirm that SIS17 acts upon HDAC11 in PMNs and not the epithelial cells in the transmigration model, we generated H441 $HDAC11^{-/-}$ cells using CRISPR-Cas9 technology **(Supplementary Figure 4.7A)**. PMNs that transmigrated across H441 $HDAC11^{-/-}$ showed lower CD16, but the same CD66b and CD63 MFI as the transmigration across wild-type (WT) H441 cells as well as the same bacterial clearance ability **(Supplementary Figures 4.7B-E)**. In addition, CFASN EVs + SIS17 transmigrated PMN showed equal bacterial killing capacity as LTB4-transmigrated PMNs **(Figures 4.3E)**. SIS17 treatment did not change the rate of EV release **(Supplementary Figure 4.7F)**. Taken together, inhibition of HDAC11 in PMNs via SIS17 allows normally pathological PMNs from committing to the GRIM fate and efficient bacterial clearance.

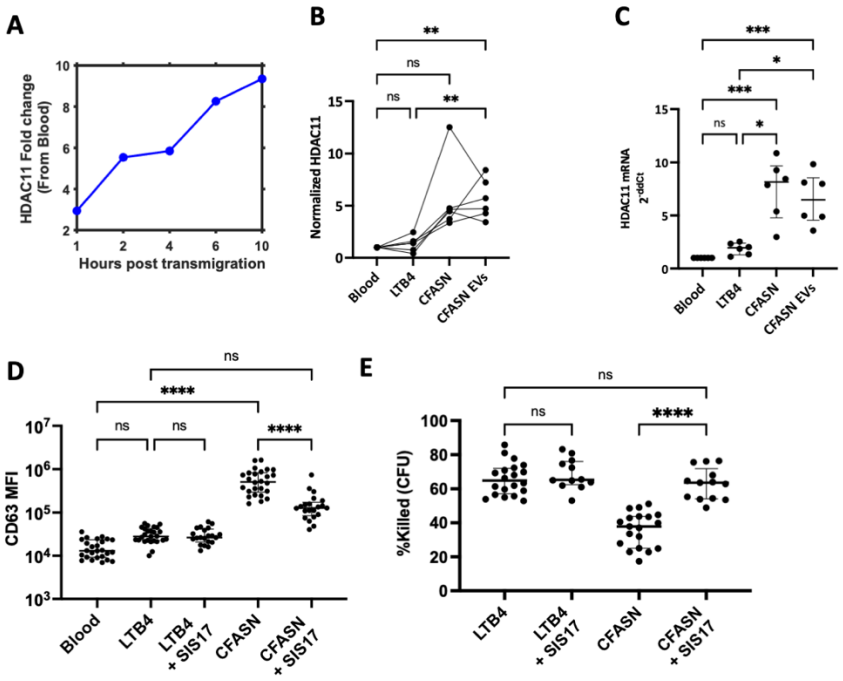

Figure 4.3: HDAC11 inhibition can prevent the induction of the GRIM phenotype. A) *PMNs transmigrated towards CFASN continuously upregulate HDAC11 transcript as measured by RNA-seq.* ***B)*** *HDAC11 protein measured by western blot in PMNs transmigrated towards each condition for 4 hours.* ***C)*** *HDAC11 mRNA is upregulated in PMNs transmigrated towards each condition for 4 hours. The small molecule drug SIS17 (25 uM), an inhibitor of HDAC11 deacylase activity was included in the apical transmigration fluid. PMNs were transmigrated for 4 hours towards each condition and then* ***D)*** *surface CD63 was measured by flow cytometry and* ***E)*** *bacteria-killing capacity. Statistics were calculated with a Kruskal-Wallis test then selected multiple comparisons between groups using Dunn's test. * p<0.0332, ** p<0.0021, ***p<0.0002*

Based on these data, HDAC11 is part of the pathway that induces the GRIM phenotype in PMNs. Since CD66b+ PMN-derived EVs are crucial for the induction of the GRIM phenotype, we sought to determine whether the CFASN EVs contained HDAC11 protein. However, even when we loaded up to 60 ug of total protein, HDAC11 could not be detected by western blot **(Supplementary Figure 4.8)**. Thus, we decided to narrow down the class of macromolecules that contributed to the ability of EVs to confer the GRIM phenotype. To identify the nature of EV contents that play a role in GRIMming of PMNs we treated the purified CFASN EVs with UV light to denature and inhibit potential activity of nucleic acids, trypsin to degrade proteins associated with the surface of the EV, or TritonX-100 to degrade the membrane. After

treatment, samples were washed with PBS + 2.5 mM EDTA and then immediately used in the transmigration model. Each treatment had an effect compared to the PBS-treated sample on primary granule release as measured by CD63 **(Supplementary Figure 4.9A)**. These effects could be explained by the following 1) The vesicular nature of the EV aids in delivery. Whatever the pathological factor is, the lack of encapsulation or association with an EV renders it inactive or unable to enter the recipient PMN; 2) UV-inactivation having an effect suggests that the pathological factor is a nucleic acid, likely RNA; and 3) trypsin, which can only degrade surface proteins because the EV protects intra-EV protein content may decrease efficacy of the EV to deliver the pathological cargo. In summary, the pathological factor that causes a PMN to become GRIM is likely an RNA, but delivery is enhanced by EV "carrier effects" (Askenase, 2021, 2022). The surface proteins of EVs facilitate the effective delivery and the EV protects the RNA cargo from degradation. These carrier effects enhance the efficiency in which EVs become GRIM.

In order to determine what RNAs could be differentially expressed in transmigrating PMNs we extracted total RNA using Trizol from PMNs transmigrated towards either CFASN EVs or LTB4 control after 4 hours. The originating blood PMNs were used as a baseline for normalization. Each transcriptional profile was distinct from the others by principle component analysis (PCA) **(Figures 4.4A)**, but that PC1, which also accounted for the largest variation (65.9%) between the groups was mostly as a result of the transmigration process. In accordance with this, LTB4 and CFASN EV transmigrated PMNs showed very little variation in PC1. We noted that the top 100 contributors to PC2 between CFASN EV and LTB4 transmigrated PMNs were significantly enriched for GO cellular component terms relating to mitochondria function

and vesicle formation, including extracellular vesicles **(Supplementary Figure 4.10A)**. In line with this, there were many mitochondria RNAs differentially expressed in between GRIM PMNs and LTB4 PMNs including 12/13 of the proteins encoded by the mitochondrial DNA **(Figures 4.4B)**. Of the proteins encoded by the mitochondrial genome, 10 were differentially expressed and in greater abundance in CFASN EV transmigrated PMNs. MT-ATP8 is present equally both populations of cells, while MT-RNR2 and MT-RNR1 were more highly expressed in LTB4 transmigrated PMNs **(Figures 4.4B)**. This likely contributes to the increase in reactive oxygen species (ROS) production, from which PMNs are the most potent producers, and oxidative stress that is observed in the CF airways (Kettle et al., 2014; Winterbourn et al., 2016). High concentration of mitochondrial transcripts may be a sign of apoptotic cells however, GRIM cells are alive and non-apoptotic (Tirouvanziam et al., 2008) and were >80% viable after the 4 h transmigration as measured by ethidium bromide/acridine orange staining **(Supplementary Figure 4.10B)** as well as flow cytometry **(Supplementary Figure 4.10C)**. The strongest contributor to the differences between LTB4 and CFASN EV transmigrated PMNs outside of the mitochondrial genes was the long noncoding RNA (lncRNA), MALAT1, which was much higher expressed in LTB4-transmgirated PMNs than CFASN EV-transmigrated PMNs **(Figures 4.4B)**. MALAT1 has been shown to be involved in the persistence of many cancers and promote inflammation through macrophages and dendritic cells (Li et al., 2021; Zhou et al., 2021; Kumar and Mishra, 2022; Mu et al., 2022; Shyu et al., 2022). In addition, MALAT1 is expressed in developing and mature PMNs and may be related to the activity of FOXO1 and STAT1 (Grieshaber-Bouyer et al., 2021). MALAT1 has also been shown to be associated with EVs from a variety of cell types suggesting that it may have a role in cell-to-cell communication.

We developed an electroporation protocol to transfect primary blood PMNs with endotoxin-free plasmid DNA. The plasmids were a two-part expression vector in which position one was either a strong CMV promoter for the expression of mRNAs or lncRNAs or a U6 promoter for siRNAs, while position two expressed GFP under the control of the EF1α promoter with a mutated Bsa1 site to facilitate Golden Gate cloning (Wagner et al., 2018) **(Figures 4.4C)**. Since the transfection of PMNs was not 100% efficient we used the positive expression of EGFP to demarcate cells that successfully received the plasmid, and presumably expressed the transgene in position one, while cells that were GFP negative were not expressing the transgene **(Supplementary Figure 4.11A).** To show the relevance of this expression system we first electroporated primary human blood PMNs that would eventually transmigrate into LTB4 conditions, which would normally result in PMNs with $CD63^{lo}$ and inefficient bacteria killing. First, when expressing the control fluorescent protein mScarlet in position 1, there were no differences in CD63, CD16, or CD66b between EGFP+ and EGFP- cells **(Figures 4.4D, Supplementary Figures 4.11B,C).** In addition, at the population level there were no differences in bacteria killing ability **(Figures 4.4E).** Notably, when HDAC11 was expressed in position 1, EGFP+ cells showed higher surface CD63 than the EGFP- PMNs when transmigrating towards LTB4 indicating that HDAC11 is related to the ability of PMNs to exocytose their primary granules **(Figures 4.4D)**. In addition, inclusion of SIS17 in the apical fluid resulted in both EGFP- and EGFP+ cells presenting equal amounts of surface CD63 when HDAC11 was being expressed. We noted that alignment of the contigs aligning with MALAT1 resulted in only a portion of the lncRNA being expressed in PMNs **(Supplementary Figure 4.11D).** When this fragment of MALAT1 was expressed in transmigrating PMNs towards LTB4 we observed increased

degranulation compared to the EGFP- cells as well as the mScarlet-expressing controls **(Figures 4.4D)**. SIS17 in the apical fluid abrogated the effect of expressing either HDAC11 or MALAT1 on the amount of CD63 present on the surface of transmigrating PMNs **(Figures 4.4D)**.

Although it is unclear whether HDAC11 protein and MALAT1 RNA are direct binding partners they both appear in the same pathway related to PMN degranulation and bacterial killing ability based on the ability of SIS17 to mitigate the effects of MALAT1 overexpression. Taken together, this suggests that MALAT1 and HDAC11 are both relevant in the induction of the GRIM phenotype in transmigrating PMNs. In line with this reasoning, expression of siRNAs targeting HDAC11 or MALAT1 under control of the U6 promoter in PMNs transmigrating towards CFASN EVs we did not observe increased surface CD63 nor CD66b in EGFP+ PMNs **(Figures 4.4E, Supplementary Figures 4.12A)**. However, CD16 decreased regardless of whether the transmigrating PMNs received the plasmid **(Supplementary Figure 4.12B)**, perhaps as a result of NE already being present in the fluid (Middelhoven et al., 2001; Dalli et al., 2013; Genschmer et al., 2019). Notably, electroporated PMNs expressing MALAT or HDAC11 transmigrated towards LTB4 showed reduced bacteria killing capacity, which was rescued by the addition of SIS17 **(Figures 4.4F)**. Similarly, knockdown of HDAC11 or MALAT1 by siRNAs increased bacteria killing capacity in PMNs transmigrated towards CFASN EVs compared to the scramble siRNA control **(Figures 4.4G)**.

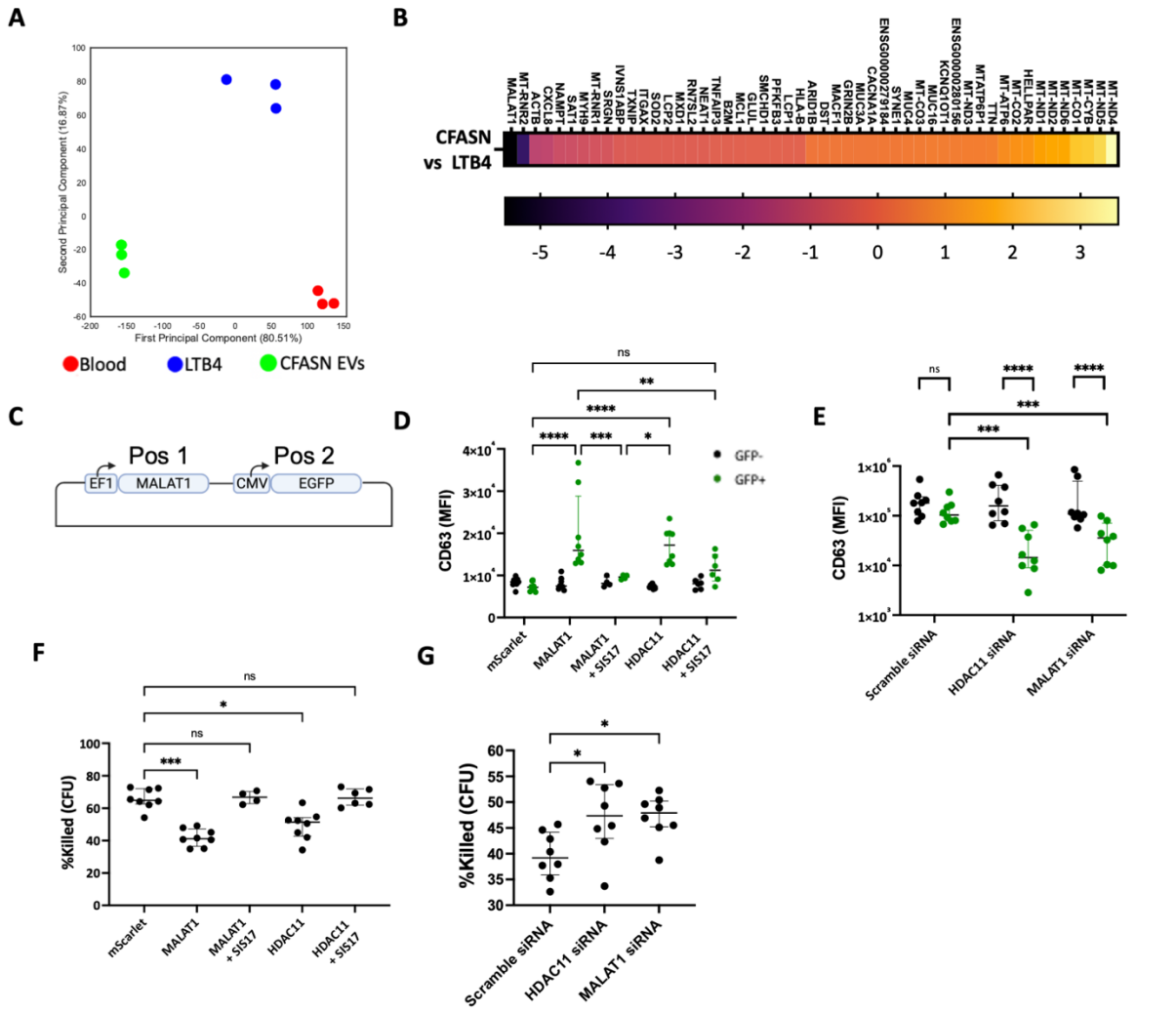

Figure 4.4: Expression or knockdown of MALAT1 or HDAC11 modulate the GRIM phenotype in airway-like PMNs. A) *PCA plot of primary human blood PMNs and PMNs transmigrated towards LTB4 or CFASN EVs.* ***B)*** *The top 25 upregulated and downregulated genes contributing to PC2 between LTB4 and CFASN EV-transmigrated PMNs.* ***C)*** *A dual expression plasmid encoding the expression of two parts. In position 1, MALAT1, HDAC11, or a control fluorescent protein mScarlet were expressed under the control of the EF1a promoter or siRNAs targeting MALAT1 or HDAC11 or a scramble control were included downstream of the U6 promoter. For all plasmids, EGFP was expressed off of the CMV promoter in position 2. Cells expressing EGFP were also expected to be expressing the construct in position 1. Blood PMNs were electroporated with each plasmid and then transmigrated towards the above conditions for 4 hours. Cells expressing EGFP were determined by flow cytometry. Surface CD63 was determined by flow cytometry in PMNs transmigrated towards* ***D)*** *LTB4 or* ***E)*** *CFASN EVs. The population of transmigrated PMNs were incubated with PA01 at an MOI of 1 and then the amount of bacteria remaining after 1 hour incubation was calculated. Statistics were calculated with a Kruskal-Wallis test then selected multiple comparisons between groups using Dunn's test. * p<0.0332, ** p<0.0021, ***p<0.0002*

The expression of lncRNA MALAT1 is sufficient to cause PMNs to become GRIM. In addition, GRIM PMNs are able to release pathological EVs that can differentiate naïve PMNs into GRIM PMNs. Based on evidence of MALAT1 being packaged into EVs from other cell types,

we next sought to determine the amount of MALAT1 transcript in both the cellular and EV compartments of GRIM PMNs and LTB4 control PMNs. We first confirmed that the knockdown and overexpression of MALAT1 were successful by qRT-PCR **(Figure 4.5A)**. However, when quantifying MALAT1 in the cellular compartment we observed lower levels of MALAT1 in PMNs transmigrated towards CFASN EVs than LTB4 **(Figure 4.5A)**. Yet, paradoxically, CFASN secondary EVs had more MALAT1 than LTB4 secondary EVs **(Figure 4.5B)**. This suggests that MALAT1 is actively loaded into EVs from GRIM PMNs, but retained intracellularly by LTB4-transmgirated PMNs. We also observed that MALAT1 was significantly higher in LTB4 transmigrated PMNs than CFASN EV transmigrated PMNs by RNA-seq **(Figure 4.4B).**

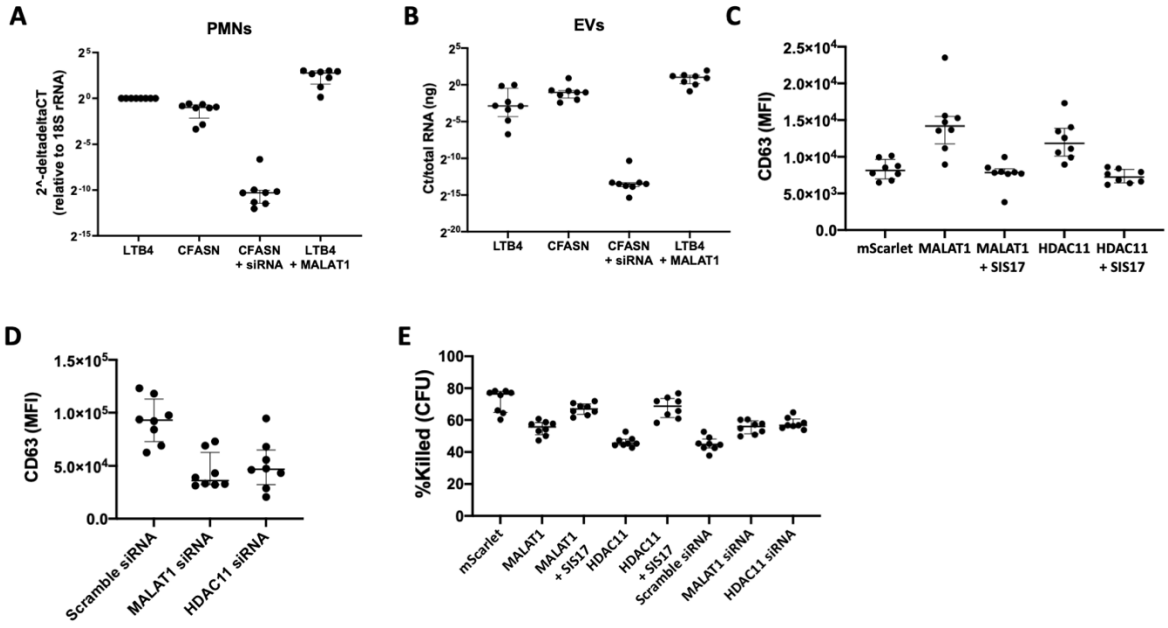

Figure 4.5: Expression of MALAT1 or HDAC11 can induce inflammation over multiple waves of recruited PMNs A) *MALAT1 RNA levels relative to 18S rRNA was calculated by qRT-PCR.* ***B)*** *PMNs were transmigrated towards LTB4 or CFASN EVs and electroporated with a mock plasmid or plasmids expressing MALAT1 siRNA or overexpression of MALAT1 and then allowed to release EVs for 12 hours. MALAT1 in the secreted EVs was calculated by qRT-PCR and normalized to the total amount of RNA. Naïve PMNs were generated towards EVs from PMNs treated with the labeled conditions and* ***D,E)*** *surface CD63 was measured by flow cytometry and* ***F)*** *bacteria-killing capacity was determined. Statistics have not yet been calculated due to insufficient repeats*

CFASN EV transmigrated PMNs released EVs that were then able to differentiate naïve PMNs into GRIM PMNs **(Figures 4.2C,D)**. EVs from MALAT1- and HDAC11- transfected PMNs were isolated and then used in the apical fluid to condition naïve PMNs. PMNs that transmigrated towards EVs from MALAT1-transfected and HDAC11-transfected PMNs showed elevated surface CD63 **(Figures 4.5C).** As before, the effects of the transfection were mitigated with SIS17 was included **(Figures 4.5C)**. In addition, EVs from CFASN EV transmigrated PMNs transfected with MALAT1 or HDAC11 siRNA were unable to condition naïve PMNs into the GRIM phenotype as shown by surface CD63 and bacteria killing **(Figures 4.5D,E).** MALAT1 and HDAC11-induced PMNs were both able to generate feed-forward activation of naïve PMNs, while inhibition or knockdown prevented transfer of the GRIM phenotype.

Since MALAT1 was readily packaged into EVs by GRIM PMNs and could condition naïve PMNs in the *in vitro* transmigration system, MALAT1 transcript in EVs may also be a biomarker of disease severity. To this end, EVs were isolated from the expectorated sputum of adult patients (n=90) that had been admitted to the hospital for an acute pulmonary exacerbation (APE) in the past year. Sputum that was collected within 1-4 days since the APE were contained significantly more copies of MALAT1 transcript than sputum that was collected 3-6 months since the APE. MALAT1 concentration in sputum 1 year after the APE had a median much lower than even the 3-6 month cohort but was not statistically significant likely due to low sample number **(Figures 4.6A).** Lung function as a measurement of forced expiratory volume relative to forced vital capacity (%FEV1) is known to decrease following an APE (Sanders et al., 2010). In addition, PMN-related factors such as NE and methionine sulfoxide concentration are also known to correlate with the decline in %FEV1 (Chandler et al., 2018; Margaroli et al., 2019). In line with

this observations MALAT1 concentration in EVs isolated from patient sputa strongly correlated with %FEV1 **(Figures 4.6B)**. Since MALAT1 may be transcribed by multiple cell types present in the airways including various epithelial cells more work must be done in order to determine the role of MALAT1+ EVs on PMNs both in early pathogenesis of airway disease as well as late-stage disease.

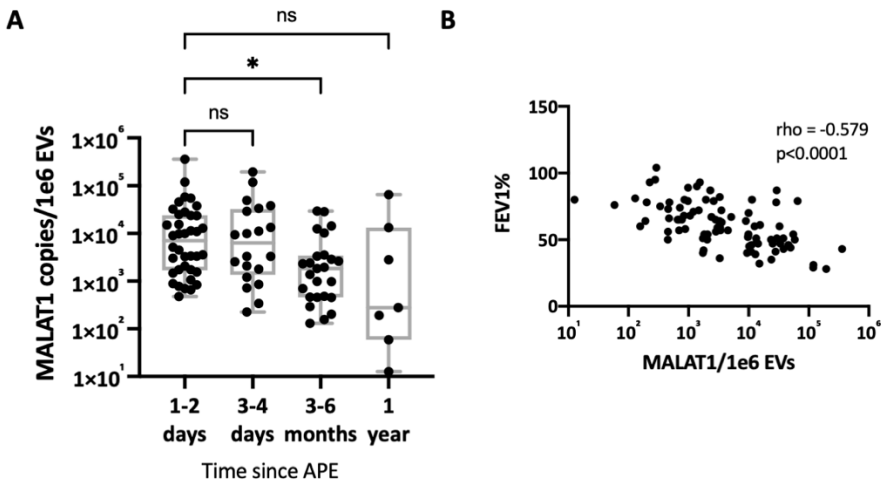

Figure 4.6: MALAT1 in EVs from CF sputum strongly correlates with exacerbation status and lung function. *Sputum was collected during inpatient visits were conducted 1-4 days after an acute pulmonary exacerbation and outpatient visits were conducted in stable condition at least 3-12 months from the exacerbation.* ***A)*** *MALAT1 was purified from total EVs and concentration was measured by qRT-PCR (n=90). Statistics were calculated with a Kruskal-Wallis test then selected multiple comparisons between groups using Dunn's test. * p<0.0332, ** p<0.0021, ***p<0.0002* ***B)*** *MALAT1 in EV concentration was correlated with %FEV lung function (n=89). One patient did not have a recorded %FEV1 and was thus excluded.* Statistics were calculated with a Spearman's correlation.

DISCUSSION

Although HEMT has been quite successful for treating CF airway disease most patients still experience chronic inflammation and gradual worsening of lung function over time (Hisert et al., 2017; Perrem and Ratjen, 2019; Zaher et al., 2021; Saluzzo et al., 2022). Furthermore, not all patients have access to these life-altering therapies or are ineligible due to their CFTR mutation status (Guo et al., 2022). There are also patients under two years of age for which HEMT is not yet approved. In this age group disease progression and airway inflammation has already begun based on the observation of GRIM PMNs in the airway lumen (Chandler et al., 2018). Further, this run-away inflammation cannot handle invading pathogens and may even act as a scaffold for opportunistic infections (Yonker et al., 2015; Lin and Kazmierczak, 2017). Thus, new therapies must be developed with the purpose to realign the poise of recruited PMNs cells in order to effectively clear pathogens and mitigate structural tissue damage (Perrem and Ratjen, 2019). The need for these host-directed therapies has also risen as multidrug resistant bacteria becomes more prevalent (Rutter et al., 2017; Hahn et al., 2018).

However, the mechanisms promoting the differentiation into GRIM PMNs, including their lack of bacterial clearance and the ability of short-lived cells to maintain a chronic phenotype, remain poorly understood. EVs in the lung, which display integrins and lipids such as phosphatidyl serine (Mulcahy et al., 2014), are particularly prone to be taken up by scavenger cells such as PMNs, and thus are primed to modulate the activity of these cells. Due to the large number of PMNs and PMN-derived EVs present in the airways, we hypothesized that EVs derived from activated and inflammatory CF airway PMNs could cause naïve PMNs, newly immigrated into the lung, to acquire a phenotype similar to that of the originating PMN. In this study we have shown that CFASN contains 1e10 EVs/mL and has a remarkable ability to

differentiate naïve airway PMNs into pathological entities with high rates of exocytosis and yet, paradoxically fail to clear bacteria. PMN-derived, CD66b+ EVs released from GRIM PMNs contained the lncRNA, MALAT1, which caused the upregulation of HDAC11 and induced the GRIM phenotype **(Figures 4.7)**. The expression of either MALAT1 or HDAC11 was necessary and sufficient for the induction of the GRIM phenotype including neglect of bacteria. Taken together, PMN-derived EVs promote feed-forward inflammatory signaling in populations of PMNs.

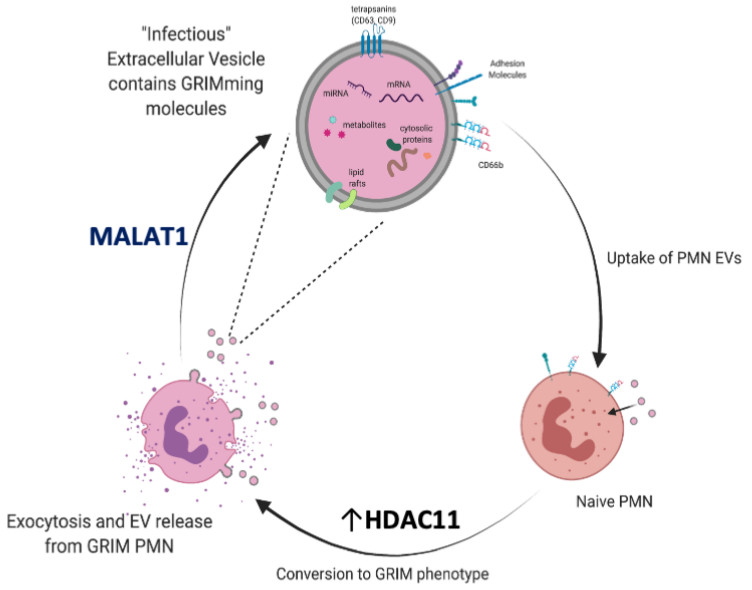

Figure 4.7: Extracellular vesicle lncRNA MALAT1 drives HDAC11 dependent chronic inflammation in airway neutrophils. *GRIM PMNs present in the airways release EVs, either microvesicles or exosomes, which contain the lncRNA MALAT1. These EVs are taken up by naïve, newly immigrated PMNs, which then upregulate expression of HDAC11. HDAC11+ PMNs become GRIM and then release EVs with MALAT1 continuing the process of feed-forward inflammation.*

EVs derived from PMNs in the blood have anti-inflammatory (Gasser and Schifferli, 2004; Pliyev et al., 2014; Rhys et al., 2018) and bactericidal effects (Timar et al., 2013), however few studies have investigated EVs from PMNs in the lung nor the functional role of these EVs in CF and other inflammatory airway diseases. PMN-derived EVs also contained membrane-bound

NE, which occludes the inhibitory domain and thus was less prone to inhibition by antiproteases than its unbound and soluble form (Owen et al., 1995; Genschmer et al., 2019; Amjadi et al., 2021). NE+ PMN-derived EVs were also sufficient to cause emphysema in mice (Genschmer et al., 2019). Furthermore, PMN-derived EVs also carry MPO, which was shown to damage vascular endothelial cells (Pitanga et al., 2014), while in the intestinal mucosa tissue-infiltrating PMNs released EVs carrying MPO, which was more potent than soluble MPO, and inhibited epithelial wound healing (Slater et al., 2017). Taken together, conjugation of effector molecules to the membrane of an EV may change the physical properties and structure thereby modifying the kinetics and potency of effector molecules.

Similarly, EVs may alter the way that potentially inflammatory damaged associated molecular patterns (DAMPs) are sensed. For example, EVs containing oxidized mitochondria did not activate the typical pattern recognition receptors that released oxidized mitochondria do and did not stimulate IL-6 production (Todkar et al., 2021). It has been demonstrated in a variety of contexts that EVs can contain various DAMPs both compartmentalized within the EVs or associated with the surface of the EV including DNA and histones, dsRNA, mitochondria, and HMGB1 (Yanez-Mo et al., 2015; Park et al., 2018; Neri et al., 2022). In addition, we recently showed that airway GRIM PMNs can release EVs that contain activate caspase-1 that can activate inflammasome signaling in airway epithelial cells bypassing the canonical requirement for signal #1 and signal #2 (Forrest et al., 2022). Another study found that EVs from activated blood neutrophils could induce endothelial inflammation via miR-142-3p and miR-451 in a model of ANCA-associated vasculitis (Glemain et al., 2022). EVs from swarming PMNs contained both the chemoattractant LTB4 and LTA4H, the enzyme that synthesizes LTB4 (Dalli et al.,

2013). These EVs were able to stimulate PMN chemotaxis (Majumdar et al., 2021). We did not measure the concentration of LTB4 or LTA4H in our batches of purified EVs, however the EVs alone were unable to induce PMN transmigration. Although the methods used to determine PMN movement were disparate, the differing ability of PMN-derived EVs to induce other PMNs to migrate may be due to potential heterogeneity in the EV population released by PMNs.

During the initiation of diapedesis, PMNs will begin to alter their membrane morphology and secrete both soluble factors and small particles as they roll along the surface of activated endothelium. Some of these structures were recently described as elongated neutrophil-derived structures (ENDS). ENDS did not contain any of the organelles of the rolling PMN such as mitochondria, ER, or DNA and histones as detected by various organelle localizing dyes and STORM imaging (Marki et al., 2021). Furthermore, ENDS contained the DAMPS S100A8 and S100A9 which were only able to be detected once the ENDS were degraded. In this way, released particles, particularly those from primed or activated PMNs, may not only be able to affect and activate other cells in the environment, but also continue to do long after the producing cells and migrated to another region of the tissue or apoptosed. It is evident based on morphology, protein, RNA and DNA contents and the timing during transmigrating when which the particle is released that ENDS, migrasomes, and EVs are distinct structures each with a unique function. During the short lifespan of a PMN, these cells are able to functionalize a release a wide variety of particles as well as soluble factors that are able to quickly modulate the local environment. It is still unclear whether ENDS, migrasomes, and GRIM EVs can all be released by a single PMN as a cascade during transmigration or each factor only arises from heterogenous populations of PMNs each with a unique function, and perhaps inflammatory

potential. In addition, it must still be determined what factors promote the release of each subset of particle. Is the propensity for synthesis and release of each particle affected by differences in granulopoiesis in the bone marrow, association with various DAMPs or PAMPs or the specific contents scavenged therein? Despite the large numbers of PMNs present in many inflammatory diseases, there has been little investigation into the contents and downstream functional roles of PMN-EVs, particularly on the receiving PMN-population.

PMNs are particularly sensitive to the contents within EVs and process their contents readily (Akbar et al., 2022). While we have demonstrated that uptake of MALAT1 within EVs causes airway-like PMNs to become GRIM via HDAC11 it still remains unclear how many transcripts of MALAT1 as well as how many EVs are necessary for this phenomenon to occur. Similarly, although we demonstrate that the population of CD66b+ EVs contain MALAT1, questions regarding whether each EV contains MALAT1 and how much MALAT1 remain unanswered. It is clear that miRNAs packaged within EVs can affect recipient cells, yet it has also been demonstrated that the number of miRNAs/EV is likely too low to have an effect based on prior cell biology studies of miRNA mechanisms of actions. It has been proposed that so-called 'carrier effects' of EVs, that is the ability of EVs to enhance efficiency and efficacy of cargo beyond the results of simple biochemical assays, can account for this discrepancy (Askenase, 2021). Similarly, the carrier effects of PMN-derived EVs via integrins and other surface proteins may increase the probability of MALAT1 delivery**.** Additionally, scavenger cells such as PMNs are able to process and partially preserve the degradation products of the lysosome for antigen presentation. EVs may be able to coopt similar mechanisms to allow for escape and utilization of transcripts. As innate immune cells PMNs are able to respond

remarkably fast to stimuli. After just 1-4 hours of transmigration into CFASN bactericidal activity (Margaroli et al., 2021). Further fractionation into just the contained EVs was also sufficient to induce similar phenotypic changes. PMNs incubated with sufficient conditioning to allow these PMNs to release their own pathological EVs. On a per cell basis, PMNs appear more sensitive to EVs able to be affected by 10^3-10^4 EVs/cell over the course of 4 hours (although not every cell necessarily receives the same number of EVs) compared to other cell types which require the addition ~100 times more EVs/cell and potential inclusion of membrane-penetrating peptides to enhance cargo delivery over 24-72 hours (Mathieu et al., 2019; Somiya and Kuroda, 2021; Breyne et al., 2022; O'Brien et al., 2022; Zhang et al., 2022). This suggests that airway PMNs, and perhaps PMNs in other tissues, are exceptionally proficient at rapidly responding to the stressors and information packaged within EVs. A recent study showed that Airway EVs, likely released by type II alveolar epithelial cells contain dsDNA, both intra-EV and associated with the outside of the EV. These stimulate PMNs to release CXCL1 and CXCL2 via TLR9 signaling and promoted PMN reverse-transmigration to the bone marrow (Liu et al., 2022). This study also overlaid proteomic analysis of airways EVs with scRNA-seq data to conclude that non-immune cells generate most of the EVs present in the airways. While an interesting method, and perhaps specific to their mouse models and human disease landscape it may not account for the buildup of EVs over time during chronic disease or that immune cells may more readily clear their own EVs from the environment.

We demonstrated that inhibition of HDAC11 by the small molecule drug, SIS17 and knockdown with siRNA normalize exocytosis and bacterial killing in typically-GRIM inducing conditions. HDAC11 has previously been shown to be essential for PMN development and

regulate the ability of mature PMNs to migrate (Sahakian et al., 2017). In addition, IL-10 for which HDAC11 is known to inhibit the expression of (Villagra et al., 2009; Cheng et al., 2014), is notably absent or only present at low levels in the CF airways (Osika et al., 1999; Colombo et al., 2005; Giacalone et al., 2022). Since SIS17 inhibits the deacylase function of PMNs (Son et al., 2019) it is likely that the targets of HDAC11 that control the induction of the GRIM fate are post-translationally modified to contain myristoyl and palmitoyl moieties on lysines (Cao et al., 2019). However, SIS17 may also affect the deacetylation functions of HDAC11 at a low level since we observe an increase in IL-10 protein when SIS17 is used. Furthermore, HDAC11 also regulates the stability of IFNAR1 via SHMT2 ubiquitylation (Cao et al., 2019). Type I IFN signaling via IFNAR has been shown to regulate PMN activation and $IFNAR^{-/-}$ PMNs had a lower threshold for activation and release of granule proteins (Xin et al., 2010). In order to determine the targets of HDAC11 in PMNs in a more unbiased approach the reagent Alk14, a palmitic acid analog with a terminal alkyne group for click chemistry, could be used with and without SIS17 or HDAC11 siRNA present (Cao et al., 2019; Son et al., 2019). Lastly, the role of one-carbon metabolism via SHMT2 and the role of EVs acting as an important carbon source as well as fueling beta-oxidation may also be relevant. In skeletal muscle cells, HDAC11 has been observed to localize to the mitochondria (Hurtado et al., 2021; Nunez-Alvarez et al., 2021). We have not yet determined the localization of HDAC11 in GRIM PMNs however we have shown upregulation and packaging of many mitochondrial genes in EVs. Furthermore, HDAC11 may also regulate protein-cargo loading into EVs since palmitoylation has been demonstrated to be a pro-EV localization motif (Fabbiano et al., 2020; O'Brien et al., 2022). HDAC11 controlling the

EV loading of RNA-binding proteins that bind MALAT1 may be one mechanism for the generation of GRIM-inducing EVs.

MATERIALS AND METHODS

Human subjects and samples. Samples were accrued per Emory University IRB-approved protocols. Informed consent was obtained before sample collection from a total of 90 adults with CF **(Supplementary Table 4.1)** and 8 HC adults. CF was diagnosed using a quantitative iontophoresis test and/or documentation of two identifiable CFTR mutations. Neutrophils were purified from whole blood from healthy control (HC) and CF donors as previously described (Tirouvanziam et al., 2008) and used for transmigration experiments (below), flow cytometry, or RNA extraction. Sputum was collected from HC subjects by induction, and from CF patients by expectoration and processed as previously described (Tirouvanziam et al., 2008) to yield live neutrophils and airway supernatant (ASN). Airway PMNs were analyzed by flow and image cytometry. ASN was stored at -80˚C until use for EV purification (below) or transmigration experiments (below).

In vitro transmigration experiments. The model was set up as described (Forrest et al., 2018; Dobosh et al., 2021). The H441 Club cell line is grown on Alvetex scaffolds (ReproCELL, Glasgow, UK) coated with rat-tail collagen (Sigma) for 2 weeks at air liquid interface with 2% v/v Ultroser G (Crescent Chemical, Islandia, NY) in 50/50 DMEM/F12 supplemented with 1% v/v penicillin/streptomycin (Forrest et al., 2018; Grunwell et al., 2019). This setup requires manual flipping of filters prior to transmigration (Dobosh et al., 2021). The filters are transferred to RPMI media with LTB4 (100 nM) with or without EVs from CFASN or fractions thereof (e.g., flow-through of 300 kDa MWCO column devoid of EVs, EVs purified from CFASN, EVs purified from conditioned media). Subsequently, 10^6 cells are loaded onto the Alvetex scaffold for transmigration which was allowed to occur for 4 hours at 37˚C under 5% CO_2. Since we observed that EVs alone could not induce transmigration of PMNs all conditions included LTB4

at 100 nM. Transmigrated PMNs were used for media conditioning (below), flow cytometry, western blot, qRT-PCR and RNA-seq analyses.

Isolation of nucleic acids. For isolation of RNA from PMNs, 0.75 mL of TriPure (Roche) was added per 10^6 cells or 10^{10} EVs. Then chloroform (Sigma) was added and spun following the manufacturer's protocol. Due to the small amount of expected RNA yield, the aqueous phase (containing the RNA) was mixed 1:1 with 100% ethanol (Sigma) and loaded onto an RNA clean and concentrator-5 column (Zymo). RNA was isolated following the manufacturer's protocol.

Quantification of MALAT1 RNA via qRT-PCR. Total RNA is reverse-transcribed using SuperScript IV (ThermoFisher) and an anchored oligo-$d(T)_{20}$ primer followed by amplification with a primer probe pair which targets MALAT1 **(Supplementary Table 4.2)** and Luna Universal Probe qPCR Master Mix (New England Biolabs) was used to amplify the cDNA. A standard curve to calculate copy number was also generated using the MALAT1 expression plasmid **(Supplementary Table 4.3)** which contains the expected binding sequence

RNA quantification and quality control. RNA was initially quantified by Nanodrop 1000 spectrophotometer (ThermoScientific). For samples that would be analyzed by RNA-seq, an aliquot was further quality controlled by an Agilent Bioanalyzer 2100.

RNA-sequencing of PMNs. For *RNASeq,* purified RNA was given to the Yerkes Genomics Core for processing. Briefly, rRNA is depleted and the TruSeqRNA Sample Preparation v2 kit and LS protocol is used. All the produced Fastq files from single end reads were aligned to the human reference genome (GRCh38.p13- Ensembl) using the alignment tool HISAT2 (version 2.1.0), using the default settings. Then, BAM files reads were sorted using SAMtools. The resulting BAM files were used as input to determine read counts using FeatureCounts (1.5.2).

All processed counts were used to conducted differential expression analysis using DEseq2, considering as differentially expressed genes, genes with fold changes > 2 folds, and a False discovery rate < 0.1. Finally, to understand the functions of the differentially expressed genes Metacore server is used against pathway maps and networks. RNA-seq data has not yet been made available, but can be given upon request. This dataset will be deposited to GEO for publication

Generation of EVs from conditioned media. PMNs (electroporated with plasmids or not) transmigrated towards LTB4 or CFASN EVs for 4 hours were incubated in RPMI at a density of 1e6 cells/mL for 12 hours and then EVs were purified as described below.

Purification of EVs. EVs were isolated from ASN or conditioned media by taking the supernatant from sequential centrifugations at 800, 3,000*,* and 20,000 x *g,* applying to a 300 kDa MWCO (Vivaspin 500, Sartorius, Germany) followed by a 3,000 x *g* spin. Characterization of EVs was by nanoparticle tracking analysis (NTA), flow cytometry and transmission electron microscopy

Cloning and Electroporation of Plasmids. Plasmids for electroporation into PMNs were generated using a modified modular Golden Gate cloning protocol (Wagner et al., 2018) **(Modified Overhangs given in Supplementary Table 4.4)**. These plasmids allowed for parts (promoters, 5'UTRs, ORFs, siRNAs and 3'UTRs) to be cloned as lvl0 plasmids. There were two different lvl1 destination vectors designated as position 1 (pos1) and position 2 (pos2), which can then be combined into a lvl2 destination vector. Lvl0 parts and all destination vectors have not yet been deposited to Addgene, but will be upon publication of the associated manuscript.

1e6 Primary blood PMNs were washed and resuspended in 100 uL P3 buffer with 4 ug of plasmid DNA. The recipe for P3 buffer is: 5mM KCl, 15mM $MgCl_2$; 90 mM NaCl; 10 mM Glucose; 0.4 mM $Ca(NO_3)_2$; 40 mM Na_2HPO_4/NaH_2PO_4 pH 7.2 (Chicaybam et al., 2016). Sample was electroporated at 150 V for 5 ms in a 0.2 cm cuvette. Samples were immediately washed once with DMEM + 10% FBS and then washed twice and resuspended in RPMI and applied to the transmigration filter.

Data Analysis. Statistical analyses were preformed using Prism 9.0.0 (GraphPad, La Jolla, CA, USA). Comparisons between two groups was performed with a Mann-Whitney U-test (unpaired) with a threshold of * for $p<0.05$, ** for $p<0.01$, and *** for $p<0.001$, and between two or more groups with a Kruskal-Wallis test and Dunn's multiple comparisons, * $p<0.0332$, ** $p<0.0021$, ***$p<0.0002$.

Characterization of EVs by nanoparticle tracking analysis, flow cytometry, and electron microscopy. Concentration and size of EVs was determined using the Nanosight NS3000 (Malvern Panalytical, Westborough, MA, USA). For flow cytometry, 30 µL of magnetic beads coated with streptavidin (SVM-80-5 Spherotech, Lake Forest, IL, USA) and washed with PBS + 2.5 mM EDTA then incubated with 10 µL of biotinylated antibody (0.5 mg/mL, Biolegend for 2 hours rotating at 4 ˚C brought to a final volume of 200 µL with PBS + EDTA. Biotinylated antibodies were CD63: 353018, CD66b: 305120, CD326: 324216. CD63 is expressed on many EVs. CD66b is to immunoprecipitate neutrophil-derived EVs, and CD326 is to immunoprecipitate epithelial-derived EVs.(Takao et al., 2018; Genschmer et al., 2019)Beads were washed 3 times with PBS + EDTA and then approximately $2x10^9$ EVs were applied to the beads and rotated overnight at 4˚C. Bead:EV conjugates were washed 3 times with PBS + EDTA

then stained with FLICA and run on a Cytoflex S flow cytometer (Beckman Coulter, Pasadena, CA, USA).

For electron microscopy, EVs were applied to a discharged formvar-carbon coated grid. Excess liquid was wicked away and 1% uranyl acetate stain was added, then wicked away. The samples were air-dried at room temperature. Grids were visualized on a Hitachi 7700 TEM at 80 kV.

Flow cytometry analysis of neutrophils. Blood and airway cells from CF and HC subjects, and from the in vitro transmigration model, were stained with fluorescently labeled antibodies CD63 (H5C6), CD66b (G10F5), EpCAM (9C4), and CD16 (3G8) (Biolegend, San Diego CA, USA), and NE (95034) (R&D Systems, Minneapolis, MN, USA). Cells were also stained with the Zombie Aqua or NIR probe (Biolegend) to determine viability.. Data were acquired on a Cytoflex S Flow Cytometer and compensation and analysis were performed using FlowJo software 10.6.1 (Becton Dickinson and Company, Franklin Lakes, NJ, USA). The voltages across all acquisitions were calibrated using Spherotech Rainbow Calibration Particles (RCP-30-5) to ensure that all samples were acquired under the same conditions and the cytometer was performing as expected.

Western Blot analysis of neutrophils and EVs. 10^6 neutrophils were pelleted and then resuspended in RIPA + HALT protease inhibitor cocktail (Thermo Fisher Scientific, Waltham MA, USA) with additional PMSF added (1 mM). EVs (~$2x10^9$) were concentrated on the 300 kDa MWCO column and then lysed in RIPA + protease inhibitor cocktail. Primary antibodies diluted in TBST+BSA were TSG101 (1:1000, 4A10, Abcam, Cambridge, UK), calnexin (1:1000, ab10286, Abcam) anti-CD63 (1:15000 System Biosciences EXOAB-CD63A-1), anti-GAPDH (1:400, sc-47724,

Santa Cruz), anti-HDAC11 (1:1000, ab166907, Abcam). Secondary antibodies were goat anti-rabbit IRdye 800 CW and goat anti-mouse IRdye 680RD (both 1:15000, LICOR, Lincoln NE, USA). Images were taken on a LICOR ODYSSEY per manufacturer guidelines. Images were analyzed in ImageJ 1.52.

REFERENCES

1. Akbar, N., Braithwaite, A.T., Corr, E.M., Koelwyn, G.J., van Solingen, C., Cochain, C., Saliba, A.E., Corbin, A., Pezzolla, D., Moller Jorgensen, M.*, et al.* (2022). Rapid Neutrophil Mobilisation by VCAM-1+ Endothelial Extracellular Vesicles. Cardiovasc Res. 10.1093/cvr/cvac012.
2. Amjadi, M.F., Avner, B.S., Greenlee-Wacker, M.C., Horswill, A.R., and Nauseef, W.M. (2021). Neutrophil-Derived Extracellular Vesicles Modulate the Phenotype of Naive Human Neutrophils. J Leukoc Biol *110*, 917-925. 10.1002/JLB.3AB0520-339RR. PMC8423865
3. Askenase, P.W. (2021). Exosomes Provide Unappreciated Carrier Effects That Assist Transfers of Their miRNAs to Targeted Cells; I. They Are 'the Elephant in the Room'. RNA Biol *18*, 2038-2053. 10.1080/15476286.2021.1885189. PMC8582996
4. Askenase, P.W. (2022). Exosome Carrier Effects; Resistance to Digestion in Phagolysosomes May Assist Transfers to Targeted Cells; II Transfers of miRNAs Are Better Analyzed Via Systems Approach as They Do Not Fit Conventional Reductionist Stoichiometric Concepts. Int J Mol Sci *23*. 10.3390/ijms23116192. PMC9181154
5. Blanter, M., Gouwy, M., and Struyf, S. (2021). Studying Neutrophil Function in Vitro: Cell Models and Environmental Factors. J Inflamm Res *14*, 141-162. 10.2147/JIR.S284941. PMC7829132
6. Bost, P., De Sanctis, F., Cane, S., Ugel, S., Donadello, K., Castellucci, M., Eyal, D., Fiore, A., Anselmi, C., Barouni, R.M.*, et al.* (2021). Deciphering the State of Immune Silence in Fatal COVID-19 Patients. Nat Commun *12*, 1428. 10.1038/s41467-021-21702-6. PMC7935849
7. Breyne, K., Ughetto, S., Rufino-Ramos, D., Mahjoum, S., Grandell, E.A., de Almeida, L.P., and Breakefield, X.O. (2022). Exogenous Loading of Extracellular Vesicles, Virus-Like Particles, and Lentiviral Vectors with Supercharged Proteins. Commun Biol *5*, 485. 10.1038/s42003-022-03440-7. PMC9120435
8. Brown, R.K., Wyatt, H., Price, J.F., and Kelly, F.J. (1996). Pulmonary Dysfunction in Cystic Fibrosis Is Associated with Oxidative Stress. European Respiratory Journal *9*, 334-339. Doi 10.1183/09031936.96.09020334.
9. Cao, J., Sun, L., Aramsangtienchai, P., Spiegelman, N.A., Zhang, X., Huang, W., Seto, E., and Lin, H. (2019). HDAC11 Regulates Type I Interferon Signaling through Defatty-Acylation of SHMT2. Proc Natl Acad Sci U S A *116*, 5487-5492. 10.1073/pnas.1815365116. PMC6431144
10. Chandler, J.D., Margaroli, C., Horati, H., Kilgore, M.B., Veltman, M., Liu, H.K., Taurone, A.J., Peng, L., Guglani, L., Uppal, K.*, et al.* (2018). Myeloperoxidase Oxidation of Methionine Associates with Early Cystic Fibrosis Lung Disease. Eur Respir J *52*. 10.1183/13993003.01118-2018. PMC7034951
11. Cheng, F., Lienlaf, M., Perez-Villarroel, P., Wang, H.W., Lee, C., Woan, K., Woods, D., Knox, T., Bergman, J., Pinilla-Ibarz, J.*, et al.* (2014). Divergent Roles of Histone Deacetylase 6 (Hdac6) and Histone Deacetylase 11 (HDAC11) on the Transcriptional Regulation of Il10 in Antigen Presenting Cells. Mol Immunol *60*, 44-53. 10.1016/j.molimm.2014.02.019. PMC4020151

12. Chicaybam, L., Barcelos, C., Peixoto, B., Carneiro, M., Limia, C.G., Redondo, P., Lira, C., Paraguassu-Braga, F., Vasconcelos, Z.F., Barros, L.*, et al.* (2016). An Efficient Electroporation Protocol for the Genetic Modification of Mammalian Cells. Front Bioeng Biotechnol *4*, 99. 10.3389/fbioe.2016.00099. PMC5253374
13. Colombo, C., Costantini, D., Rocchi, A., Cariani, L., Garlaschi, M.L., Tirelli, S., Calori, G., Copreni, E., and Conese, M. (2005). Cytokine Levels in Sputum of Cystic Fibrosis Patients before and after Antibiotic Therapy. Pediatric pulmonology *40*, 15-21. 10.1002/ppul.20237.
14. Dalli, J., Montero-Melendez, T., Norling, L.V., Yin, X., Hinds, C., Haskard, D., Mayr, M., and Perretti, M. (2013). Heterogeneity in Neutrophil Microparticles Reveals Distinct Proteome and Functional Properties. Mol Cell Proteomics *12*, 2205-2219. 10.1074/mcp.M113.028589. PMC3734580
15. Dittrich, A.S., Kuhbandner, I., Gehrig, S., Rickert-Zacharias, V., Twigg, M., Wege, S., Taggart, C.C., Herth, F., Schultz, C., and Mall, M.A. (2018). Elastase Activity on Sputum Neutrophils Correlates with Severity of Lung Disease in Cystic Fibrosis. Eur Respir J *51*. 10.1183/13993003.01910-2017.
16. Dobosh, B., Giacalone, V.D., Margaroli, C., and Tirouvanziam, R. (2021). Mass Production of Human Airway-Like Neutrophils Via Transmigration in an Organotypic Model of Human Airways. STAR Protoc *2*, 100892. 10.1016/j.xpro.2021.100892. PMC8551927
17. Dobosh, B., Zandi, K., Giraldo, D.M., Goh, S.L., Musall, K., Aldeco, M., LeCher, J., Giacalone, V.D., Yang, J., Eddins, D.J.*, et al.* (2022). Baricitinib Attenuates the Proinflammatory Phase of COVID-19 Driven by Lung-Infiltrating Monocytes. Cell Rep *39*, 110945. 10.1016/j.celrep.2022.110945.
18. Elborn, J.S. (2016). Cystic Fibrosis. Lancet *388*, 2519-2531. 10.1016/S0140-6736(16)00576-6. 27140670
19. Fabbiano, F., Corsi, J., Gurrieri, E., Trevisan, C., Notarangelo, M., and D'Agostino, V.G. (2020). RNA Packaging into Extracellular Vesicles: An Orchestra of RNA-Binding Proteins? J Extracell Vesicles *10*, e12043. 10.1002/jev2.12043. PMC7769857
20. Farrell, P., Ferec, C., Macek, M., Frischer, T., Renner, S., Riss, K., Barton, D., Repetto, T., Tzetis, M., Giteau, K.*, et al.* (2018). Estimating the Age of P.(Phe508del) with Family Studies of Geographically Distinct European Populations and the Early Spread of Cystic Fibrosis. Eur J Hum Genet *26*, 1832-1839. 10.1038/s41431-018-0234-z. PMC6244163
21. Fine, N., Tasevski, N., McCulloch, C.A., Tenenbaum, H.C., and Glogauer, M. (2020). The Neutrophil: Constant Defender and First Responder. Front Immunol *11*, 571085. 10.3389/fimmu.2020.571085. PMC7541934
22. Forrest, O.A., Dobosh, B., Ingersoll, S.A., Rao, S., Rojas, A., Laval, J., Alvarez, J.A., Brown, M.R., Tangpricha, V., and Tirouvanziam, R. (2022). Neutrophil-Derived Extracellular Vesicles Promote Feed-Forward Inflammasome Signaling in Cystic Fibrosis Airways. J Leukoc Biol. 10.1002/JLB.3AB0321-149R.
23. Forrest, O.A., Ingersoll, S.A., Preininger, M.K., Laval, J., Limoli, D.H., Brown, M.R., Lee, F.E., Bedi, B., Sadikot, R.T., Goldberg, J.B.*, et al.* (2018). Frontline Science: Pathological Conditioning of Human Neutrophils Recruited to the Airway Milieu in Cystic Fibrosis. J Leukoc Biol *104*, 665-675. 10.1002/JLB.5HI1117-454RR. PMC6956843

24. Gasser, O., and Schifferli, J.A. (2004). Activated Polymorphonuclear Neutrophils Disseminate Anti-Inflammatory Microparticles by Ectocytosis. Blood *104*, 2543-2548. 10.1182/blood-2004-01-0361.
25. Genschmer, K.R., Russell, D.W., Lal, C., Szul, T., Bratcher, P.E., Noerager, B.D., Abdul Roda, M., Xu, X., Rezonzew, G., Viera, L.*, et al.* (2019). Activated PMN Exosomes: Pathogenic Entities Causing Matrix Destruction and Disease in the Lung. Cell *176*, 113-126 e115. 10.1016/j.cell.2018.12.002. PMC6368091
26. Giacalone, V.D., Moncada-Giraldo, D., Margaroli, C., Brown, M.R., Silva, G.L., Chandler, J.D., Peng, L., Tirouvanziam, R., Guglani, L., and Program, I.-C. (2022). Pilot Study of Inflammatory Biomarkers in Matched Induced Sputum and Bronchoalveolar Lavage of 2-Year-Olds with Cystic Fibrosis. Pediatric pulmonology *n/a*. 10.1002/ppul.26023.
27. Glemain, A., Neel, M., Neel, A., Andre-Gregoire, G., Gavard, J., Martinet, B., Le Bloas, R., Riquin, K., Hamidou, M., Fakhouri, F.*, et al.* (2022). Neutrophil-Derived Extracellular Vesicles Induce Endothelial Inflammation and Damage through the Transfer of miRNAs. J Autoimmun *129*, 102826. 10.1016/j.jaut.2022.102826.
28. Grieshaber-Bouyer, R., and Nigrovic, P.A. (2019). Neutrophil Heterogeneity as Therapeutic Opportunity in Immune-Mediated Disease. Front Immunol *10*, 346. 10.3389/fimmu.2019.00346. PMC6409342
29. Grieshaber-Bouyer, R., Radtke, F.A., Cunin, P., Stifano, G., Levescot, A., Vijaykumar, B., Nelson-Maney, N., Blaustein, R.B., Monach, P.A., Nigrovic, P.A.*, et al.* (2021). The Neutrotime Transcriptional Signature Defines a Single Continuum of Neutrophils across Biological Compartments. Nat Commun *12*, 2856. 10.1038/s41467-021-22973-9. PMC8129206
30. Grunwell, J.R., Giacalone, V.D., Stephenson, S., Margaroli, C., Dobosh, B.S., Brown, M.R., Fitzpatrick, A.M., and Tirouvanziam, R. (2019). Neutrophil Dysfunction in the Airways of Children with Acute Respiratory Failure Due to Lower Respiratory Tract Viral and Bacterial Coinfections. Sci Rep *9*, 2874. 10.1038/s41598-019-39726-w. PMC6393569
31. Guo, J., Garratt, A., and Hill, A. (2022). Worldwide Rates of Diagnosis and Effective Treatment for Cystic Fibrosis. J Cyst Fibros *21*, 456-462. 10.1016/j.jcf.2022.01.009.
32. Hahn, A., Burrell, A., Fanous, H., Chaney, H., Sami, I., Perez, G.F., Koumbourlis, A.C., Freishtat, R.J., and Crandall, K.A. (2018). Antibiotic Multidrug Resistance in the Cystic Fibrosis Airway Microbiome Is Associated with Decreased Diversity. Heliyon *4*, e00795. 10.1016/j.heliyon.2018.e00795. PMC6143701
33. Headland, S.E., Jones, H.R., D'Sa, A.S., Perretti, M., and Norling, L.V. (2014). Cutting-Edge Analysis of Extracellular Microparticles Using Imagestream(X) Imaging Flow Cytometry. Sci Rep *4*, 5237. 10.1038/srep05237. PMC4050385
34. Hisert, K.B., Heltshe, S.L., Pope, C., Jorth, P., Wu, X., Edwards, R.M., Radey, M., Accurso, F.J., Wolter, D.J., Cooke, G.*, et al.* (2017). Restoring Cystic Fibrosis Transmembrane Conductance Regulator Function Reduces Airway Bacteria and Inflammation in People with Cystic Fibrosis and Chronic Lung Infections. Am J Respir Crit Care Med *195*, 1617-1628. 10.1164/rccm.201609-1954OC. PMC5476912
35. Hurtado, E., Nunez-Alvarez, Y., Munoz, M., Gutierrez-Caballero, C., Casas, J., Pendas, A.M., Peinado, M.A., and Suelves, M. (2021). HDAC11 Is a Novel Regulator of Fatty Acid Oxidative Metabolism in Skeletal Muscle. FEBS J *288*, 902-919. 10.1111/febs.15456.

36. Ingersoll, S.A., Laval, J., Forrest, O.A., Preininger, M., Brown, M.R., Arafat, D., Gibson, G., Tangpricha, V., and Tirouvanziam, R. (2015). Mature Cystic Fibrosis Airway Neutrophils Suppress T Cell Function: Evidence for a Role of Arginase 1 but Not Programmed Death-Ligand 1. J Immunol *194*, 5520-5528. 10.4049/jimmunol.1500312. PMC4433848
37. Kettle, A.J., Turner, R., Gangell, C.L., Harwood, D.T., Khalilova, I.S., Chapman, A.L., Winterbourn, C.C., Sly, P.D., and Arest, C.F. (2014). Oxidation Contributes to Low Glutathione in the Airways of Children with Cystic Fibrosis. Eur Respir J *44*, 122-129. 10.1183/09031936.00170213.
38. Kumar, S., and Mishra, S. (2022). Malat1 as Master Regulator of Biomarkers Predictive of Pan-Cancer Multi-Drug Resistance in the Context of Recalcitrant Nras Signaling Pathway Identified Using Systems-Oriented Approach. Sci Rep *12*, 7540. 10.1038/s41598-022-11214-8. PMC9085754
39. Kutil, Z., Novakova, Z., Meleshin, M., Mikesova, J., Schutkowski, M., and Barinka, C. (2018). Histone Deacetylase 11 Is a Fatty-Acid Deacylase. ACS Chem Biol *13*, 685-693. 10.1021/acschembio.7b00942.
40. Laucirica, D.R., Schofield, C.J., McLean, S.A., Margaroli, C., Agudelo-Romero, P., Stick, S.M., Tirouvanziam, R., Kicic, A., Garratt, L.W., Western Australian Epithelial Research, P*., et al.* (2022). Pseudomonas Aeruginosa Modulates Neutrophil Granule Exocytosis in an in Vitro Model of Airway Infection. Immunol Cell Biol *100*, 352-370. 10.1111/imcb.12547. PMID: 35318736
41. Laval, J., Touhami, J., Herzenberg, L.A., Conrad, C., Taylor, N., Battini, J.L., Sitbon, M., and Tirouvanziam, R. (2013). Metabolic Adaptation of Neutrophils in Cystic Fibrosis Airways Involves Distinct Shifts in Nutrient Transporter Expression. J Immunol *190*, 6043-6050. 10.4049/jimmunol.1201755.
42. Letsiou, E., Teixeira Alves, L.G., Felten, M., Mitchell, T.J., Muller-Redetzky, H.C., Dudek, S.M., and Witzenrath, M. (2021). Neutrophil-Derived Extracellular Vesicles Activate Platelets after Pneumolysin Exposure. Cells *10*. 10.3390/cells10123581. PMC8700313
43. Li, C., Ni, Y.Q., Xu, H., Xiang, Q.Y., Zhao, Y., Zhan, J.K., He, J.Y., Li, S., and Liu, Y.S. (2021). Roles and Mechanisms of Exosomal Non-Coding RNAs in Human Health and Diseases. Signal Transduct Target Ther *6*, 383. 10.1038/s41392-021-00779-x. PMC8578673
44. Lin, C.K., and Kazmierczak, B.I. (2017). Inflammation: A Double-Edged Sword in the Response to Pseudomonas Aeruginosa Infection. J Innate Immun *9*, 250-261. 10.1159/000455857. PMC5469373
45. Liu, B., Jin, Y., Yang, J., Han, Y., Shan, H., Qiu, M., Zhao, X., Liu, A., Jin, Y., and Yin, Y. (2022). Extracellular Vesicles from Lung Tissue Drive Bone Marrow Neutrophil Recruitment in Inflammation. J Extracell Vesicles *11*, e12223. 10.1002/jev2.12223. PMC9122834
46. Lorincz, A.M., Schutte, M., Timar, C.I., Veres, D.S., Kittel, A., McLeish, K.R., Merchant, M.L., and Ligeti, E. (2015). Functionally and Morphologically Distinct Populations of Extracellular Vesicles Produced by Human Neutrophilic Granulocytes. J Leukoc Biol *98*, 583-589. 10.1189/jlb.3VMA1014-514R.
47. Majumdar, R., Tavakoli Tameh, A., Arya, S.B., and Parent, C.A. (2021). Exosomes Mediate LTB4 Release During Neutrophil Chemotaxis. PLoS Biol *19*, e3001271. 10.1371/journal.pbio.3001271. PMC8262914

48. Makam, M., Diaz, D., Laval, J., Gernez, Y., Conrad, C.K., Dunn, C.E., Davies, Z.A., Moss, R.B., Herzenberg, L.A., Herzenberg, L.A.*, et al.* (2009). Activation of Critical, Host-Induced, Metabolic and Stress Pathways Marks Neutrophil Entry into Cystic Fibrosis Lungs. Proc Natl Acad Sci U S A *106*, 5779-5783. 10.1073/pnas.0813410106. PMC2667067
49. Margaroli, C., Garratt, L.W., Horati, H., Dittrich, A.S., Rosenow, T., Montgomery, S.T., Frey, D.L., Brown, M.R., Schultz, C., Guglani, L.*, et al.* (2019). Elastase Exocytosis by Airway Neutrophils Is Associated with Early Lung Damage in Children with Cystic Fibrosis. Am J Respir Crit Care Med *199*, 873-881. 10.1164/rccm.201803-0442OC. PMC6444666
50. Margaroli, C., Moncada-Giraldo, D., Gulick, D.A., Dobosh, B., Giacalone, V.D., Forrest, O.A., Sun, F., Gu, C., Gaggar, A., Kissick, H.*, et al.* (2021). Transcriptional Firing Represses Bactericidal Activity in Cystic Fibrosis Airway Neutrophils. Cell Rep Med *2*, 100239. 10.1016/j.xcrm.2021.100239. PMC8080108
51. Margaroli, C., and Tirouvanziam, R. (2016). Neutrophil Plasticity Enables the Development of Pathological Microenvironments: Implications for Cystic Fibrosis Airway Disease. Mol Cell Pediatr *3*, 38. 10.1186/s40348-016-0066-2. PMC5136534
52. Marki, A., Buscher, K., Lorenzini, C., Meyer, M., Saigusa, R., Fan, Z., Yeh, Y.T., Hartmann, N., Dan, J.M., Kiosses, W.B.*, et al.* (2021). Elongated Neutrophil-Derived Structures Are Blood-Borne Microparticles Formed by Rolling Neutrophils During Sepsis. J Exp Med *218*. 10.1084/jem.20200551. PMC7721910
53. Mathieu, M., Martin-Jaular, L., Lavieu, G., and Thery, C. (2019). Specificities of Secretion and Uptake of Exosomes and Other Extracellular Vesicles for Cell-to-Cell Communication. Nat Cell Biol *21*, 9-17. 10.1038/s41556-018-0250-9.
54. Middelhoven, P.J., Van Buul, J.D., Hordijk, P.L., and Roos, D. (2001). Different Proteolytic Mechanisms Involved in Fc Gamma Riiib Shedding from Human Neutrophils. Clin Exp Immunol *125*, 169-175. 10.1046/j.1365-2249.2001.01548.x. PMC1906091
55. Mitchell, T.C. (2018). A Grim Fate for Human Neutrophils in Airway Disease. J Leukoc Biol *104*, 657-659. 10.1002/JLB.5CE0418-162R. PMC7309533
56. Moreno-Yruela, C., Galleano, I., Madsen, A.S., and Olsen, C.A. (2018). Histone Deacetylase 11 Is an Epsilon-N-Myristoyllysine Hydrolase. Cell Chem Biol *25*, 849-856 e848. 10.1016/j.chembiol.2018.04.007.
57. Mu, X., Shen, Z., Lin, Y., Xiao, J., Xia, K., Xu, C., Chen, B., Shi, R., Zhu, A., Sun, X.*, et al.* (2022). Lncrna-Malat1 Regulates Cancer Glucose Metabolism in Prostate Cancer Via Mybl2/Mtor Axis. Oxid Med Cell Longev *2022*, 8693259. 10.1155/2022/8693259. PMC9086835 publication of this paper.
58. Mulcahy, L.A., Pink, R.C., and Carter, D.R. (2014). Routes and Mechanisms of Extracellular Vesicle Uptake. J Extracell Vesicles *3*, 24641. 10.3402/jev.v3.24641. PMC4122821
59. Neri, T., Celi, A., Tine, M., Bernardinello, N., Cosio, M.G., Saetta, M., Nieri, D., and Bazzan, E. (2022). The Emerging Role of Extracellular Vesicles Detected in Different Biological Fluids in Copd. Int J Mol Sci *23*. 10.3390/ijms23095136. PMC9101666
60. Nunez-Alvarez, Y., Hurtado, E., Munoz, M., Garcia-Tunon, I., Rech, G.E., Pluvinet, R., Sumoy, L., Pendas, A.M., Peinado, M.A., and Suelves, M. (2021). Loss of HDAC11 Accelerates Skeletal Muscle Regeneration in Mice. FEBS J *288*, 1201-1223. 10.1111/febs.15468.

61. O'Brien, K., Ughetto, S., Mahjoum, S., Nair, A.V., and Breakefield, X.O. (2022). Uptake, Functionality, and Re-Release of Extracellular Vesicle-Encapsulated Cargo. Cell Rep *39*, 110651. 10.1016/j.celrep.2022.110651.
62. Osika, E., Cavaillon, J.M., Chadelat, K., Boule, M., Fitting, C., Tournier, G., and Clement, A. (1999). Distinct Sputum Cytokine Profiles in Cystic Fibrosis and Other Chronic Inflammatory Airway Disease. Eur Respir J *14*, 339-346. 10.1034/j.1399-3003.1999.14b17.x.
63. Owen, C.A., Campbell, M.A., Sannes, P.L., Boukedes, S.S., and Campbell, E.J. (1995). Cell Surface-Bound Elastase and Cathepsin G on Human Neutrophils: A Novel, Non-Oxidative Mechanism by Which Neutrophils Focus and Preserve Catalytic Activity of Serine Proteinases. J Cell Biol *131*, 775-789. 10.1083/jcb.131.3.775. PMC2120617
64. Park, S.J., Kim, J.M., Kim, J., Hur, J., Park, S., Kim, K., Shin, H.J., and Chwae, Y.J. (2018). Molecular Mechanisms of Biogenesis of Apoptotic Exosome-Like Vesicles and Their Roles as Damage-Associated Molecular Patterns. Proc Natl Acad Sci U S A *115*, E11721-E11730. 10.1073/pnas.1811432115. PMC6294905
65. Perrem, L., and Ratjen, F. (2019). Anti-Inflammatories and Mucociliary Clearance Therapies in the Age of CFTR Modulators. Pediatric pulmonology *54 Suppl 3*, S46-S55. 10.1002/ppul.24364.
66. Pillay, J., den Braber, I., Vrisekoop, N., Kwast, L.M., de Boer, R.J., Borghans, J.A., Tesselaar, K., and Koenderman, L. (2010). In Vivo Labeling with 2h2o Reveals a Human Neutrophil Lifespan of 5.4 Days. Blood *116*, 625-627. 10.1182/blood-2010-01-259028.
67. Pitanga, T.N., de Aragao Franca, L., Rocha, V.C., Meirelles, T., Borges, V.M., Goncalves, M.S., Pontes-de-Carvalho, L.C., Noronha-Dutra, A.A., and dos-Santos, W.L. (2014). Neutrophil-Derived Microparticles Induce Myeloperoxidase-Mediated Damage of Vascular Endothelial Cells. BMC cell biology *15*, 21. 10.1186/1471-2121-15-21. PMC4059455
68. Pliyev, B.K., Kalintseva, M.V., Abdulaeva, S.V., Yarygin, K.N., and Savchenko, V.G. (2014). Neutrophil Microparticles Modulate Cytokine Production by Natural Killer Cells. Cytokine *65*, 126-129. 10.1016/j.cyto.2013.11.010.
69. Reusch, N., De Domenico, E., Bonaguro, L., Schulte-Schrepping, J., Bassler, K., Schultze, J.L., and Aschenbrenner, A.C. (2021). Neutrophils in COVID-19. Front Immunol *12*, 652470. 10.3389/fimmu.2021.652470. PMC8027077
70. Rhys, H.I., Dell'Accio, F., Pitzalis, C., Moore, A., Norling, L.V., and Perretti, M. (2018). Neutrophil Microvesicles from Healthy Control and Rheumatoid Arthritis Patients Prevent the Inflammatory Activation of Macrophages. EBioMedicine *29*, 60-69. 10.1016/j.ebiom.2018.02.003. PMC5925578
71. Rosales, C. (2018). Neutrophil: A Cell with Many Roles in Inflammation or Several Cell Types? Front Physiol *9*, 113. 10.3389/fphys.2018.00113. PMC5826082
72. Rutter, W.C., Burgess, D.R., and Burgess, D.S. (2017). Increasing Incidence of Multidrug Resistance among Cystic Fibrosis Respiratory Bacterial Isolates. Microb Drug Resist *23*, 51-55. 10.1089/mdr.2016.0048.
73. Sahakian, E., Chen, J., Powers, J.J., Chen, X., Maharaj, K., Deng, S.L., Achille, A.N., Lienlaf, M., Wang, H.W., Cheng, F.*, et al.* (2017). Essential Role for Histone Deacetylase 11 (HDAC11) in Neutrophil Biology. J Leukoc Biol *102*, 475-486. 10.1189/jlb.1A0415-176RRR. PMC6608079

74. Saluzzo, F., Riberi, L., Messore, B., Lore, N.I., Esposito, I., Bignamini, E., and De Rose, V. (2022). CFTR Modulator Therapies: Potential Impact on Airway Infections in Cystic Fibrosis. Cells *11*. 10.3390/cells11071243. PMC8998122
75. Sanders, D.B., Bittner, R.C., Rosenfeld, M., Hoffman, L.R., Redding, G.J., and Goss, C.H. (2010). Failure to Recover to Baseline Pulmonary Function after Cystic Fibrosis Pulmonary Exacerbation. Am J Respir Crit Care Med *182*, 627-632. 10.1164/rccm.200909-1421OC. PMC5450763
76. Shyu, K.G., Wang, B.W., Fang, W.J., Pan, C.M., and Lin, C.M. (2022). Exosomal Malat1 Derived from High Glucose-Treated Macrophages up-Regulates Resistin Expression Via miR-150-5p Downregulation. Int J Mol Sci *23*. 10.3390/ijms23031095. PMC8834900
77. Slater, T.W., Finkielsztein, A., Mascarenhas, L.A., Mehl, L.C., Butin-Israeli, V., and Sumagin, R. (2017). Neutrophil Microparticles Deliver Active Myeloperoxidase to Injured Mucosa to Inhibit Epithelial Wound Healing. J Immunol *198*, 2886-2897. 10.4049/jimmunol.1601810. PMC5360559
78. Somiya, M., and Kuroda, S.i. (2021). Reporter Gene Assay for Membrane Fusion of Extracellular Vesicles. Journal of Extracellular Vesicles *10*, e12171. https://doi.org/10.1002/jev2.12171.
79. Son, S.I., Cao, J., Zhu, C.L., Miller, S.P., and Lin, H. (2019). Activity-Guided Design of HDAC11-Specific Inhibitors. ACS Chem Biol *14*, 1393-1397. 10.1021/acschembio.9b00292. PMC6893910
80. Sumagin, R. (2021). Emerging Neutrophil Plasticity: Terminally Differentiated Cells No More. J Leukoc Biol *109*, 473-475. 10.1002/JLB.1CE0720-378R. PMC7906924
81. Takao, M., Nagai, Y., Ito, M., and Ohba, T. (2018). Flow Cytometric Quantitation of Epcam-Positive Extracellular Vesicles by Immunomagnetic Separation and Phospholipid Staining Method. Genes Cells *23*, 963-973. 10.1111/gtc.12645.
82. Thery, C., Witwer, K.W., Aikawa, E., Alcaraz, M.J., Anderson, J.D., Andriantsitohaina, R., Antoniou, A., Arab, T., Archer, F., Atkin-Smith, G.K.*, et al.* (2018). Minimal Information for Studies of Extracellular Vesicles 2018 (MISEV2018): A Position Statement of the International Society for Extracellular Vesicles and Update of the MISEV2014 Guidelines. J Extracell Vesicles *7*, 1535750. 10.1080/20013078.2018.1535750. PMC6322352
83. Timar, C.I., Lorincz, A.M., Csepanyi-Komi, R., Valyi-Nagy, A., Nagy, G., Buzas, E.I., Ivanyi, Z., Kittel, A., Powell, D.W., McLeish, K.R.*, et al.* (2013). Antibacterial Effect of Microvesicles Released from Human Neutrophilic Granulocytes. Blood *121*, 510-518. 10.1182/blood-2012-05-431114. PMC3548170
84. Tirouvanziam, R., Gernez, Y., Conrad, C.K., Moss, R.B., Schrijver, I., Dunn, C.E., Davies, Z.A., Herzenberg, L.A., and Herzenberg, L.A. (2008). Profound Functional and Signaling Changes in Viable Inflammatory Neutrophils Homing to Cystic Fibrosis Airways. Proc Natl Acad Sci U S A *105*, 4335-4339. 10.1073/pnas.0712386105. PMC2393742
85. Todkar, K., Chikhi, L., Desjardins, V., El-Mortada, F., Pepin, G., and Germain, M. (2021). Selective Packaging of Mitochondrial Proteins into Extracellular Vesicles Prevents the Release of Mitochondrial Damps. Nat Commun *12*, 1971. 10.1038/s41467-021-21984-w. PMC8009912
86. Villagra, A., Cheng, F., Wang, H.W., Suarez, I., Glozak, M., Maurin, M., Nguyen, D., Wright, K.L., Atadja, P.W., Bhalla, K.*, et al.* (2009). The Histone Deacetylase HDAC11 Regulates

the Expression of Interleukin 10 and Immune Tolerance. Nat Immunol *10*, 92-100. 10.1038/ni.1673. PMC3925685
87. Wagner, T.E., Becraft, J.R., Bodner, K., Teague, B., Zhang, X., Woo, A., Porter, E., Alburquerque, B., Dobosh, B., Andries, O*., et al.* (2018). Small-Molecule-Based Regulation of RNA-Delivered Circuits in Mammalian Cells. Nat Chem Biol *14*, 1043-1050. 10.1038/s41589-018-0146-9.
88. Winterbourn, C.C., Kettle, A.J., and Hampton, M.B. (2016). Reactive Oxygen Species and Neutrophil Function. Annu Rev Biochem *85*, 765-792. 10.1146/annurev-biochem-060815-014442.
89. Xin, L., Vargas-Inchaustegui, D.A., Raimer, S.S., Kelly, B.C., Hu, J., Zhu, L., Sun, J., and Soong, L. (2010). Type I Ifn Receptor Regulates Neutrophil Functions and Innate Immunity to Leishmania Parasites. J Immunol *184*, 7047-7056. 10.4049/jimmunol.0903273. PMC4159077
90. Yanez-Mo, M., Siljander, P.R., Andreu, Z., Zavec, A.B., Borras, F.E., Buzas, E.I., Buzas, K., Casal, E., Cappello, F., Carvalho, J*., et al.* (2015). Biological Properties of Extracellular Vesicles and Their Physiological Functions. J Extracell Vesicles *4*, 27066. 10.3402/jev.v4.27066. PMC4433489
91. Yonker, L.M., Cigana, C., Hurley, B.P., and Bragonzi, A. (2015). Host-Pathogen Interplay in the Respiratory Environment of Cystic Fibrosis. J Cyst Fibros *14*, 431-439. 10.1016/j.jcf.2015.02.008. PMC4485938
92. Zaher, A., ElSaygh, J., Elsori, D., ElSaygh, H., and Sanni, A. (2021). A Review of Trikafta: Triple Cystic Fibrosis Transmembrane Conductance Regulator (CFTR) Modulator Therapy. Cureus *13*, e16144. 10.7759/cureus.16144. PMC8266292
93. Zhang, Y., Huang, M., Jiang, L., Li, T., Wang, J., Zhao, L., and Zhou, J. (2022). Autophagy Inhibitors Enhance Biomolecular Delivery Efficiency of Extracellular Vesicles. Biochem Biophys Res Commun *603*, 130-137. 10.1016/j.bbrc.2022.03.006.
94. Zhou, Q., Liu, L., Zhou, J., Chen, Y., Xie, D., Yao, Y., and Cui, D. (2021). Novel Insights into Malat1 Function as a Microrna Sponge in Nsclc. Front Oncol *11*, 758653. 10.3389/fonc.2021.758653. PMC8578859

This chapter has been published in Cell Reports (Dobosh et al., 2022)

Chapter 5: BARICITINIB ATTENUATES THE PROINFLAMMATORY PHASE OF COVID-19 DRIVEN BY LUNG-INFILTRATING MONOCYTES

ABSTRACT

SARS-CoV-2-infected subjects are generally asymptomatic during initial viral replication, but may suffer severe immunopathology after the virus has receded and monocytes have infiltrated the airways. In bronchoalveolar lavage fluid from severe COVID-19 patients, monocytes express mRNA encoding inflammatory mediators and contain SARS-CoV-2 transcripts. We leverage a human small airway model of infection and inflammation whereby primary blood monocytes transmigrate across SARS-CoV-2-infected lung epithelium to characterize viral burden, gene expression and inflammatory mediator secretion by epithelial cells and monocytes. In this model, lung-infiltrating monocytes acquire SARS-CoV-2 from the epithelium and upregulate expression and secretion of inflammatory mediators, mirroring *in vivo* data. Combined use of baricitinib (Janus kinase inhibitor) and remdesivir (nucleoside analog) enhances antiviral signaling and viral clearance by SARS-CoV-2-positive monocytes while decreasing secretion of pro-neutrophilic mediators associated with acute respiratory distress syndrome. These findings highlight the role of lung-infiltrating monocytes in COVID-19 pathogenesis and their importance as a therapeutic target.

INTRODUCTION

Coronavirus disease of 2019 (COVID-19) continues to be a rapidly evolving pandemic caused by the lung-tropic Severe Acute Respiratory Syndrome Coronavirus-2 (SARS-CoV-2) (Weston and Frieman, 2020). COVID-19 symptoms range from asymptomatic to mild to severe, and the course of lung disease can be broadly categorized into three phases (Blanco-Melo et al., 2020). In the first phase of "immune avoidance", the virus infects epithelial cells and replicates rapidly for about 3-6 days while avoiding activation of canonical antiviral responses like type I interferon (IFN) (Acharya et al., 2020; Tay et al., 2020). Respiratory symptoms occur in those patients that may progress to a second phase of "cytokine release syndrome" (CRS) involving the infiltration of blood monocytes into the lung (Henderson et al., 2020; Merad and Martin, 2020), during which the viral titers decline. Eventually, in the second week post-infection, some patients will enter into a third, life-threatening, phase of acute respiratory distress syndrome (ARDS), featuring high levels of CXCL8[4], IL-1β and other pro-inflammatory mediators resulting in neutrophil recruitment (Coperchini et al., 2020; Tang et al., 2020). Considering the distinct phases of COVID-19 (Gordon et al., 2020), antiviral drugs like remdesivir may be particularly effective if given early (epithelial and monocytic stages), while immunomodulators such as dexamethasone and the JAK1/2 inhibitor baricitinib may be impactful later (monocytic and neutrophilic stages) (Beigel et al., 2020; Kalil et al., 2021; Perez-Alba et al., 2021).

Severe cases of COVID-19 have a dysfunctional immune response largely reflected by the CRS and decreases in most immune cells in the systemic compartment including T, B, and NK cells (Tan et al., 2020) as well as monocytes, eosinophils, and basophils (Qin et al., 2020).

[4] CXCL8 is referred to as IL-8 outside of this chapter.

Meanwhile, neutrophil counts and the neutrophil-to-lymphocyte ratio are elevated in the blood of patients with severe COVID-19 (Qin et al., 2020; Zhang et al., 2020). It is not yet known what underlying circumstances cause such changes in some patients, but not others. As a result, the timing of therapeutics, in particular host-directed treatment targeting the immune system, needs to be paid close attention to in relation to the course of disease to avoid suppressing antiviral responses in early stages or promoting further damage in late stages. Understanding mechanistic effects of antiviral and immunomodulatory drugs during the course of COVID-19 requires models that can recapitulate the complex interactions between SARS-CoV-2, host epithelial cells and lung-infiltrating leukocytes (Mason, 2020). To this end, we adapted a small airway model of infection and inflammation (Dobosh et al., 2021) previously developed and validated by our group to study lung-infiltrating leukocytes in cystic fibrosis (CF) and ARDS (Forrest et al., 2018; Grunwell et al., 2019). This model features a human lung epithelium (HLE) monolayer differentiated at air-liquid interface (ALI) that enables luminal infection with SARS-CoV-2 and subsequent infiltration by primary human leukocytes.

Mimicking the early, epithelium-restricted, stage of SARS-CoV-2 infection in humans (Ravindra et al., 2021), HLE-ALI cells infected with SARS-CoV-2 *in vitro* did not upregulate canonical antiviral pathways nor express inflammatory cytokines. Next, we observed by reanalysis of a previously published dataset of single cell RNA-seq of bronchoalveolar lavage fluid (BALF) from patients with severe COVID-19 (Liao et al., 2020) that lung-infiltrating monocytes express *CXCL8* and *IL-1β* and contain transcripts from SARS-CoV-2; both features were recapitulated by lung-infiltrating monocytes *in vitro*. CXCL8 and IL-1β are critical to the development of ARDS via recruitment and activation of neutrophils (Donnelly et al., 1993; Zhou

et al., 2020). We next leveraged this model to investigate the effects on HLE-ALI cells and lung-infiltrating monocytes of remdesivir and baricitinib, two drugs which have been granted emergency use authorization by the U.S. Food and Drug Administration as single and combined therapies. While remdesivir blocked progression of viral replication in both cell types, baricitinib selectively enhanced the expression of antiviral genes in lung-infiltrating monocytes. Both drugs used alone or in combination enhanced viral clearance in monocytes. Taken together, our findings confirm that lung-infiltrating monocytes are a critical target for COVID-19 treatment.

RESULTS

Antiviral signaling in human lung epithelium differentiated at air liquid interface is blocked by SARS-CoV-2 and is not rescued by baricitinib and/or remdesivir.

Critical aspects of virus-host interactions in the lung are species-specific, which makes models of the human lung particularly relevant for mechanistic investigations. Here, we differentiated a human lung epithelium for two weeks at ALI on a scaffold enabling *en masse* transmigration of leukocytes to simultaneously investigate the dynamics of luminal infection by viruses and leukocyte infiltration following epithelial infection **(Figure 5.1A)**. SARS-CoV-2-infected HLE-ALI cells showed minimal amounts of extracellular ATP compared to OC43- and IAV-infected cells up to 48 hours post-infection at an MOI of 0.1 **(Figure 5.1B)**. This suggests that the 48-hour timepoint and MOI may be appropriate conditions to study SARS-CoV-2 infection in the absence of substantial epithelial cell toxicity. Next, we conducted a multiplexed qRT-PCR assay of infected HLE-ALI cells at different input concentrations of virus over 72 hours of infection and observed that HLE-ALI cells infected with SARS-CoV-2 and OC43 downregulated antiviral genes in contrast to IAV-infected cells **(Figure 5.1C)**. For example, core interferon pathway genes *IFNA1, IFNLR1, IFNL1, IFNG, IFNB1*, and to a lesser extent *IFNAR1* were all lowered in cells infected with coronaviruses, while the same genes were dramatically increased in IAV-infected cells. Similarly, expression of inflammatory mediators such as *IL1*α, *IL-1*β, and *CXCL8* were consistently downregulated in SARS-CoV-2-infected cells although *IL1*α expression was observed in HLE-ALI cells infected with OC43. Of note, a subset of allergy-associated genes such as *IL4, IL13, IL4R*, *IL13RA1,* and the common γ-chain *IL2RG*, were upregulated in most of the SARS-CoV-2 infection conditions. Also of interest, infection with SARS-CoV-2 at an MOI = 1

showed upregulation of *ACE2* throughout the course of infection, suggesting that the virus may be able to enhance its own infection efficiency.

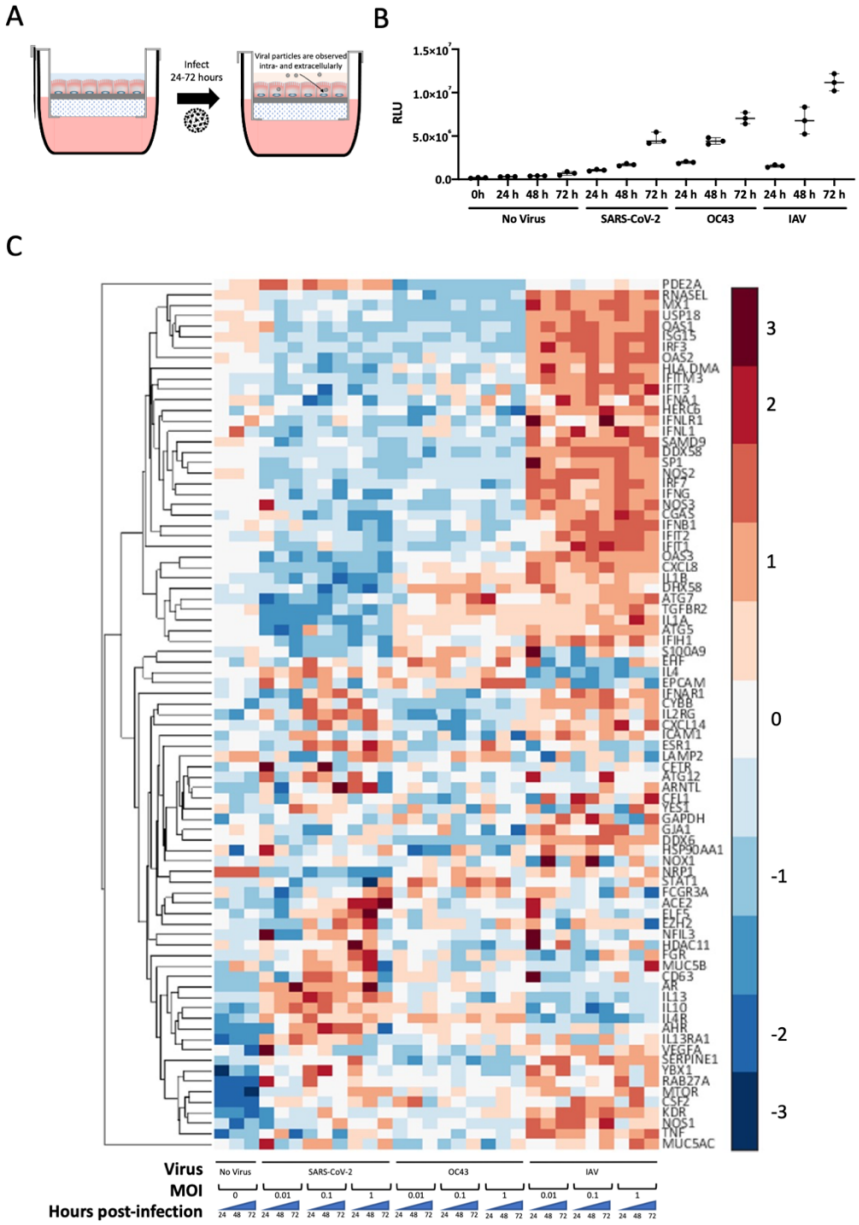

Figure 5.1. [HLE-ALI cells grown at air-liquid interface can be infected by OC43, SARS-CoV-2 and Influenza and exhibit different transcriptional responses.] (A) Experimental scheme illustrating the infection of human lung epithelium (HLE) differentiated at air-liquid interface (ALI) with Influenza A strain A/PR8/1934 (IAV), beta coronaviruses OC43 or SARS-CoV-2, Isolate USA-WA1/2020 for 24-72 hrs. (B) Extracellular ATP generated by HLE-ALI cells infected with IAV, OC43 or SARS-CoV-2 at an MOI of 0.1 for 24-72 hrs was measured using a luciferase assay. Plotted is the median with interquartile range. No statistics were calculated due to low sample number. (C) Multiplexed qRT-PCR of HLE-ALI cells infected with either no virus or Influenza A strain A/PR8/1934, beta coronaviruses OC43 or SARS-CoV-2, Isolated USA-WA1/2020 for 24-72 hrs at MOIs of either 0.01, 0.1, or 1. Data was normalized using the delta delta Ct method relative to GAPDH and the no virus condition at time 0, and then z-score normalized. Values shown are the average of biological triplicates.

In order to better understand the global changes in the infected HLE-ALI cells we then sequenced their entire transcriptome. As before, infection with influenza strain A/PR8/1934 (IAV; MOI 0.1) induced canonical antiviral signaling in HLE-ALI cells, most notably IFITM1/2/3, ISG15, and OAS1/2/3, while infection with betacoronaviruses (MOI 0.1) OC43 and SARS-CoV-2, Isolate USA-WA1/2020 did not (Figure 5.2A, Supplementary Table 5.1). Across all infections, 50 Gene Ontology (GO) terms were significantly enriched (Supplementary Table 5.2). Most genes enriched in HLE-ALI cells infected with IAV related to the immune response, particularly the response to virus and immune effector processes. In contrast, the enrichment profiles of HLE-ALI cells infected with OC43 and SARS-CoV-2 related to cellular processes such as localization, transport and metabolism (Figure 5.2B). Many of the antiviral genes upregulated in IAV-infected HLE-ALI cells were not upregulated in OC43 and SARS-CoV-2 infections (Figure 5.2C). Additionally, the genes associated with cellular processes in SARS-CoV-2-infected cells were similarly downregulated or remained unchanged in IAV-infected cells **(Figure 5.2C, Supplementary Table 5.2, row 9)**.

Further analysis of the RNA-seq dataset revealed that at 48 hr post-infection with SARS-CoV-2 at an MOI = 0.1, HLE-ALI cells had the greatest number of uniquely differentially expressed genes (DEGs) compared to the uninfected time = 0 control (**Supplementary Figure 5.1)**. At both 24- and 48-hr post-infection these DEGs showed dramatic changes in pathways associated with metabolic processes showing that the HLE-ALI cells were affected by infection with SARS-CoV-2 despite the avoidance of canonical anti-viral signaling **(Supplementary Figure 5.1B, Supplementary Table 5.3)**.

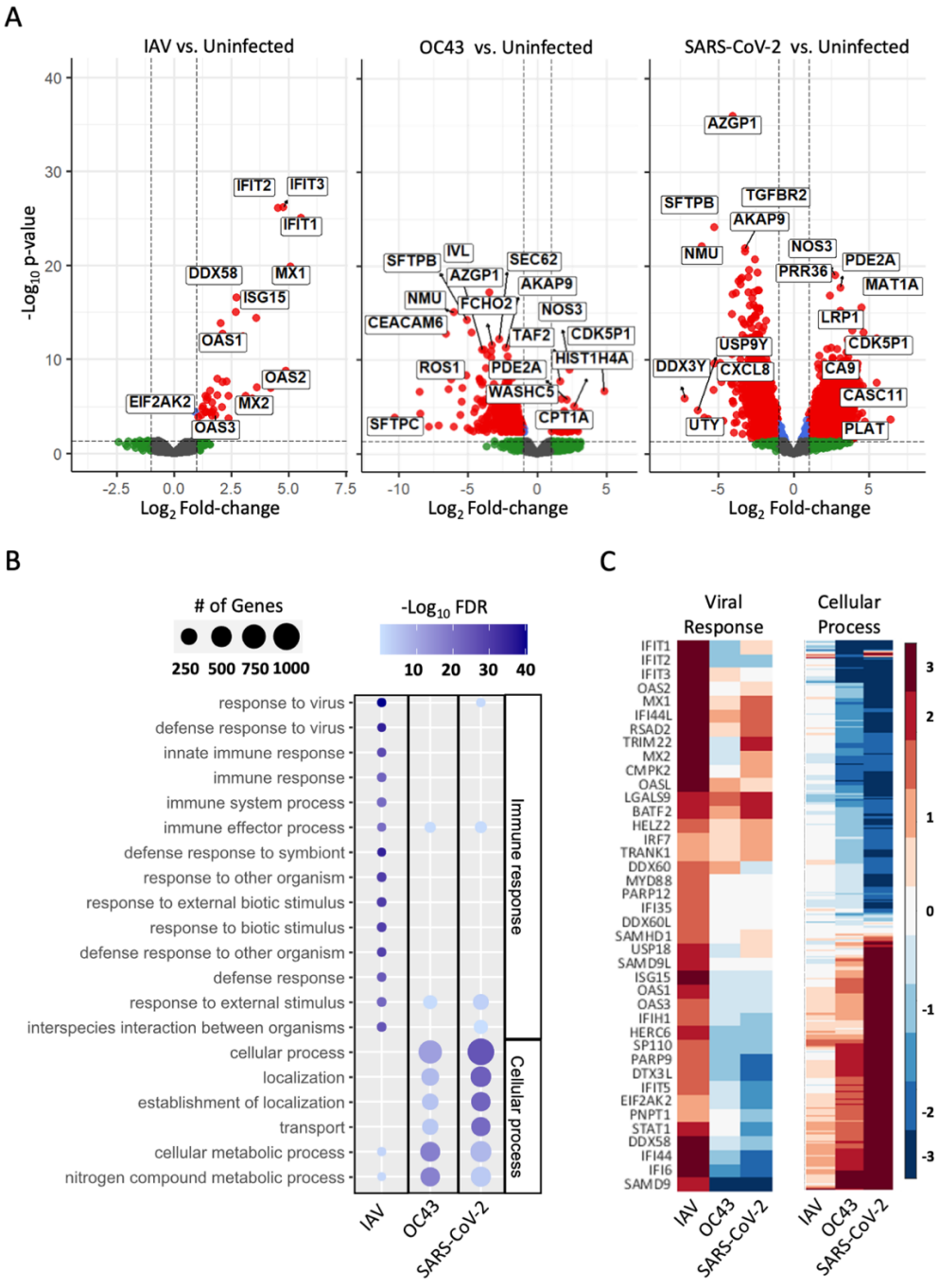

Figure 5.2: [SARS-CoV-2 prevents induction of an antiviral response in differentiated human lung epithelium.] Human lung epithelium (HLE) differentiated at air-liquid interface (ALI) were infected at an MOI of 0.1 with Influenza A strain A/PR8/1934 (IAV), beta coronaviruses OC43 or SARS-CoV-2, Isolate USA-WA1/2020 for 48 hr from which total RNA was extracted and library prepared following the protocol of the TruSeq RNA Sample Preparation kit. (A) Volcano plots of differentially expressed genes in HLE-ALI cells infected with Influenza A strain A/PR8/1934 or the betacoronaviruses compared to uninfected cells. (B) Gene ontology enrichment profiles of the differentially expressed genes (DEGs) in HLE-ALI cells infected with IAV, OC43, or SARS-CoV-2. Gene names associated with each GO term are in Supplementary Table 5.2. (C) Heatmaps of targeted analysis of genes associated with the viral response or cellular process pathways. Gene names associated with the cellular process terms are in Supplementary Table 5.2, row 9, and raw expression values are in Supplementary Table 5.1.

Following SARS-CoV-2 infection of the lung epithelium, subjects may remain asymptomatic or progress toward COVID-19. *In vivo* studies suggest that the pivotal response distinguishing asymptomatic from symptomatic subjects is the induction of a proinflammatory phase driven by lung-infiltrating monocytes (Falasca et al., 2020; Li et al., 2021). To investigate this key process in our model, we applied primary human blood monocytes to the basolateral side of SARS-CoV-2 infected HLE-ALI cells and allowed them to transmigrate across. To mimic *in vivo* conditions, the epithelial phase of infection was allowed to proceed for 48 hr without any drug treatment, while the monocytic phase was studied for another 24 hr in vehicle control (no drug condition) or in the presence of baricitinib (1 μM) and/or remdesivir (1 μM) **(Figure 5.3A)**. The chemoattractants, CCL2 (250 pg/mL) and LTB4 (100 nM), were used in all conditions.

To understand the impact of monocyte transmigration on the epithelium, we identified DEGs in HLE-ALI cells pre- vs. post-transmigration. From these DEGs, we listed the top-10 GO enrichment profiles **(Supplementary Figure 5.2, Supplementary Table 5.4)**. Following transmigration by monocytes, HLE-ALI cells showed an enrichment in genes related to the regulation of cell communication, signaling and multicellular organismal processes, which was abrogated when HLE-ALI cells had been infected by SARS-CoV-2 prior to monocyte transmigration **(Supplementary Figure 5.2)**. Moreover, in the absence of SARS-CoV-2, transmigration of monocytes showed much fewer DEGs in the HLE-ALI cells **(Supplementary Figure 5.3A)** than when monocyte transmigration occurred in the presence of virus **(Supplementary Figure 5.1A)**. Approximately 55% of the upregulated DEGs were shared in all conditions, suggesting that these genes are commonly expressed by HLE-ALI cells during the

course of transmigration. Furthermore, most of the uniquely downregulated genes were observed in the no drug condition, suggesting that remdesivir and baricitinib have minimal effects on HLE-ALI cells unless they are infected by SARS-CoV-2 **(Supplementary Figure 5.3A)**. Many of the GO terms observed were related to changes in cellular morphology and metabolic remodeling (**Supplementary Figure 5.3B, Supplementary Table 5.5)**. Similarly, about 59% of the upregulated DEGs and 34% of the downregulated genes were shared by all conditions **(Supplementary Figure 5.4A),** and many of the same metabolic process GO terms were observed. Notably however, the no drug condition showed an enrichment of GO terms associated with MHC class II antigen presentation **(Supplementary Figure 5.4B, Supplementary Table 5.6)**.

Moreover, in concordance with the biological processes identified in SARS-CoV-2-infected HLE-ALI cells pre-transmigration by monocytes **(Figure 5.2B)**, SARS-CoV-2-infected HLE-ALI cells post-transmigration still failed to induce genes included under the response to virus or immune system processes GO terms **(Supplementary Figure 5.5)**. Taken together, these findings suggest that during early SARS-CoV-2 infection, epithelial antiviral responses are delayed or blocked while favoring cellular and metabolic processes and regulation of communication. Remdesivir treatment did not induce an enrichment of these pathways when SARS-CoV-2 was present. Baricitinib treatment, however, promoted an enrichment in GO terms related to the regulation of cell communication and signaling in the SARS-CoV-2-infected epithelium post-transmigration, suggesting that this drug can affect epithelial signaling **(Supplementary Figure 5.2, Supplementary Figure 5.4)**.

After transmigration across SARS-CoV-2 infected HLE-ALI cells, human monocytes induce proinflammatory signaling, which is attenuated by baricitinib treatment.

To investigate the expression profile of lung-infiltrating monocytes during SARS-CoV-2 infection (compared to uninfected conditions), a set of 67 genes was measured by multiplexed qRT-PCR and grouped by unsupervised clustering **(Figure 5.3B)**. Nucleic acid signaling sensor (*CGAS* and *STING1*, *DDX58*, *OAS1/2/3*), kinase (*TBK1*), effector (*RNAse L*), and transcription factor (*IRF3*, *IRF7*) genes as well as critical neutrophil chemoattractant genes such as *CXCL8* and *IL-1*β were upregulated in monocytes recruited across SARS-CoV-2-infected HLE-ALI cells. The same set of genes were extracted from the RNA-seq dataset of the HLE-ALI cells pre- and post-transmigration. Although the post-transmigration HLE-ALI cells did not show global enrichment of antiviral pathways by analysis of GO terms compared to the pre-transmigration control, specific antiviral genes such as *DDX58* and *OAS1/2/3* and the pro-neutrophilic chemokine *CXCL8* were also upregulated **(Supplementary Figure 5.5)**. This response was not affected by treatment with baricitinib and/or remdesivir.

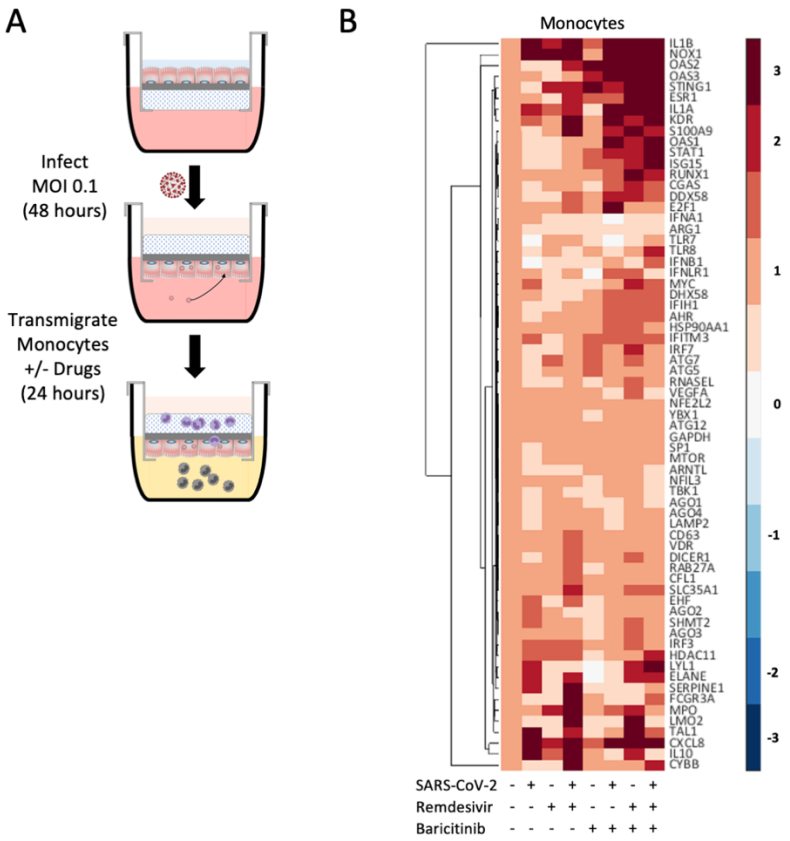

Figure 5.3. [Lung-recruited primary human monocytes induce proinflammatory signaling after transmigration across a SARS-CoV-2 infected epithelium.] (A) Schematic diagram of the monocyte transmigration process: HLE-ALI cells were differentiated at ALI for two weeks, infected with SARS-CoV-2 at an MOI of 0.1 for 48 hr, after which 10^6 monocytes were transmigrated across the infected epithelium towards LTB4 (100 nM) and CCL2 (250 pg/mL) for 24 hr, in the absence or presence of remdesivir (1 µM) and/or baricitinib (1 µM). All conditions contained 0.1% v/v DMSO. (B) Heatmaps of selected genes from each treatment condition. Monocyte mRNA was analyzed by multiplexed qRT-PCR and first normalized to GAPDH using the delta delta Ct method, then z-score normalized.

Computational analysis of a publicly available single-cell RNASeq (scRNA-seq) dataset from the bronchoalveolar lavage fluid (BALF) of COVID-19 patients hospitalized with COVID-19 (Liao et al., 2020) confirmed that lung-infiltrating monocytes (differentiated from macrophages by exclusion of the macrophage gene *MARCO*) displayed elevated *CXCL8* and *IL-1β* in patients with severe rather than mild disease **(Figure 5.4A, Supplementary Figure 5.6)**. To our knowledge this is the only dataset that has obtained scRNA-seq from BALF of hospitalized

patients spanning mild and severe COVID-19, pre-remdesivir. Another study, which analyzed BALF from patients with severe COVID-19 found that there was expression of numerous inflammatory cytokines in BALF cells from a variety of cell types, particularly neutrophils (Bost et al., 2021). However, that study was conducted later during the course of the COVID-19 pandemic and did not report on BALF from relatively milder COVID-19.

Epithelial cells recovered in BALF of severe COVID-19 patients upregulated cell-death-associated pathways and downregulated genes associated with antigen presentation, both of which may promote inflammation by innate immune cells **(Figure 5.4B, Supplementary Table 5.7)**. In addition to *CXCL8* mentioned above, infiltrated monocytes present in the BALF of severe COVID-19 patients upregulated many chemokines, such as *CCL4, CCL7, CCL4L2, CCL3, CXCL2, CXCL3,* and *CCL2*, most of which are potent monocyte and macrophage chemoattractants and actually downregulated pathways associated with antigen presentation, similar to the epithelial cells **(Figure 5.4B, Supplementary Table 5.8).** In addition, patients with severe disease showed a greater number of neutrophils in BALF compared to those with mild COVID-19, in whom monocytes and T-cells were more abundant. These responses are consistent with those observed in lung-infiltrating monocytes produced *in vitro* **(Figure 5.3B)**.

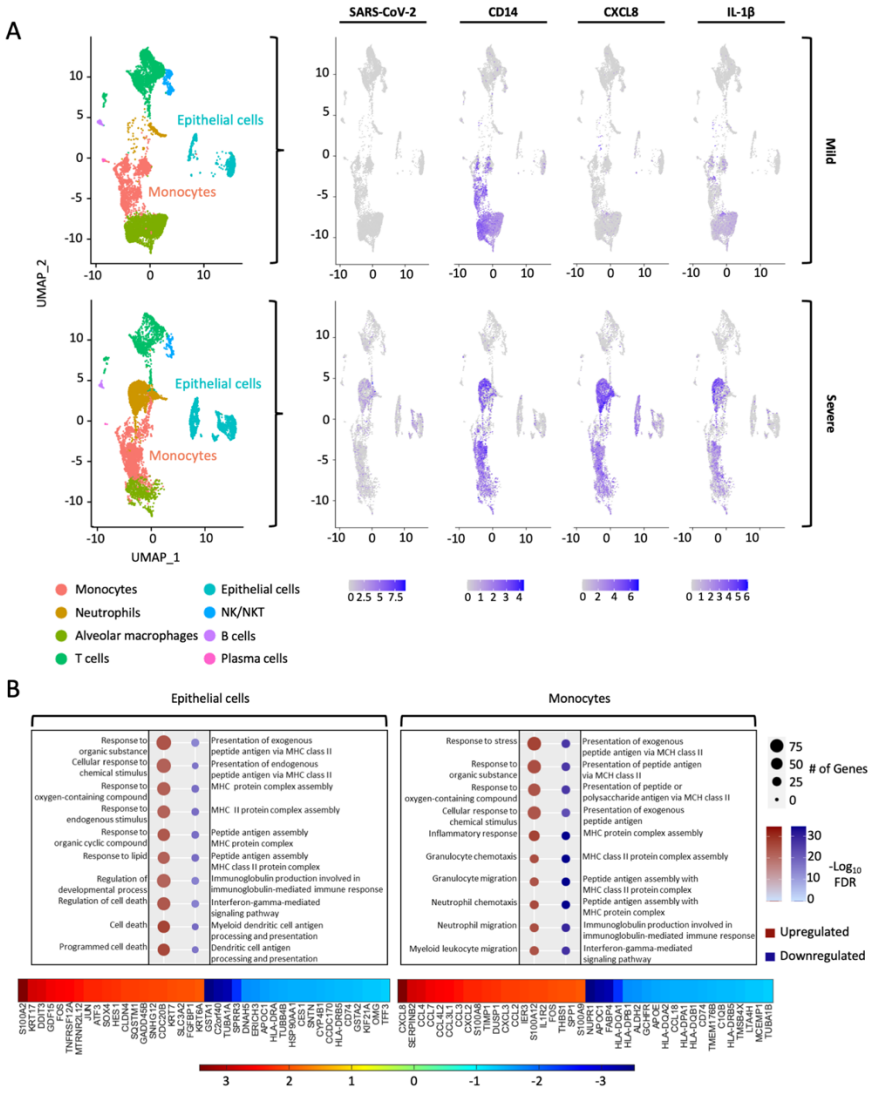

Figure 5.4. [Single-cell RNA-seq of BALF from patients hospitalized with mild or severe COVID-19 shows that monocytes harbor SARS-CoV-2 genomes and express CXCL8 and IL-1β among other chemokines.] (A) Combined UMAP plots of scRNASeq from n=3 mild patients and n=3 severe patients. Seurat was used to normalize gene barcodes and generate UMAP clustering plots. Expression values for SARS-CoV-2, CD14, CXCL8, and IL-1β were overlaid onto the UMAP plot. (B) DEGs in cells identified as epithelial cells or monocytes between the severe and mild patient groups were investigated. Enriched pathways for each cell type were plotted based on whether they were up- or down-regulated (severe vs. mild). The top 20 up- and down-regulated genes were listed for both cell types and plotted as a heatmap.

Next, we sought to confirm that changes in the expression of immune mediator genes was reflected in protein levels present in the apical aspect of our small airway model. Monocyte transmigration following SARS-CoV-2 infection of the epithelium led to increased extracellular levels of CRS-associated mediators such as CXCL8, IL-1β, IL-10, GM-CSF, IL-1α, IL-6, G-CSF, TNF-α, VEGFA and IFN-γ in the fluid compared to conditions where monocyte transmigration was conducted in the absence of virus **(Figure 5.5A**). While remdesivir treatment did not alter mediator levels, baricitinib treatment alone and in combination with remdesivir decreased extracellular IL-10 levels. This coincided with a decrease in *IL-10* transcripts in lung-infiltrating monocytes, but not epithelial cells **(Figure 5.3B, Supplementary Figure 5.5)**. Baricitinib treatment also increased extracellular CXCL8 levels, while its combination with remdesivir decreased IL-1α, IL-1β, IL-6, TNF-α, VEGFA, and IFN-γ levels **(Figure 5.5A)**.

Treatment with baricitinib and remdesivir decreases total viral burden in lung-infiltrating monocytes, which acquire SARS-CoV-2 from infected epithelium.

Importantly, the JAK1/2 pathway can promote leukocyte recruitment in the lung, and in our model treatment with the JAK1/2 inhibitor baricitinib decreased the number of lung-infiltrating monocytes **(Figure 5.5B),** which we determined by a qPCR-based DNA quantitation method **(Supplementary Figure 5.7A)**. As expected, remdesivir treatment decreased the viral burden in the HLE-ALI cells **(Figure 5.5C)** as measured by qRT-PCR **(Supplementary Figure 5.7B, Supplementary Figure 5.7C)**, despite the 48 hours afforded to the virus to infect epithelial cells prior to treatment.

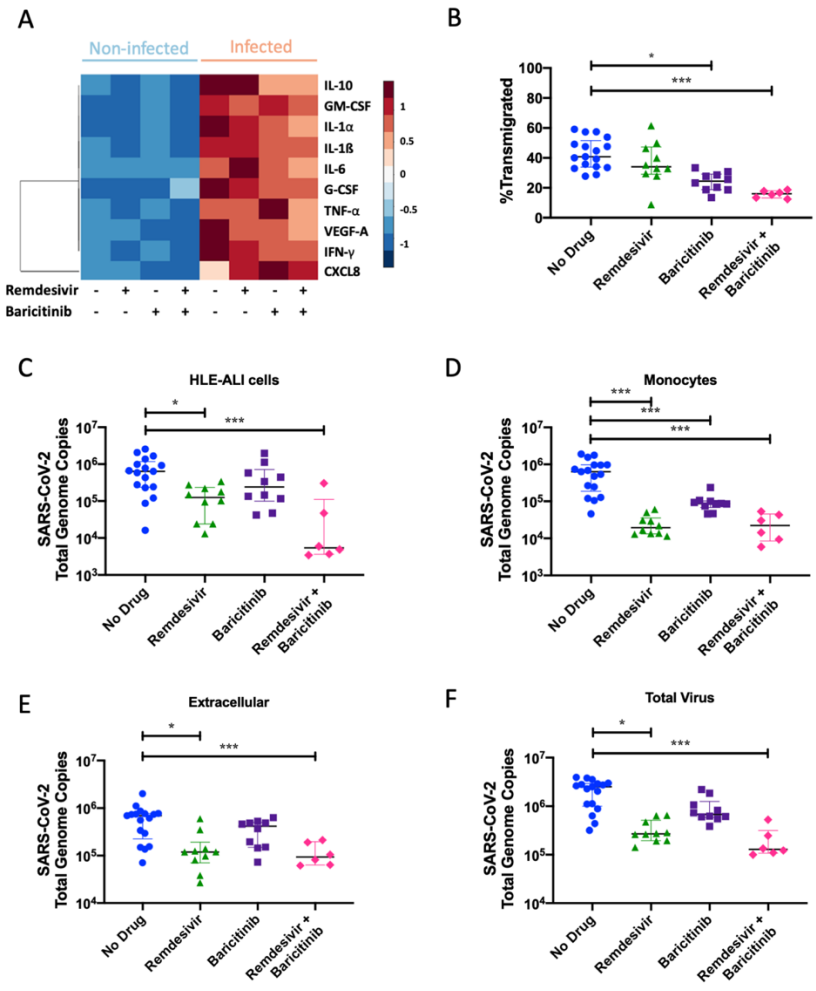

Figure 5.5. *[Lung-infiltrating monocytes release inflammatory mediators and harbor replicative SARS-CoV-2.] **(A)** Inflammatory mediators in the apical fluid following transmigration were quantified by a multiplexed electrochemiluminescent assay. The z-score for each mediator in each condition was calculated and plotted. **(B)** Transmigration efficiency of monocytes was calculated by dividing the number of monocytes in the apical fluid after 24 hours by the input number of cells. **(C-E)** RNA was extracted from each component of the model (epithelium, lung-infiltrating monocytes, extracellular fluid) and reverse transcribed. Total SARS-CoV-2 genome copies were calculated. **(F)** The sum of each of the components of the model was calculated to depict the total amount of virus remaining in the system after monocytes were allowed to transmigrate for 24 hr. All statistics were calculated using the Mann-Whitney U-test in Prism between the "No Drug" and Treatment group. * p<0.05, ** p<0.01, ***p<0.001. Shown is the median with the interquartile range.*

Our re-analysis of publicly available scRNASeq data from lung-infiltrating monocytes in the BALF of patients with severe COVID-19 revealed that some of them harbored SARS-CoV-2 transcripts **(Figure 5.4A)**. In severe COVID-19 patients included in another BALF study, infiltrating monocytes also contained SARS-CoV-2, although the vast majority of viral transcripts

were found in the neutrophil compartment (Bost et al., 2021). Similarly, lung-infiltrating monocytes in our model, which were not directly infected but rather were made to cross an infected epithelium, also contained SARS-CoV-2 genome copies as determined by qRT-PCR **(Figure 5.5D, Supplementary Figure 5.7D).** The total viral burden in lung-infiltrating monocytes was decreased in all treatment conditions, with the greatest effect being contributed by remdesivir. Absolute quantification of SARS-CoV-2 in both epithelial and monocytic compartments showed similar results as relative quantification of SARS-CoV-2 to *GAPDH* and *18S rRNA* transcripts (**Supplementary Figure 5.8A-D)**. SARS-CoV-2 genome copies were also detectable in the extracellular fluid, and were decreased by treatment with remdesivir alone and combined with baricitinib **(Figure 5.5E)**. Altogether, remdesivir decreased total virus in all compartments of the transmigration model, while baricitinib did not have a noticeable effect despite lowering the number of genome copies in the recruited monocytes **(Figure 5.5F)**.

In the 72 hours during which the virus was applied to the HLE-ALI cells from start to finish of transmigration experiments, HLE-ALI cells had a median of 6.3×10^5 viral genome copies in the absence of drugs, which is about 5x the initial input **(Figure 5.5C)**. To determine if viral replication occurred, we assessed SARS-CoV-2 N-subgenome relative to *18S rRNA* transcripts in HLE-ALI cells. There was a detectable amount of N-subgenome that remained unchanged in conditions including remdesivir. However, treatment with baricitinib resulted in an $\sim 2^4$-fold increase in the N-subgenome relative amount **(Supplementary Figure 5.7E)**. Relative to *18S rRNA* transcript, all treatment conditions increased the amount of N-subgenome compared to the untreated control in monocytes (remdesivir: $\sim 2^1$; baricitinib: $\sim 2^3$; remdesivir+baricitinib: $\sim 2^1$) **(Supplementary Figure 5.7F)**.

In order to gain a better understanding of how SARS-CoV-2 enters monocytes we analyzed the expression of surface ACE2 and also included various treatments during transmigration known to affect SARS-CoV-2 entry into cells. Blood monocytes were found to express surface ACE2 as measured by flow cytometry, and ACE2 appeared to be slightly upregulated upon transmigration **(Supplementary Figure 5.9A).** The observation that immune cells, including monocytes and macrophages, express ACE2 and thus could be susceptible to direct SARS-CoV-2 infection has been validated by many groups (Abassi et al., 2020). Accordingly, the inclusion of soluble ACE2 (200 μg/mL, also contained a C-terminal 10xHis-tag) lowered the amount of SARS-CoV-2 observed in the monocytes as other groups have shown (Monteil et al., 2020; Krishnamurthy et al., 2021). Next, the use of the antibiotic dalbavancin (1 μM), which has been shown to bind to the ACE2 receptor (Wang et al., 2021), also decreased the amount of SARS-CoV-2 in transmigrated monocytes. As a control, the use of either soluble ACE2 or dalbavancin did not decrease the amount of OC43 in the monocytes **(Supplementary Figure 5.9B)**. The dynamin GTPase inhibitor and pinocytosis blocker Dynasore (80 μM) and endocytosis inhibitor pitstop2 (15 μM) also inhibited SARS-CoV-2 entry into monocytes. Taken together, SARS-CoV-2 likely enters monocytes through a variety of mechanisms including ACE2 receptor-mediated endocytosis either with or without the aid of clathrin (Bayati et al., 2021), as well as pinocytosis.

Treatment with baricitinib and remdesivir decreases the rate of viral clearance and replication in lung-infiltrating monocytes harboring SARS-CoV-2.

Since SARS-CoV-2 genome copies were detectable in lung-infiltrating monocytes, we examined whether these genomes were replication-competent. To this end, we isolated and washed lung-infiltrating monocytes via negative selection with anti-CD326 beads to remove contaminating epithelial cells, and incubated the purified monocytes in fresh medium for 72 hours **(Figure 5.6A)**. Every 24 hours, RNA and protein were isolated from the monocytes and the extracellular fluid. In the absence of drug, viral genome copies in monocytes increased from 0 to 48 hours, and then plateaued **(Figure 5.6B)** while extracellular viral genome copies steadily increased across the 72 hours **(Figure 5.6C)**. Since baricitinib induced the expression of several antiviral genes and remdesivir reduced viral genome copies in lung-infiltrating monocytes in our model, we next tested the effect of these drugs on viral propagation upon an additional 72 hours of culture. As expected, treatment with remdesivir abrogated the replication of the virus and few genome copies were detected in monocytes. Treatment with baricitinib decreased viral genome copies in monocytes at 48- and 72-hour timepoints, suggesting that this drug may also promote clearance of virus by lung-infiltrating monocytes. Furthermore, treatment with remdesivir alone or in combination with baricitinib resulted in a stark decrease in levels of *N-subgenome* in monocytes at all timepoints **(Figure 5.6D)**. Treatment with baricitinib also lowered *N-subgenome* in monocytes compared to the untreated control at 48- and 72-hour timepoints.

Since the virus replicated its genome in lung-infiltrating monocytes, we next sought to determine whether infectious particles could be formed from these cells. To this end, the extracellular fluid from monocyte cultures collected at 48- and 72-hour timepoints were applied to virus-permissive VeroE6 cells. Remarkably, no plaques or cytopathic effects were observed

(Figure 5.6E, Supplementary Figure 5.10), an observation repeated with a foci assay. These findings suggest that although lung-infiltrating monocytes in our *in vitro* model are amenable to *SARS-CoV-2* genome replication, a blockade exists in these cells that results in abortive virus.

Finally, to better understand the inflammatory state of lung-infiltrating monocytes harboring viral genome copies, we performed a multiplexed electrochemiluminescent assay to quantify mediators released by these cells. While extracellular IL-10 levels steadily increased from 0 to 48 hours in the absence of drugs, treatment with baricitinib alone or in combination with remdesivir kept those levels low **(Figure 5.6F)**. Treatment with remdesivir alone increased extracellular IL-10 levels, although not to the same levels as in the untreated control conditions. Extracellular levels of CXCL8 and IL-1β were higher in the absence of drug at 0- and 24-hour timepoints than in all treatment groups. However, treatment with baricitinib lowered the magnitude of IL-1β increase, suggesting that this drug may promote lower grade neutrophilic inflammation. Although treatment with remdesivir resulted in lower levels of CXCL8 and IL-1β **(Figure 5.6G,H)**, it elevated levels of IL-1α compared to the untreated control condition at 24- and 48-hour timepoints **(Supplementary Figure 5.11A)**. IFN-γ increased over time in the untreated control condition but remained low in all treatment groups **(Supplementary Figure 5.11B)**, while no effects were observed with IL-6, TNF-α, G-CSF, GM-CSF, and VEGF-A **(Supplementary Figure 5.11C-G)**.

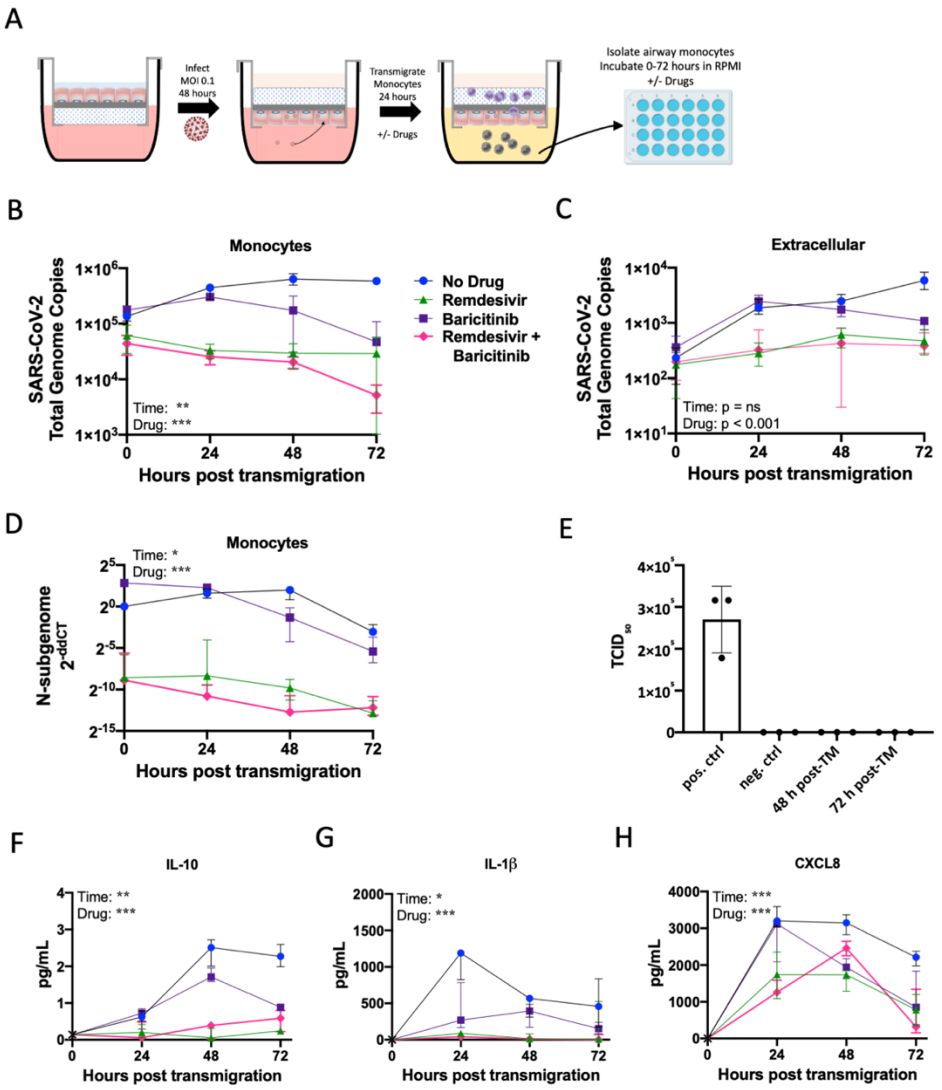

*Figure 5.6. [Treatment with baricitinib and remdesivir increases the rate of viral clearance in lung-infiltrating monocytes.] (A) Schematic of the experimental setup to quantify replication of the virus in monocytes. Then, HLE-ALI cells were infected with SARS-CoV-2 at an MOI 0.1 for 48 hours, after which 106 monocytes were transmigrated across the infected epithelium towards LTB4 (100 nM) and CCL2 (250 pg/mL) for 24 hr, in the absence / presence of remdesivir (1 µM) and/or baricitinib (1 µM). Monocytes were washed and purified by negative depletion using anti-CD326 beads to remove contaminating epithelial cells and placed into medium with no drug, remdesivir (1 µM) and/or baricitinib (1 µM) for 0-72 hr. All conditions contained 0.1% v/v DMSO. (B) Quantification of total SARS-CoV-2 genome copies in the monocytes. (C) Quantification of the amount of virus in the extracellular fluid at each time point. (D) Quantification of the N-subgenome in monocytes at each time point. Data was normalized to 18S rRNA in the untreated condition at 0 hr using the delta delta Ct method. (E) The extracellular fluid was layered onto VeroE6 cells to perform a plaque assay from which a TCID50 was calculated. The positive was the direct application of 2.5 x 104 genome copies of SARS-CoV-2 to the cells. (F-H) Inflammatory mediators were measured using an electrochemiluminescent assay. All statistics were calculated with a two-way ANOVA, main effects model in Prism with Geisser-Greenhouse Correction applied. * p<0.05, ** p<0.01, ***p<0.001. Shown is the median with the interquartile range.*

DISCUSSION

COVID-19 includes an early viral phase, and a later immune phase. Upon infection by SARS-CoV-2, differentiated epithelial cells in the small airway model show enhanced pro-apoptotic signaling and attenuated type I IFN signaling, which may allow for enhanced viral propagation during early disease and prevent mounting of an effective innate immune response by epithelial and myeloid cells. An ineffective innate immune response with suboptimal type I IFN signaling can impede development of subsequent type II IFN (IFNγ)-dependent adaptive immune responses (Zuniga et al., 2015), as occurs in severe COVID-19 (Rao et al., 2020). Prior studies noted that SARS-CoV-2-infected human lung tissue failed to upregulate IFN genes during infection, and that in patients with severe COVID-19, lung-infiltrating monocytes showed a reduced IFN signature compared to patients with mild disease (Chu et al., 2020; Schulte-Schrepping et al., 2020). In contrast with prior studies that did not combine differentiated epithelial cells with infiltrating leukocytes (Vanderheiden et al., 2020), our small airway model did show increased IFNγ release upon SARS-CoV-2 infection.

As viral burden wanes, host responses may devolve into CRS, featuring proinflammatory mediators supporting monocyte infiltration combined with high IL-10 levels, which act to initially limit neutrophil recruitment (Eroshenko et al., 2020). To overcome the barrier posed by IL-10, lung-infiltrating virus-infected monocytes may synthesize additional CXCL8, which eventually results in neutrophil infiltration leading to ARDS. Moreover, high levels of monocyte-derived IL-1β can also overcome IL-10 blockade and promote neutrophilic inflammation (Dinarello, 2018). Lung-infiltrating monocytes in our model were infected by SARS-CoV-2 from the epithelium. They subsequently increased expression of pro-inflammatory genes including

CXCL8 and IL-1β, among other changes in their transcriptional poise likely to contribute to further inflammation. This mirrors in vivo findings that infiltrating monocytes isolated from the BALF of severe COVID-19 patients contain SARS-CoV-2 transcripts and increased expression of CXCL8 and IL-1β and multiple other chemokines including CCL4, CCL7, CCL3, and CCL2. These findings implicate lung-infiltrating monocytes as key contributors to COVID-19 progression. Thus, our model recapitulates the distinct phases in the clinical progression of COVID-19 including initial immune avoidance in epithelial cells, recruitment of airway monocytes, and the release of inflammatory molecules reflective of CRS, and later, ARDS.

Although the viral products detected in lung-infiltrating monocytes were abortive, these cells may yet act as a reservoir of virus or as a continuing source of inflammatory cytokines and contribute not only to fueling the CRS, but also pave the way for neutrophil-driven ARDS. Furthermore, it is possible that replicative SARS-CoV-2 in airway monocytes serves as a continual source of dsRNA-stimulation resulting in inflammatory cytokine release contributing to symptomatology seen in so-called “long-haulers”, i.e., patients who have relatively mild disease weeks or even months after the initial infection. Indeed, it was previously observed that CD16+ blood monocytes expressed SARS-CoV-2 S1 spike protein up to 15 months after initial SARS-CoV-2 infection, despite the inability to isolated full-length viral RNA (Patterson et al., 2021). The finding that monocytes harbor cell-associated SARS-CoV-2 copies has been observed by others and poses a key therapeutic opportunity for early host-directed disease intervention. In one study, blood monocytes were able to be infected by SARS-CoV-2 in an antibody-dependent manner, triggering inflammasome activation and contributing to severe COVID-19 pathology (Junqueira et al., 2021). In another study, circulating lymphomononuclear cells

including monocytes as well as T- and B-cells were susceptible to SARS-CoV-2 infection (Pontelli et al., 2020). A third study described that blood monocytes and differentiated macrophages could be infected by SARS-CoV-2, resulting in abortive viral products (Boumaza et al., 2021). However, these prior instances were in blood monocytes, not lung-infiltrating cells as used in our study, which we previously showed to acquire a distinct transcriptional poise (Ford et al., 2021). Recently, another group showed that tissue-resident alveolar macrophages take up and replicate SARS-CoV-2, after which a type I IFN response ensued (Sefik et al., 2022).

In the ACTT-1 clinical trial, the antiviral remdesivir showed greatest clinical benefits (improved time to recovery) in patients with an ordinal oxygen score of 4 or 5 (not receiving or receiving low-flow oxygen, respectively) compared to a placebo, suggesting that antivirals will work best in early-stage disease (Beigel et al., 2020). The ACTT-2 trial evaluated baricitinib in combination with remdesivir against baricitinib alone (Kalil et al., 2021). The combined treatment shortened total time to recovery, had more improvement in symptoms and fewer adverse events than the control group. The efficacy of combined baricitinib and remdesivir treatment was greatest in patients that had an ordinal score of 6 at baseline (receiving high-flow oxygen or a non-invasive ventilation), indicating the profound effects of baricitinib on more severe late-stage disease. In the subset of patients that started treatment at an ordinal score of 6, time to recovery was shorted from 18 days in the group to 10 days in the combination group (Kalil et al., 2021).

In rhesus macaques infected with SARS-CoV-2, baricitinib given alone from 2-10 days post-infection suppressed pro-inflammatory cytokine production in lung macrophages, reduced recruitment of neutrophils, and resulted in reduced lung pathology compared to the control

group. However, viral load in nasal and throat swabs as well as BALF was unchanged (Hoang et al., 2021). Other groups have proposed that in addition to its immunomodulatory effects via JAK1/2 inhibition, baricitinib treatment may have a direct effect on SARS-CoV-2 viral entry via ACE2 by inhibiting numb-associated kinases to prevent clathrin-mediated endocytosis (Stebbing et al., 2020). Our study supports the notion that treatment with baricitinib (alone and in combination with remdesivir) reduces viral load in lung-infiltrating monocytes, and that baricitinib (alone and in combination with remdesivir) reduces viral replication and the release of inflammatory mediators. Meanwhile, an exploratory trial evaluating baricitinib plus standard of care vs. a placebo plus standard of care found that the treatment group had a lower mortality rate at both 28 and 60 days, although ventilator-free days and length of hospital duration were unchanged (Ely et al., 2022). At such late timepoints post-infection, viral titers are low and baricitinib is likely functioning primarily as an immunomodulator.

Findings presented here are made relevant to the clinical prevention and resolution of COVID-19 by, first, comparing our in vitro data to in vivo single cell RNA-seq data from patients with severe COVID-19, and second, by using the approved drugs remdesivir and baricitinib. These drugs may now be tested in combination with or as comparators for emerging therapies to bring to trial. Findings here suggest that candidate drugs can affect the epithelium and lung-infiltrating leukocytes in different and sometimes divergent ways with regards to their impact on antiviral and immune signaling, notably. For this reason, the use of our small airway model as a testing platform for candidate COVID-19 drugs overcomes some limitations associated with using non-human / non-lung in vitro models.

In conclusion, we showed that human lung epithelial cells differentiated at ALI propagate SARS-CoV-2 and fail to induce antiviral signaling, but can recruit monocytes. These lung-infiltrating monocytes are in turn infected by SARS-CoV-2 yet successfully induce host antiviral pathways while also activating IL-1β and CXCL8 transcription. Critically, we show that virus-laden, IL-1β and CXCL8-positive monocytes are also present in vivo in the lung fluid of patients with severe, but not mild, COVID-19. Finally, we show that treatment with the JAK1/2 inhibitor baricitinib combined with the antiviral drug remdesivir decreases monocyte recruitment through the virus-infected epithelium and viral burden in both cell types and also alters signaling pathways in monocytes. Taken together, our findings establish that lung-infiltrating monocytes retain virus and contribute to the pathogenesis of COVID-19 and thus must be appropriately targeted for successful resolution of the disease.

Limitations of the study: while the human small airway model leveraged here can be generated with primary epithelial cells (Laucirica et al., 2022), the present study relies on a club cell line. In addition, blood monocytes transmigrated in the model are from healthy subjects. Use of primary monocytes from patients may shed information on disease course in light of the observations that they may behave abnormally in severe COVID-19 (Qin et al., 2020). Finally, this study uses the Washington strain of SARS-CoV-2. Follow-up studies combining primary airway epithelial cells and monocytes from infected subjects, and other SARS-CoV-2 variants of interest [e.g., Delta (B.1.617.2) or Omicron (B.1.1.529)] may help identify host/virus interactions causing the divergence between asymptomatic, mild and severe cases.

ACKNOWLEDGMENTS

This study was supported by NSF EAGER award 2032273 (to RT, RFS and KZ) and Woodruff Health Science Center COVID-19 CURE award (to RT, RFS, KZ, MB and VS). RFS is also funded in part by NIH grant R01MH116695. We thank Dr. Matt Frieman (University of Maryland) for sharing primer sequences targeting the N-subgenome of SARS-CoV-2. We thank Dalia Gulick, Naima Djeddar and Gregory Gibson (Georgia Tech) for assisting with multiplexed qRT-PCR. Research reported in this publication was supported in part by the Pediatrics/Winship Flow Cytometry Core of Winship Cancer Institute of Emory University, Children's Healthcare of Atlanta. Graphical Abstract was generated in Biorender. SARS-CoV-2, Isolate USA-WA1/2020 was obtained from BEI Resources, Manassas, VA.

AUTHOR CONTRIBUTIONS

BD, KZ, DMG, SLG, KM, MA, JLC, VG, JK, DE, JY performed and analyzed experiments. MB, VS, EG provided conceptualization and input for the work. BD, KZ, DMG, RT, RFS wrote the original manuscript. RFS and RT conceptualized the experiments. All authors reviewed and edited the manuscript.

DECLARATION OF INTERESTS

RFS is the inventor of the use of baricitinib for coronavirus infections and receives royalties from Eli Lilly and Company. His conflict of interest has been reviewed and approved by Emory University. All other authors have declared that no conflict of interest exists. Contents within this manuscript are included in patent USPTO 10670594.

MATERIALS AND METHODS

Resource availability. Lead Contact: Requests for further information should be directed to and will be fulfilled by the lead contact, Rabindra Tirouvanziam (tirouvanziam@emory.edu). Materials Availability: This study did not generate new unique reagents. Data and Code availability: RNA-seq data has been deposited at GEO and are available as of the date of publication. It can be accessed under accession: GSE186460.

In vitro transmigration experiments and infection with virus. The H441 Club cell line is grown on Alvetex scaffolds (ReproCELL, Glasgow, UK) coated with rat-tail collagen (Sigma) for 2 weeks at air liquid interface with 2% v/v Ultroser G (Crescent Chemical, Islandia, NY) in 50/50 DMEM/F12 supplemented with 1% v/v penicillin/streptomycin (Forrest et al., 2018; Grunwell et al., 2019). The filters are then flipped and placed into fresh media in the bottom of the well. Virus (PR8: A/Puerto Rico/8/1934; OC43; or NR-52281, SARS-CoV-2 Isolate USA-WA1/2020) is added to the media such that that the multiplicity of infection (MOI) is 0.1 and incubated for 24 hours (unless otherwise indicated). This setup requires manual flipping of filters prior to transmigration (Dobosh et al., 2021), a delicate process to perform in BSL3 conditions. Thus, the epithelial cells must be infected while the cells are submerged and no longer at ALI, which may introduce artifacts reminiscent of pneumonia. The filters are transferred to RPMI media with LTB4 (100 nM) and CCL2 (250 pg/mL) with or without additional drugs. Baricitinib and remdesivir were each used at a final concentration of 1 μM. The untreated condition contained 0.1% v/v DMSO as a vehicle control. Blood monocytes were purified using RosetteSep (StemCell). A total of 10^6 cells is loaded onto the Alvetex scaffold for transmigration which was

allowed to occur for 24 hours **(Figure 5.1A)**. After transmigration, TriPure (Roche) was added to epithelial cells and frozen at -80 ˚C.

Isolation of monocytes from transmigration fluid. To purify transmigrated cells in a low volume-manner and without the use of a centrifuge, we conjugated 8 μm magnetic beads coated in streptavidin (Spherotech) with biotinylated antibodies targeting CD45 and CD115. Beads and cells were incubated at room temperature for 15 min and the supernatant was removed. The bead precipitate was resuspended in TriPure and frozen at -80 ˚C.

Isolation of nucleic acids. For isolation of RNA (and DNA) from epithelial cells, after thawing, chloroform (Sigma) was added to the TriPure and RNA was extracted using the standard purification procedure in the manufacturer's protocol followed by a sodium acetate precipitation to further clean the RNA. For isolation of RNA (and DNA) from monocytes, the tubes were thawed and placed on a magnet to remove the beads from solution. The TriPure supernatant was transferred to a clean tube and chloroform was added and spun following the manufacturer's protocol. Due to the small amount of expected RNA yield, the aqueous phase (containing the RNA) was mixed 1:1 with 100% ethanol (Sigma) and loaded onto an RNA clean and concentrator-5 column (Zymo). RNA was isolated following the manufacturer's protocol. DNA was isolated from the organic phase following the manufacturer's protocol.

Cell counting by DNA quantification. Traditional cell counting by hemocytometer was not available in the BSL3. To solve this problem, an estimate of cell number was achieved by

quantifying the amount of DNA in the sample. The extracted genomic DNA is amplified using a primer and probe pair which bind an exon-intron junction of AP endonuclease 1 (APEX1; **Supplementary Table 5.9)**. These sequences appear once in the genome and the primers and probe do not exhibit off-target amplification. A standard curve to calculate copy number was generated using a double stranded gBlock from IDT which contains the expected binding sequence **(Supplementary Table 5.10)**. The copy number was then divided by two to account for diploidy and multiplied by the dilution factor to estimate the total number of cells. Naturally, this number is an estimate as dividing cells as well as dead cells, which have not yet fully degraded their DNA, will elevate the count resulting in an overestimate of the total cell yield.

Flow cytometric analysis of monocytes. Purified blood monocytes from blood before and after transmigration across HLE-ALI cells with or without infection with SARS-CoV-2 were stained (R&D Systems) for the presence of surface ACE2 and then measured by flow cytometry on a Cytoflex S (Beckman Coulter).

eATP assay. 100 µL of extracellular fluid was centrifuged at 800 xg for 10 minutes and then used with the Promega Realtime-Glo Extracellular ATP Assay following the manufacturer's instructions. Luminescence was measured on a SpectraMax iD3 (Molecular Devices).

Quantification of viral RNA via qRT-PCR. Total RNA is reverse-transcribed using SuperScript IV (ThermoFisher) and an anchored oligo-d$(T)_{20}$ primer followed by amplification with a primer

probe pair which targets the N gene **(Supplementary Table 5.9)** and Luna Universal Probe qPCR Master Mix (New England Biolabs) was used to amplify the cDNA. A standard curve to calculate copy number was also generated using a double stranded gBlock from IDT which contains the expected binding sequence **(Supplementary Table 5.10)**.

qRT-PCR. RNA is reverse-transcribed using SuperScript IV and anchored oligo-d$(T)_{20}$ primers to make a cDNA library that can be used multiple times. cDNA is amplified using relevant primer pairs **(Supplementary Table 5.9)** and SYBR Green in an Applied Biosystems 7500. Data are analyzed via the ddCt method for 18S rRNA and GAPDH (loading controls).

RNA quantification and quality control. RNA was initially quantified by Nanodrop 1000 spectrophotometer (ThermoScientific). For samples that would be analyzed by RNA-seq, an aliquot was further quality controlled by an Agilent Bioanalyzer 2100.

Transcriptomic analysis of monocytes. Isolated RNA was reverse transcribed using Superscript IV Reverse Transcriptase (ThermoFisher Scientific) and an anchored oligo-d$(T)_{20}$ primer following the manufacturer's protocol. A Fluidigm Biomark machine and Delta Gene Assay chip (96x96) was used to conduct multiplexed qPCR of 96 genes and 96 samples. Data was analyzed using a modified version of the jpouch script available in Github (https://github.com/jpouch/qPCR-Biomark; Date of Access: May 31st, 2020).

RNA-sequencing of epithelial cells. For *RNASeq,* purified RNA was given to the Yerkes Genomics Core for processing. Briefly, rRNA is depleted and the TruSeqRNA Sample Preparation v2 kit and LS protocol is used. All the produced Fastq files from single end reads were aligned to the human reference genome (GRCh38.p13- Ensembl) using the alignment tool HISAT2 (version 2.1.0), using the default settings. Then, BAM files reads were sorted using SAMtools. The resulting BAM files were used as input to determine read counts using FeatureCounts (1.5.2). All processed counts were used to conducted differential expression analysis using DEseq2, considering as differentially expressed genes, genes with fold changes > 2 folds, and a False discovery rate < 0.1. Finally, to understand the functions of the differentially expressed genes Metacore server is used against pathway maps and networks. RNA-seq data has been deposited at GEO and are available as of the date of publication. It can be accessed under accession: GSE186460.

Protein extraction*.* Once the DNA was removed from the organic phase, the supernatant was mixed 1:1 with 1% v/v SDS and loaded onto a 3,000 kDa MWCO column (Sartorius) and spun at 3,000 xg for 2 minutes. The column was buffer exchanged with 500 µL of 1% v/v SDS five times.

Quantification of inflammatory mediators. Ten mediators (CXCL8, G-CSF, GM-CSF, IFNalpha, IL-1alpha, IL1beta, IL-6, IL-10, IL-18, TNFalpha) were measured using a chemiluminescent assay according to the manufacturer's protocol (U-plex; Meso Scale Diagnostics). In general, to measure CXCL8, samples had to be diluted 1:10, but for all other cytokines we did not need to dilute the samples.

Single-cell RNA sequencing. The scRNA-seq FASTQs data from BALF of mild and severe patients were acquired from the Gene Expression Omnibus (GEO) database under accession code GSE145926 (Liao et al., 2020). The Cell Ranger Software (v.3.1.0) was used to perform barcode processing and single-cell 5' unique molecular identifier (UMI) counting. To detect SARS-CoV-2 reads, a customized reference was built by integrating human GRCh38 and SARS-CoV-2 genome (severe acute respiratory syndrome coronavirus 2 isolate Wuhan-Hu-1, complete genome, GenBank MN908947.3). Specifically, splicing-aware aligner STAR was used in FASTQs alignment. Cell barcodes were then determined based on the distribution of UMI counts automatically. The filtered gene-barcode matrices were first normalized using 'LogNormalize' methods in Seurat v.3 with default parameters. The top 2,000 variable genes were then identified using the 'vst' method by the FindVariableFeatures function. To remove the batch effect between the mild and the critical datasets, the standard integration workflow of Seurat v.3 was used with the first 30 dimensions from canonical correlation analysis (CCA) as the input of the 'FindTransferAnchors()' function. PCA was performed using the top 2,000 variable genes of the integrated matrix. Then UMAP was performed on the top 30 principal components for visualizing the cells. Meanwhile, graph-based clustering was performed on the PCA-reduced data for clustering analysis with Seurat v.3. The resolution was set to 0.8 to obtain the UMAP. RNA-seq data has been deposited at GEO and are available as of the date of publication. It can be accessed under accession: GSE186460.

SUPPLEMENTARY FIGURES

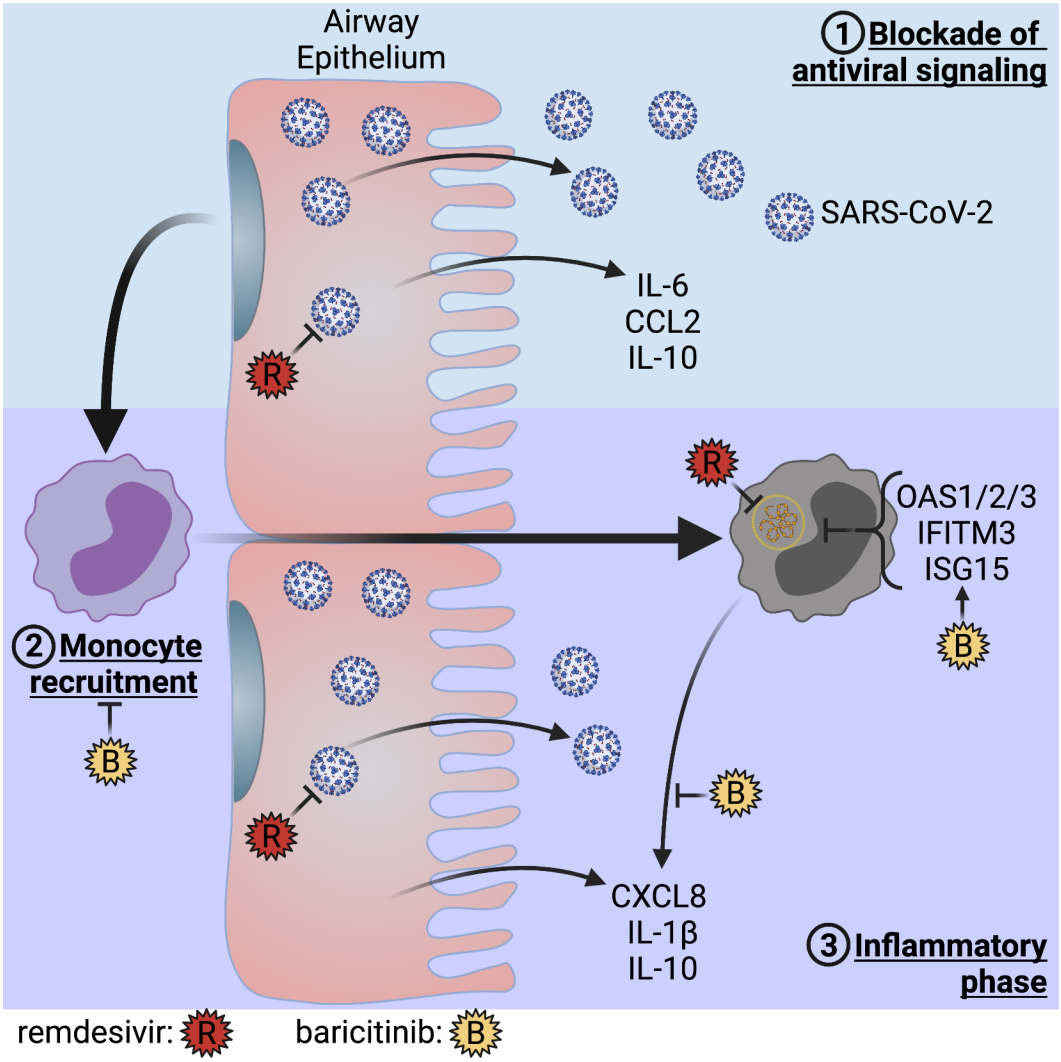

Graphical abstract. *Antiviral and proinflammatory signaling are suppressed in the initial epithelial phase of SARS-CoV-2 lung infection, but enhanced upon monocyte infiltration into the virus-infected lung. This phased response is modeled in a novel small airway model of infection and inflammation in vitro model to evaluate the mechanistic effects of COVID-19 drugs such as the antiviral drug remdesivir and JAK1/2 inhibitor baricitinib.*

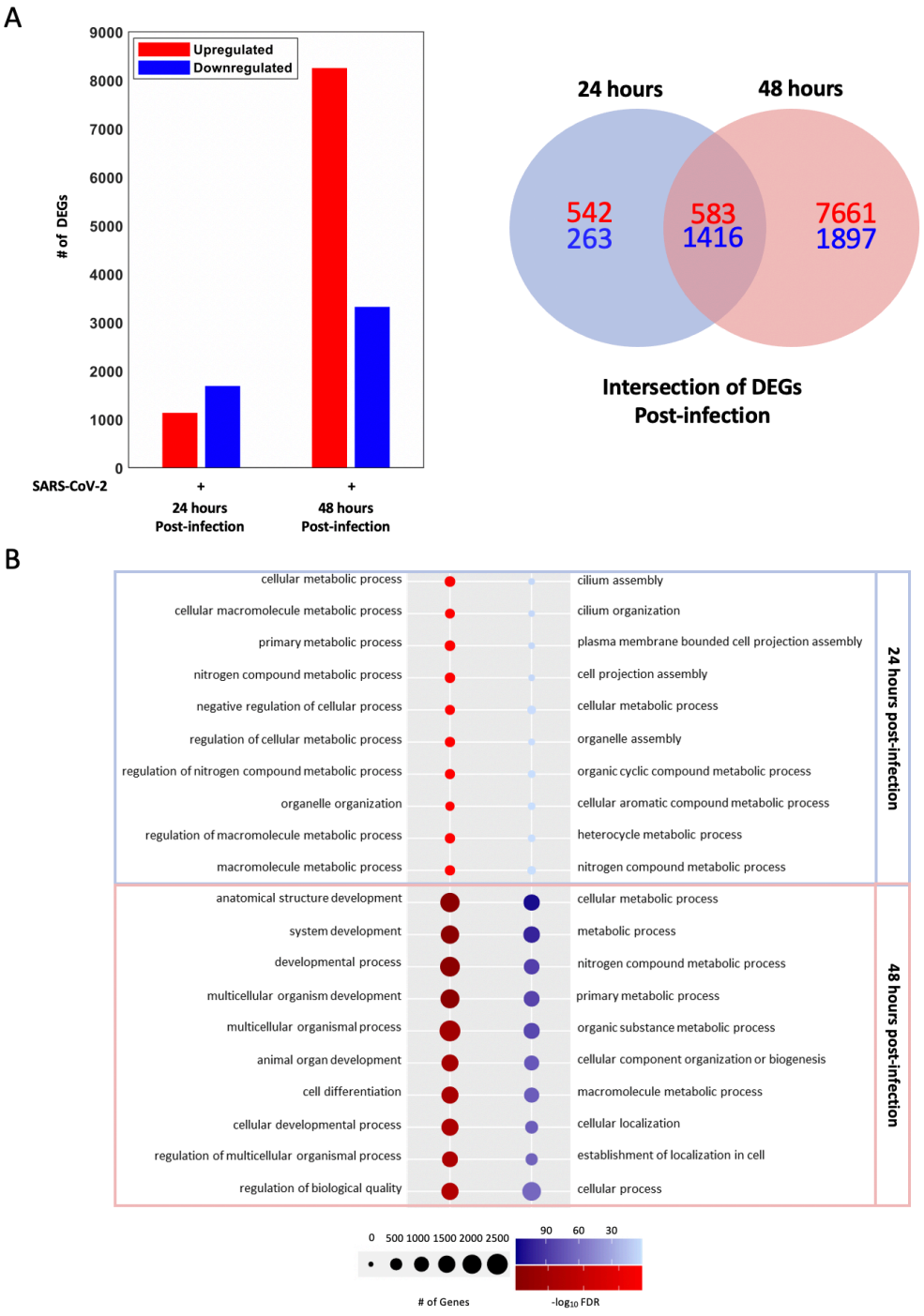

Supplementary Figure 5.1. Related to Figure 5.2. A) Number of upregulated and downregulated DEGs from the RNA-seq data (n=3 biological replicates) of HLE-ALI cells infected with SARS-CoV-2 for either 24- or 48-hours. B) GO processes enriched in HLE-ALI cells at either 24- or 48 hr post-infection with SARS-CoV-2. GO terms were only generated using the uniquely DEGs between the two conditions.

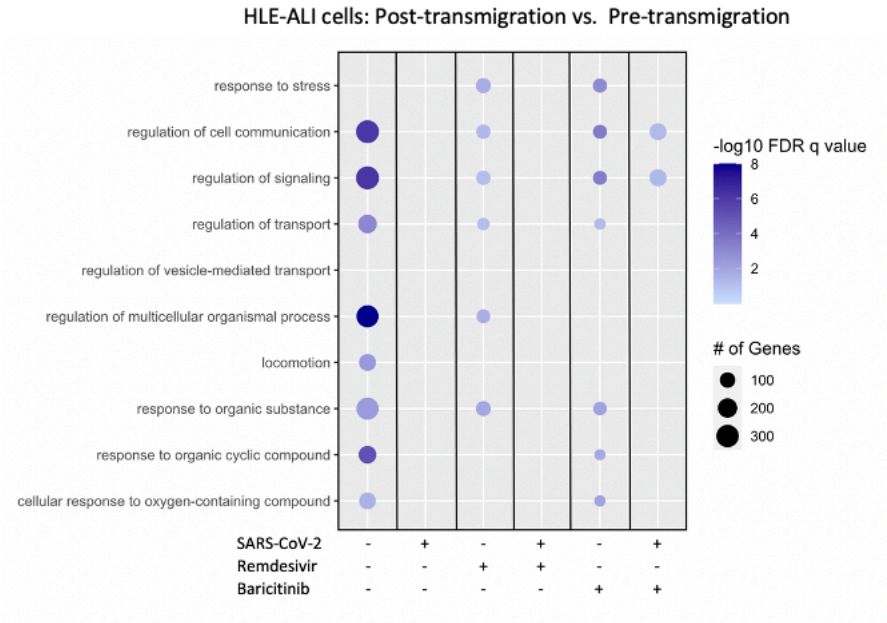

Supplementary Figure 5.2. Related to Figure 5.3B. A) Enriched GO terms of the HLE-ALI cells pre- and post- transmigration under each drug and infection condition (n=3 biological replicates).

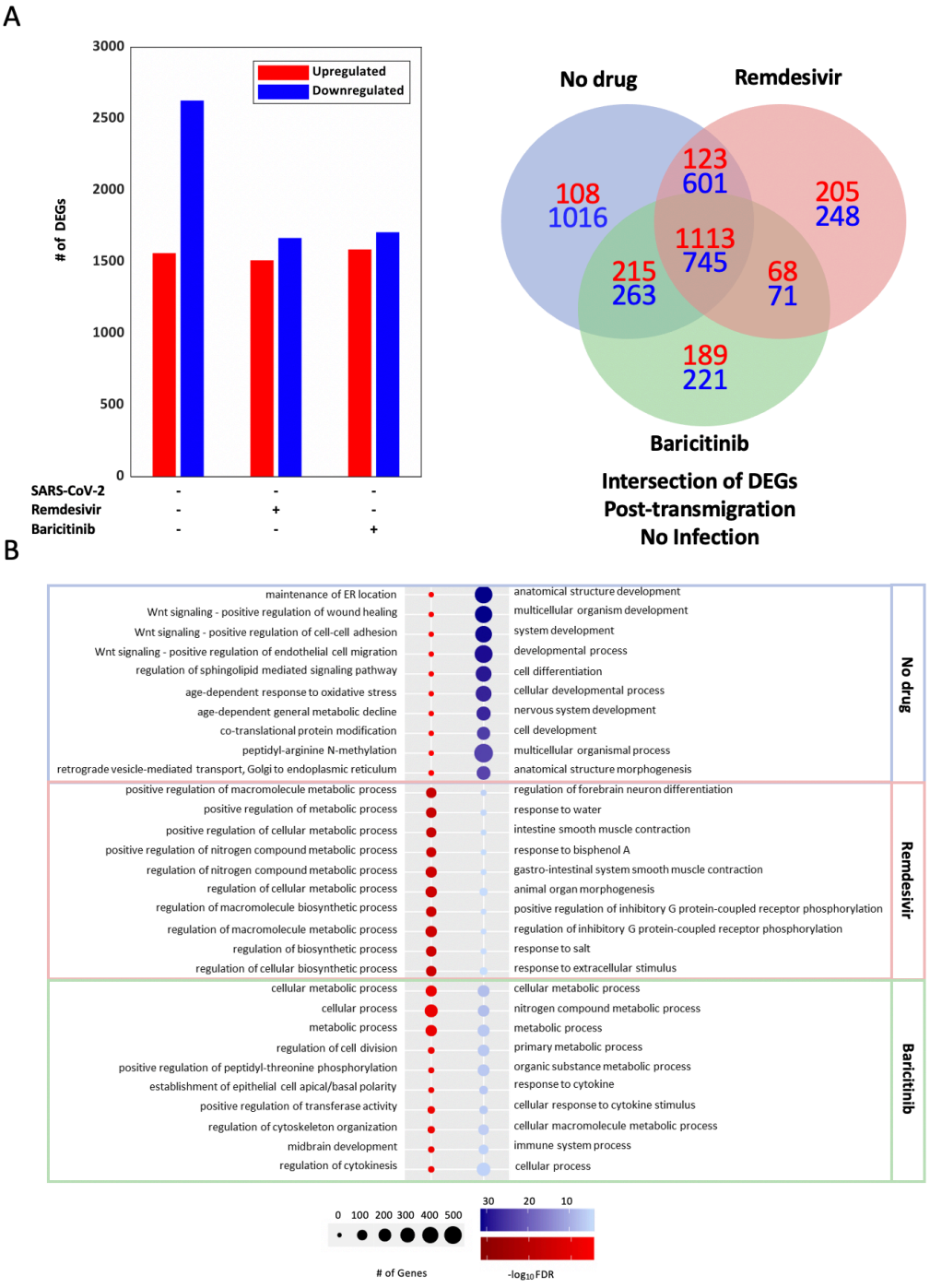

Supplementary Figure 5.3. Related to Figure 5.3B. A) Number of upregulated and downregulated DEGs from the RNA-seq data of HLE-ALI cells that were not infected with SARS-CoV-2 after transmigration of monocytes in the presence of either vehicle, remdesivir, or baricitinib (n=3 biological replicates). B) GO processes enriched in HLE-ALI cells after transmigration of monocytes in the presence of either vehicle, remdesivir, or baricitinib. GO terms were only generated using the uniquely DEGs between the three conditions.

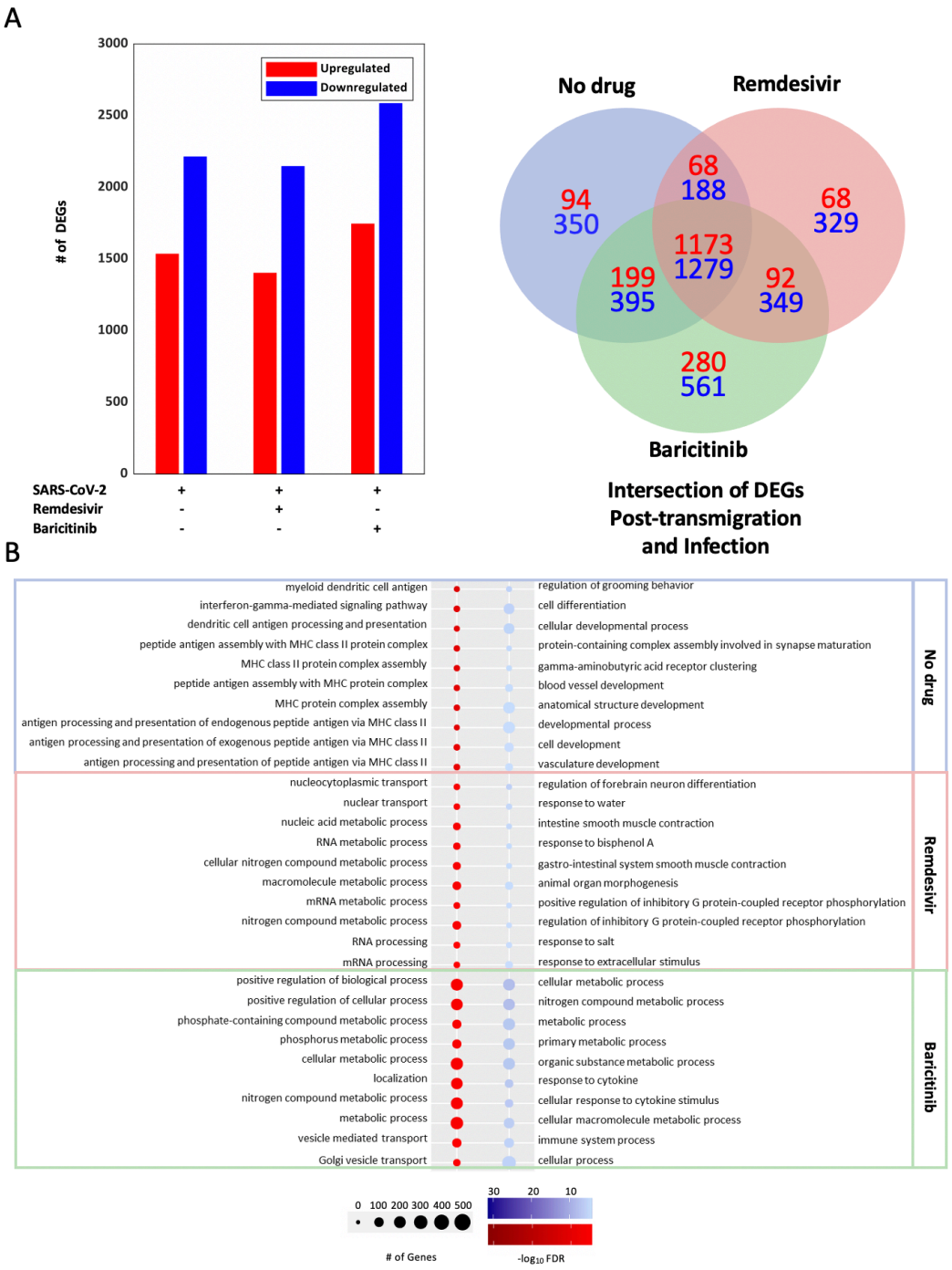

Supplementary Figure 5.4. Related to Figure 5.3B. A) Number of upregulated and downregulated DEGs from the RNA-seq data of HLE-ALI cells infected with SARS-CoV-2 after transmigration of monocytes in the presence of either vehicle, remdesivir, or baricitinib (n=3 biological replicates). B) GO processes enriched in HLE-ALI cells after transmigration of monocytes in the presence of either vehicle, remdesivir, or baricitinib. GO terms were only generated using the uniquely DEGs between the three conditions.

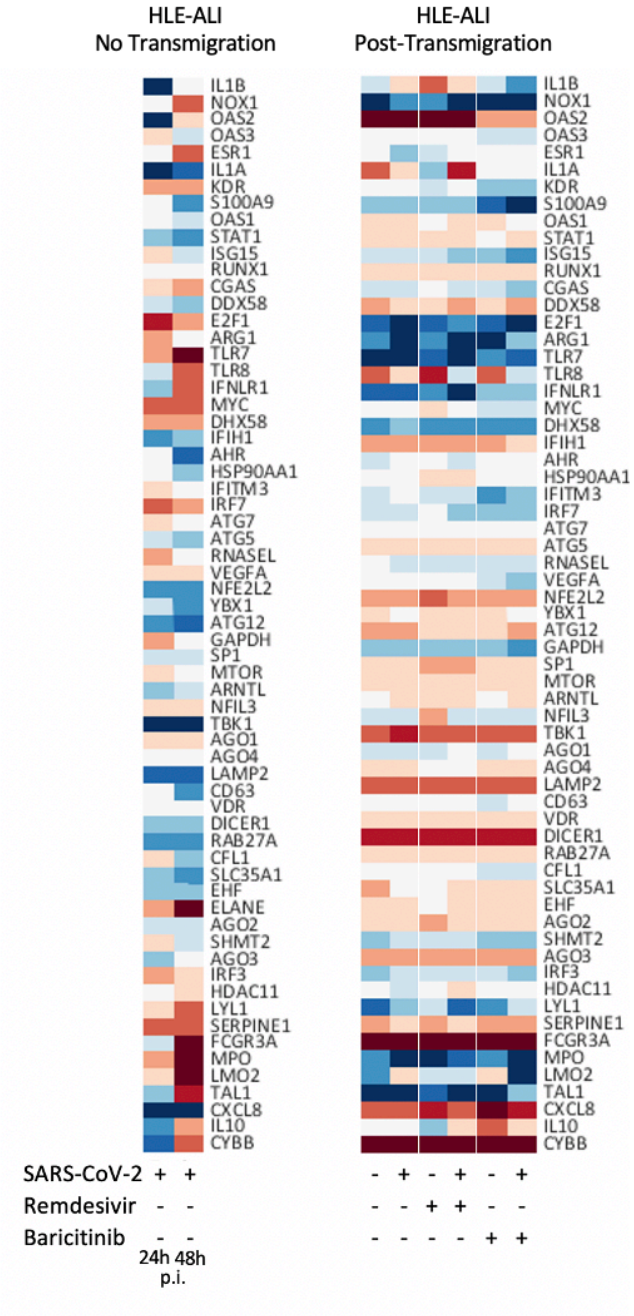

Supplementary Figure 5.5. Related to Figure 5.3B. A) Normalized expression values of a set of genes extracted from the RNA-seq data of HLE-ALI cells under each treatment condition (n=3 biological replicates). The set of genes was selected to be the same as the genes selected for qRT-PCR of the monocytes in Figure 5.3B. If a gene was not identified in the RNA-seq data of the HLE-ALI cells then it was not listed.

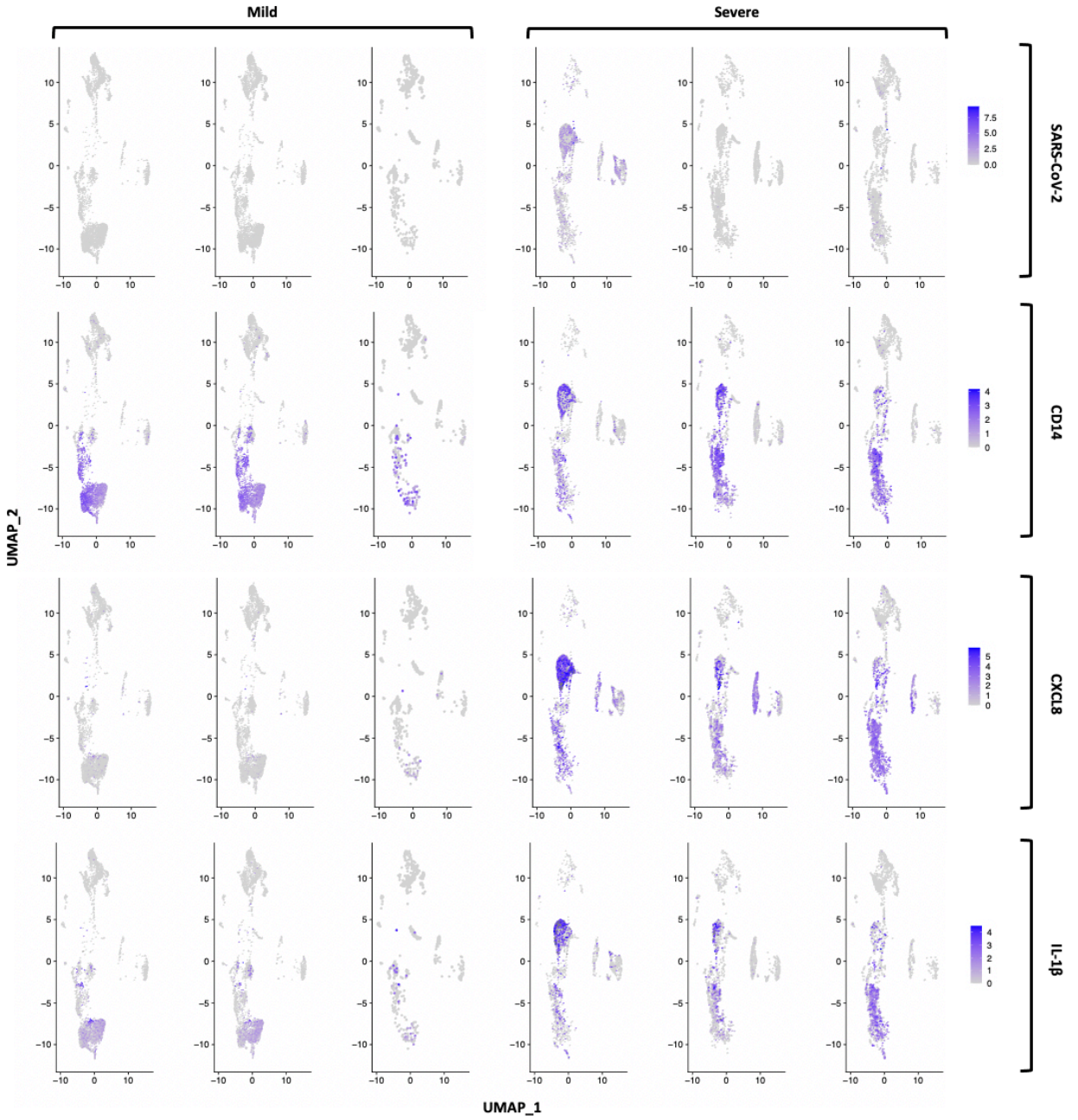

Supplementary Figure 5.6. Related to Figure 5.4A. Individual UMAPs of scRNA-seq data of BALF from patients hospitalized with either mild or severe COVID-19. Original scRNA-seq data is publicly available under accession code GSE145926 (Liao et al., 2020).

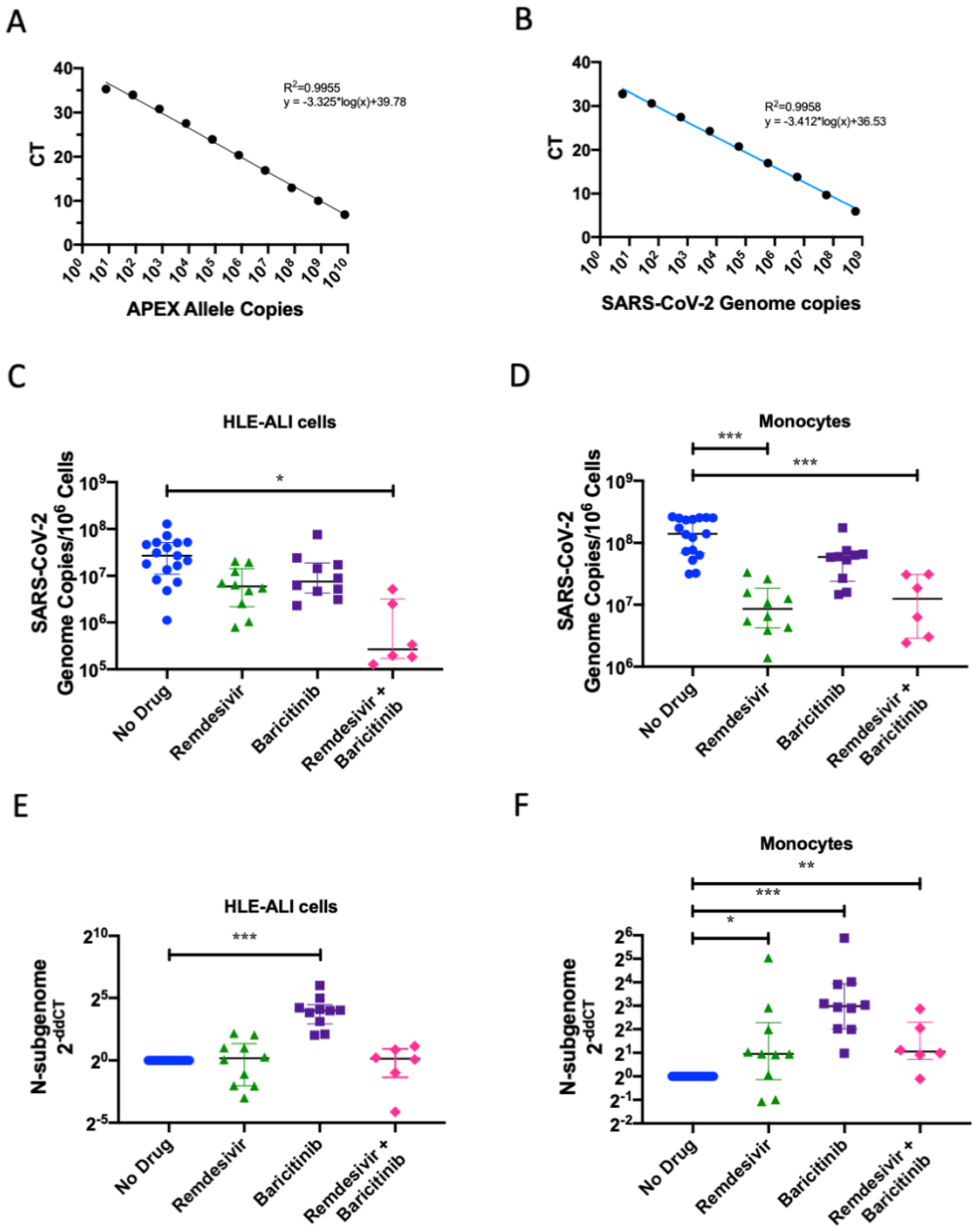

*Supplementary Figure 5.7. Related to Figure 5.5. SARS-CoV-2 genome copies in each compartment relative to cell number and N-subgenome calculations. (A) In order to calculate cell number a standard curve was used to estimate the number of alleles of APEX present (see Supplementary Tables 9 and 10). This number was transformed by the following calculation to obtain an estimate for cell number: (calculated gene copies) / 2*dilution factor (B) A standard curve was generated to calculate the total number of SARS-CoV-2 genome copies (see Supplementary Tables 9 and 10). (C,D) Calculated SARS-CoV-2 genome copies in each cell was normalized by dividing by the number of cells present. (E) Primers aligning to the N-subgenome were used to quantify the replication competency of the virus. Data were normalized using the delta delta Ct method to 18S rRNA (see Supplementary Tables 9 and 10). (n=17 for the no drug condition, n=10 for the baricitinib and remdesivir alone conditions, and n=6 for the combined baricitinib and remdesivir conditions). All statistics were calculated using the Mann-Whitney U-test in Prism. * p<0.05, ** p<0.01, ***p<0.001.*

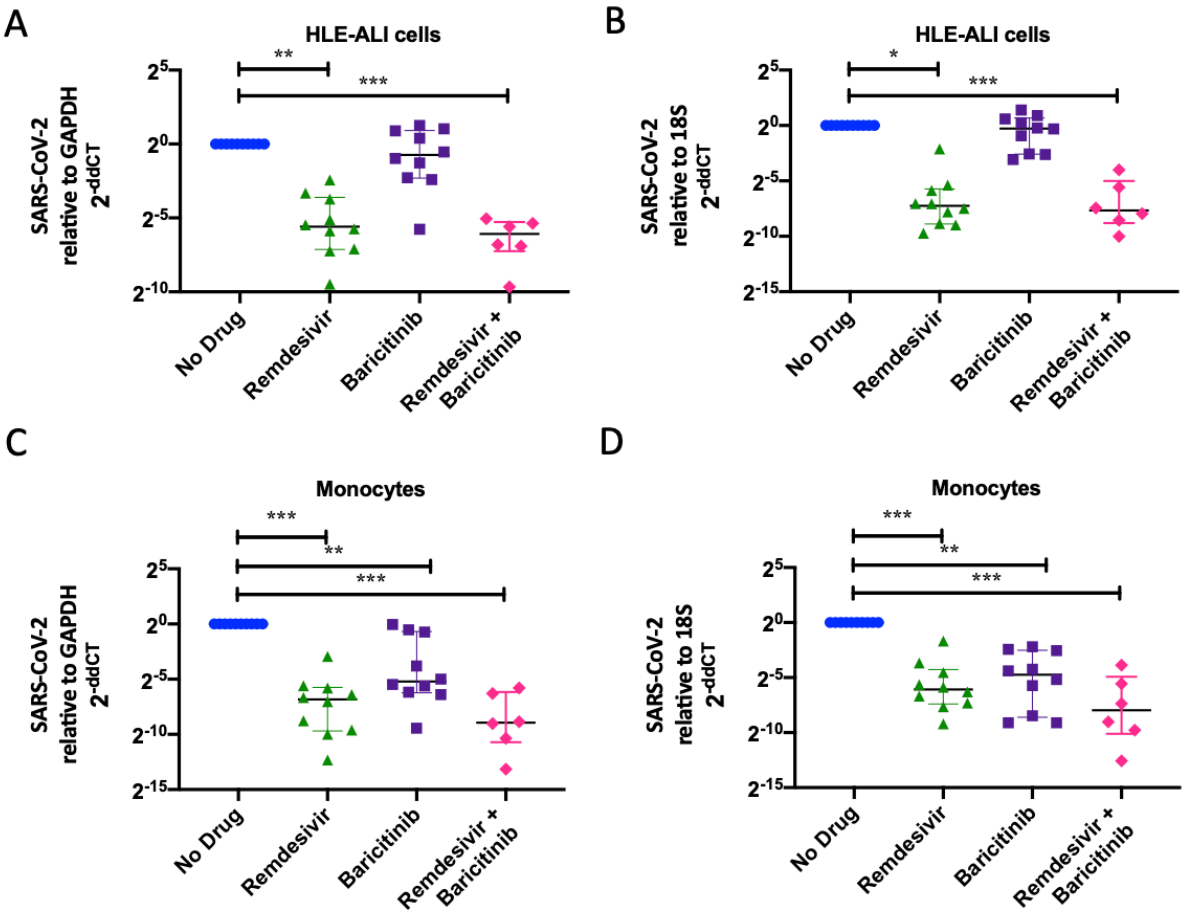

*Supplementary Figure 5.8. Related to Figure 5.5. (A-D) Calculated SARS-CoV-2 genome copies in each cell was normalized to either GAPDH (A,C) or 18S rRNA (B,D) in either HLE-ALI cells (A,B) or monocytes (C,D) using the delta delta Ct method (see Supplementary Tables 9 and 10). (n=10 for the no drug condition and the baricitinib and remdesivir alone conditions, and n=6 for the combined baricitinib and remdesivir conditions). All statistics were calculated using the Mann-Whitney U-test in Prism. * p<0.05, ** p<0.01, ***p<0.001.*

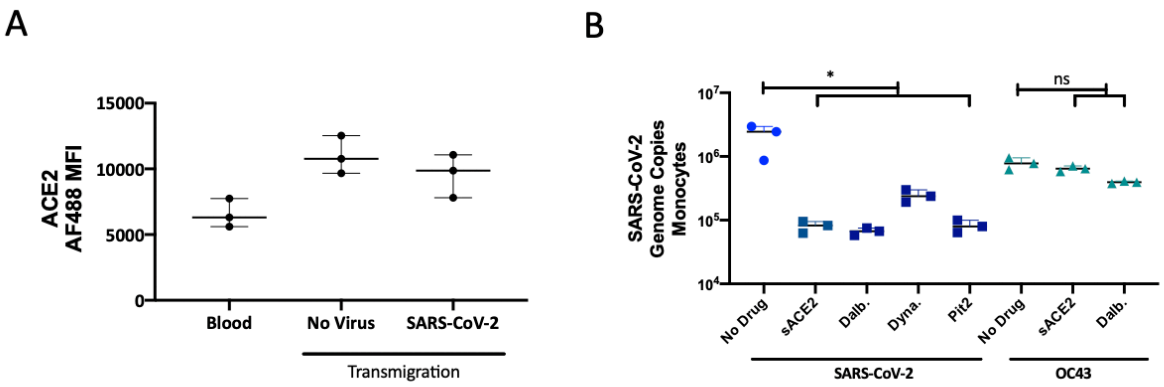

*Supplementary Figure 5.9. Related to Figure 5.5. A) Purified blood monocytes from blood before and after transmigration across HLE-ALI cells with or without infection with SARS-CoV-2 were stained for the presence of surface ACE2 and then measured by flow cytometry (n=3 biological replicates). B) Monocytes were transmigrated across HLE-ALI cells infected with either SARS-CoV-2 or OC43. In the apical fluid were soluble ACE2 (200 µg/mL), dalbavancin (1 µM), Dynasore (80 µM) or pitstop2 (15 µM) (n=3 biological replicates). Statistics were calculated using a Mann-Whitney U-test in Prism. * p<0.05, ** p<0.01, ***p<0.001.*

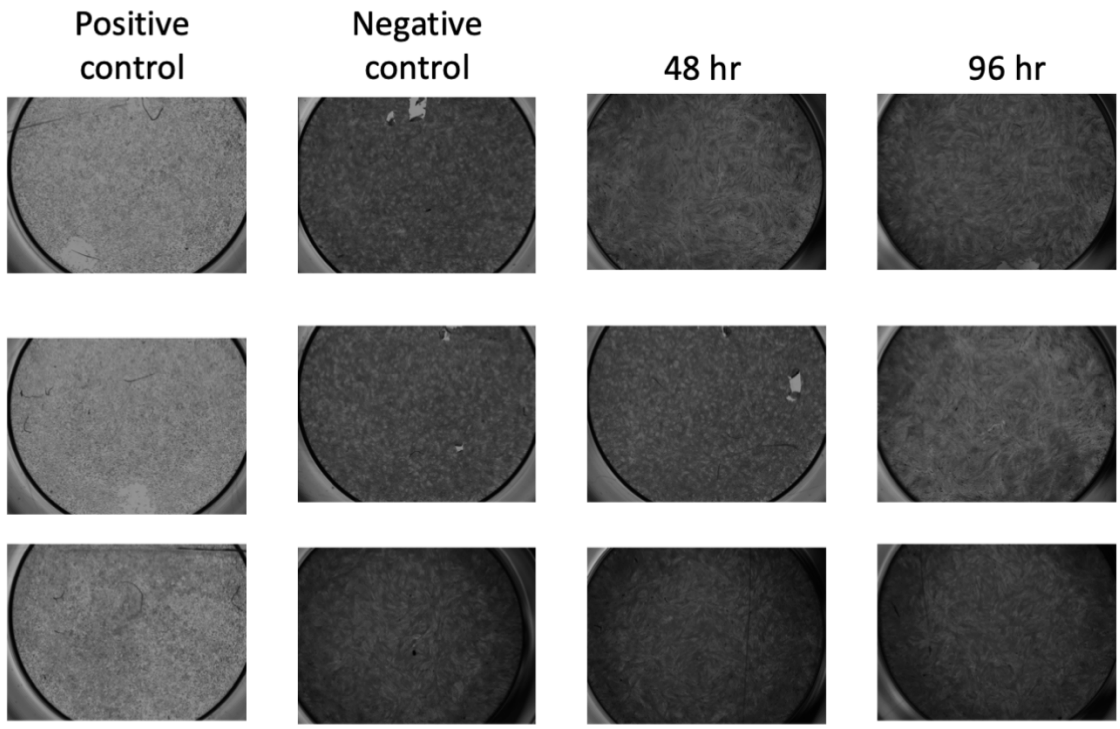

Supplementary Figure 5.10 (related to Figure 5.6E). Plaque assay. The extracellular fluid was layered onto VeroE6 cells to perform a plaque assay. The positive control was the direct application of 2.5 x 104 genome copies of SARS-CoV-2 to the cells.

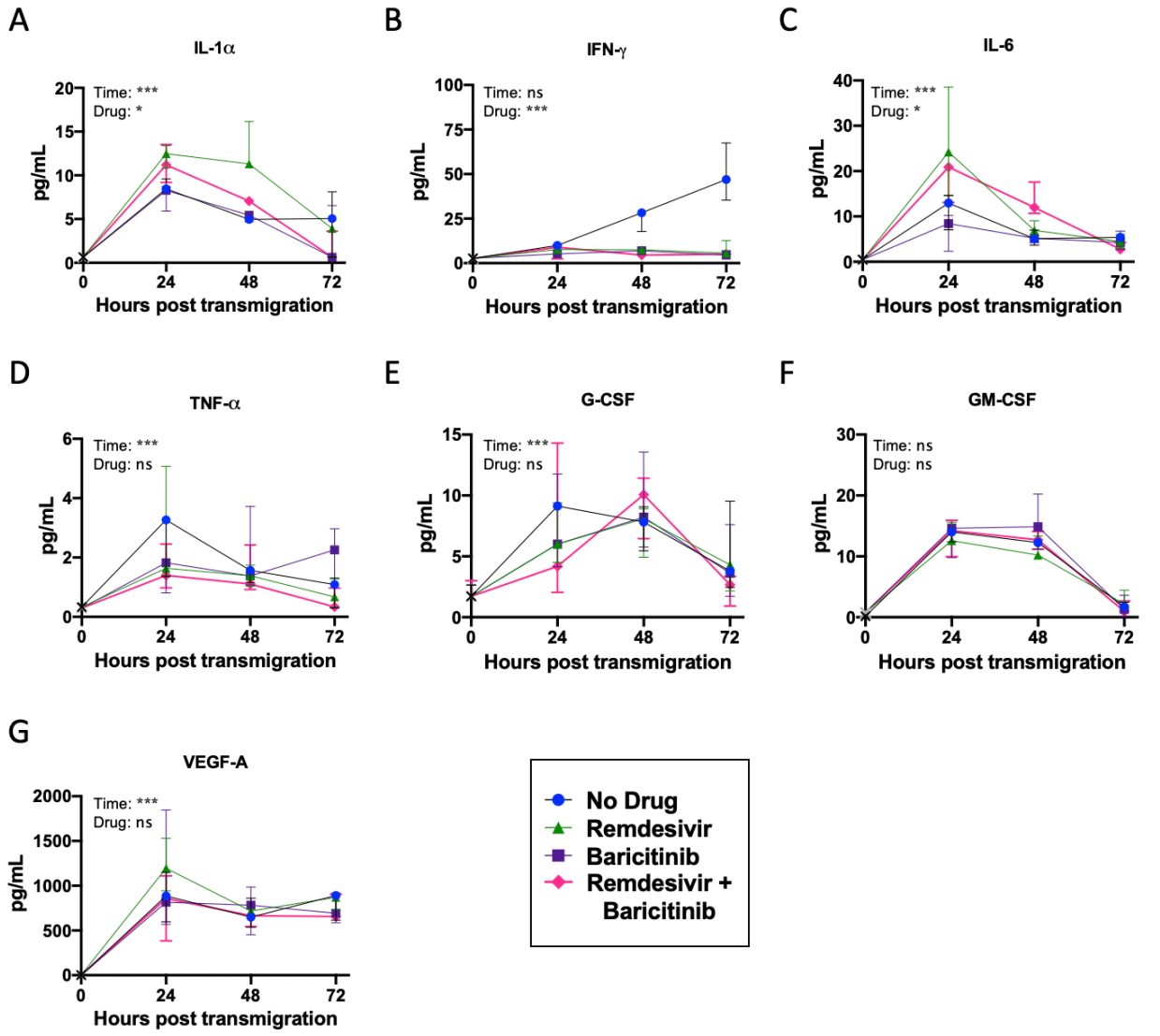

*Supplementary Figure 5.11 (related to Figure 5.6). Inflammatory mediators from each of the monocyte treatment conditions were quantified using an electrochemiluminescent assay from n=3 biological replicates. All statistics were calculated with a two-way ANOVA, main effects model in Prism with Geisser-Greenhouse correction applied. * p<0.05, ** p<0.01, ***p<0.001. Shown are median and interquartile range.*

REFERENCES

1. Abassi, Z., Knaney, Y., Karram, T., and Heyman, S.N. (2020). The Lung Macrophage in SARS-CoV-2 Infection: A Friend or a Foe? Front Immunol *11*, 1312. 10.3389/fimmu.2020.01312. PMC7291598
2. Acharya, D., Liu, G., and Gack, M.U. (2020). Dysregulation of Type I Interferon Responses in COVID-19. Nat Rev Immunol *20*, 397-398. 10.1038/s41577-020-0346-x. PMC7249038
3. Bayati, A., Kumar, R., Francis, V., and McPherson, P.S. (2021). SARS-CoV-2 Infects Cells after Viral Entry Via Clathrin-Mediated Endocytosis. J Biol Chem *296*, 100306. 10.1016/j.jbc.2021.100306. PMC7816624
4. Beigel, J.H., Tomashek, K.M., Dodd, L.E., Mehta, A.K., Zingman, B.S., Kalil, A.C., Hohmann, E., Chu, H.Y., Luetkemeyer, A., Kline, S.*, et al.* (2020). Remdesivir for the Treatment of Covid-19 - Final Report. N Engl J Med *383*, 1813-1826. 10.1056/NEJMoa2007764. PMC7262788
5. Blanco-Melo, D., Nilsson-Payant, B.E., Liu, W.C., Uhl, S., Hoagland, D., Moller, R., Jordan, T.X., Oishi, K., Panis, M., Sachs, D.*, et al.* (2020). Imbalanced Host Response to SARS-CoV-2 Drives Development of COVID-19. Cell *181*, 1036-1045 e1039. 10.1016/j.cell.2020.04.026. PMC7227586
6. Bost, P., De Sanctis, F., Cane, S., Ugel, S., Donadello, K., Castellucci, M., Eyal, D., Fiore, A., Anselmi, C., Barouni, R.M.*, et al.* (2021). Deciphering the State of Immune Silence in Fatal COVID-19 Patients. Nat Commun *12*, 1428. 10.1038/s41467-021-21702-6. PMC7935849
7. Boumaza, A., Gay, L., Mezouar, S., Bestion, E., Diallo, A.B., Michel, M., Desnues, B., Raoult, D., La Scola, B., Halfon, P.*, et al.* (2021). Monocytes and Macrophages, Targets of Severe Acute Respiratory Syndrome Coronavirus 2: The Clue for Coronavirus Disease 2019 Immunoparalysis. J Infect Dis *224*, 395-406. 10.1093/infdis/jiab044. PMC7928817
8. Chu, H., Chan, J.F., Wang, Y., Yuen, T.T., Chai, Y., Hou, Y., Shuai, H., Yang, D., Hu, B., Huang, X.*, et al.* (2020). Comparative Replication and Immune Activation Profiles of SARS-CoV-2 and SARS-CoV in Human Lungs: An Ex Vivo Study with Implications for the Pathogenesis of COVID-19. Clin Infect Dis *71*, 1400-1409. 10.1093/cid/ciaa410. PMC7184390
9. Coperchini, F., Chiovato, L., Croce, L., Magri, F., and Rotondi, M. (2020). The Cytokine Storm in COVID-19: An Overview of the Involvement of the Chemokine/Chemokine-Receptor System. Cytokine Growth Factor Rev *53*, 25-32. 10.1016/j.cytogfr.2020.05.003. PMC7211650
10. Dinarello, C.A. (2018). Overview of the IL-1 Family in Innate Inflammation and Acquired Immunity. Immunol Rev *281*, 8-27. 10.1111/imr.12621. PMC5756628
11. Dobosh, B., Giacalone, V.D., Margaroli, C., and Tirouvanziam, R. (2021). Mass Production of Human Airway-Like Neutrophils Via Transmigration in an Organotypic Model of Human Airways. STAR Protoc *2*, 100892. 10.1016/j.xpro.2021.100892. PMC8551927
12. Dobosh, B., Zandi, K., Giraldo, D.M., Goh, S.L., Musall, K., Aldeco, M., LeCher, J., Giacalone, V.D., Yang, J., Eddins, D.J.*, et al.* (2022). Baricitinib Attenuates the Proinflammatory Phase of COVID-19 Driven by Lung-Infiltrating Monocytes. Cell Rep *39*, 110945. 10.1016/j.celrep.2022.110945.
13. Donnelly, S.C., Strieter, R.M., Kunkel, S.L., Walz, A., Robertson, C.R., Carter, D.C., Grant, I.S., Pollok, A.J., and Haslett, C. (1993). Interleukin-8 and Development of Adult Respiratory

Distress Syndrome in at-Risk Patient Groups. Lancet *341*, 643-647. 10.1016/0140-6736(93)90416-e. PMID: 8095568
14. Ely, E.W., Ramanan, A.V., Kartman, C.E., de Bono, S., Liao, R., Piruzeli, M.L.B., Goldman, J.D., Saraiva, J.F.K., Chakladar, S., Marconi, V.C*., et al.* (2022). Efficacy and Safety of Baricitinib Plus Standard of Care for the Treatment of Critically Ill Hospitalised Adults with COVID-19 on Invasive Mechanical Ventilation or Extracorporeal Membrane Oxygenation: An Exploratory, Randomised, Placebo-Controlled Trial. Lancet Respir Med *10*, 327-336. 10.1016/S2213-2600(22)00006-6. PMC8813065
15. Eroshenko, N., Gill, T., Keaveney, M.K., Church, G.M., Trevejo, J.M., and Rajaniemi, H. (2020). Implications of Antibody-Dependent Enhancement of Infection for SARS-CoV-2 Countermeasures. Nat Biotechnol *38*, 789-791. 10.1038/s41587-020-0577-1. PMID: 32504046
16. Falasca, L., Nardacci, R., Colombo, D., Lalle, E., Di Caro, A., Nicastri, E., Antinori, A., Petrosillo, N., Marchioni, L., Biava, G*., et al.* (2020). Postmortem Findings in Italian Patients with COVID-19: A Descriptive Full Autopsy Study of Cases with and without Comorbidities. J Infect Dis *222*, 1807-1815. 10.1093/infdis/jiaa578. PMC7543426
17. Ford, B.D., Moncada Giraldo, D., Margaroli, C., Giacalone, V.D., Brown, M.R., Peng, L., and Tirouvanziam, R. (2021). Functional and Transcriptional Adaptations of Blood Monocytes Recruited to the Cystic Fibrosis Airway Microenvironment in Vitro. Int J Mol Sci *22*. 10.3390/ijms22052530. PMC7959310
18. Forrest, O.A., Ingersoll, S.A., Preininger, M.K., Laval, J., Limoli, D.H., Brown, M.R., Lee, F.E., Bedi, B., Sadikot, R.T., Goldberg, J.B*., et al.* (2018). Frontline Science: Pathological Conditioning of Human Neutrophils Recruited to the Airway Milieu in Cystic Fibrosis. J Leukoc Biol *104*, 665-675. 10.1002/JLB.5HI1117-454RR. PMC6956843
19. Gordon, D.E., Jang, G.M., Bouhaddou, M., Xu, J., Obernier, K., White, K.M., O'Meara, M.J., Rezelj, V.V., Guo, J.Z., Swaney, D.L*., et al.* (2020). A SARS-CoV-2 Protein Interaction Map Reveals Targets for Drug Repurposing. Nature *583*, 459-468. 10.1038/s41586-020-2286-9. PMC7431030
20. Grunwell, J.R., Giacalone, V.D., Stephenson, S., Margaroli, C., Dobosh, B.S., Brown, M.R., Fitzpatrick, A.M., and Tirouvanziam, R. (2019). Neutrophil Dysfunction in the Airways of Children with Acute Respiratory Failure Due to Lower Respiratory Tract Viral and Bacterial Coinfections. Sci Rep *9*, 2874. 10.1038/s41598-019-39726-w. PMC6393569
21. Henderson, L.A., Canna, S.W., Schulert, G.S., Volpi, S., Lee, P.Y., Kernan, K.F., Caricchio, R., Mahmud, S., Hazen, M.M., Halyabar, O*., et al.* (2020). On the Alert for Cytokine Storm: Immunopathology in COVID-19. Arthritis Rheumatol *72*, 1059-1063. 10.1002/art.41285. PMC7262347
22. Hoang, T.N., Pino, M., Boddapati, A.K., Viox, E.G., Starke, C.E., Upadhyay, A.A., Gumber, S., Nekorchuk, M., Busman-Sahay, K., Strongin, Z*., et al.* (2021). Baricitinib Treatment Resolves Lower-Airway Macrophage Inflammation and Neutrophil Recruitment in SARS-CoV-2-Infected Rhesus Macaques. Cell *184*, 460-475 e421. 10.1016/j.cell.2020.11.007. PMC7654323
23. Junqueira, C., Crespo, A., Ranjbar, S., Ingber, J., Parry, B., Ravid, S., de Lacerda, L.B., Lewandrowski, M., Clark, S., Ho, F*., et al.* (2021). SARS-CoV-2 Infects Blood Monocytes to

Activate NLRP3 and AIM2 Inflammasomes, Pyroptosis and Cytokine Release. medRxiv. 10.1101/2021.03.06.21252796. PMC7987031
24. Kalil, A.C., Patterson, T.F., Mehta, A.K., Tomashek, K.M., Wolfe, C.R., Ghazaryan, V., Marconi, V.C., Ruiz-Palacios, G.M., Hsieh, L., Kline, S.*, et al.* (2021). Baricitinib Plus Remdesivir for Hospitalized Adults with Covid-19. N Engl J Med *384*, 795-807. 10.1056/NEJMoa2031994. PMC7745180
25. Krishnamurthy, S., Lockey, R.F., and Kolliputi, N. (2021). Soluble ACE2 as a Potential Therapy for COVID-19. Am J Physiol Cell Physiol *320*, C279-C281. 10.1152/ajpcell.00478.2020. PMC7938633
26. Laucirica, D.R., Schofield, C.J., McLean, S.A., Margaroli, C., Agudelo-Romero, P., Stick, S.M., Tirouvanziam, R., Kicic, A., Garratt, L.W., Western Australian Epithelial Research, P.*, et al.* (2022). Pseudomonas Aeruginosa Modulates Neutrophil Granule Exocytosis in an in Vitro Model of Airway Infection. Immunol Cell Biol *100*, 352-370. 10.1111/imcb.12547. PMID: 35318736
27. Li, M., Zhang, Y., Lu, J., Li, L., Gao, H., Ma, C., Dai, E., and Wei, L. (2021). Asymptomatic COVID-19 Individuals Tend to Establish Relatively Balanced Innate and Adaptive Immune Responses. Pathogens *10*. 10.3390/pathogens10091105. PMC8468997
28. Liao, M., Liu, Y., Yuan, J., Wen, Y., Xu, G., Zhao, J., Cheng, L., Li, J., Wang, X., Wang, F.*, et al.* (2020). Single-Cell Landscape of Bronchoalveolar Immune Cells in Patients with COVID-19. Nat Med *26*, 842-844. 10.1038/s41591-020-0901-9. PMID: 32398875
29. Mason, R.J. (2020). Pathogenesis of COVID-19 from a Cell Biology Perspective. Eur Respir J *55*. 10.1183/13993003.00607-2020. PMC7144260
30. Merad, M., and Martin, J.C. (2020). Pathological Inflammation in Patients with COVID-19: A Key Role for Monocytes and Macrophages. Nat Rev Immunol *20*, 355-362. 10.1038/s41577-020-0331-4. PMC7201395
31. Monteil, V., Kwon, H., Prado, P., Hagelkruys, A., Wimmer, R.A., Stahl, M., Leopoldi, A., Garreta, E., Hurtado Del Pozo, C., Prosper, F.*, et al.* (2020). Inhibition of SARS-CoV-2 Infections in Engineered Human Tissues Using Clinical-Grade Soluble Human ACE2. Cell *181*, 905-913 e907. 10.1016/j.cell.2020.04.004. PMC7181998
32. Patterson, B.K., Francisco, E.B., Yogendra, R., Long, E., Pise, A., Rodrigues, H., Hall, E., Herrera, M., Parikh, P., Guevara-Coto, J.*, et al.* (2021). Persistence of Sars Cov-2 S1 Protein in CD16+ Monocytes in Post-Acute Sequelae of COVID-19 (PASC) up to 15 Months Post-Infection. Front Immunol *12*, 746021. 10.3389/fimmu.2021.746021. PMC8784688
33. Perez-Alba, E., Nuzzolo-Shihadeh, L., Aguirre-Garcia, G.M., Espinosa-Mora, J., Lecona-Garcia, J.D., Flores-Perez, R.O., Mendoza-Garza, M., and Camacho-Ortiz, A. (2021). Baricitinib Plus Dexamethasone Compared to Dexamethasone for the Treatment of Severe COVID-19 Pneumonia: A Retrospective Analysis. J Microbiol Immunol Infect *54*, 787-793. 10.1016/j.jmii.2021.05.009. PMC8253716
34. Pontelli, M.C., Castro, I.A., Martins, R.B., Veras, F.P., Serra, L., Nascimento, D.C., Cardoso, R.S., Rosales, R., Lima, T.M., Souza, J.P.*, et al.* (2020). Infection of Human Lymphomononuclear Cells by SARS-CoV-2. bioRxiv. 10.1101/2020.07.28.225912. PMC8132220

35. Qin, C., Zhou, L., Hu, Z., Zhang, S., Yang, S., Tao, Y., Xie, C., Ma, K., Shang, K., Wang, W*., et al.* (2020). Dysregulation of Immune Response in Patients with Coronavirus 2019 (COVID-19) in Wuhan, China. Clin Infect Dis *71*, 762-768. 10.1093/cid/ciaa248. PMC7108125
36. Rao, V.U.S., Arakeri, G., Subash, A., Rao, J., Jadhav, S., Suhail Sayeed, M., Rao, G., and Brennan, P.A. (2020). COVID-19: Loss of Bridging between Innate and Adaptive Immunity? Med Hypotheses *144*, 109861. 10.1016/j.mehy.2020.109861. PMC7245229
37. Ravindra, N.G., Alfajaro, M.M., Gasque, V., Huston, N.C., Wan, H., Szigeti-Buck, K., Yasumoto, Y., Greaney, A.M., Habet, V., Chow, R.D*., et al.* (2021). Single-Cell Longitudinal Analysis of SARS-CoV-2 Infection in Human Airway Epithelium Identifies Target Cells, Alterations in Gene Expression, and Cell State Changes. PLoS Biol *19*, e3001143. 10.1371/journal.pbio.3001143. PMC8007021
38. Schulte-Schrepping, J., Reusch, N., Paclik, D., Bassler, K., Schlickeiser, S., Zhang, B., Kramer, B., Krammer, T., Brumhard, S., Bonaguro, L*., et al.* (2020). Severe COVID-19 Is Marked by a Dysregulated Myeloid Cell Compartment. Cell *182*, 1419-1440 e1423. 10.1016/j.cell.2020.08.001. PMC7405822
39. Sefik, E., Qu, R., Junqueira, C., Kaffe, E., Mirza, H., Zhao, J., Brewer, J.R., Han, A., Steach, H.R., Israelow, B*., et al.* (2022). Inflammasome Activation in Infected Macrophages Drives COVID-19 Pathology. bioRxiv, 2021.2009.2027.461948. 10.1101/2021.09.27.461948. PMC8491846
40. Stebbing, J., Krishnan, V., de Bono, S., Ottaviani, S., Casalini, G., Richardson, P.J., Monteil, V., Lauschke, V.M., Mirazimi, A., Youhanna, S*., et al.* (2020). Mechanism of Baricitinib Supports Artificial Intelligence-Predicted Testing in COVID-19 Patients. EMBO Mol Med *12*, e12697. 10.15252/emmm.202012697. PMC7300657
41. Tan, M., Liu, Y., Zhou, R., Deng, X., Li, F., Liang, K., and Shi, Y. (2020). Immunopathological Characteristics of Coronavirus Disease 2019 Cases in Guangzhou, China. Immunology *160*, 261-268. 10.1111/imm.13223. PMC7283723
42. Tang, D., Comish, P., and Kang, R. (2020). The Hallmarks of COVID-19 Disease. PLoS Pathog *16*, e1008536. 10.1371/journal.ppat.1008536. PMC7244094
43. Tay, M.Z., Poh, C.M., Renia, L., MacAry, P.A., and Ng, L.F.P. (2020). The Trinity of COVID-19: Immunity, Inflammation and Intervention. Nat Rev Immunol *20*, 363-374. 10.1038/s41577-020-0311-8. PMC7187672
44. Vanderheiden, A., Ralfs, P., Chirkova, T., Upadhyay, A.A., Zimmerman, M.G., Bedoya, S., Aoued, H., Tharp, G.M., Pellegrini, K.L., Manfredi, C*., et al.* (2020). Type I and Type III Interferons Restrict SARS-CoV-2 Infection of Human Airway Epithelial Cultures. J Virol *94*. 10.1128/JVI.00985-20. PMC7495371
45. Wang, G., Yang, M.L., Duan, Z.L., Liu, F.L., Jin, L., Long, C.B., Zhang, M., Tang, X.P., Xu, L., Li, Y.C*., et al.* (2021). Dalbavancin Binds ACE2 to Block Its Interaction with SARS-CoV-2 Spike Protein and Is Effective in Inhibiting SARS-CoV-2 Infection in Animal Models. Cell Res *31*, 17-24. 10.1038/s41422-020-00450-0. PMC7705431
46. Weston, S., and Frieman, M.B. (2020). COVID-19: Knowns, Unknowns, and Questions. mSphere *5*, e00203-00220. 10.1128/mSphere.00203-20. PMC7082143
47. Zhang, B., Zhou, X., Zhu, C., Song, Y., Feng, F., Qiu, Y., Feng, J., Jia, Q., Song, Q., Zhu, B*., et al.* (2020). Immune Phenotyping Based on the Neutrophil-to-Lymphocyte Ratio and IgG

Level Predicts Disease Severity and Outcome for Patients with COVID-19. Front Mol Biosci *7*, 157. 10.3389/fmolb.2020.00157. PMC7350507

48. Zhou, Z., Ren, L., Zhang, L., Zhong, J., Xiao, Y., Jia, Z., Guo, L., Yang, J., Wang, C., Jiang, S*., et al.* (2020). Heightened Innate Immune Responses in the Respiratory Tract of COVID-19 Patients. Cell Host Microbe *27*, 883-890 e882. 10.1016/j.chom.2020.04.017. PMC7196896
49. Zuniga, E.I., Macal, M., Lewis, G.M., and Harker, J.A. (2015). Innate and Adaptive Immune Regulation During Chronic Viral Infections. Annu Rev Virol *2*, 573-597. 10.1146/annurev-virology-100114-055226. PMC4785831

Chapter 6: SUMMARY AND FUTURE DIRECTIONS

MUSINGS ON COMMUNICATION VIA EVS

EVs are small biological particles carrying lipids, carbohydrates, proteins and nucleic acids ubiquitously released by all cells during both homeostasis and disease conditions, and can serve as biomarkers of disease diagnosis and pathogenesis (Mulcahy et al., 2014; Mathieu et al., 2019). EVs present an interesting medium by which autocrine and paracrine signaling may occur to steer the inflammatory response, depending upon their contents (Mulcahy et al., 2014; Tkach and Thery, 2016; Mathieu et al., 2019). The mechanisms for sorting cargo into EVs are complex and not completely understood and differ depending on the cell type being observed and the phenotype of the producing cell at the moment of EV biogenesis.

At any given time, a cell may be either producing and/or receiving EVs. Thus, a cell can be either a net producer or a net recipient of EVs. A cell that is a net producer will modulate the phenotype of other cells, whereas a recipient cell will alter its phenotype in response to the EVs that it processes. In the context of the recursive and feed-forward inflammatory process driven by MALAT1+ PMN EVs in CF airways **(See Chapter 4)**, a GRIM PMN having established residence in CF airways for a few hours would be considered a producer cell. Meanwhile a naïve, newly immigrated PMN would be a recipient cell. From this, it is clear that cells can change from a recipient cell to a producer cell. It should also be possible for a cell to go from being a producer cell to a recipient cell. The transition between these phenotypes may be a result of a premade transcriptional/translational program or because of input from the EV population or other extracellular stimuli. This also begs the question of whether a cell is predisposed to becoming either a recipient or producer cell and how sensitive a cell is to changing its status between

producer and recipient. In addition, since the population of EVs secreted by a cell are not homogenous, perhaps a cell can be a producer of one subset of EVs (perhaps a pathogenic entity), while still being a net recipient. For example, scavenger cells could remove EVs from environments laden with debris after an infection or injury while still releasing EVs to promote the resolution of an immune response (Wang et al., 2020b; Hu et al., 2021; Yang et al., 2022). Indeed, the general premise for the concept of producer and recipient cells can be observed in cytokine responses as well as when leukocytes enter a tissue in response to a stimuli (the leukocyte is a net recipient, while the damaged cells, and perhaps bystander cells, within the tissues are net producers). As infiltrating leukocytes come into contact with the site of inflammation, they may release their own mediators, thus transitioning to a net producer state.

Due to the ubiquitous nature of EVs, it is difficult to determine what qualities of both the producer cell and recipient cell populations are involved in EV transfer and cell-to-cell communication. The producer cell determines physical aspects of the EV such as the intra-EV cargo, the lipid, carbohydrate, and protein contents of the membrane. This includes the surface protein and glycans, which comes together to form the size, sphericity, viscosity, and 'stickiness' of the particle. This 'sticky factor' is particularly confounding because an EV can then potentially sponge extracellular material made by other 'pseudo-producer' cells, which may be observed in the protein-corona that many EVs have. The recipient cell on the other hand displays receptors and ligands recognized by cognate ligands and receptors on EVs. These determine the mechanism of uptake of the particle by macropinocytosis, phagocytosis, or receptor-mediated endocytosis, which is also determined in large part by what the producer cell displays on the surface of its EVs (Mulcahy et al., 2014). The recipient cell also expresses

factors that determine whether and how the lysosome degrades the contents of EVs that have been taken up (Dellar et al., 2022; O'Brien et al., 2022). This in turn impacts how the recipient cell reacts to the EV cargo. Does a particular miRNA become functional and bind to its cognate sequence or does it become degraded into ribonucleotides for transcription or as an alternative energy source? Do deoxyribonucleotides become substrates for cyclization and agonistic activation of the STING receptor? Similarly, do EV lipids feed into formation of membranes for organelles, become fuel for beta-oxidation or become attached post-translationally to proteins (Skotland et al., 2020)? While researchers have merely scratched the surface of the transfer of functional effector cargo on recipient cells, the effect of the "non-functional" cargo has yet to be explored in any significant detail.

Scavenger cells, which by nature consume a lot of extracellular material including large numbers of EVs, may be uniquely poised to degrade EVs and contents therein, as well as adapt to their environment as a result of the packaged biomolecules. How many EVs does it take for a scavenger cell to see its phenotype change? Essentially, what is their minimum infective dose? In related research on viral infection, it has been shown that small numbers of viruses infecting a cell, results in inefficient viral replication and difficulty with evading the host immune response (Santiana et al., 2018; Andreu-Moreno and Sanjuan, 2020). In order to prevent the production of pathogenic EVs we must determine when PMNs are releasing or producing EVs. Similarly, to prevent the induction of a pathogenic fate, we must determine which cells are more likely to take up an EV since it is likely that not all PMNs maintain the same rate of pinocytosis, endocytosis and other EV uptake mechanisms. Thus, a proper EV-directed therapy must prevent both the production as well as the uptake/processing of pathogenic EVs.

Due to the nature of the feed-forward inflammation presented in this work **(See Chapter 3, Chapter 4)**, if either the production or uptake of pathogenic EVs can be prevented, then the presence of inflammatory PMNs that neglect bacteria should be cleared. The population of PMNs at any given time in the airways is quite heterogenous being comprised of PMNs that just immigrated to cells that have been present for around a day and every timepoint between. Arguably, each of these cells will potentially release unique populations of EVs as well as have varying responses to each of the EV populations.

FUTURE DIRECTIONS REGARDING PMN-DRIVEN INFLAMMATION

One of the major aspects of this thesis that may not be as obvious as the conceptual additions to PMN, monocyte, and EV biology, is that the standard toolbox of molecular biology applies to PMNs. Very few groups have manipulated neutrophils with any kind of exogenous genetic material (i.e., plasmids, mRNA, siRNA, or viral vectors.). One group electroporated human blood PMNs with a plasmid expressing EGFP, beta-galactosidase as well as p47 (Johnson et al., 2006). In addition, they showed that upon stimulation, PMNs express the transgene after just two hours post-transfection (although they did not share data from earlier timepoints). In another study, PMNs were electroporated with plasmids expressing PKCε fused to EGFP (Tamassia et al., 2012). Of note, transfection with a plasmid expressing just EGFP were also able to stimulate PMNs via the TLR4 pathway (Tamassia et al., 2012). In our studies, we expressed the null transcript mScarlet or a scramble siRNA to account for these effects. To our knowledge, no other group has shown functional transfection of primary human PMNs nor successful knockdown of transcripts as result of an siRNA being expressed off of a plasmid **(See Chapter**

4). Thus, we can begin to generate libraries of miRNAs/siRNAs, utilize reporter constructs, conduct CRISPR screens and much more. This allows for a new level of screening for PMN-targeted therapeutics.

HDAC11 and MALAT1

It is still unclear what the targets of HDAC11 are in PMNs, since this enzyme acts both as a histone deacetylase as well as a lysine defatty acylase (de-palmitoylase/myristoylase) (Lin et al., 2013; Cao et al., 2019). To approach this problem, the most direct biological approach would be to incubate the cells with Alk14, a palmitic acid analog with a terminal alkyne group available for copper-catalyzed click chemistry that gets post-translationally added in the same manner as natural long-chain palmitoyl groups (Zheng et al., 2016; Cao et al., 2019). Including inhibitors of HDAC11, such as SIS17 or FT895 or HDAC11 knockdowns or knockouts would lend specificity of this approach for HDAC11 (Martin et al., 2018; Son et al., 2019; Li et al., 2020).

Alternatively, we can attempt to predict targets that are palmitoylated (or myristoylated) (Ren et al., 2008) and determine whether we observe changes in the target protein amounts based on the acquired EV proteomics. For example, the Src family tyrosine protein kinase Lyn, which has traditionally been studied for its role in B-cell differentiation, proliferation, and survival (Brodie et al., 2018) is also present in other cells, including PMNs. Lyn has previously been shown to rapidly phosphorylate substrates in response to PMN stimulation (Gaudry et al., 1995) and promoting PMN chemotaxis to wounds in zebrafish (Yoo et al., 2011). Additionally, Lyn was shown to be packaged within EVs from multiple cell types and this Lyn localization to EVs is dependent on palmitoylation and myristoylation of its N-terminal signal peptide (Liang et al., 2001; Morinaga et al., 2017; O'Brien et al., 2022; Whitley et al., 2022).

Proteomics data from our group show that upon overexpression of HDAC11 in PMNs, Lyn is no longer present in EVs suggesting that palmitoylated-Lyn is a substrate of HDAC11, although this has to be further corroborated **(Figure 6.).** The transcriptional coactivator YES has been shown to be palmitoylated in the same fashion as Lyn and colocalizes with it (Sato et al., 2009). According to early transcriptomic data from our group (Cammarata-Mouchtouris, unpublished), YES and YES-associated protein (YAP) are differentially expressed in PMNs transmigrated to CF airway fluid when treated with the HDAC11 inhibitor SIS17. YES and YAP1 have also been shown to bind and colocalize with MALAT1 (Wang et al., 2014; Sun et al., 2016). Although many of these steps still need to be validated, it is possible that HDAC11 affects the ability of Lyn, YES, and YAP to colocalize to EVs and that in turn, colocalization of MALAT1 in EVs is also affected, thereby interrupting the feed-forward cycle of disease.

As menitoned earlier, LLPCs may contribute to the determination of EV cargo, as evidenced by the promotion of miRNA-223 loading of into exosomes by the LLPC-enriched ribonucleoprotein YBX1 (Liu et al., 2021). Multiple post-translational modifications impact the activity and localization of YBX1 including ubiquitination, acetylation, methylation, and phosphorylation. These post-translation modifications are also relevant for the formation of LLPCs in general (Owen and Shewmaker, 2019), and phosphorylation of YBX1 regulates its loading into EVs (Kossinova et al., 2017). One study argued that MALAT1 and YBX-1 exist within the same network, although it failed to show an interaction between the two molecules in certain cancers (Kumar and Mishra, 2022). Another study found that MALAT1 was not co-immunoprecipitated with YBX-1 in oral squamous cell carcinoma (Xu et al., 2017).

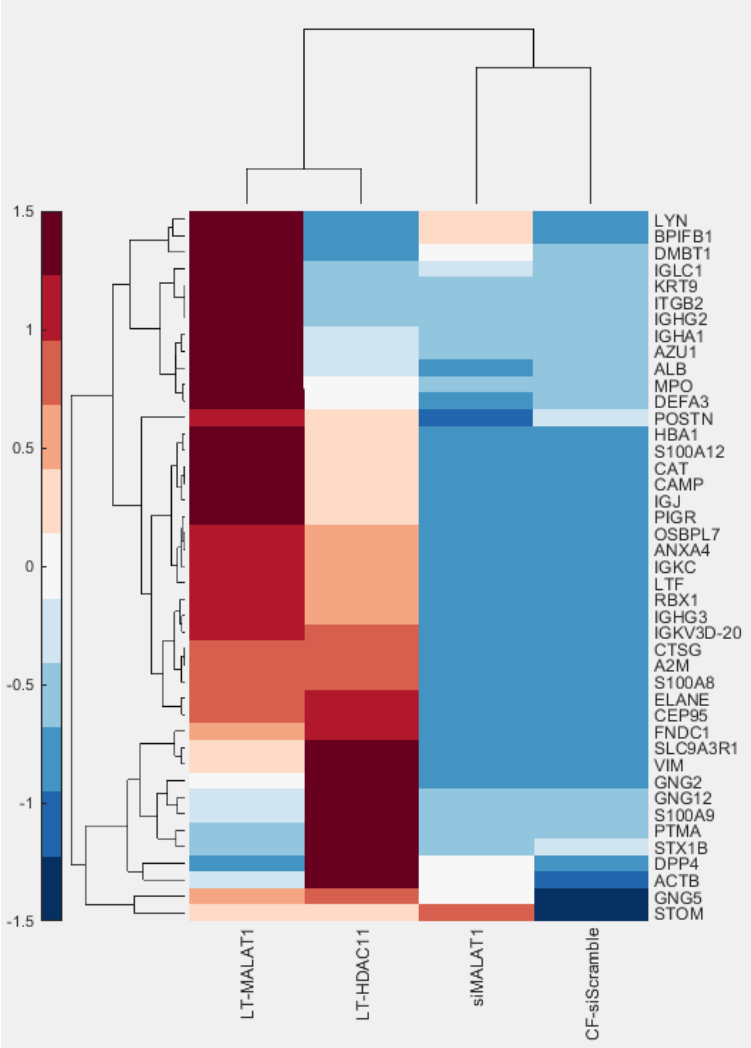

Figure 6.1: Changes in EV protein content following mRNA/siRNA transfection in airway-recruited human PMNs. Primary human blood PMNs were transfected with plasmids expressing either MALAT1 or HDAC11 and then transmigrated towards LTB4 or transfected with a plasmid expressing a scramble siRNA or siRNA targeting MALAT1 and transmigrated towards CFASN EVs for 4 hours. PMNs were purified and allowed to condition RPMI media for 12 hours after which total protein was extracted from purified EVs, digested by trypsin and analyzed by mass spectrometry.

Potential Mechanisms Regulating HDAC11

The Lyn/YES/YAP axis is one potential mechanism by which HDAC11 may affect MALAT1 localization to EVs. While we have clearly shown that PMN activation by HDAC11 and MALAT1 via EVs is a feed-forward process, how MALAT1 causes HDAC11 upregulation remains unknown. One possibility is that HDAC11 may be regulated post-transcriptionally by miRNA145-5p binding specifically to its 3'UTR sequence (Lin et al., 2013; Shinohara et al., 2017; Wang et al., 2020a).

Multiple studies have shown that miRNA145-5p[5] is readily packaged within EVs both in vitro and in vivo (Shinohara et al., 2017; Lutful Kabir et al., 2018; Sanz-Rubio et al., 2018; Jara et al., 2021; Zhang et al., 2021). One study has even linked miRNA145-5p within EVs to HDAC11 inhibition in tumor-associated macrophages and the downstream promotion of an M2 phenotype (Shinohara et al., 2017) proving the concept that EVs can regulate HDAC11 in immune cells. MALAT1, and the fragment of MALAT1 that we observe in our GRIM EVs has also been shown to act as a sink or sponge for miRNA145-5p, preventing it from degrading target transcripts (Lu et al., 2016; Liu et al., 2019). Similarly, the lncRNA TUG1 sponges miRNA145-5p and attenuates NF-kB during IAV infection (Tu et al., 2021). Interestingly miRNA145-5p also regulates CFTR and has been shown to be increased by expression of ΔF508 CFTR, endoplasmic reticulum stress, allergy, and viral infections (Collison et al., 2011; Gillen et al., 2011; Oglesby et al., 2013; Viart et al., 2015; Lutful Kabir et al., 2018; Bezzerri et al., 2021)

We surmise that miRNA145-5p is naturally present in EVs, perhaps as a mechanism to regulate PMN-induced inflammation via degradation of HDAC11 transcripts and that expression of MALAT1 prevents degradation of HDAC11 by sponging away miRNA145-5p. In this way, PMN inflammation driven by HDAC11 continues until the stress has been resolved. In the case or CF however, the stress of the epithelial cells is never resolved and thus PMNs are always present in an inflammatory state. There may be other factors affecting miRNA145 and promoting PMN activation. One is the transcription factor C/EBPβ (implicated in emergency granulopoiesis and PMN activation) which binds the promoter for miRNA145 to suppress its transcription (Sachdeva et al., 2012) potentially limiting the resolution of PMN inflammation by HDAC11.

[5] Not to be confused with miRNA451-5p, which is also readily packaged within EVs.

The NCBI gene annotation for HDAC11 lists an alternative polyadenylation site that has not been experimentally validated **(Figure 6.2)**. Of note, the main miRNA145-5p binding site identified in prior literature (Lin et al., 2013; Wang et al., 2020a) (colored arrows on **Figure 6.A**) is downstream of this alternative polyadenylation sequence (first blue polyA motif in **Figure 6.2A).** Furthermore, during a time-course of transmigration towards CFASN, which also continuously upregulated HDAC11 (**Figure 6.2B**), the aligned contigs from the RNA-seq dataset might show differential alignment across the 3'UTR in accordance with usage of this alternative polyadenylation site **(Figure 6.2B)**. Thus, HDAC11 transcript stability may be further regulated by poly-A binding protein complexes, a mechanism which has not been explored in PMNs due to the traditional dogma that these cells are transcriptionally silent – and a dogma that of course has now been shown to be incorrect by our group and others (Hu et al., 2016; Grieshaber-Bouyer et al., 2021; Margaroli et al., 2021).

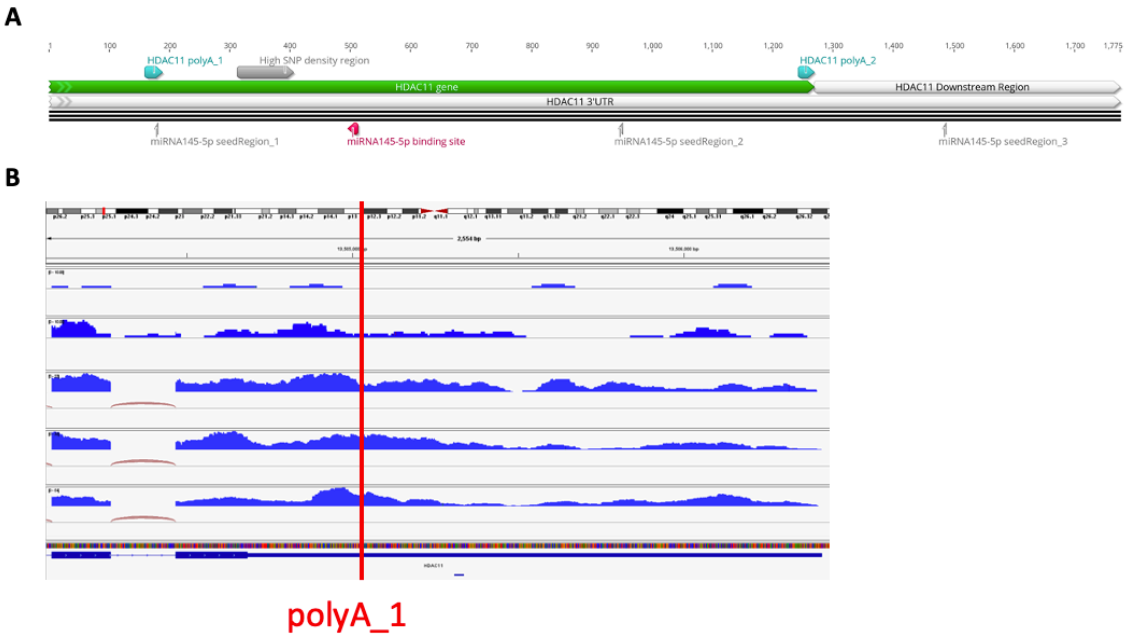

Figure 6.2: Homo sapiens HDAC11 3'UTR structure (green) with immediate downstream region also present. The canonical miRNA145-5p site is labeled in red, with three other potential miRNA145-5p seed binding regions also labeled in light gray. HDAC11 also has a region of high SNP density, which may regulate other interactions. There are two annotated polyadenylation sites for HDAC11. HDAC11 polyA_2 is the canonical polyadenylation site.

Metabolism and HDAC11

Metformin is a metabolic modulator that downregulates glucose-dependent PMN activation, ROS production and inflammation (Zmijewski et al., 2008; Piwkowska et al., 2010). We have also previously shown that metformin modulates GRIM PMNs by decreasing their metabolic activity, granule release, and oxidant production as well as oxygen consumption, but had no effect on bacteria killing capacity (Forrest et al., 2018). It will be interesting to determine how metformin treatment of GRIM PMNs affects their expression of HDAC11.

It was also found that PMNs precursors in the BM require autophagy of accumulated lipid droplets and fatty acid oxidation in order to overcome a block at the level of glycolysis and proceed with normal differentiation (Riffelmacher et al., 2017). The transcriptional poise of transmigrating PMNs into the airways seems to unlock developmental pathways such as mTOR, SP1 and cMyc (Margaroli et al., 2021). The uptake and autophagy of EVs may provide fuel for PMN activation and the repackaging of activating/pathogenic factors into newly generated EVs. This provides a basis for PMNs, and likely other scavenger cells, to process EVs, break them down into more basic components followed by repackaging and release into the environment. Hence, feed-forward PMN inflammation could potentially be prevented by lipase inhibitors or the addition of free fatty acids to block processing of EVs. SIS17 inhibits the defatty acylase activity of HDAC11 (Son et al., 2019) and induction of the GRIM fate **(See Chapter 4).** This inhibition decreases the available pool of lipids and thus may prevent subsequent breakdown of long chain fatty acids into acyl-CoA and fueling of fatty acid oxidation.

Mitochondria are organelles that are highly concentrated in proteins that are post-translationally modified with a wide range of acyl-lipids, which are chemically diverse (Ringel et

al., 2018). Long-chain modifications such as myristoylation and palmitoylation, partially regulated by HDAC11, are only a subset of the many acyl-lysine modifications that can occur (Pougovkina and de Boer, 2016). In addition, transmigrating PMNs transfer mitochondria to nearby cells with special EVs termed migrasomes (Ma et al., 2015) and may receive damaged mitochondria from other cells for subsequent recycling (Jiao et al., 2021), although how the PMN handles the received mitochondria is unclear. Mitochondria may be transferred to and by immune cells in other contexts as well, such as via nanotubes formed with cancer cells. Inhibition of nanotube formation and mitochondrial transfer increased efficacy of PD-1 checkpoint therapy in a breast cancer model (Saha et al., 2022).

In skeletal muscle cells HDAC11 has been observed to localize to mitochondria and show opposing activity with carnitine palmitoyl transferase (CPT1a) as well as inhibit the production of IL-10 (Hurtado et al., 2021; Nunez-Alvarez et al., 2021). HDAC11 has been shown to inhibit IL-10 in other contexts as well by competing with HDAC6 for the IL-10 promoter region – this may explain the low levels of IL-10 observed in the CF airways (Lin et al., 2013; Mukherjee et al., 2014). Interestingly, we observed that PMNs treated with SIS17, a drug that inhibits the deacylase activity of HDAC11, but not its histone deacetylation activity, increased their production of IL-10 **(See Chapter 4).**

HERVs

Links between virion formation and budding with EV synthesis have already been summarized earlier **(See Chapter 1)** as well as by other authors (Gould et al., 2003; Nolte-'t Hoen et al., 2016; van der Grein et al., 2022). There are remnants of ancient viruses that have been integrated into the genome known as endogenous retroviruses (ERVs), a subset of which

are human ERVs (HERVs). What was once referred to as “junk DNA” is now know to contain various regulatory regions and subsequences of ERVs. There are many subsets of HERVs, but the most well-studied is HERV-K, which has numerous locations throughout the human genome and plays a role in embryogenesis and cancer progression (Belshaw et al., 2004; Garcia-Montojo et al., 2018). In addition, expression of EZH2 in Ewing sarcoma cancer cells suppresses LINE-1 retrotransposons, multiple ERVs and IFNβ and antiviral signaling via MX1 and OAS1 (Jayabal et al., 2021). Although HERV genes are generally considered silenced in adult cells they may be expressed as a stress response including during SARS-CoV-2, influenza, or HIV infection (Li et al., 2014; Young et al., 2014; Denner, 2021; Kitsou et al., 2021; Temerozo et al., 2022). In fact, ERVs may compete with exogenous viruses for access to receptors as well as host factors necessary for viral replication such as nucleotides and amino acids and promote the production of defective virions (Srinivasachar Badarinarayan and Sauter, 2021). Alternatively, HERVs may also activate innate sensing pathways including interferon, RIG-I, MDA5, and OAS (Li et al., 2014; Chitrakar et al., 2021; Kuriyama et al., 2021; Song et al., 2021; Guo et al., 2022; Yan et al., 2022). PMNs from pulmonary arterial hypertension patients released NE on EVs and neutrophil extracellular traps (NETs) (Taylor et al., 2022). These PMNs also expressed HERV-K Env protein, IFIT1, RIGI-I, PKR and were more sensitized to IFN signaling by upregulation of IFNAR1, IFNAR2, and IFNGR2 (Taylor et al., 2022). Data acquired from a prior member of our lab, Thomas Bonneaud, showed the expression of HERV-E env and HERV-K env by PCR (data not shown) in LTB4 and CFASN transmigrated PMNs and reanalysis of the time course transcriptome (Margaroli et al., 2021) confirmed expression of multiple HERV genes **(Figure 6.3).** Exploring the

role of HERVs in the context of pathological EVs production and pro-inflammatory signaling by PMNs is a promising approach in which our group is engaging.

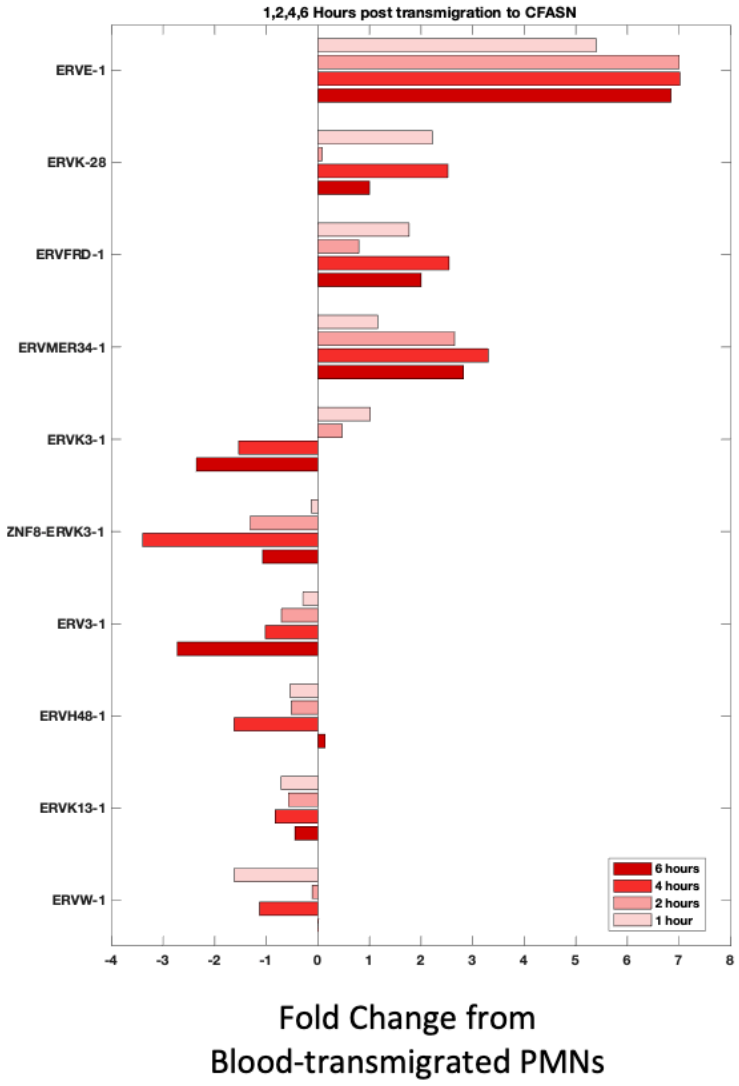

Figure 6.3: RNA-seq analysis of HERV-related genes in CFASN transmigrated PMNs from 1-6 hours compared to blood PMNs. Shown are the rapid dynamics of transcript for 10 HERVs during the process of transmigration of naïve human primary blood PMNs to CFASN in our model.

REFERENCES

1. Andreu-Moreno, I., and Sanjuan, R. (2020). Collective Viral Spread Mediated by Virion Aggregates Promotes the Evolution of Defective Interfering Particles. mBio *11*. 10.1128/mBio.02156-19. PMC6946798
2. Belshaw, R., Pereira, V., Katzourakis, A., Talbot, G., Paces, J., Burt, A., and Tristem, M. (2004). Long-Term Reinfection of the Human Genome by Endogenous Retroviruses. Proc Natl Acad Sci U S A *101*, 4894-4899. 10.1073/pnas.0307800101. PMC387345
3. Bezzerri, V., Gentili, V., Api, M., Finotti, A., Papi, C., Tamanini, A., Olioso, D., Duca, M., Tedesco, E., Leo, S.*, et al.* (2021). ACE2 Expression and Localization Are Regulated by CFTR: Implications Beyond Cystic Fibrosis. bioRxiv, 2021.2011.2019.469220. 10.1101/2021.11.19.469220.
4. Brodie, E.J., Infantino, S., Low, M.S.Y., and Tarlinton, D.M. (2018). Lyn, Lupus, and (B) Lymphocytes, a Lesson on the Critical Balance of Kinase Signaling in Immunity. Front Immunol *9*, 401. 10.3389/fimmu.2018.00401. PMC5837976
5. Cao, J., Sun, L., Aramsangtienchai, P., Spiegelman, N.A., Zhang, X., Huang, W., Seto, E., and Lin, H. (2019). HDAC11 Regulates Type I Interferon Signaling through Defatty-Acylation of SHMT2. Proc Natl Acad Sci U S A *116*, 5487-5492. 10.1073/pnas.1815365116. PMC6431144
6. Chitrakar, A., Solorio-Kirpichyan, K., Prangley, E., Rath, S., Du, J., and Korennykh, A. (2021). Introns Encode Dsrnas Undetected by Rig-I/Mda5/Interferons and Sensed Via Rnase L. Proc Natl Acad Sci U S A *118*. 10.1073/pnas.2102134118. PMC8609619
7. Collison, A., Mattes, J., Plank, M., and Foster, P.S. (2011). Inhibition of House Dust Mite-Induced Allergic Airways Disease by Antagonism of microRNA-145 Is Comparable to Glucocorticoid Treatment. J Allergy Clin Immunol *128*, 160-167 e164. 10.1016/j.jaci.2011.04.005.
8. Dellar, E.R., Hill, C., Melling, G.E., Carter, D.R.F., and Baena-Lopez, L.A. (2022). Unpacking Extracellular Vesicles: RNA Cargo Loading and Function. Journal of Extracellular Biology *1*, e40. 10.1002/jex2.40.
9. Denner, J. (2021). Porcine Endogenous Retroviruses and Xenotransplantation, 2021. Viruses *13*. 10.3390/v13112156. PMC8625113
10. Forrest, O.A., Ingersoll, S.A., Preininger, M.K., Laval, J., Limoli, D.H., Brown, M.R., Lee, F.E., Bedi, B., Sadikot, R.T., Goldberg, J.B.*, et al.* (2018). Frontline Science: Pathological Conditioning of Human Neutrophils Recruited to the Airway Milieu in Cystic Fibrosis. J Leukoc Biol *104*, 665-675. 10.1002/JLB.5HI1117-454RR. PMC6956843
11. Garcia-Montojo, M., Doucet-O'Hare, T., Henderson, L., and Nath, A. (2018). Human Endogenous Retrovirus-K (Hml-2): A Comprehensive Review. Crit Rev Microbiol *44*, 715-738. 10.1080/1040841X.2018.1501345. PMC6342650
12. Gaudry, M., Gilbert, C., Barabe, F., Poubelle, P.E., and Naccache, P.H. (1995). Activation of Lyn Is a Common Element of the Stimulation of Human Neutrophils by Soluble and Particulate Agonists. Blood *86*, 3567-3574. 10.1182/blood.V86.9.3567.bloodjournal8693567.
13. Gillen, A.E., Gosalia, N., Leir, S.H., and Harris, A. (2011). Microrna Regulation of Expression of the Cystic Fibrosis Transmembrane Conductance Regulator Gene. Biochem J *438*, 25-32. 10.1042/BJ20110672. PMC4323381

14. Gould, S.J., Booth, A.M., and Hildreth, J.E. (2003). The Trojan Exosome Hypothesis. Proc Natl Acad Sci U S A *100*, 10592-10597. 10.1073/pnas.1831413100. PMC196848
15. Grieshaber-Bouyer, R., Radtke, F.A., Cunin, P., Stifano, G., Levescot, A., Vijaykumar, B., Nelson-Maney, N., Blaustein, R.B., Monach, P.A., Nigrovic, P.A.*, et al.* (2021). The Neutrotime Transcriptional Signature Defines a Single Continuum of Neutrophils across Biological Compartments. Nat Commun *12*, 2856. 10.1038/s41467-021-22973-9. PMC8129206
16. Guo, E., Xiao, R., Wu, Y., Lu, F., Liu, C., Yang, B., Li, X., Fu, Y., Wang, Z., Li, Y.*, et al.* (2022). Wee1 Inhibition Induces Anti-Tumor Immunity by Activating Erv and the Dsrna Pathway. J Exp Med *219*. 10.1084/jem.20210789. PMC8628262 Biotechnology, GSK, ImmunoMET, Ionis, Lilly, PDX Pharmaceuticals, Signalchem Lifesciences, Symphogen, Tarveda, Turbine, Zentalis Pharmaceuticals, Catena Pharmaceuticals, HRD assay to Myriad Genetics, DSP to Nanostring, Adelson Medical Research Foundation, Breast Cancer Research Foundation, Komen Research Foundation, Ovarian Cancer Research Foundation, Prospect Creek Foundation, Nanostring Center of Excellence, Ionis (Provision of tool compounds), and Genentech during the conduct of the study; and personal fees, non-financial support, and "other" from Amphista, AstraZeneca, Chrysallis Biotechnology, GSK, ImmunoMET, Ionis, Lilly, PDX Pharmaceuticals, Signalchem Lifesciences, Symphogen, Tarveda, Turbine, Zentalis Pharmaceuticals, Catena Pharmaceuticals, HRD assay to Myriad Genetics, DSP to Nanostring, Adelson Medical Research Foundation, Breast Cancer Research Foundation, Komen Research Foundation, Ovarian Cancer Research Foundation, Prospect Creek Foundation, Nanostring Center of Excellence, Ionis (Provision of tool compounds), and Genentech outside the submitted work. No other disclosures were reported.
17. Hu, Q., Lyon, C.J., Fletcher, J.K., Tang, W., Wan, M., and Hu, T.Y. (2021). Extracellular Vesicle Activities Regulating Macrophage- and Tissue-Mediated Injury and Repair Responses. Acta Pharm Sin B *11*, 1493-1512. 10.1016/j.apsb.2020.12.014. PMC8245807
18. Hu, Z., Jiang, K., Frank, M.B., Chen, Y., and Jarvis, J.N. (2016). Complexity and Specificity of the Neutrophil Transcriptomes in Juvenile Idiopathic Arthritis. Scientific Reports *6*, 27453. 10.1038/srep27453.
19. Hurtado, E., Nunez-Alvarez, Y., Munoz, M., Gutierrez-Caballero, C., Casas, J., Pendas, A.M., Peinado, M.A., and Suelves, M. (2021). HDAC11 Is a Novel Regulator of Fatty Acid Oxidative Metabolism in Skeletal Muscle. FEBS J *288*, 902-919. 10.1111/febs.15456.
20. Jara, D., Carvajal, P., Castro, I., Barrera, M.-J., Aguilera, S., González, S., Molina, C., Hermoso, M., and González, M.-J. (2021). Type I Interferon Dependent Hsa-Mir-145-5p Downregulation Modulates Muc1 and TLR4 Overexpression in Salivary Glands from Sjögren's Syndrome Patients. In Frontiers in immunology, pp. 685837.
21. Jayabal, P., Ma, X., and Shiio, Y. (2021). Ezh2 Suppresses Endogenous Retroviruses and an Interferon Response in Cancers. Genes Cancer *12*, 96-105. 10.18632/genesandcancer.218. PMC8711646
22. Jiao, H., Jiang, D., Hu, X., Du, W., Ji, L., Yang, Y., Li, X., Sho, T., Wang, X., Li, Y.*, et al.* (2021). Mitocytosis, a Migrasome-Mediated Mitochondrial Quality-Control Process. Cell *184*, 2896-2910 e2813. 10.1016/j.cell.2021.04.027.

23. Johnson, J.L., Ellis, B.A., Munafo, D.B., Brzezinska, A.A., and Catz, S.D. (2006). Gene Transfer and Expression in Human Neutrophils. The Phox Homology Domain of P47phox Translocates to the Plasma Membrane but Not to the Membrane of Mature Phagosomes. BMC Immunol *7*, 28. 10.1186/1471-2172-7-28. PMC1712351
24. Kitsou, K., Kotanidou, A., Paraskevis, D., Karamitros, T., Katzourakis, A., Tedder, R., Hurst, T., Sapounas, S., Kotsinas, A., Gorgoulis, V.*, et al.* (2021). Upregulation of Human Endogenous Retroviruses in Bronchoalveolar Lavage Fluid of COVID-19 Patients. Microbiol Spectr *9*, e0126021. 10.1128/Spectrum.01260-21. PMC8510252
25. Kossinova, O.A., Gopanenko, A.V., Tamkovich, S.N., Krasheninina, O.A., Tupikin, A.E., Kiseleva, E., Yanshina, D.D., Malygin, A.A., Ven'yaminova, A.G., Kabilov, M.R.*, et al.* (2017). Cytosolic YB-1 and NSUN2 Are the Only Proteins Recognizing Specific Motifs Present in mRNAs Enriched in Exosomes. Biochim Biophys Acta Proteins Proteom *1865*, 664-673. 10.1016/j.bbapap.2017.03.010.
26. Kumar, S., and Mishra, S. (2022). Malat1 as Master Regulator of Biomarkers Predictive of Pan-Cancer Multi-Drug Resistance in the Context of Recalcitrant Nras Signaling Pathway Identified Using Systems-Oriented Approach. Sci Rep *12*, 7540. 10.1038/s41598-022-11214-8. PMC9085754
27. Kuriyama, Y., Shimizu, A., Kanai, S., Oikawa, D., Motegi, S.I., Tokunaga, F., and Ishikawa, O. (2021). Coordination of Retrotransposons and Type I Interferon with Distinct Interferon Pathways in Dermatomyositis, Systemic Lupus Erythematosus and Autoimmune Blistering Disease. Sci Rep *11*, 23146. 10.1038/s41598-021-02522-6. PMC8632942
28. Li, F., Nellaker, C., Sabunciyan, S., Yolken, R.H., Jones-Brando, L., Johansson, A.S., Owe-Larsson, B., and Karlsson, H. (2014). Transcriptional Derepression of the Ervwe1 Locus Following Influenza a Virus Infection. J Virol *88*, 4328-4337. 10.1128/JVI.03628-13. PMC3993755
29. Li, G., Tian, Y., and Zhu, W.G. (2020). The Roles of Histone Deacetylases and Their Inhibitors in Cancer Therapy. Front Cell Dev Biol *8*, 576946. 10.3389/fcell.2020.576946. PMC7552186
30. Liang, X., Nazarian, A., Erdjument-Bromage, H., Bornmann, W., Tempst, P., and Resh, M.D. (2001). Heterogeneous Fatty Acylation of Src Family Kinases with Polyunsaturated Fatty Acids Regulates Raft Localization and Signal Transduction. J Biol Chem *276*, 30987-30994. 10.1074/jbc.M104018200.
31. Lin, L., Hou, J., Ma, F., Wang, P., Liu, X., Li, N., Wang, J., Wang, Q., and Cao, X. (2013). Type I Ifn Inhibits Innate IL-10 Production in Macrophages through Histone Deacetylase 11 by Downregulating microRNA-145. J Immunol *191*, 3896-3904. 10.4049/jimmunol.1203450.
32. Liu, C., Ren, S., Zhao, S., and Wang, Y. (2019). Lncrna Malat1/Mir-145 Adjusts Il-1beta-Induced Chondrocytes Viability and Cartilage Matrix Degradation by Regulating Adamts5 in Human Osteoarthritis. Yonsei Med J *60*, 1081-1092. 10.3349/ymj.2019.60.11.1081. PMC6813144
33. Liu, X.M., Ma, L., and Schekman, R. (2021). Selective Sorting of microRNAs into Exosomes by Phase-Separated YBX1 Condensates. Elife *10*. 10.7554/eLife.71982. PMC8612733
34. Lu, H., He, Y., Lin, L., Qi, Z., Ma, L., Li, L., and Su, Y. (2016). Long Non-Coding RNA Malat1 Modulates Radiosensitivity of Hr-Hpv+ Cervical Cancer Via Sponging Mir-145. Tumour Biol *37*, 1683-1691. 10.1007/s13277-015-3946-5.

35. Lutful Kabir, F., Ambalavanan, N., Liu, G., Li, P., Solomon, G.M., Lal, C.V., Mazur, M., Halloran, B., Szul, T., Gerthoffer, W.T.*, et al.* (2018). Microrna-145 Antagonism Reverses TGF-beta Inhibition of F508del CFTR Correction in Airway Epithelia. Am J Respir Crit Care Med *197*, 632-643. 10.1164/rccm.201704-0732OC. PMC6005236
36. Ma, L., Li, Y., Peng, J., Wu, D., Zhao, X., Cui, Y., Chen, L., Yan, X., Du, Y., and Yu, L. (2015). Discovery of the Migrasome, an Organelle Mediating Release of Cytoplasmic Contents During Cell Migration. Cell Res *25*, 24-38. 10.1038/cr.2014.135. PMC4650581
37. Margaroli, C., Moncada-Giraldo, D., Gulick, D.A., Dobosh, B., Giacalone, V.D., Forrest, O.A., Sun, F., Gu, C., Gaggar, A., Kissick, H.*, et al.* (2021). Transcriptional Firing Represses Bactericidal Activity in Cystic Fibrosis Airway Neutrophils. Cell Rep Med *2*, 100239. 10.1016/j.xcrm.2021.100239. PMC8080108
38. Martin, M.W., Lee, J.Y., Lancia, D.R., Jr., Ng, P.Y., Han, B., Thomason, J.R., Lynes, M.S., Marshall, C.G., Conti, C., Collis, A.*, et al.* (2018). Discovery of Novel N-Hydroxy-2-Arylisoindoline-4-Carboxamides as Potent and Selective Inhibitors of HDAC11. Bioorg Med Chem Lett *28*, 2143-2147. 10.1016/j.bmcl.2018.05.021.
39. Mathieu, M., Martin-Jaular, L., Lavieu, G., and Thery, C. (2019). Specificities of Secretion and Uptake of Exosomes and Other Extracellular Vesicles for Cell-to-Cell Communication. Nat Cell Biol *21*, 9-17. 10.1038/s41556-018-0250-9.
40. Morinaga, T., Yanase, S., Okamoto, A., Yamaguchi, N., and Yamaguchi, N. (2017). Recruitment of Lyn from Endomembranes to the Plasma Membrane through Calcium-Dependent Cell-Cell Interactions Upon Polarization of Inducible Lyn-Expressing Mdck Cells. Sci Rep *7*, 493. 10.1038/s41598-017-00538-5. PMC5428707
41. Mukherjee, S., Mukherjee, B., Mukhopadhyay, R., Naskar, K., Sundar, S., Dujardin, J.C., and Roy, S. (2014). Imipramine Exploits Histone Deacetylase 11 to Increase the Il-12/IL-10 Ratio in Macrophages Infected with Antimony-Resistant Leishmania Donovani and Clears Organ Parasites in Experimental Infection. J Immunol *193*, 4083-4094. 10.4049/jimmunol.1400710.
42. Mulcahy, L.A., Pink, R.C., and Carter, D.R. (2014). Routes and Mechanisms of Extracellular Vesicle Uptake. J Extracell Vesicles *3*, 24641. 10.3402/jev.v3.24641. PMC4122821
43. Nolte-'t Hoen, E., Cremer, T., Gallo, R.C., and Margolis, L.B. (2016). Extracellular Vesicles and Viruses: Are They Close Relatives? Proc Natl Acad Sci U S A *113*, 9155-9161. 10.1073/pnas.1605146113. PMC4995926
44. Nunez-Alvarez, Y., Hurtado, E., Munoz, M., Garcia-Tunon, I., Rech, G.E., Pluvinet, R., Sumoy, L., Pendas, A.M., Peinado, M.A., and Suelves, M. (2021). Loss of HDAC11 Accelerates Skeletal Muscle Regeneration in Mice. FEBS J *288*, 1201-1223. 10.1111/febs.15468.
45. O'Brien, K., Ughetto, S., Mahjoum, S., Nair, A.V., and Breakefield, X.O. (2022). Uptake, Functionality, and Re-Release of Extracellular Vesicle-Encapsulated Cargo. Cell Rep *39*, 110651. 10.1016/j.celrep.2022.110651.
46. Oglesby, I.K., Chotirmall, S.H., McElvaney, N.G., and Greene, C.M. (2013). Regulation of Cystic Fibrosis Transmembrane Conductance Regulator by microRNA-145, -223, and -494 Is Altered in Deltaf508 Cystic Fibrosis Airway Epithelium. J Immunol *190*, 3354-3362. 10.4049/jimmunol.1202960.

47. Owen, I., and Shewmaker, F. (2019). The Role of Post-Translational Modifications in the Phase Transitions of Intrinsically Disordered Proteins. Int J Mol Sci *20*. 10.3390/ijms20215501. PMC6861982
48. Piwkowska, A., Rogacka, D., Jankowski, M., Dominiczak, M.H., Stepinski, J.K., and Angielski, S. (2010). Metformin Induces Suppression of Nad(P)H Oxidase Activity in Podocytes. Biochem Biophys Res Commun *393*, 268-273. 10.1016/j.bbrc.2010.01.119.
49. Pougovkina, O., and de Boer, V.C.J. (2016). Protein Lysine Acylation: Abundance, Dynamics and Function. In Sirtuins, R.H. Houtkooper, ed. (Dordrecht: Springer Netherlands), pp. 41-69.
50. Ren, J., Wen, L., Gao, X., Jin, C., Xue, Y., and Yao, X. (2008). Css-Palm 2.0: An Updated Software for Palmitoylation Sites Prediction. Protein Eng Des Sel *21*, 639-644. 10.1093/protein/gzn039. PMC2569006
51. Riffelmacher, T., Clarke, A., Richter, F.C., Stranks, A., Pandey, S., Danielli, S., Hublitz, P., Yu, Z., Johnson, E., Schwerd, T.*, et al.* (2017). Autophagy-Dependent Generation of Free Fatty Acids Is Critical for Normal Neutrophil Differentiation. Immunity *47*, 466-480 e465. 10.1016/j.immuni.2017.08.005. PMC5610174
52. Ringel, A.E., Tucker, S.A., and Haigis, M.C. (2018). Chemical and Physiological Features of Mitochondrial Acylation. Mol Cell *72*, 610-624. 10.1016/j.molcel.2018.10.023. PMC6498146
53. Sachdeva, M., Liu, Q., Cao, J., Lu, Z., and Mo, Y.Y. (2012). Negative Regulation of Mir-145 by C/Ebp-Beta through the Akt Pathway in Cancer Cells. Nucleic Acids Res *40*, 6683-6692. 10.1093/nar/gks324. PMC3413133
54. Saha, T., Dash, C., Jayabalan, R., Khiste, S., Kulkarni, A., Kurmi, K., Mondal, J., Majumder, P.K., Bardia, A., Jang, H.L.*, et al.* (2022). Intercellular Nanotubes Mediate Mitochondrial Trafficking between Cancer and Immune Cells. Nat Nanotechnol *17*, 98-106. 10.1038/s41565-021-01000-4.
55. Santiana, M., Ghosh, S., Ho, B.A., Rajasekaran, V., Du, W.L., Mutsafi, Y., De Jesus-Diaz, D.A., Sosnovtsev, S.V., Levenson, E.A., Parra, G.I.*, et al.* (2018). Vesicle-Cloaked Virus Clusters Are Optimal Units for Inter-Organismal Viral Transmission. Cell Host Microbe *24*, 208-220 e208. 10.1016/j.chom.2018.07.006. PMC6226266
56. Sanz-Rubio, D., Martin-Burriel, I., Gil, A., Cubero, P., Forner, M., Khalyfa, A., and Marin, J.M. (2018). Stability of Circulating Exosomal miRNAs in Healthy Subjects. Sci Rep *8*, 10306. 10.1038/s41598-018-28748-5. PMC6037782
57. Sato, I., Obata, Y., Kasahara, K., Nakayama, Y., Fukumoto, Y., Yamasaki, T., Yokoyama, K.K., Saito, T., and Yamaguchi, N. (2009). Differential Trafficking of Src, Lyn, Yes and Fyn Is Specified by the State of Palmitoylation in the Sh4 Domain. Journal of Cell Science *122*, 965-975. 10.1242/jcs.034843.
58. Shinohara, H., Kuranaga, Y., Kumazaki, M., Sugito, N., Yoshikawa, Y., Takai, T., Taniguchi, K., Ito, Y., and Akao, Y. (2017). Regulated Polarization of Tumor-Associated Macrophages by Mir-145 Via Colorectal Cancer-Derived Extracellular Vesicles. J Immunol *199*, 1505-1515. 10.4049/jimmunol.1700167.
59. Skotland, T., Sagini, K., Sandvig, K., and Llorente, A. (2020). An Emerging Focus on Lipids in Extracellular Vesicles. Adv Drug Deliv Rev *159*, 308-321. 10.1016/j.addr.2020.03.002.

60. Son, S.I., Cao, J., Zhu, C.L., Miller, S.P., and Lin, H. (2019). Activity-Guided Design of HDAC11-Specific Inhibitors. ACS Chem Biol *14*, 1393-1397. 10.1021/acschembio.9b00292. PMC6893910
61. Song, Y., Hou, G., Diep, J., Ooi, Y.S., Akopyants, N.S., Beverley, S.M., Carette, J.E., Greenberg, H.B., and Ding, S. (2021). Inhibitor of Growth Protein 3 Epigenetically Silences Endogenous Retroviral Elements and Prevents Innate Immune Activation. Nucleic Acids Res *49*, 12706-12715. 10.1093/nar/gkab1070. PMC8682784
62. Srinivasachar Badarinarayan, S., and Sauter, D. (2021). Switching Sides: How Endogenous Retroviruses Protect Us from Viral Infections. J Virol *95*. 10.1128/JVI.02299-20. PMC8315955
63. Sun, D., Li, X., He, Y., Li, W., Wang, Y., Wang, H., Jiang, S., and Xin, Y. (2016). Yap1 Enhances Cell Proliferation, Migration, and Invasion of Gastric Cancer in Vitro and in Vivo. Oncotarget *7*, 81062-81076. 10.18632/oncotarget.13188. PMC5348376
64. Tamassia, N., Bazzoni, F., Le Moigne, V., Calzetti, F., Masala, C., Grisendi, G., Bussmeyer, U., Scutera, S., De Gironcoli, M., Costantini, C.*, et al.* (2012). Ifn-B Expression Is Directly Activated in Human Neutrophils Transfected with Plasmid DNA and Is Further Increased Via TLR-4–Mediated Signaling. The Journal of Immunology *189*, 1500-1509. 10.4049/jimmunol.1102985.
65. Taylor, S., Isobe, S., Cao, A., Contrepois, K., Benayoun, B.A., Jiang, L., Wang, L., Melemenidis, S., Ozen, M.O., Otsuki, S.*, et al.* (2022). Endogenous Retroviral Elements Generate Pathologic Neutrophils in Pulmonary Arterial Hypertension. Am J Respir Crit Care Med. 10.1164/rccm.202102-0446OC.
66. Temerozo, J.R., Fintelman-Rodrigues, N., Dos Santos, M.C., Hottz, E.D., Sacramento, C.Q., de Paula Dias da Silva, A., Mandacaru, S.C., Dos Santos Moraes, E.C., Trugilho, M.R.O., Gesto, J.S.M.*, et al.* (2022). Human Endogenous Retrovirus K in the Respiratory Tract Is Associated with COVID-19 Physiopathology. Microbiome *10*, 65. 10.1186/s40168-022-01260-9. PMC9024070
67. Tkach, M., and Thery, C. (2016). Communication by Extracellular Vesicles: Where We Are and Where We Need to Go. Cell *164*, 1226-1232. 10.1016/j.cell.2016.01.043.
68. Tu, Y.H., Guo, Y., Ji, S., Shen, J.L., and Fei, G.H. (2021). The Influenza a Virus H3n2 Triggers the Hypersusceptibility of Airway Inflammatory Response Via Activating the lncRNA Tug1/Mir-145-5p/Nf-Kappab Pathway in Copd. Front Pharmacol *12*, 604590. 10.3389/fphar.2021.604590. PMC8029562
69. van der Grein, S.G., Defourny, K.A.Y., Rabouw, H.H., Goerdayal, S.S., van Herwijnen, M.J.C., Wubbolts, R.W., Altelaar, M., van Kuppeveld, F.J.M., and Nolte-'t Hoen, E.N.M. (2022). The Encephalomyocarditis Virus Leader Promotes the Release of Virions inside Extracellular Vesicles Via the Induction of Secretory Autophagy. Nat Commun *13*, 3625. 10.1038/s41467-022-31181-y.
70. Viart, V., Bergougnoux, A., Bonini, J., Varilh, J., Chiron, R., Tabary, O., Molinari, N., Claustres, M., and Taulan-Cadars, M. (2015). Transcription Factors and miRNAs That Regulate Fetal to Adult CFTR Expression Change Are New Targets for Cystic Fibrosis. Eur Respir J *45*, 116-128. 10.1183/09031936.00113214.
71. Wang, J., Wang, H., Zhang, Y., Zhen, N., Zhang, L., Qiao, Y., Weng, W., Liu, X., Ma, L., Xiao, W.*, et al.* (2014). Mutual Inhibition between Yap and Srsf1 Maintains Long Non-Coding

RNA, Malat1-Induced Tumourigenesis in Liver Cancer. Cell Signal *26*, 1048-1059. 10.1016/j.cellsig.2014.01.022.
72. Wang, W., Ding, B., Lou, W., and Lin, S. (2020a). Promoter Hypomethylation and Mir-145-5p Downregulation- Mediated HDAC11 Overexpression Promotes Sorafenib Resistance and Metastasis of Hepatocellular Carcinoma Cells. Front Cell Dev Biol *8*, 724. 10.3389/fcell.2020.00724. PMC7434871
73. Wang, Y., Zhao, M., Liu, S., Guo, J., Lu, Y., Cheng, J., and Liu, J. (2020b). Macrophage-Derived Extracellular Vesicles: Diverse Mediators of Pathology and Therapeutics in Multiple Diseases. Cell Death Dis *11*, 924. 10.1038/s41419-020-03127-z. PMC7595091
74. Whitley, J.A., Kim, S., Lou, L., Ye, C., Alsaidan, O.A., Sulejmani, E., Cai, J., Desrochers, E.G., Beharry, Z., Rickman, C.B.*, et al.* (2022). Encapsulating Cas9 into Extracellular Vesicles by Protein Myristoylation. J Extracell Vesicles *11*, e12196. 10.1002/jev2.12196. PMC8982324
75. Xu, Z., Han, X., Tang, Z., Tian, G., Gao, J., and Xu, X. (2017). Interaction between Malat-1, Ccr7 and Correlated Genes in Oral Squamous Cell Carcinoma. Int J Clin Exp Pathol *10*, 10730-10739. PMC6965852
76. Yan, J., Zhao, Y., Du, J., Wang, Y., Wang, S., Wang, Q., Zhao, X., Xu, W., and Zhao, K. (2022). RNA Sensor Mda5 Suppresses Line-1 Retrotransposition by Regulating the Promoter Activity of Line-1 5'-Utr. Mob DNA *13*, 10. 10.1186/s13100-022-00268-0. PMC9003951
77. Yang, K., Fan, M., Wang, X., Xu, J., Wang, Y., Tu, F., Gill, P.S., Ha, T., Liu, L., Williams, D.L.*, et al.* (2022). Lactate Promotes Macrophage Hmgb1 Lactylation, Acetylation, and Exosomal Release in Polymicrobial Sepsis. Cell Death Differ *29*, 133-146. 10.1038/s41418-021-00841-9. PMC8738735
78. Yoo, S.K., Starnes, T.W., Deng, Q., and Huttenlocher, A. (2011). Lyn Is a Redox Sensor That Mediates Leukocyte Wound Attraction in Vivo. Nature *480*, 109-112. 10.1038/nature10632. PMC3228893
79. Young, G.R., Mavrommatis, B., and Kassiotis, G. (2014). Microarray Analysis Reveals Global Modulation of Endogenous Retroelement Transcription by Microbes. Retrovirology *11*, 59. 10.1186/1742-4690-11-59. PMC4222864
80. Zhang, S., Wu, J., Zhu, X., Song, H., Ren, L., Tang, Q., Xu, X., Liu, C., Zhang, J., Hu, W.*, et al.* (2021). A Novel Approach to Identify the Mechanism of Mir-145-5p Toxicity to Podocytes Based on the Essential Genes Targeting Analysis. Mol Ther Nucleic Acids *26*, 749-759. 10.1016/j.omtn.2021.09.005. PMC8526908
81. Zheng, B., Jarugumilli, G.K., Chen, B., and Wu, X. (2016). Chemical Probes to Directly Profile Palmitoleoylation of Proteins. Chembiochem *17*, 2022-2027. 10.1002/cbic.201600403. PMC5113023
82. Zmijewski, J.W., Lorne, E., Zhao, X., Tsuruta, Y., Sha, Y., Liu, G., Siegal, G.P., and Abraham, E. (2008). Mitochondrial Respiratory Complex I Regulates Neutrophil Activation and Severity of Lung Injury. Am J Respir Crit Care Med *178*, 168-179. 10.1164/rccm.200710-1602OC. PMC2453511

ABBREVIATIONS

Term	Abbreviation
forced exhaled volume in one second compared to the full, forced vital capacity	%FEV1
asymmetrical flow field flow fractionation	aF4
argonaute-2	Ago2
air-liquid interface	ALI
palmitic acid alkyne	alk14
acute respiratory distress syndrome	ARDS
arginase-1	ARG1
apoptosis-associated speck-like protein	ASC
bronchoalveolar lavage fluid	BAL
bone marrow	BM
CCAAT enhancer binding proteins	C/EBP
caspase activation and recruitment domain	CARD
cystic fibrosis	CF
cystic fibrosis sputum airway supernatant	CFASN
common lymphoid progenitor	CLP
common myeloid progenitor	CMP
chronic obstructive pulmonary disease	COPD
coronavirus disease 2019	COVID-19
carnitine palmitoyl transferase	CPT
cAMP-response element binding	CREB
cytokine release syndrome	CRS
damage associated molecular pattern	DAMP
dendritic cell	DC
dynamic light scattering	DLS
double-stranded RNA	dsRNA
Epstein-Barr virus	EBV
enhanced green fluorescent protein	EGFP
epithelial sodium channel	ENaC
elongated neutrophil-derived structures	ENDS
endogenous retroviruses	ERVs
Extracellular Vesicle	EV
formyl methionine leucine phenylalanine	fMLF
forward scatter	FSC
gDNA	genomic DNA
granulocyte-monocyte progenitor	GMP

granule release, immunoregulatory activities toward T-cells and macrophages and metabolic licensing	GRIM
gRNA	guide RNA
highly effective modulator therapy	HEMT
human endogenous retroviruses	HERVs
human immunodeficiency virus	HIV
human lung epithelium	HLE
hematopoietic stem cells	HSCs
influenza A	IAV
intercellular adhesion molecule-1	ICAM-1
interferon	IFN
interleukin	IL
interleukin-1	IL-1
Janus kinase	JAK
lactate dehydrogenase	LDH
liquid-liquid phase condensate	LLPC
long non-coding RNA	lncRNA
leukotriene A4 hydrolase	LTA4H
Leukotriene B4	LTB4
myelin and lymphocyte	MAL
c-Mer tyrosine kinase	MerTK
Major Histocompatibility Complex	MHC
microRNA	miRNA
matrix metalloprotease 9	MMP9
myeloperoxidase	MPO
messenger RNA	mRNA
mitochondria DNA	mtDNA
mechanistic target of rapamycin	mTOR
mitochondrial RNA	mtRNA
molecular weight cut-off	MWCO
neutrophil elastase	NE
neutrophil extracellular trap	NETosis
PMN-restricted precursor	NeuP
NOD-, LRR- and pyrin domain-containing protein 3	NLRP3
NOD-like receptors	NLRs
nanoluciferase	nluc
nitric oxide synthase	NOS
nanoparticle tracking analysis	NTA
pathogen associated molecualr pattern	PAMP

polymorphonuclear neutrophil	PMN
qRT-PCR	quantitative reverse transcription polymerase chain reaction
RNA-binding domains	RBD*
Receptor-binding domain	RBD*
RNA-binding protein	RBP
ribonucleoproteins	RNP
reactive oxygen species	ROS
ribosomal RNA	rRNA
severe acute respiratory syndrome coronavirus-2	SARS-CoV-2
single-cell RNASeq	scRNA-seq
small interfering RNA	siRNA
single particle interferometric reflectance imaging sensing	SP-IRIS
spanning-tree progression analysis of density-normalized events	SPADE
side scatter	SSC
signal transducer and activator of transcription	STAT
T-cell receptor	TCR
Transmission electron microscopy	TEM
Toll-like receptor	TLR
tumor necrosis factor	TNF
transfer RNA	tRNA
violet side scatter	V-SSC
whole blood	WB
YES-associated protein	YAP